University of Strathclyde Engineering

Royal Charter since 1964
Useful Learning since 1796

Performance and Energy Efficiency of Low Irradiance Antimicrobial Violet-Blue Light for Environmental Decontamination Applications

A thesis presented in fulfilment of the requirement for the degree of

Doctor of Philosophy

Lucy Goodwin Sinclair

2024

Department of Electronic and Electrical Engineering

University of Strathclyde

Glasgow, UK

This thesis is the result of the author's original research. It has been composed by the author and has not been previously submitted for examination which has led to the award of a degree.

Signed: 

Dated: 06/06/2024

This thesis was supported by a UK Engineering and Physical Sciences Research Council (EPSRC) Doctoral Training Partnership from 2019-2024.

Reference: EP/R513349/1.

ACKNOWLEDGEMENTS

I would firstly like to extend the greatest thank you to my supervisor, Dr Michelle Maclean, for her immeasurable support, guidance and encouragement throughout the course of this study. I am so grateful to have had the opportunity to work in Michelle's research group, and I cannot thank her enough for her generous time, ideas, enthusiasm and kindness over the last few years. I would also like to thank Professor Scott MacGregor, and Professor John Anderson, for their expertise and assistant throughout.

I also would like to thank the technical staff at the Department of Electronic and Electrical Engineering, including Andy Carlin, Sean Doak, Frank Cox, Conor Bradley, Cameron Hunter and Louis Cooper, for their technical expertise, along with Katie Henderson at the Department of Biomedical Engineering, for her laboratory guidance. I would additionally like to thank Maureen Cooper, for her administrative assistance.

I would also like to thank fellow ROLEST PhD students and friends, Caitlin, David, Sarah, Alyssa, Ruairidh, Justine, Laura and Ross, with whom it has been a pleasure to share my PhD experience with over the last few years.

Finally, I would like to thank my family, especially my Mum, Dad, Julie, Gran and Papa, and Jack, for always supporting and encouraging me in everything I do. I lovingly dedicate this thesis to each of you.

ABSTRACT

Healthcare associated infections are one of the most frequent adverse events to occur during healthcare delivery, affecting 7-15% of patients with an estimated mortality of 10%. The healthcare environment plays a significant role in the transmission of pathogens which can instigate such infections. Environmental decontamination technologies which use UV-light or chemicals can be employed to control infection-inducing pathogen spread, but are limited to episodic use in vacant rooms due to safety restrictions. Antimicrobial 405-nm violet-blue visible light has emerged as an alternative technology, due to its inherent safety at low irradiance levels, enabling its use for continuous decontamination of air and exposed surfaces within occupied settings. The research of this PhD generated new information pertaining to low irradiance 405-nm light and its efficacy for environmental decontamination.

Initial experiments investigated the broad-spectrum bactericidal efficacy of 405-nm light at exposure levels typically employed for decontamination in occupied settings ($\leq$0.5 mW cm^{-2}), with results indicating successful inactivation of surface-seeded nosocomial bacteria within practical exposure times. Bactericidal efficacy was then evaluated under exposure conditions emulating realistic clinical deployment – namely, exposure to a range of possible illuminating irradiances; desiccated on clinical surfaces; associated with biological substrates; and presented as biofilms – with results indicating significant inactivation in all instances using irradiances $\geq$0.005 mW cm^{-2}. Subsequent experiments established an enhancement in the germicidal efficiency of 405-nm light, on a per-unit-dose basis, when employed using low irradiances, analogous to levels employed for environmental decontamination, in comparison to higher irradiances; highlighting the energy efficiency of such lighting systems. Further testing demonstrated the ability of low irradiance 405-nm light to inactivate a SARS-CoV-2 surrogate in both minimal and biologically-relevant media, with reductions significantly enhanced in the latter, likely due to the presence of photosensitive components; overall indicating its ability to control transmission of SARS-CoV-2, and potentially other respiratory viruses, within occupied environments.

This research significantly advances fundamental knowledge of the germicidal efficiency of low irradiance 405-nm light, furthering clinical delivery of this novel environmental decontamination technology which holds potential to reduce healthcare associated infection acquisition and thus address current challenges associated with infection prevention and control within healthcare settings.

TABLE OF CONTENTS

LIST OF FIGURES

LIST OF TABLES

LIST OF ABBREVIATIONS

●OH	Hydroxyl radical
$^1O_2$	Singlet oxygen
$^3O_2$	Oxygen
aHP	Aerosolised hydrogen peroxide
AMR	Antimicrobial resistance
ARHAI	Antimicrobial Resistance & Healthcare Associated Infection
BCCM/LMG	Belgian Coordinated Collections of Microorganisms
BSI	Bloodstream infections
$CaCl_2$	Calcium chloride
Carboxy-H_2DCFDA	6-carboxy-2',7'-dichlorodihydrofluorescein diacetate
CAPP	Cold atmospheric pressure plasma
CDC	Centers for Disease Control and Prevention
CFU	Colony forming units
ClO_2	Chlorine Dioxide
COVID-19	Coronavirus Disease 19
CUV	Continuous ultraviolet
CVC	Central venous catheter
DNA	Deoxyribonucleic acid
DSM/DSMZ	German Collection of Microorganisms
ECDC	European Centre for Disease Prevention and Control
EDS	Environmental decontamination system
EPS	Extracellular polymeric substance
EPSRC	Engineering and Physical Sciences Research Council
ESKAPE	*Enterococcus faecium*, *Staphylococcus aureus*, *Klebsiella pneumoniae*, *Acinetobacter baumannii*, *Pseudomonas aeruginosa* and *Enterobacter* spp.
FWHM	Full-width half-maximum
GE	Germicidal efficiency

H_2O_2	Hydrogen peroxide
HAI	Healthcare-associated infection
HCW	Healthcare worker
HIC	High income countries
HSE	Health and Safety Executive
IC	Internal conversion
ICNIRP	International Commission on Non-Ionizing Radiation Protection
ICU	Intensive care unit
ISC	Intersystem crossing
K_2HPO_4	Dipotassium phosphate
KCl	Potassium chloride
KrCl	Krypton Chloride
LED	Light emitting diode
LMIC	Low-to-middle income countries
LRTI	Lower respiratory tract infections
MDR	Multidrug resistant
$MgSO_4$	Magnesium sulphate
MRSA	Methicillin-resistant *Staphylococcus aureus*
MSSA	Methicillin-sensitive *Staphylococcus aureus*
NA	Nutrient agar
NaCl	Sodium chloride
$NaHCO_3$	Sodium bicarbonate
NB	Nutrient broth
NCTC	National collection of type cultures
NHS	National Health Service
NICE	National Institute for Health and Care Excellence
NPSA	National Patient Safety Agency
$O2^{\bullet-}$	Superoxide
O_3	Ozone

PBS	Phosphate buffered saline
PDT	Photodynamic therapy
PFU	Plaque forming units
PVC	Polyvinyl chloride
ROS	Reactive oxygen species
$S_{\geq 1}$	Singlet excited state
S_0	Singlet ground state
SARS-CoV-2	Severe acute respiratory syndrome coronavirus 2
SD	Standard deviation
SOD	Superoxide dismutase
SSI	Surgical site infections
T_1	Triplet excited state
TFTC	Too few to count
TNTC	Too numerous to count
TSA	Tryptone soya agar
TSB	Tryptone soya broth
UTI	Urinary tract infection
UV	Ultraviolet
VPHP	Vapour phase hydrogen peroxide
VR	Vibrational relaxation
VRE	Vancomycin-resistant *Enterococci*
WHO	World Health Organization
δ-ALA	δ-aminolaevulinic acid

CHAPTER 1

Introduction and Research Aims

1.0 Overview

Healthcare-associated infections (HAIs) are the most frequent adverse event to occur during healthcare delivery (WHO, 2011) and are globally associated with increased mortality, morbidity, durations of hospital stay and healthcare costs (NICE, 2016). It is well-recognised that the healthcare environment plays a significant role in the transmission of pathogens which can instigate such infections (Dancer, 2009, 2014), and an estimated 70% of HAIs are considered avoidable with improved infection prevention and control measures (WHO, 2022a). Nosocomial pathogens can persist on surfaces for extended periods of time even after cleaning, and patients admitted to rooms previously occupied by infected individuals have shown to be more susceptible to infection acquisition from contaminated surfaces (Mitchell *et al.*, 2015; Shams *et al.*, 2016). The problem is exacerbated by the increasing threat of multi-drug resistant (MDR) organisms, which are becoming decreasingly susceptible to available antimicrobials and routine cleaning procedures (WHO, 2011). As a consequence, there is an increasing necessity for novel and improved strategies to effectively decontaminate healthcare environments to prevent HAIs and enhance public safety.

In response to such concerns, a novel disinfection technology, termed the 405-nm light Environmental Decontamination System (EDS), has recently been developed for continuous environmental decontamination (Anderson *et al.*, 2008; Maclean *et al.*, 2010). The violet-blue 405-nm light wavelengths emitted from these systems excite photosensitive porphyrin molecules within microbial cells, initiating the production of reactive oxygen species (ROS) which induces widespread cellular damage and ultimately cell death (Hamblin *et al.*, 2005; Maclean *et al.*, 2008a). Due to the use of visible violet-blue light, these systems have the advantage that they can be employed to provide a continuous decontamination effect to the air and exposed surfaces within occupied environments (Anderson *et al.*, 2008), and various clinical studies have successfully demonstrated their ability to both safely reduce

general bacterial contamination levels within healthcare settings and subsequently reduce HAI rates therein (Maclean *et al.*, 2010, 2013a; Bache *et al.*, 2012a, 2018a; Murrell *et al.*, 2019). To enable the safe, continuous use of the EDS in the presence of room occupants, these systems have been designed to utilise low irradiance levels of typically ≤0.5 mW cm^{-2} (Anderson *et al.*, 2008; ICNIRP, 2013). The majority of studies which have thus far exemplified the fundamental antimicrobial action of 405-nm light inactivation, however, have typically utilised higher irradiance levels (up to approximately 200 mW cm^{-2}) to demonstrate such effects (Hamblin *et al.*, 2005; Guffey and Wilborn, 2006; Murdoch *et al.*, 2012; McKenzie *et al.*, 2014; Tomb *et al.*, 2014; Moorhead *et al.*, 2016b). As such, further evidence is required to fully determine the antimicrobial efficacy of low irradiance 405-nm light, and how it compares to that of higher irradiance exposures.

1.1 Aims of the Study

To further its clinical translatability, this thesis aimed to investigate key research areas associated with the 405 nm light EDS technology and its implementation for continuous environmental decontamination. These included:

(1) Investigating the broad-spectrum antibacterial efficacy of the 405-nm light EDS;
(2) Investigating the antibacterial efficacy of the 405-nm light EDS under bacterial exposure conditions representative of those associated with practical clinical deployment;
(3) Establishing the germicidal efficiency of, and cytotoxic responses of bacteria to, low irradiance 405-nm light in comparison to higher irradiance exposures on a per unit dose basis; and,
(4) Investigating the antiviral efficacy of the 405-nm light EDS.

This research will generate important new information on this emerging infection control technology, particularly in terms of its antimicrobial efficacy and germicidal efficiency, which will be crucial in the development of low power, energy efficient antimicrobial lighting systems with a view to minimising hospital contamination levels and subsequently reducing the transmission of nosocomial pathogens.

A brief overview of the research focus of each chapter in this thesis is as follows:

Chapter 2 – *Background and Literature Review*: discusses HAIs, common routes of transmission and current methods of environmental decontamination in healthcare. The chapter then introduces the novel 405-nm light EDS and, more broadly, 405-nm light in terms of its mechanism of action, antimicrobial efficacy, and research gaps yet to be addressed.

Chapter 3 – *General Methodology*: provides details of the microbiological cultivation and preparation techniques, light sources and optical equipment, and data and statistical analysis techniques required to conduct experimental studies within this thesis.

Chapter 4 – *Antibacterial Efficacy of the 405-nm Light EDS*: characterises the optical irradiance output profile of a ceiling-mounted 405-nm light EDS when installed in a typical room setting, and then quantifies the broad-spectrum bactericidal efficacy of 405-nm light within this irradiance range for the inactivation of nosocomial bacteria. This chapter also investigates the effects of contaminant position from the light source on inactivation efficacy, employing *Staphylococcus aureus* and *Pseudomonas aeruginosa* as model organisms.

Chapter 5 – *405-nm Light EDS Operational Considerations*: expands upon the work conducted in the previous chapter by investigating the bactericidal efficacy of the 405-nm light EDS using contaminant exposure conditions representative of those likely to be encountered in dynamic healthcare environments. This includes exposures: to the lower range of irradiance levels produced by the 405-nm light EDS in a typical room setting; when bacteria are suspended in minimal, organic and biologically-relevant media, and seeded onto clinically-relevant surfaces; and when bacteria are presented in monolayer and mature biofilms formed on microtiter plate wells and clinically-relevant surfaces. To do this, a miniaturised 405-nm light EDS was designed and profiled such that exposures could be conducted practically on a laboratory bench.

Chapter 6 – *Bactericidal Efficacy and Energy Efficiency of Low Irradiance 405-nm Light*: investigates the broad-spectrum bactericidal efficacy and energy efficiency of low versus high irradiance 405-nm light, on a per unit energy basis, for the inactivation of surface-seeded and liquid-suspended ESKAPE (*Enterococcus faecium, S. aureus, K. pneumoniae, Acinetobacter baumannii, Pseudomonas aeruginosa and Enterobacter cloacae*) pathogens. Based on these findings, associated

mechanisms of damage elicited in response to such exposures was examined for *S. aureus* and *P. aeruginosa*.

Chapter 7 – *Antiviral Efficacy of Low Irradiance 405-nm Light*: investigates the antiviral efficacy of the 405-nm light EDS for inactivation of a SARS-CoV-2 surrogate, bacteriophage phi6. The susceptibility of phi6 is investigated at both low and high seeding densities and when suspended in both minimal and biologically-relevant suspension media; to additionally determine the influence of population and suspension media on viral susceptibility. For comparison, preliminary investigations into the susceptibility of phi6 to higher irradiances of 405-nm light are also included.

Chapter 8 – *Conclusions and Recommendations for Future Work*: summarises the key findings from each experimental chapter, overall highlighting the pertinence of 405-nm light for environmental decontamination and its potential to augment clinical infection control practices. Recommendations for future work, in consideration of the work conducted in this thesis, is also discussed.

CHAPTER 2

Background and Literature Review

2.0 Overview

The healthcare environment plays a significant role in the transmission of nosocomial infections, and this chapter provides background about healthcare-associated infections, common routes of infection transmission within healthcare settings – with a focus on environmental transmission – and current methods of environmental decontamination in healthcare. Further, and more specifically, the chapter will then introduce the novel 405-nm light EDS and, more broadly, 405-nm light, in terms of its mechanism of action, antimicrobial efficacy, and fundamental research questions yet to be addressed.

2.1 Healthcare-Associated Infections

HAIs are defined as infections which occur during the period of care within a hospital or healthcare facility which were not present or incubating at the time of admission, including infections acquired within a healthcare facility that do not arise until after discharge, and occupational infections acquired by staff (WHO, 2011).

HAIs are the most frequent adverse event to occur during healthcare delivery worldwide (WHO, 2011). The acquisition of HAIs is associated with prolonged hospital stays, long-term disability, increased resistance towards antimicrobial treatments, additional medical expenditure and excessive morbidity and mortality in hospitalised patients (NICE, 2016). On average, one in every ten affected patients will die as a result of their HAI (WHO, 2023). The continuing persistence of HAIs, coupled with the emerging threat of antimicrobial resistance (AMR), highlights the necessity for improved strategies to prevent such infections and enhance patient and public safety.

The global burden of HAIs is largely under-reported due to a lack of efficient surveillance systems, particularly in low-to-middle-income countries (LMICs) (Vilar-Compte *et al*., 2017; WHO, 2022a).

From the available data, the WHO recently reported that an estimated 15 and 7% of acute-care patients in LMICs and high-income countries (HICs), respectively, are thought to acquire at least one HAI during their stay (WHO, 2011; 2022a). The implications of HAIs are heightened within LMICs compared to HICs due to fewer effective infection prevention and control programmes, a lack of professional training, insufficient medical supplies and diagnostic tools, inadequate organisational infrastructure and poverty-related factors including basic sanitation (Bardossy and Zervos, 2016; Vilar-Compte *et al.*, 2017; WHO, 2022a).

Nevertheless, HAI acquisition in HICs is still a significant public health concern. In Europe, an estimated 98,000 patients, equating to one in every fifteen, will bear at least one HAI during their hospital stay (ECDC, 2017); with rates heightened for patients in intensive care, where approximately one in every five are affected (ECDC, 2024). Annually, these infections directly conduce approximately 37,000 deaths and contribute towards a further 110,000; in addition to 16 million extra hospital stay days and direct healthcare costs amounting to €7 billion (WHO, 2011). In the UK, the total annual cost of HAIs on the NHS is estimated to be £774 million (Manoukian, *et al.,* 2021). In Scotland alone, an estimated 5% of inpatients will acquire a HAI during their stay (Health Protection Scotland, 2012); accounting for 58,000 extra bed stays and costs of £46.4 million annually (Manoukian, *et al.,* 2021).

The most prevalent HAIs reported globally, described in greater detail in Table 2.1, are urinary tract infections (UTIs), surgical site infections (SSIs), bloodstream infections (BSIs) and lower respiratory tract infections (LRTIs) (WHO, 2011). In Scotland, the prevalence of these infections in acute adult hospital inpatients is 24.5%, 16.5%, 8.7% and 23.9%, respectively (Health Protection Scotland, 2017d).

Table 2.1 Common HAIs, their clinical relevance, causes, commonly associated pathogens and current preventative measures.

HAI	Definition	Clinical Relevance	Causes	Commonly Associated Pathogens	Current Preventive Measures
UTI	An infection involving any part of the urinary tract including the urethra, bladder, ureters and/or kidneys (Tan and Chlebicki, 2016).	• One of the most common HAI (Tan and Chlebicki, 2016). • Associated with frequent infection reoccurrence, pyelonephritis with sepsis, renal damage in young children, pre-term birth and complications with frequent antimicrobial use (Flores-Mireles *et al.*, 2015)	• ~70-80% attributable to urinary catheters (Nicolle, 2014) • Although often essential – ~17.5% of Europe inpatients require one during treatment (Zarb *et al.*, 2012) – urinary catheters can result in bacteriuria and biofilm colonisation; increasing morbidity and mortality rates in hospitalised patients (Flores-Mireles *et al.*, 2015)	• Predominant uropathogen is *Escherichia coli* (Kucheria *et al.,* 2005); others include *Klebsiella pneumoniae*, *Staphylococcus aureus*, *Staphylococcus saprophyticus*, *Enterococcus faecalis*, *Proteus mirabilis*, *Pseudomonas aeruginosa*, *Acinetobacter* spp. and *Candida* spp. (Mandal *et al.*, 2012; Flores-Mireles *et al.*, 2015; Tan and Chlebicki, 2016).	• Antibiotics: 60-80% of inpatients with an indwelling catheter will receive antimicrobials and, due to the likelihood of infections reoccurring or becoming chronic, frequent retreatment or long-term antibiotic prophylaxis is common (Nicolle, 2014)
SSI	An infection which occurs ≤30 days following a surgical procedure (or ≤90 days if an implant has been placed) and affect the area of the body in which the surgery was performed (ECDC, 2017c).	• Second most common HAI in Europe affecting >500,000 people and costing ~€19 billion/ annum (WHO, 2018) • Associated with morbidity, mortality, readmission, reoperation, intensive care unit admissions, prolonged post-operative hospital stays and high economic burden (Owens and Stoessel, 2008; Cassini *et al.*, 2016; Badia *et al.*, 2017)	Typically, attributable to either: • Patient's endogenous skin microflora, mucous membranes or hollow viscera (Reichman and Greenberg, 2009) • Environment, surgical personnel or tools brought into the sterile field during the procedure	From each source, respectively: • *S. aureus* (accounting for 20-30%), with the involvement of MDR pathogens, particularly methicillin-resistance *S. aureus* (MRSA), increasing drastically (WHO, 2018) • *S. aureus*, coagulase-negative staphylococci, *Enterococcus* spp. and *E. coli* (Spagnolo *et al.*, 2013)	• Good patient preparation, aseptic practice, attention to surgical technique and antimicrobial prophylaxis (Berríos-Torres *et al.*, 2017) • General heating, ventilation and air conditioning systems to control airborne transmission of infectious particles (Spagnolo *et al.,* 2013)
BSI	An infection defined by the presence of viable bacterial or fungal microorganisms in the bloodstream (Viscoli, 2016).	• In Europe, ~1.2 million episodes of BSIs occur each year, accounting for over 157,000 deaths (Goto and Al-Hasan, 2013) • BSIs are the costliest HAI/ case in Scotland due to associated hospital stays, averaging 11.4 additional days (Manoukian *et al.*, 2021)	• Intravascular devices, particularly central venous catheters (CVCs), represent the most common cause (Gahlot *et al.*, 2014a) • CVC insertion can significantly increase hospital costs and lead to prolonged lengths of stay, with an associated mortality rate of 12-25% (CDC, 2011)	• Bacteria of the skin microflora including *S. aureus*, *P. aeruginosa*, coagulase negative staphylococci, *E. coli*, *K. pneumoniae* and *A. baumannii* (Parameswaran *et al.*, 2010) • Patients in occupied rooms are more likely to develop a BSI than those in private rooms, suggesting measures to reduce environmental spread are essential	• Antibiotic treatment is standard • Technologies incorporating catheters and dressings infused with antiseptics or antibiotics have recently been developed (Gahlot *et al.*, 2014a)
LRTI	An infection localised to the airways (bronchitis, bronchiolitis, influenza and whooping cough) or lungs (pneumonia).	• Amongst acute Scottish inpatients, LRTIs account for almost a quarter of all HAI reported and more than a third of antimicrobials prescribed for infections (Health Protection Scotland, 2017d)	Hospital-acquired pneumonia is the most commonly reported LRTI (Health Protection Scotland, 2017d) and is predominantly caused by intubation and mechanical ventilation, which interferes with host defence mechanisms and encourages biofilm formation on the inner tube surface (Adair *et al.*, 1999; Zolfaghari *et al.*, 2011; Hunter, 2012; Mietto *et al.*, 2013)	• ESKAPE pathogens account for 80% of all ventilator-associated LRTI (Chi kala*et al.*, 2012; Sandiumenge *et al.*, 2012) • Early onset infection typically caused by antibiotic-sensitive bacteria such as *Streptococcus* spp., *S. aureus, E. coli*, *K. pneumoniae* and *Enterobacter* spp.; late onset infection typically caused by MDR bacteria such as MRSA, *Acinetobacter* spp., *P. aeruginosa* and ESBL (Hunter, 2012; Kalanuria *et al.*, 2014)	• Limited-spectrum antibiotics for early onset VAP and broad-spectrum antibiotics for late onset VAP (American Thoracic Society, 2005) • Novel preventative measures with focus on poor infection practices and contamination of respiratory equipment are essential (Koenig *et al.*, 2006)

2.2 Nosocomial Pathogens and their Transmission

The causation and spread of HAIs are dependent on a linked sequence of events termed the chain of infection (Figure 2.1) which will be discussed in this section as a means of understanding the various ways in which infectious agents can be transmitted and instigate infection within healthcare.

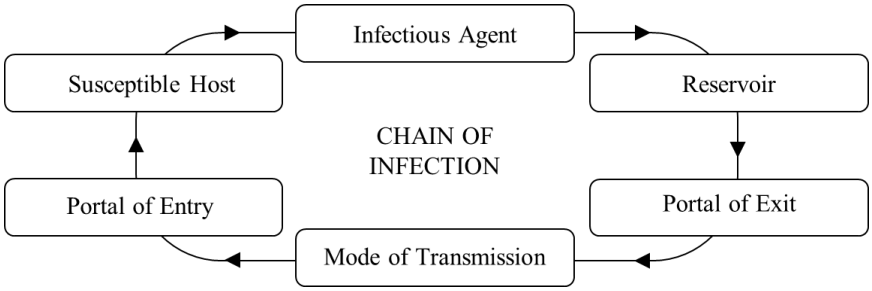

Figure 2.1 Chain of infection within healthcare: the instigation of infection begins with an infectious agent residing in a favoured reservoir; the infectious agent will then leave this reservoir via a suitable portal of exit, and using a mode of transmission, can enter and infect a susceptible host (van Seventer and Hochberg, 2016).

2.2.1 Infectious Agents

Various nosocomial pathogens are capable of inducing infection within healthcare settings depending upon patient populations, healthcare facilities and the care environment. Given the scope of this thesis, this section will detail bacterial and viral species associated with HAIs.

2.2.1.1 Bacteria

Bacteria are responsible for approximately 90% of all reported HAIs (Khan *et al.*, 2015). In a recent Scottish survey, 40.4% of HAIs reported were caused by Gram-negative bacilli and 20.2% by *S. aureus* (Health Protection Scotland, 2017d). The ESKAPE pathogens (Table 2.2) collectively represent the leading cause of nosocomial infections worldwide (Santajit and Indrawattana, 2016). In LMICs, they are associated with the highest mortality risks and healthcare costs of all MDR infectious agents; primarily due to their notorious resilience to common antibiotics and antibacterial treatments (Founou *et al.*, 2017). The WHO recently published a list of global MDR 'priority' pathogens which pose the greatest threat to human health and urgently require research and development of new antibiotic treatments or other infection control interventions (WHO, 2017). Therein, the ESKAPE pathogens were appointed high and critical priority status (WHO, 2017)

Table 2.2 ESKAPE pathogens, associated clinical disease, their common healthcare reservoirs, resistive characteristics and clinical significance.

Bacteria	Gram Stain/ Morphology	Associated Clinical Disease	Healthcare Reservoirs	Resistive Characteristics	Clinical Significance
Enterococcus faecium	+ Cocci	UTI; Intra-abdominal and Pelvic Infection; Wound Infections; Bacteraemia; Endocarditis; Neonatal Sepsis; Meningitis	• Skin and gut microbiota • Contaminated environmental surfaces (Pendleton *et al.*, 2013)	MDR, including: vancomycin, ampicillin, linezolid, teicoplanin, piperacillin, cephalosporin (De Oliveira *et al.*, 2020)	• Up to 46.3% and 80% of clinical isolates in Europe and US are currently vancomycin resistant, respectively (Zhou *et al.*, 2020) • 1/3 of mortality in European hospitals associated with *Enterococcus* spp. HA-BSI between 2010-2020 were attributed to VRE (Brinkwirth *et al.*, 2021)
Staphylococcus aureus	+ Cocci	LRTI; SSI; Bacteraemia; Pneumonia; Cardiovascular Infections	• Skin and mucosa microbiota • Contaminated environmental surfaces (Pendleton *et al.*, 2013)	MDR, including: aminoglycosides, β-lactams, chloramphenicol, trimethoprim, macrolides, tetracycline, fluoroquinolones (De Oliveira *et al.*, 2020)	• The most commonly isolated HAI-causing ESKAPE pathogen in Scotland, responsible for 20.2% and 25% of infections in acute adult and paediatric inpatients (Cairns *et al.*, 2018) • In the UK, ~5-25% of MRSA strains are resistant to oxacillin (Lee *et al.*, 2018)
Klebsiella pneumoniae	- Bacillus	Neonatal Septicaemia; Septicaemia; Bacteraemia; Pneumonia; Wound Infections; SSI	• Respiratory tract and gut microbiota • Contaminated environmental surfaces (Pendleton *et al.*, 2013)	Pandrug and MDR, including: polymyxins, carbapenems, fluoroquinolones, 3rd-gen. cephalosporins, aminoglycosides, tetracyclines (De Oliveira *et al.*, 2020)	• ~32.8% of global nosocomial infections are due to MDR *K. pneumoniae* isolates (Asri *et al.*, 2021) • Mortality rate of carbapenem resistant *K. pneumoniae* infections (42.1%) double that of carbapenem-susceptible *K. pnumoniae* infections (21.2%) (Xu *et al.*, 2017)
Acinetobacter baumannii	- Coccobacillus	Bacteraemia; UTI; Pneumonia; Wound Infections	• Contaminated environmental surfaces (Pendleton *et al.*, 2013)	MDR, including: carbapenems, polymyxins, β-lactams, tigecycline, ceftazidime, fourth-gen. cephalosporins (De Oliveira *et al.*, 2020)	• Extremely persistent in the environment, with evidence of its ability to survive on dry inanimate surfaces for up to 5 months (Kramer *et al.*, 2006) • The mortality rate of nosocomial *A. baumannii* infections has been recorded as high as 44% (Alrahmany *et al.*, 2022)
Pseudomonas aeruginosa	- Bacillus	Wound Infections; Meningitis; Uti; Necrotising Pneumonia; SSI; Bacteraemia	• Skin, respiratory tract and digestive tract microbiota • Contaminated water sources (e.g. sink drains, toilets, etc) • Contaminated environmental surfaces (CDC, 2019)	MDR, including: first- and second-gen. cephalosporins, piperacillin-tazobactam, aminoglycosides, quinolones, carbapenems, polymyxins (De Oliveira *et al.*, 2020)	• Responsible for ~700,000 deaths per year (Qin *et al.*, 2022) • The most frequently isolated organism in ICU-acquired pneumonia (ECDC, 2016)
Enterobacter spp.	- Bacillus	LRTI; UTI; Gastrointestinal Tract Infections	• Gut microbiota • Contaminated water sources (e.g. sink drains, toilets, etc) (Davin-Regli *et al.*, 2019)	Pandrug and MDR, including: carbapenems, fourth-gen. cephalosporins, Fluoroquinolones, β-lactams, polymyxins (De Oliveira *et al.*, 2020)	• Currently resistant to almost all available antimicrobial drugs, except tigecycline and colistin (Santajit and Indrawattana, 2016) • *E. cloacae*, which causes 90-99% of Enterobacter infections in humans, is associated with an inpatient mortality rate of 15.1% (Song *et al.*, 2010)

2.2.1.2 Viruses

Viral pathogens account for 1-5% of all HAI-inducing pathogens (Aitken and Jeffries, 2001) and are typically transmitted via blood products, faecal matter or respiratory routes (WHO, 2002). Nosocomial bloodborne viruses, such as hepatitis B, C and human immunodeficiency virus type 1, are commonly transmitted through unsafe and improper needle practice via blood transfusions or in dialysis units (Aitken and Jeffries, 2001); with 30% of these due to failures following infection control procedures (Singh *et al.*, 2022). Pathogens transmitted via the faecal-oral route, including rotavirus, calicivirus, hepatitis A and E (Aitken and Jeffries, 2001), typically replicate in the intestines and are spread through improper hand hygiene practices or failures in sanitation systems (Gerba, 2009). Respiratory viruses, including respiratory syncytial virus, norovirus, influenza A and B, adenovirus, rhinovirus and coronavirus (Aitken and Jeffries, 2001), are the most common causative agent of disease in humans (Boncristiani, 2009) and represent a major cause of mortality, causing approximately 2.7 million deaths worldwide in 2015 (Troeger *et al.*, 2017). In light of the recent Coronavirus Disease 19 (COVID-19) pandemic, this study took a particular focus on severe acute respiratory syndrome coronavirus 2 (SARS-CoV-2) and further detail about this virus is provided in Chapter 7.

2.2.1.3 Antimicrobial Resistance

AMR is the situation whereby a disease-causing microorganism develops the ability to survive exposure to an antimicrobial agent which would have previously been considered an effective treatment (WHO, 2021a). The global emergence and spread of MDR pathogens, decreasingly susceptible to available antimicrobials, threatens the ability to treat and prevent common infections. It is considered one of the top ten global public health threats facing humanity today (WHO, 2021a): in 2019, approximately 1.27 million global deaths were directly attributable, and it is predicted to cause 10 million deaths by 2050; matching the global death toll of cancer (O'Neill, 2016; Antimicrobial Resistance Collaborators, 2022).

Antimicrobial Resistance Mechanisms in Bacteria

The modern 'antibiotic era' – inaugurated with the discovery of penicillin by Sir Alexander Fleming in 1928 (Lee Ventola, 2015) – incited production of various novel classes of antibiotics, revolutionising modern medicine and consequently saving many lives (Office for National Statistics, 2017). However, this was followed by a cyclic pattern of antibiotic production and subsequent drug resistance. By the

1950s, penicillin resistance was a significant clinical problem (Lee Ventola, 2015). Novel beta-lactam antibiotics were developed in response; however, cases of methicillin-resistant *S. aureus* (MRSA) were identified less than a year later (Harkins *et al.*, 2017). This urged development of vancomycin; which was followed by the discovery of vancomycin-resistant enterococci (Cetinkaya *et al.*, 2000). Resistance has been observed to the vast majority of antibiotics currently available (Lee Ventola, 2015) and, since the 1980s, the production of novel antibiotics has significantly decreased (HM Government, 2019).

Bacteria typically demonstrate either intrinsic resistance, due to general adaptive processes not necessarily linked to a specific class of antimicrobials (*P. aeruginosa*, for example, is resistant to common antimicrobials due to its low outer membrane permeability, expression of efflux pumps which can expel antibiotic materials, and ability to produce antibiotic-inactivating enzymes (Pang *et al.*, 2019)); or acquired resistance, typically through genetic mutation or acquisition via horizontal transfer from another strain/ species – with mechanisms including thickening of cell walls, encoding proteins to prevent drug penetration and onset of mutants lacking porin channels to inhibit influx of chemicals (Jori *et al.*, 2006) – due to evolutionary pressure to evade antimicrobial susceptibility (Reygaert, 2018). Examples of these mechanisms are presented in Figure 2.2.

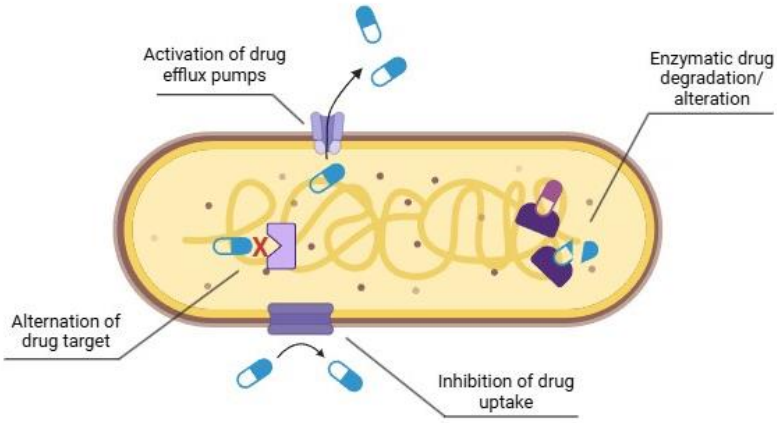

Figure 2.2 Antimicrobial resistance mechanisms in bacterial cells. Image created with BioRender.com.

The rise and spread of MDR bacteria have created a new generation of hospital 'superbugs' which are increasingly difficult to treat with existing therapeutics. Emerging strains of *S. aureus*, for example, have shown resistance towards vancomycin, which was considered a last line of defence (Smith *et al.*, 1999) and MRSA is associated with high global mortality rates (Founou *et al.*, 2017). Carbapenem-resistant and ESBL-producing Gram-negative bacteria are also of concern, accounting for all critical

organisms on the WHO's recently published list of MDR pathogens requiring novel therapeutics (WHO, 2017). In Europe, one third of HAI-causing bacteria are believed to be MDR phenotypes (ECDC, 2017).

Antimicrobial Resistance Mechanisms in Viruses

Viruses principally confer resistance through various naturally occurring random point mutations: some enter a latency period, whereby antivirals are generally ineffective; some adopt various serotypes which are unlikely be effectively treated by one antiviral; and some have high mutation rates during their replication cycle, increasing the likelihood of clinical resistance (Vere Hodge and Field, 2011). Further, viruses with segmented genomes, such as influenza, can generate resistance through genetic reassortment upon infecting a host cell; producing progeny viruses with novel genomes (Vere Hodge and Field, 2011). Resistance has developed to most available antivirals, including antiretroviral drugs to treat HIV (WHO, 2021a), with prolonged antiviral drug exposure and ongoing viral replication due to immunosuppression key contributing factors (Strasfeld and Chou, 2010). In light of the COVID-19 pandemic, the potential for SARS-CoV-2 to confer resistance mechanisms is of significant concern. Although not fully understood, recent findings have demonstrated its ability to already mutate and escape the effects of Remdesivir, which is routinely used to treat hospitalised COVID-19 patients (Szemiel *et al.*, 2021).

Clinical Impact

Although naturally occurring, AMR can be accelerated by factors including: the misuse and overuse of antimicrobials, lack of access to clean drinking water and sanitation, limited quality diagnostics and treatments, poor infection control practices, a lack of appropriate legislation enforcement, agricultural use of antibiotics in livestock feedstuff, increased global travelling and poor education (Dadgostar, 2019; WHO, 2021a). HAI instigated by MDR pathogens, compared to sensitive pathogens, doubles the likelihood of complication development and triples the likelihood of death (Cecchini *et al.*, 2015), and is associated with greater healthcare costs due to prolonged hospital stays, additional diagnostic tests and therapies (Serra-Burriel *et al.*, 2020). Without action, AMR is estimated to account for a cumulative economic output of $100 trillion globally by 2050 (O'Neill, 2016). As the antimicrobial pipeline continues to decrease and MDR pathogens continue to emerge, the end of the antibiotic era is imminent and development of novel therapeutics with minimal likelihood of tolerance development is crucial.

2.2.2 Sources of Infection

Nosocomial pathogens commonly arise from either an endogenous source, such as the patient's natural microflora, or exogeneous sources, primarily through contact transmission (Khan *et al.*, 2017).

Endogenous Sources

Human skin acts as a physical barrier to prevent invasion of foreign pathogens (Byrd *et al.*, 2018). It also hosts various microorganisms, with up to one million residing on just one square centimetre (Weyrich *et al.*, 2015). The majority are harmless commensal microbiota which protect against foreign pathogens by both acting on the host's immune system to induce protective responses and directly inhibiting growth via production of antimicrobial products and competition for nutrients and adhesion sites (Byrd *et al.*, 2018; Khan *et al.*, 2019). *Staphylococcus epidermidis*, for example, which is the most commonly isolated bacteria from healthy human skin, has been shown to produce bacteriocins and β-defensins which initiate an enhanced immune response and inhibit growth of invading pathogens including *S. aureus* (Lai and Gallo, 2010). Skin microbiota can, however, induce infection if immune responses are hampered or if the skin surface is breached (Khan *et al.*, 2017). *S. aureus*, for example, is a commensal which asymptomatically colonises the skin/ mucosal surfaces of approximately 1 in 3 individuals (Gorwitz *et al.*, 2008); however, upon entering the body, is the leading cause of bacteraemia, infective endocarditis, skin, soft tissue and device-related infections (Tong *et al.*, 2015; Grogan *et al.*, 2019).

Exogenous Sources

Approximately 20-40% of HAIs arise due to cross infection via healthcare workers (HCWs) hands, via direct patient contact or indirect contact with contaminated surfaces (Weber *et al.*, 2010). Various surfaces/ objects within the 'patient zone' can serve as pathogen reservoirs, with colonisation dependent on factors including surface type/ orientation, environmental conditions and frequency of contact (Suleyman *et al.*, 2018). 'High-touch' surfaces in close proximity to patients are thought to provide the biggest risk of HAI transmission (Otter *et al.*, 2013; Suleyman *et al.*, 2018) and thus should be cleaned more frequently (CDC, 2023). Huslage *et al*. (2010) recently defined, based on observations of contact frequency, the bed rail, bed surface, supply cart, over-bed table and intravenous pump as the top five most frequently touched hospital surfaces. Water sources are also a prominent reservoir for pathogens

including *Pseudomonas* spp., which can be transmitted from sinks to hands during handwashing (Franco *et al.*, 2020).

Nosocomial bacteria often survive on healthcare surfaces for extended periods of time due to their aptitude for the temperate hospital environment (Kramer *et al.*, 2006; Dancer, 2014). Certain microorganisms, such as *S. aureus*, persist better under low humidity conditions, whilst certain Gram-negative bacteria survive better at high humidity; primarily due to the cell wall enabling higher tolerance of dry conditions (Kramer and Assadian, 2014). Suspension media can also be influential: Fedorenko *et al*. (2020) recently reported significantly higher levels of SARS-CoV-2 survival on glass surfaces when suspended in evaporated saliva microdroplets compared to minimal media; with saliva proteins believed to offer the virion protection. Bacterial endospores also survive longer than their vegetative counterparts (Otter and French, 2009): the outer spore layers detoxify chemicals, the spore coat protects from heat and desiccation and the inner spore membrane restricts access of toxic chemicals (Setlow, 2014). Bacteria can also develop biofilms – an assemblage of surface-associated microbial cells enclosed in an extracellular polymeric substance (EPS) matrix – in response to environmental stress which structurally aid survival: growth rate is reduced, the hydrated EPS prevents desiccation, exchange of extrachromosomal DNA occurs quicker, and the up and down regulation of specific genes to confer resistance against environmental influences (Donlan, 2002). The ESKAPE pathogens have been found to survive on common hospital surfaces for up to four weeks (Katzenberger *et al*., 2021). MRSA, often shed from infected individuals, has been shown to resist desiccation and survive on hospital surfaces for up to one year (Wagenvoort *et al.*, 2000). Further, vancomycin-resistant *Enterococci* (VRE) has been shown to survive several years on surfaces (Suleyman *et al.*, 2018) and is the most frequently isolated MDR bacteria in nosocomial transmission events (Erb *et al.*, 2016). The risk of infection is additionally heightened for individuals admitted to rooms previously occupied by infected patients (Huang *et al.*, 2006).

2.2.3 Modes of Transmission

Infectious particles can be transferred and instigate infection via multiple routes of transmission including contact, droplet and airborne transmission.

2.2.3.1 Contact Transmission

Contact transmission – either direct or indirect – is the most frequent mode of nosocomial infection transfer (NHS, 2022). Direct contact transmission typically occurs via direct physical contact between the skin or mucosa of an infected individual and that of a susceptible host (van Seventer and Hochberg, 2016). This includes bacterial and viral conjunctivitis and respiratory viruses such as SARS-CoV-2 (van Seventer and Hochberg, 2016; Leung, 2021). During regular care activities, such as lifting patients and taking vital signs, HCW hands can easily become contaminated (Casewell and Phillips, 1977), with up to 300 colony forming units (CFU) of bacteria previously found on HCW fingertips following direct patient contact (Pittet *et al.*, 1999). Hand hygiene is one of the most effective measures in HAI prevention (Pittet, 2001) and, when used correctly, can lower hospital stays and rates of patient morbidity, mortality and complications (Ahmadipour *et al.*, 2022). However, poor compliance to these measures is often demonstrated due to various factors including insufficient hand washing supplies, high workloads, understaffing, and limited education (Pittet, 2001). Indirect contact transmission occurs when an infected individual contaminates a surface or fomite with pathogens and a susceptible host then later comes into contact with this contaminated material. Infectious pathogens are shed from patients into the environment via the skin or excretion/secretion of bodily fluids such as vomit, faeces, blood and respiratory droplets, which can then settle on environmental surfaces. Contamination of hospital surfaces in patient areas via this shedding is widely reported to play an important role in the development of HAIs (Weber *et al.*, 2010). HCWs frequently touch patients and surfaces, and thus can act as transmission vectors if the environment is contaminated and hygiene measures are not adhered to (Huslage *et al.*, 2010). Hayden *et al*. (2008) found 70% of HCWs in a tertiary-care teaching hospital who touched VRE-positive patients and their immediate environment contaminated their hands or gloves; with 52% becoming contaminated following contact with the environment only. Further, Sasahara *et al*. (2016) found 76% of HCWs hands in a tertiary-care hospital were contaminated with either *Bacillus subtilis, Bacillus cereus and Clostridium difficile* spores (mean of 468.3 CFU hand^{-1}) following nine working hours, with a significant positive correlation between hand contamination level and the length of time since last handwashing.

2.2.3.2 Transmission through the Air

Infectious pathogens can be dispersed from an infected individual through various expiratory activities. In response to the COVID-19 pandemic, the WHO have recently updated their official terminology used to describe the transmission of pathogens through the air in order to better reflect the complexities associated with such transmission and enable clearer and more effective communication of public health strategies (WHO, 2024). Comprehensively, pathogens may be transmitted through the air via either airborne transmission/inhalation or direct deposition (WHO, 2024). Airborne transmission/inhalation occurs when pathogens expelled into the air, as described above, enter, through inhalation, the respiratory tract of another individual (WHO, 2024). In such instances, the infectious particles can travel various distances before being inhaled by the host (WHO, 2024). Direct deposition occurs when a pathogen expelled into the air follows a short-range semi-ballistic trajectory and is then directly deposited on the exposed facial mucosal surfaces of another individual (WHO, 2024). The type of organism, particle size, settling velocity, relative humidity and airflow can each influence the length of time that an infectious particle can be suspended in the air, and thus the distance over which it can travel (WHO, 2014). Prolonged suspension time enables wide distribution of aerosolised particles throughout hospital buildings, and as such, ventilation conditions play a considerable role in transmission (Beggs, 2003). Most aerosolised infectious particles in healthcare settings are generated from infected individuals via expelled respiratory droplets or medical aerosol-generating procedures (WHO, 2014). Dougall *et al*. (2019) demonstrated a correlation between the mean counts of airborne bacteria within inpatient isolation rooms and the duration of patient stay and room activity levels: an average increase in air bioburden of 103%, 197% and 145% during patient personal hygiene activities, when more than three staff members were in the room and during bed sheet changes, respectively.

2.2.4 Risk Factors

Various predisposing factors, including those related to the patient, healthcare delivery and the environment, may increase the likelihood of HAI acquisition.

Patient-related factors

Higher risk age groups include the elderly, due to greater likelihood of long-term care facility stays, age-associated co-morbidities, chronic in-dwelling devices and extensive healthcare delivery exposure

(Gruber *et al.*, 2013). Neonates are also of higher risk, primarily due to the immaturity of their immune system, frequent use of broad-spectrum antimicrobials, extended hospital stays and long-term use of invasive devices (Legeay *et al.*, 2015). Immunocompromised patients are also at higher risk, primarily due to the severity of their underlying conditions and consequential ongoing diagnostic, monitoring and therapeutic procedures (Lim, 1997; Al-Tawfiq and Tambyah, 2014), with a recent study finding vulnerable patients admitted to Scottish hospitals for cancer, cardiovascular disease, chronic renal failure and diabetes were at significantly higher risk than all other patients (Stewart *et al.*, 2021).The risk of HAI is substantially heightened with increasing duration of hospital stays: a case-control study in an emergency department found for every extra hour that an emergency-intubated blunt trauma patient stayed in hospital, the risk of developing healthcare-acquired pneumonia increased by around 20% (Carr *et al.*, 2007). Minimising unnecessary hospitalisations is a significant problem, with approximately 350,000 patients across NHS England currently spending over three weeks in acute hospitals each year (NHS England, 2019).

Healthcare delivery-related factors

The risk of HAI development heightens upon increasing exposure to invasive devices (van der Kooi *et al.*, 2007). Central venous catheters (CVCs) pose the greatest risk, and are the main cause of bacteraemia and septicaemia in hospitalised patients (Gahlot *et al.*, 2014). During surgical procedures, pathogens may enter open incisions – further exacerbated by prolonged exposures and inadequacies in the surgical scrub or antiseptic preparation of the skin (Cheadle, 2006) – with SSIs estimated to account for 16.5% of inpatient HAIs within NHS Scotland in 2019 (ARHAI Scotland, 2020). Infections instigated by MDR bacteria are associated with increased severity: for example, MRSA infections are associated with greater co-morbidities, complications, hospital stays and mortality compared to methicillin-sensitive *S. aureus* (MSSA) infections (Cosgrove *et al.*, 2003; Hanberger *et al.*, 2011; Chatterjee *et al.*, 2018).

Environmental factors

HAI prevalence is highest in intensive care units (ICUs) compared to all other hospital wards (WHO, 2011): a national point prevalence survey in Scotland found 11.4% of ICU patients had a HAI at any given time, compared to just 4% of medical patients and 6.5% of surgical patients (Health Protection Scotland, 2017d). Globally, an estimated 30% and 88.9% of adult ICU patients in HICs and LMICs,

respectively, are affected by at least one HAI during their stay (WHO, 2011). This is primarily due to greater likelihood of emergency admissions, prolonged hospital stays, intravenous material placement and immuno-suppressed and neutropenic patients (WHO, 2011). Burns patients are also at significantly higher risk due to breakdown of the skin barrier/immunosuppression when exposed to significant thermal injuries (Church *et al.*, 2006). If patients survive the initial 72 h after a burn injury, infections are considered the most common cause of death therein (Lachiewicz *et al.*, 2017).

Stiller *et al*. (2016) additionally observed a strong correlation between ward design and HAI rates, identifying single patient rooms and hand rub dispensers near patient beds as important infection control facilitators. Air-conditioning systems can harbour dust and moisture, increasing contamination risk: HEPA filters are efficient in reducing contamination, however are typically only used in high risk areas instead of general wards and clinics (Wu *et al.*, 2021). Mitchell *et al*. (2018) also found a decrease in staffing levels, measured in terms of nurse-to-patient ratio or nursing hours per patient day, increases the risk; potentially due to high levels of burnout leading to lapses in infection control procedures (Cimiotti *et al.*, 2012).

Up to 70% of HAIs are considered avoidable with improved infection prevention and control measures (WHO, 2022a). Although complete eradication is unfeasible and unrealistic, implementation of efficient and stringent control measures to hinder infection acquisition is essential for improving patient outcomes and relieving financial burden on healthcare systems (Health Protection Scotland, 2019).

2.3 Environmental Decontamination in Healthcare

High standards of decontamination play an important role in minimising the risk and controlling outbreaks of HAIs (Dancer, 2009a, 2014); however, the discussed complexities associated with contamination substantiates the need for a multidisciplinary approach. This section discusses both standard and ‘whole-room’ methods used for routine and terminal decontamination of hospital environments.

2.3.1 Routine and Terminal Decontamination

NHS Scotland stipulates both routine and terminal environmental cleaning must be conducted to minimise environmental contamination (Healthcare Associated Infection Task Force, 2009). Routine cleaning is conducted on a regular basis – not in response to an outbreak – and mostly targets surfaces with higher risks of contamination, i.e. those close to the patient area and frequently touched by patients and HCWs (Cobrado *et al.*, 2017; Health Protection Scotland, 2017d). These are recommended daily or at increased frequency in high-risk patient areas, such as ICUs, accident and emergency, and neonatal units, and very high-risk areas, including theatres and transplant and bone marrow units (Health Protection Scotland, 2017d). Terminal cleaning is conducted, where necessary, in addition to routine cleaning and is the procedure required to ensure that the environment used to treat patients with an alert organism or communicable disease are adequately decontaminated such to render it safe for the next patient (Healthcare Associated Infection Task Force, 2009). Once the patient has been transferred, discharged or is no longer considered infectious, all healthcare waste, fabrics and laundry is removed; reusable non-invasive care equipment is cleaned in the room prior to removal; and, using an appropriate method, all surfaces are cleaned thoroughly, starting from the least to the most contaminated point (NHSScotland, 2012).

2.3.2 Standard Decontamination Methods

Traditionally, environmental cleaning, both routine and terminal, is conducted using detergents and disinfectants. During routine cleaning, a neutral or near-neutral pH solution detergent should be used to physically remove organic matter and microorganisms from surfaces (Health Protection Scotland, 2017). This alone can be sufficient in low-risk settings, such as offices and corridors; however, within patient care areas, surfaces and non-critical items, such as bed rails, bedpans and blood pressure cuffs, must subsequently be treated with disinfectants, such as alcohol, chlorine, sodium hypochlorite and quaternary ammonium compounds, to inactivate any remaining pathogens (Rutala and Weber, 2013).

Although essential for reducing contamination, manual cleaning using detergents/disinfectants can be considered suboptimal. Despite improvements in cleaning performance in recent years, inaccessible or difficult-to-clean surfaces can still be missed or cleaned ineffectively, with findings demonstrating flat surfaces, such as countertops and bedside tables, are cleaned more duly than small, vertical surfaces,

such as doorknobs and light switches (Goodman *et al.*, 2008; Ali *et al.*, 2016; Parry *et al.,* 2022). Further, surfaces which are not routinely cleaned, such as walls and electronic equipment, are still likely to harbour pathogens for transmission (Maclean *et al.*, 2015). Although low-level disinfectants demonstrate rapid efficacy; these can often be irritants, cause material damage, and be affected by organic matter (Rutala and Weber, 2013, 2016). Individual cleaning performance can also vary and there is a potential lack of compliance amongst cleaning staff, often accredited to inadequate staffing or excessive workload (Dancer, 2009a; Goodman *et al*., 2008b). Further, organisms can persist even after discharge cleaning: a prospective microbiology study found 40% of hospital rooms sampled were contaminated with MDR organisms after routine and terminal cleaning, of which VRE was most common (Shams *et al.*, 2016); and recent findings indicate patient admitted to rooms previously occupied by individuals infected with MRSA, VRE, *C. difficile*, MDR *Acinetobacter* and *Pseudomonas* spp. were at a significantly higher risk of infection (Mitchell *et al.*, 2015).

2.3.3 Whole-Room Decontamination Methods

As a consequence of the issues associated with traditional cleaning, there has been an upsurge in the use of 'whole-room' technologies which are designed to complement standard cleaning and infection control procedures and enhance environmental decontamination. This section will discuss the key technologies currently commercially available or under development for this purpose, including gaseous and light-based disinfection methods.

2.3.3.1 Steam Cleaning

Steam cleaning systems for environmental decontamination deliver pressurised superheated (≥140 ºC) dry steam to both clean and disinfect: the pressurised steam loosens organic debris, which are then vacuum extracted into the machine, whilst the high temperatures inactivate microorganisms through irreversible coagulation and denaturation of structural proteins and enzymes (Rutala *et al.*, 2008; ARHAI Scotland Infection Control Team, 2021). It is rapidly microbicidal and sporicidal, with evidenced ability to successfully remove nosocomial pathogens, including MRSA, *Acinetobacter* and *C. difficile* spores, from clinical surfaces (NHS England, 2008). The technology does not pose chemical hazards, however, is associated with scalds and/or burns risk due to the high temperatures employed, and so rooms must be vacated with fully trained operators employed throughout. To ensure adequate

decontamination, the spray nozzle must be held at the appropriate distance for a set time; making the process intensive and time-consuming (NPSA, 2009). The technology is not recommended on temperature and/or moisture sensitive surfaces due to potential rusting, oxidation and/or damage to joints, seals and bonds (Kohli, 2018). Care must be taken not to apply the steam over electrical sockets (NPSA, 2009), and fire/smoke detectors often require disengaging prior to use (NHS England, 2008).

2.3.3.2 Hydrogen Peroxide

Hydrogen peroxide (H_2O_2) produces free hydroxyl and ferryl radicals that induce oxidative damage in cellular lipids, proteins and nucleic acids (Otter and French, 2009; Linley *et al.*, 2012). It is microbiocidal and sporicidal, and thus is commonly employed for terminal decontamination in healthcare. Two varieties of H_2O_2 based systems are currently used: aerosolised H_2O_2 (aHP) systems and vapour-phase H_2O_2 (VPHP) systems.

aHP systems, such as the GLOSAIR^{TM} 400 system (ASP, 2015) and Oxy'Pharm Nocospray (Oxy'Pharm, 2021; Figure 2.3), produce a pressure-generated fine mist of 0.5-20 μm diameter droplets by aerosolising H_2O_2 (5-6%) with additives such as silver ions (<50 ppm) and deionised water (95%) (Otter *et al.*, 2019). A 6 mL m^{-3} dose cycle is recommended in hospital rooms, during which circulating electrically charged particles will adhere to and inactivate microorganisms in the air and on exposed surfaces (Fu *et al.*, 2012). The H_2O_2 decomposes naturally, and so aeration post-treatment is not typically required. The technology has demonstrated >3 $\log_{10}$ reductions in organisms isolated from ICU patients in <3 h (Herruzo *et al.*, 2014); however, there is concern regarding its efficacy given the ability of certain pathogens to produce catalase, which degrades H_2O_2. Kelly *et al*. (2022) found aHP systems reduced bacterial contamination within an ICU by 50.7%, however, other light-based methods achieved 96.8% reductions.

VPHP systems, including the Steris 1000ED mobile generator unit (STERIS, 2021a) and Bioquell L-4 mobile generator unit (Bioquell, 2021; Figure 2.4), deliver a heat-generated vapour of aqueous H_2O_2 through a high-velocity airstream to uniformly decontamination the air and surfaces within enclosed areas (Boyce, 2009; Fu *et al.*, 2012). Steris systems continually dehumidify the air and deliver a controlled concentration of dry VPHP without reaching the dew point; thus, ensuring vapour and/or toxic residues do not condense on surfaces (STERIS, 2021b). In contrast, Bioquell systems do not

incorporate prior dehumidification, and instead deliver VPHP at an uncontrolled concentration beyond the dew point until the enclosure becomes saturated and H_2O_2 begins to condense on surfaces (Otter *et al.*, 2019). VPHP systems have demonstrated >6 $\log_{10}$ reductions in nosocomial pathogens including *C. difficile* spores, MRSA, VRE, *A. baumannii* and SARS-CoV-2 surrogates (Otter and French, 2009; Berrie *et al.*, 2011; Barbut *et al.*, 2012; Goyal *et al.*, 2014). VPHP is more widely used for whole-room decontamination than aHP due to its higher penetrating power and distribution ability: Holmdahl *et al*. (2011) reported a single VPHP system was more effective than two aHP units; and Fu *et al*. (2012a) found VPHP safer and more efficient than aHP; with ≥2 $\log_{10}$ greater reductions in MRSA, *C. difficile* and *A. baumannii*.

Figure 2.3 aHP systems: (A) Glosair 400 and (B) OxyPharm Nocospray (ASP, 2015; Oxy'Pharm, 2021).

Figure 2.4 VPHP system: Bioquell L-4 mobile generator unit (Bioquell, 2021).

Although effective, H_2O_2 is extremely toxic due to its non-selective oxidising nature, and inhalation can irritate the nose, throat, respiratory tract and, in severe cases, cause bronchitis or pulmonary oedema. Decommission and adequate sealing of rooms is thus essential prior to treatment, with experienced operator supervision required throughout. Reported cycle times can be up to 8 h (Ray *et al.*, 2010),

which could potentially reduce admission capacity and prolong bed turn over time (Otter *et al.*, 2009), and is infeasible in wards which offer 24 h emergency care (Dancer, 2014). Using VPHP systems, H_2O_2 levels can reach >450 ppm (Murdoch *et al.*, 2016) – with short-term occupational H_2O_2 exposure limits being 2.0 ppm (HSE, 2020) – and thus aeration post-treatment to catalyse the conversion of VPHP into non-toxic by-products is essential (Hall *et al.*, 2007; Rutala and Weber, 2013). Efficacy has also shown to be impeded by residual debris and soft materials, with repeated use shown to encourage erosion of plastics and polymer surfaces (Dancer, 2014).

2.3.3.3 Chlorine Dioxide

Chlorine dioxide (ClO_2) is an EPA-registered steriliser which has recently been proposed for terminal cleaning given its ability to penetrate porous surfaces and diffuse rapidly within the air to reach areas which are difficult to clean manually (Health Protection Scotland, 2017b). It is highly potent and fast-acting against bacteria, viruses and fungi due to its ability to selectively attack cellular constituents (Jefri *et al.*, 2022): unlike other oxidisers, it does not react, or reacts very slowly, with the majority of organic compounds in living tissue; and instead oxidises a small number of amino acids and inorganic ions present in cellular proteins and peptides (Noszticzius *et al.*, 2013). As such, it demonstrates broad antimicrobial capabilities: Li *et al*. (2012) demonstrated 1.8-6.6 $\log_{10}$ reductions in *C. difficile* spores from six clinically-relevant materials within 3 h of treatment; Shirasaki *et al*. (2016) demonstrated complete inhibition of *S. aureus* and *Escherichia coli* growth from an 87 m^3 lab room following 2-3 h exposure; and clinically, Lowe *et al*. (2013) demonstrated 7-10 $\log_{10}$ reductions of nosocomial bacteria including *A. baumannii*, *E. coli*, and *S. aureus* from a patient care suite in a similar time frame. There are, however, limitations associated with its use: the gas is highly explosive, limiting its ability to be stored commercially (Jin *et al.*, 2009); as a potent oxidiser, rooms must be decommissioned/sealed, which, as discussed, can negatively impact healthcare delivery (Health Protection Scotland, 2017b); and it also induces material degradation/ corrosion unless employed at extremely low (<0.9 mg/m^3) concentrations (Ning *et al.*, 2020).

2.3.3.4 Ozone

Ozone (O_3) is highly unstable and is believed to induce oxidative damage – with a very high oxidation potential – to bacterial cell walls and cytoplasmic membranes (Boer *et al.*, 2006; Zoutman *et al.*, 2011)

and viral capsid proteins and nucleic acids (Tseng and Li, 2008). The technology is not yet widely used in clinical settings; however, its fast-acting antimicrobial efficacy has been demonstrated in the literature. Moat *et al*. (2009a) demonstrated its ability to inactivate clinically-relevant bacteria, including *S. aureus*, *E. coli*, *B. cereus* and *C. difficile* spores, by >3$\log_{10}$ in a small testing room in <1 h. More recently, an automated system achieved >4 $\log_{10}$ reductions of SARS-CoV-2 surrogates on room surfaces (Franke *et al.*, 2021). Its synergistic effect in combination with other established technologies has also been demonstrated: Zoutman *et al*. (2011) observed ≥6 $\log_{10}$ reductions of surface-seeded nosocomial bacteria in 90 min using 80-ppm ozone and 1% VPHP; and Liu *et al*. (2014a) found ozone and ultraviolet C (UV-C) irradiation together were significantly more effective at reducing *Aspergillus niger* spores in comparison to each technology alone. Despite its antimicrobial efficacy, there are limitations associated with its use. As a strong oxidiser, ozone is extremely toxic and can irritate and damage the respiratory tract (Health Protection Scotland, 2017c). Training and respiratory protective equipment is required for all operators, and rooms must be vacated, decommissioned and sealed during the procedure (Moccia *et al.*, 2020). To ensure no toxic residue remains prior to room recommission, a quench gas or scrubber is often required at the end of a treatment cycle (Moat *et al.*, 2009). Further, Doan *et al*. (2012) compared the effectiveness of eight disinfection methods and found ozone to be the most expensive – costing approximately £116 per use – rendering it infeasible for widespread application.

2.3.3.5 Cold Atmospheric Pressure Plasma

Cold atmospheric pressure plasma (CAPP) is an emerging technology with potential applications for environmental decontamination. CAPP consists of an assortment of charged particles, radicals (including atomic oxygen, ozone, superoxide and oxides of nitrogen), intense electric fields and UV radiation, which are typically generated in the air at room temperature via a plasma jet or dielectric barrier discharge (O'Connor *et al.*, 2014). This process often produces a combination of these elements, inducing microbial damage through various targets: positive and negative ions electrostatically disrupt bacterial cell walls; radicals etch cell walls, interfere with cellular transport and induce DNA lesions; intense electric fields induce electroporation; and UV radiation induces DNA and intracellular protein damage (Cahill *et al.*, 2014). The technology is effective for inactivation of vegetative and sporicidal bacteria, fungi and viruses. Although not yet clinically deployed, recent studies have indicated its

potential efficacy. Cahill *et al*. (2014) demonstrated 1.7-5 $\log_{10}$ reductions in nosocomial bacteria including MRSA, VRE, *E. coli* and *A. baumannii* on clinical surfaces following just a 1.5 min treatment. Zimmermann *et al*. (2011) demonstrated up to 6 $\log_{10}$ reductions and inhibited replication of human adenovirus, which is resistant to most disinfection procedures, in 4 min. More recently, CAPP systems have demonstrated the ability to inactivate SARS-CoV-2 droplets (2×10^5 PFU in 25 µL) deposited on various surfaces including plastic, metal and cardboard in ≤3 min when the device was held at a distance of 15 mm (Chen *et al.*, 2020). CAPP can be considered advantageous over other whole-room technologies given it leaves no harmful residues and can be applied at room temperature; however, further studies are required to assess its safety and scalability (O'Connor *et al.*, 2014).

2.3.3.6 Ultraviolet Light Systems

UV-C wavelengths in the region of 250-270 nm (peaking at 254 nm) are germicidal against nucleic acid-based pathogens (Cobb, 2016). These wavelengths are strongly absorbed by DNA/RNA base pairs and induce damage primarily through dimerization of pyrimidine molecules (Dai *et al.*, 2012b) which interrupts DNA replication, transcription and translation; compromising cellular function and leading to microbial cell death (Ploydaeng *et al.*, 2021). Due to its broad-spectrum antimicrobial nature, artificial UV-C light has been widely implemented for terminal room decontamination, using either continuous or pulsed UV-C light (Ploydaeng *et al.*, 2021).

Continuous Ultraviolet Light for Whole-Room Decontamination

Continuous UV (CUV) room decontamination typically uses either a monochromatic 254 nm low-pressure or a polychromatic medium pressure mercury lamp. The Tru-D Smart UVC device (Figure 2.5) – which pioneered clinical UV-C disinfection in 2007 and continues to be one of the most widely used today – is mobile, fully automated, calculates the precise dose required, and then achieves this from a single cycle and position (Tru-D, 2024), with a dose of 12 mJ cm^{-2} recommended for inactivation of vegetative bacteria and 22 mJ cm^{-2} recommended for bacterial spores (Mahida *et al.*, 2013). Its efficacy in eradicating nosocomial pathogens from exposed surfaces has been widely demonstrated: Rutala *et al*. (2010) demonstrated ≥99.8% reductions in vegetative bacteria and spores following 15 and 50 min of use, respectively; Nerandzic *et al*. (2010) demonstrated 93% reductions of MRSA and VRE and 80% reductions in *C. difficile* spores in isolation rooms following patient discharge but prior to

standard cleaning; and Mahida *et al*. (2013) reported ≥4 $\log_{10}$ reductions of VRE, MDR *Acinetobacter* spp. and *Aspergillus* spp. from intensive therapy units in <1 h; however, this was achieved on surfaces in direct sight of the device, and the system was less effective (1.7-2.3 $\log_{10}$ reductions) in shaded areas.

Figure 2.5 Tru-D Smart UVC device (Tru-D, 2024).

Pulsed Ultraviolet Light for Whole-Room Decontamination

To reduce risks associated with mercury, there has been interest in pulsed polychromatic xenon-based UV-C flashlamps which emits UV wavelengths (200-320 nm) in short and high energy pulses, resulting in faster and more ecological decontamination than CUV (Wang *et al.*, 2005; Jinadatha *et al.*, 2014). The Light Strike Germ-Zapping Robots produced by Xenex, for example, are 4300 times more intense than a mercury lamp (Xenex, 2022), which significantly shortens treatment: for a typical isolation room, complete decontamination can be achieved in 18 min (Jinadatha *et al.*, 2014). At a distance of 1 m in a laboratory room, the device has shown to induce 8.7-9.1 $\log_{10}$ reductions of *S. aureus*, *K. pneumoniae*, *A. baumannii* and *P. aeruginosa* in 5 min, and complete eradication (7.27 $\log_{10}$ reduction) of Ebola virus in 1 min (Stibich and Stachowiak, 2016). Simmons *et al*. (2021) demonstrated >4.1 $\log_{10}$ reductions of SARS-CoV-2 on laboratory surfaces within 5 min of use. Clinically, a 2 min cycle has shown to eliminate ≥70% more surface contamination in operating rooms than that achieved by manual cleaning alone (El Haddad *et al.*, 2017).

Far UV-C Light for Whole Room Decontamination

Clinical use of UV-C light is primarily limited to unoccupied environments due the hazardous carcinogenic and cataractogenic properties associated with 254 nm exposure of human skin and tissue

(Van Kuijk, 1991; Matsumura and Ananthaswamy, 2004). There has been recent interest in the use of far UV-C (200-230 nm) light for decontamination, which, compared to conventional UV-C light, possess similar germicidal properties owing to their similar mechanism of microbial inactivation (Dai *et al.*, 2012b); however, are less penetrative in biological materials (Brenner, 2022) and, given the size difference between microbial and mammalian cells (typically 0.1-1 μm versus >10 μm diameter), is less toxic to mammalian cells (Coohill, 1986; Hessling *et al.*, 2021). Far UV-C wavelengths can typically only reach the outermost stratum of the corneum layer of the skin epidermidis, which consists of dead keratinocytes that absorb the majority of the radiation (Hessling *et al.*, 2021); and the human eye tear layer absorbs radiation and shields the corneal epithelium from damage (Kaidzu *et al.*, 2019).

Such devices predominantly use 222 nm excimer lamps filled with Krypton-Chloride (KrCl) gas (Hessling *et al.*, 2021). These wavelengths have proven effective for inactivation of various MDR and susceptible bacteria and viruses on surfaces, in liquid suspension and in aerosols (Matafonova *et al.*, 2008; Wang *et al.*, 2010; Buonanno *et al.*, 2017, 2020; Welch *et al.*, 2018; Kitagawa *et al.*, 2021; Eadie *et al.*, 2022); with evidence suggesting they are just as germicidal as conventional UV, and more efficient for bacterial endospores (Narita *et al.*, 2020). Although promising, there is limited evidence of the antimicrobial efficacy of far UV-C within whole-room environments. Eadie *et al*. (2022) recently demonstrated for the first time the ability of far UV-C to inactivate aerosolised pathogens in a 32.3 m^3 bioaerosol chamber designed to replicate a realistic room environment by means of controlled air flow, temperature and humidity: five ceiling-mounted lamps reduced aerosolised *S. aureus* by 92% in just 15 min at intensities sufficiently lower that ICNIRP exposure limits, thus rendering it safe for human exposure. Further study to establish the efficacy of these wavelengths for whole-room decontamination is essential for these systems to be considered for widespread application.

2.3.3.7 Necessity for Alternative Methods

A summary of the whole-room decontamination technologies discussed in Sections 2.3.3.1-2.3.3.6 are presented in Table 2.3. Although undoubtably effective, these technologies are associated with limitations: the most prominent being that the majority are unsafe in the presence of room occupants, and thus are restricted to terminal cleaning applications. As such, there is a necessity for alternative methods of environmental decontamination which can be safely employed in occupied settings.

Table 2.3 Comparison of 'whole-room' decontamination technologies. Adapted from Maclean *et al.* (2015).

Decontamination Technology		Description	Operational Advantages	Operational Disadvantages
Gaseous Methods	Hydrogen Peroxide Vapour	A generator releases hydrogen peroxide which forms oxidising hydroxyl and ferryl free radicals and inactivates micro-organisms by penetrating cell walls and reacting with membrane lipids, proteins and nucleic acids to prevent proper function and halt replication and infection (Ali *et al.*, 2016).	• Broad antimicrobial efficacy • Effective for terminal decontamination • Decontamination achieved quickly • Effective for whole room decontamination of air and surfaces • Environmentally friendly	• Episodic use • Exposure is toxic to people • Rooms must be vacated, sealed and out of commission before use to prevent chemical exposure or leakage • Requires experienced operators and training • Rooms can quickly become re-contaminated • Risk of material damage • Requires active catalytic conversion to aid decomposition of hydrogen peroxide into non-toxic by-products
	Chlorine Dioxide Vapour	A generator releases chlorine dioxide vapour which inactivates micro-organisms by oxidising intracellular compounds and the membrane surface to disrupt cell metabolism. The direct reaction with disulphide bonds in the cellular amino acids and RNA halts replication and infection (Shirasaki *et al.*, 2016).	• Broad antimicrobial efficacy • Effective for terminal decontamination • Decontamination achieved quickly • Effective for decontamination of air and surfaces (including hard to reach areas)	• Episodic use • Exposure is toxic to people • Rooms must be vacated, sealed and out of commission before use to prevent chemical exposure or leakage • Requires experienced operators and training • Rooms can quickly become re-contaminated • Risk of material damage • Limited commercial storage due to explosive properties of chlorine dioxide
	Ozone	A generator releases gaseous ozone which inactivates micro-organisms by inducing oxidative damage to the cell wall and cytoplasmic membrane of bacteria and fungi and lipid peroxidation and subsequent lipid envelope and protein shell damage of viruses (Boer *et al.*, 2006; Murray *et al.*, 2008).	• Broad antimicrobial efficacy • Effective for terminal decontamination • Decontamination achieved quickly • Effective for whole room decontamination of air and surfaces	• Episodic use • Exposure is toxic to humans • Rooms must be vacated, sealed and out of commission before use to prevent chemical exposure or leakage • Requires experienced operators and staff training • Rooms can quickly become re-contaminated • Risk of material corrosion damage • Requires active catalytic conversion to aid decomposition
	CAPP	Release reactive oxygen and nitrogen species (e.g. $^1O_2$, O_3 and NO_2) which disrupt bacterial cell walls, viral capsids and damage nucleic acids (Cahill *et al.*, 2014).	• Broad antimicrobial efficacy • Effective for all surface types	• Episodic use • Safety implications are not yet established • Likely to require experienced operators and training • No established systems in place at present
	Steam Cleaning	Steam technology uses superheated dry steam (<140°C) delivered under pressure at a temperature sufficient to inactivate micro-organisms and loosen dirt and sticky oils from surfaces (Oztoprak *et al.*, 2019).	• Broad antimicrobial efficacy • Effective for terminal decontamination • Decontamination achieved quickly • Incorporates vacuum extraction to also remove dirt, water and contaminants	• Episodic use • Cannot be used in the presence of people • Disruptive to normal hospital routine • Rooms can quickly become re-contaminated • Cannot treat air and is ineffective for fabrics • Only accessible surfaces can be treated • Incompatible with sensitive electronic equipment
Light Methods	UV-Light	UV-light systems illuminate micro-organisms using either continuous or pulsed light sources within the UVC region (240-260 nm) and the absorption of these photons by DNA and RNA base pairs induces the formation of thymine dimers and other mutations which halt microbial replication (Sinha & Häder, 2002).	• Broad antimicrobial efficacy • Effective for terminal decontamination • Decontamination achieved quickly • Effective for whole room decontamination of air and surfaces • No production of toxic residues	• Episodic use • Uses radiation which is toxic to people – damaging to human skin and eye tissues • Rooms must be vacated and out of commission during treatment • Rooms can quickly become re-contaminated • Microbial resistance can develop to UV light illumination • Materials may become damaged by photosensitive degradation • Efficacy limited by short range of UV wavelengths

2.4 405-nm Light Environmental Decontamination System

To address current challenges associated with effectual decontamination of clinical environments, a novel disinfection technology, termed the 405-nm light EDS, has recently been developed. The antimicrobial nature of the 405-nm light EDS, discussed in greater depth in Section 2.4.3, is owed to its emission of violet-blue visible light wavelengths: exposure to these wavelengths, with peak activity at 405-nm, induces photoexcitation of porphyrin molecules within microbial cells resulting in the production of ROS which damage and inactivate microbes (Hamblin *et al.*, 2005; Maclean *et al.*, 2008a). This section provides an overview of the 405-nm light EDS with regard to its design, characteristics and efficacy in healthcare.

2.4.1 System Overview

The 405-nm light EDS was first developed at the University of Strathclyde as a means of providing continuous decontamination to the air and exposed surfaces within occupied environments (Anderson *et al.*, 2008). For clinical use, it is designed to be implemented as a complimentary disinfection approach used in conjunction with conventional infection control measures (Anderson *et al.*, 2008; Maclean *et al.*, 2010, 2013a; Bache *et al.*, 2012a). These ceiling-mounted light sources consist of a matrix of light emitting diodes (LEDs) which emit violet-blue visible light within a narrow spectral profile centred at 405-nm (Anderson *et al.*, 2008), blended with white LEDs to ensure that the illumination produced is predominantly white and blends with standard clinical room lighting systems (Maclean *et al.*, 2010). The system is designed to continuously emit low-irradiance violet-blue light across an approximate 10 m^2 area at irradiances of approximately 0.05-0.5 mW cm^{-2}; set, on the basis of extensive laboratory experiments and international safety guidelines, to stimulate significant bacterial inactivation at levels deemed safe for continuous human exposure (Anderson *et al.*, 2008; Bache *et al.*, 2012a; ICNIRP, 2013).

The EDS technology has since been licensed from the University of Strathclyde by a number of companies including Kenall Lighting, a major US lighting company, who have successfully marketed the technology under the brand name IndigoClean™. They have produced a range of products which incorporate the technology, from standard room to operating theatre lighting (Figure 2.6).

Figure 2.6 Commercial 405-nm light EDS in (A) antimicrobial blue only mode and (B) blended mode (Kenall Manufacturing, 2017).

2.4.2 Clinical Efficacy

The antimicrobial nature of 405-nm light is discussed comprehensively in Section 2.4.3; this section focuses primarily on studies which examine clinical efficacy of the 405-nm light EDS. In all cases, the system was employed as a complementary disinfection protocol in conjunction with standard cleaning.

Initial studies by Maclean *et al*. (2010) assessed levels of staphylococcal bacteria on frequently touched surfaces in a single-bed isolation room housing an MRSA-infected burns patient with two 405-nm light EDS installed and switched on for around 14 h/day. Findings indicated increasing reductions (56-86%) over 5 days of use and rising levels (≤126%) in the 6 days following use; confirming the recontamination effect post-treatment and the necessity for a continuous disinfection approach (Maclean *et al.*, 2010). Subsequently, Bache *et al*. (2012) evaluated its efficacy for reducing surface staphylococcal bacteria contamination in a single-bed isolation room housing a burns inpatient and a burns outpatient clinic. Inpatient studies demonstrated 27-75% reductions over 2 days of use, and outpatient studies demonstrated 61% reductions over an 8 h clinic; indicating the decontamination effect is neither patient nor room dependant (Bache *et al.*, 2012a). Efficacy has also been demonstrated in non-patient clinical areas, such as nurses' stations and preparation rooms, where surface contamination as high as 193 CFU plate^{-1} has been shown (Coyle *et al.*, 2011).

Maclean *et al*. (2013a) evaluated its efficacy in an occupied ICU isolation room for surface decontamination of both staphylococcal-type and total viable bacteria, to provide a broader overview of antimicrobial activity. Findings indicated 63-67% reductions in both following 2-5 days of use; with levels returning to pre-treatment and higher levels (≤375% increase) post treatment (Maclean *et al.*,

2013a). This study additionally found that, although reductions were greater on directly illuminated surfaces (63%), significant and uniform reductions were also achieved on indirectly illuminated surfaces (48%); indicating decontamination occurs throughout the room and not just on surfaces in close proximity (Maclean *et al.*, 2013a). Further, Bache *et al*., (2018) investigated the effects of irradiance and exposure time on staphylococcal contamination levels within an occupied burns isolation room: reductions were shown to cumulatively increase upon increasing exposure time, with 53, 69 and 86% reductions observed following 2, 4 and 6 days of use, respectively; however, no correlation was demonstrated between reductions and irradiance levels, with 50-100% reductions at each sampling site regardless of irradiance. The authors suggested, given light dose is a function of irradiance and exposure time, and the irradiances employed are so low (<1 mW cm^{-2}) whilst exposure times can span several days, it is possible that exposure time is more critical in the decontamination effect (Bache *et al.*, 2018a).

Kendall Manufacturing's IndigoClean™ is available in a multitude of fixtures which emit low levels of 405-nm light (0.1-0.2 mW cm^{-2}) to decontaminate surgical rooms, procedure rooms, patient bathrooms, ORs and healthcare pharmacies (Kenall Manufacturing, 2017). Its efficacy was first demonstrated by Sandhu *et al*. (2016), who observed 88.8% and 94.9% reductions (2456 to 275 and 14 CFU $plate^{-1}$, respectively) in *S. aureus* contamination on ICU surfaces following 2 and 3 weeks of use, respectively. Further, Sutton *et al*. (2016) investigated its efficacy within a level II trauma room - an environment which cannot easily be sealed and thus renders alternative 'whole-room' decontamination methods challenging – with results demonstrating reductions in mean bacterial counts across 15 weeks of use (24.5 to 5.2 CFU $plate^{-1}$) despite mean patient minutes in the room increasing (254 to 490); highlighting its efficacy even during periods of increased room activity. Rutala *et al*. (2018) demonstrated its ability to reduce surface-seeded MRSA, VRE and MDR *Acinetobacter* by ≤90% in 24 h exposure to irradiances of 0.3-0.4 mW cm^{-2}. In a randomised control trial, Warren *et al*. (2020) demonstrated that installation of the system resulted in fewer pathogens within wound/pulmonary outpatient clinics; however, no reductions in contamination levels were presented by the end of each clinic day. It should be noted, however, that contamination levels within clinics substantially increased throughout the day (≤87%), and thus longer exposures may be necessary to achieve adequate decontamination (Warren *et al.*, 2020).

Although these studies have successfully demonstrated reductions in environmental contamination, infection prevention guidelines do not currently include the use of no-touch disinfection technologies,

such as the 405-nm light EDS, primarily due to a lack of evidence to demonstrate ensuing reductions in HAI development (Health Protection Scotland, 2017a). Recently, however, Murrell *et al*. (2019), assessed the efficacy of a 405-nm light EDS for reduction of bacterial surface contaminants within an orthopaedic OR, and its subsequent impact on SSI rate for procedures performed in the year therein. After one year of use, bacterial counts were reduced by 81% and SSI rates reduced from 1.4% in the year pre-installation to 0.4% in the year post-installation (Murrell *et al.*, 2019); proving its efficacy at both reducing environmental contamination levels and subsequent HAI rates, which is the ultimate goal of any environmental disinfection strategy. Further, the authors noted that this effect extended into an adjacent OR, where bacterial levels were reduced by 49% and SSI rates reduced from 1.2% to 0.3%; believed to be due to the positioning and shared air circulatory system between the two OR's, suggesting the system's efficacy for inactivation of airborne bacteria (Murrell *et al.*, 2019). Although promising, further exploration into this effect will be crucial in its widespread implementation.

2.4.3 Antimicrobial Mechanism of Action

Violet-blue visible light induces microbial inactivation using mechanisms analogous to photodynamic therapy (PDT); a treatment modality in which a light-activated chemical substance, termed a photosensitiser, and low intensity visible light, of specific wavelength, are combined in the presence of oxygen to produce cytotoxic species which induce localised destruction of a target cell or organism (Hamblin and Hasan, 2004). PDT was first reported by Raab (1900), who discovered the lethal combined effects of acridine red and visible light on *Paramecium caudatum*; with ensuring studies discovering the necessity of oxygen in the process (von Tappeiner, 1904). However, PDT for antimicrobial purposes was not widely implemented until the 1990's – instead emerging as a malignancy treatment – when it was realised that the "antibiotic era" was under serious threat (Jori *et al.*, 2006). Compared to conventional antibiotics, PDT is an advantageous alternative: it is non-specific and so one photosensitiser can act on various microorganisms; efficacy is independent of microbial resistance patterns, with an improbability of resistance development; it has high selectively for hyperproliferating cells including microbes; and its effects are localised, minimising damage to host tissue and/or mutagenesis (Nitzan *et al.*, 1992; Cassell and Mekalanos, 2001; Jori *et al.*, 2006). Traditionally, PDT employs non-toxic chemical dyes, porphyrins or chlorophylls as photosensitisers, which are delivered to a specific area and illuminated at the required wavelength to elicit cell damage

(Allison *et al.*, 2004). Those presently employed include halogenated xanthene's, such as Rose Bengal, phenothiazinium dyes, such as toluidine blue, and porphyrin derivatives, such as hematoporphyrin (Wilson and Yianni, 1995; Wainwright, 1998; Bertoloni *et al.*, 2000; Tanielian *et al.*, 2000). It is essential that these agents demonstrate high tissue selectivity, to minimise host cell damage; are adequately small/ soluble to penetrate membranes; demonstrate rapid clearance from normal tissues to minimise phototoxic side effects; possess a substantial triplet quantum yield to maximise ROS production; and are relatively cheap/ easy to mass manufacture (Abrahamse and Hamblin, 2016).

Research over the last 20 years, however, has indicated photosensitive additives are not necessarily required for PDT, and that violet-blue visible light possess the ability to excite naturally occurring intracellular photosensitive molecules, namely porphyrins, within microbial cells (Papageorgiou *et al*., 2000; Ashkenazi *et al*., 2003; Hamblin *et al*., 2005; Maclean, 2006; Guffey and Wilborn, 2007).

2.4.3.1 Porphyrins and the Photodynamic Inactivation Process

Porphyrins are highly pigmented organic compounds which occur naturally in both prokaryotic and eukaryotic cells and are fundamental to various biological processes including oxygen transport, electron transport, photosynthesis, pigmentation changes and catalysis reactions (Goldoni, 2002). They each consist of a basic organic porphine macrocyclic ring framework (Figure 2.7), with specific type and function derived from side-chain substitution of porphine at the methine bridges (positions 5, 10, 15 and 20) or exposed pyrrole regions (positions 1, 4, 6, 9, 11, 14, 16 and 19) with non-hydrogen atoms or groups (Lesage *et al.*, 1993; Milgrom, 1997; Josefsen and Boyle, 2008).

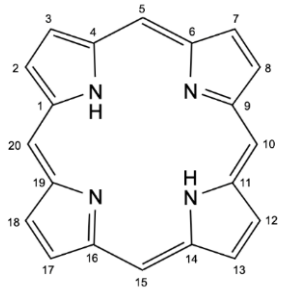

Figure 2.7 Molecular structure of porphine ($C_{20}H_{14}N_4$) which consists of a 16-atom ring containing four nitrogen atoms obtained by linking four pyrrole sub-units with four methine bridges (Josefsen and Boyle, 2008).

Porphyrins present distinctive absorption characteristics in the ultraviolet-visible (UV-Vis) spectrum (Figure 2.8). Maximum absorption, termed the Soret band, is demonstrated at approximately 400 nm,

and four weaker absorptions, termed the Q bands (I, II, III and IV), are demonstrated at approximately 450-700 nm (Goldoni, 2002; Josefsen and Boyle, 2008). The relative intensities and wavelengths of each are associated with the type and position of porphine substituents (Giovannetti, 2012).

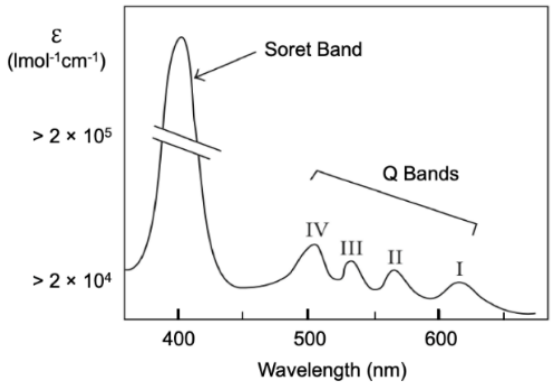

Figure 2.8 UV-Vis absorption spectrum of porphyrins. Adapted from (Josefsen & Boyle (2008).

Absorption of 405-nm light induces photoexcitation of porphyrin molecules within microbial cells, which inaugurates a sequence of actions to produce ROS and ultimately results in microbial cell death (Hamblin *et al.*, 2005; Maclean *et al.*, 2008a). The ability of endogenous porphyrins to act as photosensitisers eliminates the requirement for chemical additives, required in traditional PDT, to actuate microbial inactivation. This mechanism of photoexcitation (Figure 2.9) is described as follows.

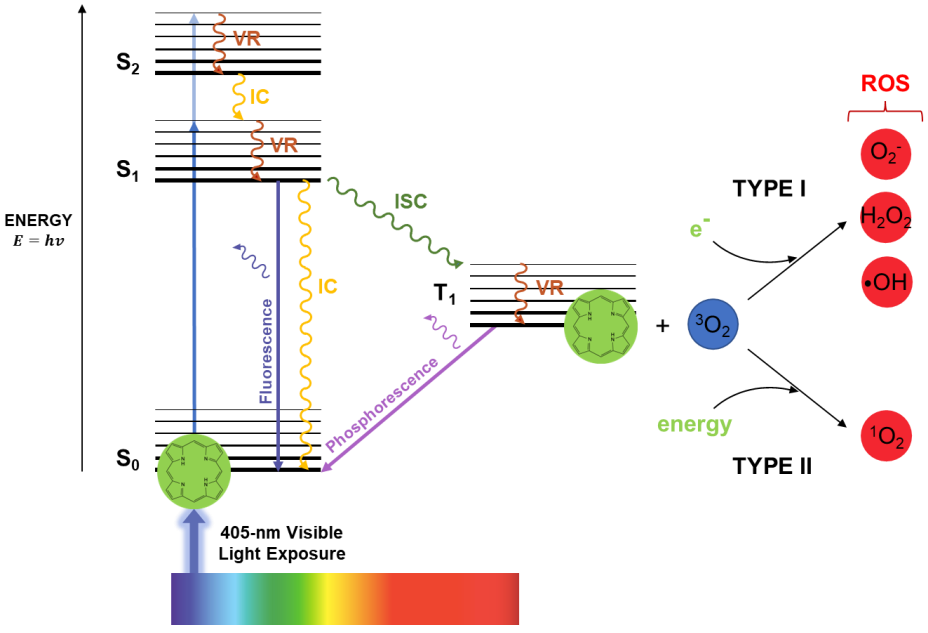

Figure 2.9 Jablonski diagram demonstrating the photoexcitation of endogenous porphyrins upon 405-nm light. Straight arrows represent radiative energy transitions; curved arrows represent non-radiative energy transitions. VR: vibrational relaxation; IC: internal conversion; ISC: intersystem crossing.

In their natural ground singlet state (S_0), porphyrins have a stable electron configuration comprising two unpaired electrons in its outermost electron orbitals with opposite spin bearing null net angular momentum (Vatansever *et al.*, 2013). Absorption of a violet-blue light photon provides sufficient quantum energy to transport a porphyrin electron from its ground state to one of many unstable and short-lived excited singlet states ($S \geq 1$) (Dai *et al.*, 2012a). Exposure to approximately 400 nm results in strong electron transmission from S_0 to S_2, giving rise to the Soret band; and photo-stimulation at approximately 450-700 nm results in weaker transmission from S_0 to S_1, giving rise to Q bands (Goldoni, 2002; Josefsen and Boyle, 2008; Dai *et al.*, 2012a). With an electron in an excited singlet state, porphyrins will rapidly endeavour to lose this excess energy and return to S_0 in order to regain stability (Abrahamse and Hamblin, 2016). If in a high vibrational level of an excited state, the electron will fall to the energetically lowest level of that state through vibrational relaxation (VR); releasing heat to its surroundings (Plaetzer *et al.*, 2009). If elevated to an excited singlet state more energetic than S1, the electron will fall to lower energetic states by internal conversion (IC); similar to VR, releasing heat to the surroundings (Plaetzer *et al.*, 2009). When at the energetically lowest level of S_1, the porphyrin will partake in one of three energy-releasing mechanisms: the electron may return to S_0 by fluorescence, which involves energy release through secondary photon emission of lower energy (approximately 630 nm) than that used for photoexcitation; the electron may return to S_0 by IC; or, most importantly for cellular inactivation (Dai *et al.*, 2012a; Vatansever *et al.*, 2013), the electron may participate in intersystem crossing (ISC), which involves spin reversal of the excited electron and subsequent transportation from S_1 to its triplet excited state (T_1) (Plaetzer *et al.*, 2009; Abrahamse and Hamblin, 2016).

In T_1, the spin reversal of the excited electron produces parallel spin to its former paired electron, and net angular momentum is no longer equal to zero (St. Denis *et al.*, 2011a) . As such, the electron is not permitted to immediately decay to its ground state: the molecule will have identical quantum numbers to that of its paired electrons; violating the Pauli Exclusion Principe (Frenkel, 1930). Accordingly, the electron can either: change its spin orientation, which is a relatively slow process, and return to S_0 through photon emission (phosphorescence); or interact with molecules abundant in the immediate environment (Dai *et al.*, 2012a). Although less energetic than S_1, T_1 is much more stable and provides a significantly longer lifespan (microseconds versus nanoseconds) for molecular interaction (Dai *et al.*,

2012a). Based on the selection rules, which specify that triplet-triplet interactions are permitted whilst triplet-singlet interactions are forbidden (Frenkel, 1930), porphyrin in T_1 can readily interact with molecular oxygen ($^3O_2$), which, uniquely, is one of few molecules inherently found as a triplet in its ground state (Dai *et al.*, 2012a).

The interaction of porphyrins with $^3O_2$ is crucial to the production of ROS, which comprise superoxide ($O2^{\bullet-}$), H_2O_2, hydroxyl radical (●OH) and singlet oxygen ($^1O_2$). ROS are natural by-products of cell activity and, at low levels, have important roles in cell signalling pathways, including aerobic respiration, metabolism and redox homeostasis, and are vital for cell survival, apoptosis and differentiation (Dröge, 2002; Bae *et al.*, 2011). Cellular antioxidant defence mechanisms have evolved to neutralise low level ROS; however, when produced in excess, ROS can overwhelm these systems and induce oxidative stress, which can damage cellular components and ultimately lead to cell death (Ray *et al.*, 2012; Vatansever *et al.*, 2013). In T_1, porphyrins can readily interact with $^3O_2$ to produce ROS by one of two photooxidative reaction pathways.

Type I pathway involves electron/hydrogen atom transfer from porphyrin in T_1 to $^3O_2$ to produce $O2^{\bullet-}$ (Plaetzer *et al.*, 2009). $O2^{\bullet-}$ is not particularly reactive, inducing limited oxidative damage alone; however, it can react with itself through dismutation, catalysed by superoxide dismutase (SOD), to yield H_2O_2; which again is not particularly reactive, however, in the presence of $O2^{\bullet-}$, produces extremely reactive ●OH via the Haber-Weiss and/or Fenton reaction (Castano *et al.*, 2004; Plaetzer *et al.*, 2009). Type II pathway involves transfer of excitation energy, as opposed to electrons, from porphyrin in T_1 to $^3O_2$. This inverses the spin of an outermost electron of $^3O_2$, resulting in the production of $^1O_2$ which, due to its electron configuration instability, is extremely short-lived and reactive (St. Denis *et al.*, 2011a).

Both pathways occur concurrently and in competition, with the relative proportions of each thought to be dependent on photosensitiser structure and micro-environment (Plaetzer *et al.*, 2009). Production of ROS is mechanically simpler via the Type II pathway (Vatansever *et al.*, 2013), and porphyrins composed of a tetrapyrrole framework tend to predominantly produce Type II $^1O_2$ over Type I ROS (Abrahamse and Hamblin, 2016). ROS-induced cellular damage is strictly localised given the short half-

life (nanoseconds) and diffusion distance (20 nm) of ROS; providing a 'therapeutic window', whereby microbial cells can be destroyed without damaging adjacent cells (Moan, 1990).

2.4.3.2 Oxidative Damage

Given its non-specific nature, overproduction of ROS, generated during the violet-blue light photodynamic inactivation process, can induce a wide range of damage to microbial cells. This section provides an overview of the current understanding of the cellular targets and the damage induced by violet-blue light exposure.

Early studies by McKenzie *et al*. (2016) indicated exposure to 405-nm light (65 mW cm^{-2} for ≤180 min) reduced the membrane integrity of both *S. aureus* and *E. coli*, based on observations of a loss of salt and bile tolerance and an increase in release of nucleic acid material into the extracellular matrix of both species upon exposure. Later studies similarly concluded that the cellular membrane was a key target in violet-blue light inactivation, with evidence of increasing membrane permeability, loss of efflux activity, changes in transmembrane potential and polarisation in various bacterial species (Biener *et al.*, 2017; Kim and Yuk, 2017; Chu *et al.*, 2019; Jeffet *et al.*, 2020; Kim and Kang, 2021; dos Anjos *et al.*, 2023). Of these, Biener *et al*. (2017) observed that, for MRSA exposure to 405-nm light (135 mW cm^{-2} for ≤30 min), membrane damage occurred drastically within the first 5 min and then continued slowly as exposure time increased; suggesting damage induced on membranes is immediate. Interestingly, dos Anjos *et al*. (2023) indicated, upon exposing *S. aureus*, *E. coli* and *P. aeruginosa* to 410-nm, sublethal doses induced measurable membrane permeabilization in the Gram-negative species, however much higher doses were required for this same effect in *S. aureus* (45.8 versus 549.6 J cm^{-2}); suggesting damage is likely dependent on species-specific variances in antioxidant/ DNA repair mechanisms.

Damage to bacterial DNA has also been found following 405-nm light inactivation, with previous studies indicating increasing DNA oxidation levels, disorganisation of chromosomes and ribosomes, A-DNA cleavage and DNA fragmentation upon exposure (Bumah *et al.*, 2013; Kim and Yuk, 2017; Djouiai *et al.*, 2018; Jeffet *et al.*, 2020; dos Anjos *et al.*, 2023). dos Anjos *et al*., (2023) indicated differences in the extent of DNA damage in different species: using doses ≤366.5 J cm^{-2}, known to induce complete inactivation, significant levels of DNA degradation were demonstrated in both *S. aureus* and *E. coli*, but none was demonstrated in *P. aeruginosa*. The authors suggested this may be due

to damage instigated upon the membrane of *P. aeruginosa* upon these exposures, which likely mitigated damage to DNA given the short lifetime of ROS: DNA is robust, and sustained ROS production is likely required to elicit damage (dos Anjos *et al.*, 2023). Djouiai *et al*. (2018) observed DNA is a major target in sporicidal bacteria.

Bacterial lipids have also shown to be cellular targets in blue-light mediated inactivation, with previous studies indicating that lipid peroxidation, particularly towards unsaturated fatty acids, are associated with cellular inactivation (Chu *et al.*, 2019; dos Anjos *et al.*, 2023). Further, Fila *et al*. (2017) demonstrated, for the first time, lethal 405-nm light exposure can inactivate multiple virulence factors of *P. aeruginosa*; and Kim and Kang (2021) indicated 405-nm light exposure results in a loss of cellular respiratory activity. Together, these studies demonstrate that damage induced by violet-blue light likely involves multiple cellular components, with many likely being targeted at any given time.

2.4.3.3 Antimicrobial Efficacy

Violet-blue light within the region of 405-nm demonstrates widespread antimicrobial efficacy towards various micro-organisms, including bacteria, fungi and viruses, presented in liquid suspension, on surfaces and in aerosols (Maclean *et al.*, 2008a, 2008b, 2009, 2013b; Murdoch *et al.*, 2010, 2012, 2013; Endarko *et al.*, 2012; McKenzie *et al.*, 2013, 2014; Tomb *et al.*, 2014, 2017b; Moorhead *et al.*, 2016a; Dougall *et al.*, 2018). Given the context of this thesis, its antibacterial and antiviral efficacy will be discussed in the following sections.

Bacterial Inactivation

The ability of violet-blue light to inactivate bacteria without requiring external photosensitisers was initially observed in *Helicobacter pylori, Propionibacterium acnes, S. aureus* and *P. aeruginosa* (Papageorgiou *et al*., 2000; Ashkenazi *et al*., 2003; Hamblin *et al*., 2005; Maclean, 2006; Guffey and Wilborn, 2007); theorised to be due to the presence of photosensitive porphyrins within exposed bacteria. Maclean *et al.* demonstrated that, within the visible spectrum, greatest antibacterial activity occurs at 405 ± 10 nm (Maclean *et al.*, 2008a) and that the presence of oxygen is essential for the photoinactivation process (Maclean *et al.*, 2008b). Multiple studies have since confirmed the presence of endogenous porphyrins at levels sufficient to elicit inactivation in numerous HAI-associated bacteria (Dai *et al.*, 2013b; Zhang *et al.*, 2014, 2016; Kumar *et al.*, 2015; Wang *et al.*, 2016), and violet-blue

light inactivation of a broad-spectrum of HAI-inducing bacterial species, including ESKAPE pathogens, has been demonstrated (Guffey and Wilborn, 2006; Enwemeka *et al.*, 2008; Maclean *et al.*, 2008a, 2009; Hoenes *et al.*, 2021; Amodeo *et al.*, 2022).

This broad-spectrum efficacy is believed to be primarily due to the non-selective and non-specific nature of damage incited by ROS (Maisch, 2015). Unlike antibiotics, which act specifically towards one cellular target (Maisch, 2009), the photo-destructive oxidative burst following 405-nm light exposure produces ROS which pervade bacteria and induce damage to various targets in a way that is not conducive to bacterial survival or resistance development (Maclean *et al.*, 2014). As such, successful inactivation of MDR bacteria, including MRSA, *A. baumannii*, *K. pneumoniae* and β-lactam resistant *E. coli*, has been demonstrated (Maclean *et al.*, 2009; Barneck *et al.*, 2016; Halstead *et al.*, 2016).

The efficacy of 405-nm light inactivation is thought to be dependent on species-specific differences in the distribution and quantity of porphyrins produced by bacteria (Nitzan *et al.*, 2004; Maclean *et al.*, 2009; Kumar *et al.*, 2015). Coproporphyrin III, protoporphyrin IX and uroporphyrin III are considered primarily responsible for inactivation (Ashkenazi *et al.*, 2003; Feuerstein *et al.*, 2005; Maclean *et al.*, 2008a, 2008b; Dai *et al.*, 2013b); with coproporphyrin most significant as it produces the majority of free radicals. Whilst examining inactivation of bacteria pre-treated with δ-aminolaevulinic acid (δ-ALA) – a naturally occurring metabolite which increases uroporphyrin, coproporphyrin and protoporphyrin production through the heme synthesis pathway (Kennedy and Pottier, 1992) – and exposed to 407-420 nm light, Nitzan *et al*. (2004) found, although total porphyrin content was higher in Gram-negative bacteria than the staphylococcal strains investigated, the coproporphyrin content of staphylococcal strains was approximately 3 orders of magnitude greater, and exposure to 100 J cm^{-2} decreased cell viability by approximately 5 orders of magnitude greater, than that of the Gram-negative bacteria. More recently, Kumar *et al*. (2015) found coproporphyrin to be approximately 3 orders of magnitude higher in Gram-positive species compared to Gram-negative species examined; and exposure to 360 J cm^{-2} achieved 1.9-4 log_{10} reductions in Gram-positive species, compared to 0-0.6 log_{10} reductions in Gram-negative species. However, no correlation was found between coproporphyrin content and inactivation efficacy within bacterial classes: for Gram-positive, coproporphyrin was significantly higher in *B. cereus* compared to *S. aureus*, yet *S. aureus* inactivation was higher; for Gram-negative, coproporphyrin was significantly lower in *E. coli* than in *S. typhimurium*, yet *E. coli*

demonstrated higher inactivation (Kumar *et al.*, 2015); suggesting other cellular factors are also likely to be influential. Certain species-specific structural differences in the cell envelope, for example, have shown to protect against light penetration (Murdoch *et al.*, 2012). Further, bacterial endospores, although successfully inactivated by 405-nm light, require higher doses than their vegetative equivalent, which is proposed to potentially be due to reduced levels of heme proteins – which are members of the porphyrin family – in the former (Abad-Lozano and Rodriguez-Valera, 1984; Maclean *et al.*, 2013b).

Viral Inactivation

Given their lack of endogenous porphyrins, the mechanism of 405-nm light viral inactivation is yet to be fully understood; however, recent studies have indicated that viral inactivation by 405-nm light is still possible in the absence of external photosensitisers. Proof of concept results demonstrated the ability of 405-nm light to inactivate *Streptomyces* bacteriophage ϕC31, as a surrogate for non-enveloped double-stranded DNA viruses (Tomb *et al.*, 2014), and feline calicivirus (FCV), as a model for norovirus (Tomb *et al.*, 2017b). In both cases, enhanced susceptibility to light treatment (88-89% less dose required for 1 $\log_{10}$ reductions) was demonstrated when microbes were exposed in nutrient-rich/biologically-relevant media as opposed to minimal suspensions; likely owing to the fact that the latter typically contains constituents predisposed to 405-nm light photosensitisation, such as mucins present within saliva, and thus can aid in the inactivation effect by impacting local oxidative damage to fundamental structures in the bacteriophage or virus (Tomb *et al.*, 2014, 2017b).

The lower susceptibility of ϕC31 and FCV in minimal media was therefore likely due to the absence of photosensitisers within viral structures; however, viral reductions were still observed, suggesting inactivation in these cases was likely due to a differing mechanism (Tomb *et al.*, 2014, 2017b). Inactivation may be due to the low-level UV-A exposure at the tail end of the 405-nm LED emission spectrum (Tomb *et al.*, 2014, 2017b), which, over extended periods, will likely cause an extent of oxidative damage to viral/phage proteins (Girard *et al.*, 2011); or due to the small portion of 420-430 nm light exposure in the 405-nm LED emission spectrum, which has previously shown to induce damage to the virion-associated reverse transcription complex of murine leukaemia virus upon extended exposure (Richardson and Porter, 2005).

As expected, viruses and bacteriophages are less susceptible to 405-nm light inactivation than vegetative bacteria, with a recent review article highlighting that, from data analysed from 79 sources, the mean dose of 380-420 nm light required for a 1 $\log_{10}$ reduction is in the region of 100 J cm^{-2} for bacteria; with up to 1 kJ cm^{-2} required for viruses and bacteriophage (Tomb *et al.*, 2018). Despite this, inactivation of various HAI-relevant viruses, such as HIV, adenovirus and norovirus, upon violet-blue light exposure has since been demonstrated (Kingsley *et al.*, 2017; Terrosi *et al.*, 2021; Ragupathy *et al.*, 2022). Further, given the relevance of the COVID-19 pandemic, there has been a recent upsurge in research which has demonstrated its ability to inactivate SARS-CoV-2 or appropriate surrogates (Biasin *et al.*, 2021; Enwemeka *et al.*, 2021; Gardner *et al.*, 2021; Lau *et al.*, 2021; Rathnasinghe *et al.*, 2021; Vatter *et al.*, 2021; Singh *et al.*, 2023). Recent studies have additionally indicated an enhanced susceptibility of enveloped versus non-enveloped viruses to 405-nm light inactivation; suggesting the lipid envelope may be capable of instigating damage (Rathnasinghe *et al.*, 2021).

2.4.4 Benefits of the 405-nm light EDS

The 405-nm light EDS offers an effective and safe alternative to clinical environment decontamination due to various unique attributes.

Safety Profile

The wavelengths employed are antimicrobial against towards various HAI-inducing pathogens (Maclean *et al.*, 2008a, 2009, 2013b; Murdoch *et al.*, 2012; Halstead *et al.*, 2016; Moorhead *et al.*, 2016a; Tomb *et al.*, 2017b), without chemical additives. Furthermore, recent studies have indicated a higher sensitivity of bacterial cells to 405-nm light inactivation than mammalian cells, meaning 405-nm light can be employed at bactericidal levels without harming human tissue (McDonald *et al.*, 2011; Dai *et al.*, 2013a, 2013b; Ramakrishnan *et al.*, 2014). This is particularly advantageous over gaseous technologies previously discussed, which are often limited by the release of harmful gas/vapours. Further, compared to UV light, 405-nm light is of much lower photon energy and, although less germicidal – requiring doses in the order of joules compared to millijoules to achieve inactivation – it is not associated with detrimental effects affiliated with UV exposure, which include long-term material degradation and radiative effects to the human eye/skin (Van Kuijk, 1991; Matsumura and Ananthaswamy, 2004; Andrady *et al.*, 2023). Violet-blue light is intrinsically safe for human exposure,

with irradiances using in the EDS selected in harmonisation with relevant international safety guidelines (Anderson *et al.*, 2008; ICNIRP, 2013). The light levels employed render negligible superficial effects on commensal skin microflora, as they are unable to penetrate to the depth of the sebaceous glands and hair follicles where these microbes reside (Maclean *et al.*, 2013a); and are considerably lower than blue light wavelengths known to negatively impact human health, which is typically around 440-nm (photo retinitis) and 460-480-nm (mood and circadian rhythm) (Lockley *et al.*, 2003; Maclean *et al.*, 2014).

Continuous Decontamination Effect

The ability to induce microbial inactivation at levels inherently safe for human exposure enables the system to advantageously be used continuously in the presence of room occupants. The 405-nm light EDS can safely, automatically and unobtrusively provide a unique continuous decontamination effect on the air and exposed surfaces in the presence of hospital staff, patients and visitors (Maclean *et al.*, 2010). Rooms do not require vacation prior to cleaning, which is both time/expenses saving and limits interruption to regular hospital activities or patient care. Further, the shedding of organisms suspended in the air and precipitated on surfaces can be addressed in real-time and between manual cleaning, which is particularly useful during periods of intense room activity, such as bed/ dressing changes and visiting times, which are associated with high bacterial transmission (Maclean *et al.*, 2013a; Dougall *et al.*, 2019). This combination of attributes enables the technology to uniquely and safely lower levels of microbial contamination within healthcare settings in efforts to minimise the risk of HAI acquisition.

Unlikelihood of Pathogen Tolerance

The misuse and overuse of antibiotics is a key driver in the emergence of MDR strains and, given the limited pipeline of antibiotic production, it is essential that novel antimicrobials with a limited likelihood of tolerance development are established (WHO, 2021a). Conventional antibiotic treatments act specifically on one distinct subcellular target through the ‘key-hole’ principle and bacteria have thus developed mechanisms to resist these specific damage approaches (Maisch, 2009; Reygaert, 2018). By contrast, violet-blue light employs a non-selective and multi-targeted damage approach in which no specific porphyrin-receptor interactions are necessary and no specific target structures are the focus of the oxidative burst (Maisch, 2015). Light-induced ROS instead pervade the pathogen and incite damage

upon various cellular structures (Maclean *et al.*, 2014), thus making it more difficult for resistance to develop.

Several studies have demonstrated an unlikelihood for bacteria to develop resistance towards 405-nm light exposure, primarily by exposing bacteria to repeated sub-lethal light treatments and reporting no change in the subsequent susceptibility of bacteria to inactivation (Zhang *et al.*, 2014; Amin *et al.*, 2016; Tomb *et al.*, 2017a; Leanse *et al.*, 2018; Wang *et al.*, 2019). Following 10 cycles of sub-lethal blue light exposure (14.6-20 mW cm^{-2}) and culture, Zhang *et al*. (2014) demonstrated an increase in susceptibility of MDR *A. baumannii* to treatment and Amin *et al*. (2016) demonstrated no change in susceptibility of MDR *P. aeruginosa* to treatment. Tomb *et al*. (2017a) exposed MSSA and MRSA to 15 cycles of sub-lethal 405-nm light (180 J cm^{-2}; 60 mW cm^{-2}) and found no significant difference ($P>0.05$) between reductions achieved before (1.3 $\log_{10}$) and after cycles (1.2-1.4 $\log_{10}$), and minimal impact on antibiotic susceptibility.

There have, however, additionally been reports of the potential for bacteria to develop tolerance towards violet-blue light, with evidence of decreased efficacy following repeated sub-lethal exposures (Guffey *et al.*, 2013; Rapacka-Zdonczyk *et al.*, 2019, 2021; Kruszewska-Naczk *et al.*, 2023). Bacterial cells have developed several mechanisms to overcome oxidative stress within their immediate environment (Casas *et al.*, 2011). ROS production is antagonised by various cellular antioxidant defence mechanisms, including the glutathione system, SOD, catalase, peroxidase and lipoamide dehydrogenase, which are up-regulated in response to oxidative stress to detoxify ROS (Maisch, 2015). Also upregulated are antioxidant enzymes, such as tryptophan and cysteamine, which aid in ROS quenching and detoxification (Henderson and Miller, 1986; Wang *et al.*, 2001); RpoH sigma factor, which stimulates expression of defence factor proteins involved in ROS quenching and detoxification (Braatsch *et al.*, 2004); and heat shock proteins, which are responsible for various cytoprotective mechanisms including acting as intra-cellular chaperones for other proteins, folding and assisting in protein conformation, preventing unwanted protein aggregation and helping to stabilise partially unfolded proteins (Rodríguez *et al.*, 2016). Useful at low oxidative stress levels, these cellular responses are often limited as oxidative stress increases to levels beyond their capacity for recovery (Kessel and Oleinick, 2009). Further, it typically takes 5-10 min for such cellular responses to commence (Wolf *et al.*, 2008), and so often irreversible cellular damage will have already occurred within this time. When ROS generation is

sufficiently high, fundamental defence protein levels will be insufficient to scavenge ROS and bacteria are unlikely to survive. These mechanisms suggest an unlikelihood that bacteria will develop resistance to 405-nm light induced ROS production. Although studies have indicated tolerance formation is possible, it is important to note that resistance formation to violet-blue light has yet to be described. It should, however, be considered that a balance likely exists between 405-nm light inactivation and ROS-mediated responses, and thus further work in this area is essential to fully understand the mechanism.

2.5 Overall Summary and Research Aims

This literature review has comprehensively examined issues associated with contamination of clinical environments, the subsequent spread of nosocomial infections, current methods of environmental decontamination, the novel 405-nm light EDS, and key fundamental concepts associated with antimicrobial 405-nm light exposure. The antimicrobial nature of 405-nm light is still a relatively recent scientific discovery and there are still various aspects which require further research. This thesis aims to generate important novel information on 405-nm light technology, with specific regard to its use at low irradiance levels for environmental decontamination applications, by investigating aspects of its fundamental photochemical inactivation mechanism. To achieve this, the following chapters will investigate low irradiance 405-nm light at levels analogous to that employed for environmental decontamination in terms of:

(1) broad-spectrum antibacterial efficacy;
(2) key operational considerations associated with practical clinical implementation;
(3) germicidal efficacy and mechanisms of inactivation, in comparison to that of higher irradiance exposures on a per-unit-dose basis; and,
(4) antiviral efficacy against a SARS-CoV-2 surrogate.

Collectively, these studies seek to advance current knowledge of this emerging technology and further its development for environmental decontamination applications, and the motivations for each are discussed in the relevant chapters.

CHAPTER 3

General Methodology

3.0 Overview

This chapter provides detail of the general methodologies required for the experimental work conducted throughout this thesis. This includes details of the microbiological cultivation and handling techniques, the optical light sources employed, and the data and statistical analysis techniques. Specific detailed protocols used for experiments are provided in subsequent chapters.

3.1 Bacterial Methodology

This section provides details of the methods required to cultivate, maintain, prepare and enumerate bacteria used for light exposure experiments.

3.1.1 Bacterial Strains

The bacterial strains employed for experimental testing throughout this thesis and their optimal growth conditions are presented in Table 3.1.

Table 3.1 Bacterial strains employed in this thesis and their associated culture requirements. [TSB: Tryptone Soya Broth; TSA: Tryptone Soya Agar; NB: Nutrient Broth; NA: Nutrient Agar. Sourced from Oxoid Ltd., UK]

Bacterial Strain	**Collection No.**	**Culture Medium**	**Culture Temp. (°C)**
Enterococcus faecium	LMG 11423	TSB/TSA	37
Staphylococcus aureus	NCTC 4135	NB/NA	37
Klebsiella pneumoniae	NCTC 9633	NB/NA	37
Acinetobacter baumannii	NCTC 12156	NB/NA	37
Pseudomonas aeruginosa	LMG 9009	NB/NA	37
Enterobacter cloacae	LMG 2783	NB/NA	37
Escherichia coli	NCTC 9001	NB/NA	37
Yersinia entercolitica	LMG 7899	NB/NA	37
Pseudomonas syringae	DSM 21482	TSB / Enriched TSA (TSA + 5 mM $MgSO_4$ and 5 mM $CaCl_2$)	25

3.1.2 Cultivation and Maintenance of Bacterial Stock Populations

Where necessary, bacterial strains were purchased from the relevant culture collection as freeze-dried cultures in glass ampoules. Upon receipt, ampoules were opened and bacterial samples rehydrated by inoculation into the appropriate media as per the relevant culture collection instructions (BCCM, 2015; DSMZ, 2014; NCTC, 2019). Once reconstituted, bacterial cultures were held for long-term storage on Microbank™ beads (Pro-Lab Diagnostics Inc., UK) at -20 °C.

To provide a source of inoculum for experimental testing, stock cultures of each bacterium were prepared at the outset of investigations for short-term storage onto agar plates and slopes. To do this, an inoculated Microbank™ bead was first streaked onto an agar plate of the appropriate growth medium and incubated (IP 250 Incubator; LTE Scientific, UK) at the required temperature for growth of that particular bacterial species for 18-24 h (Table 3.1). Once cultured, bacteria were streak plated and incubated at the required temperature for 18-24 h to obtain single colonies (Figure 3.1). A colony of this pure culture was then sub-cultured onto agar slopes and incubated at the required temperature for 18-24 h, before storing at 4°C. These slopes were then used as the regular source of inoculum for daily experimental testing. All bacterial strains cultured on agar slopes were re-streaked every 4-6 weeks and purity was checked by Gram staining.

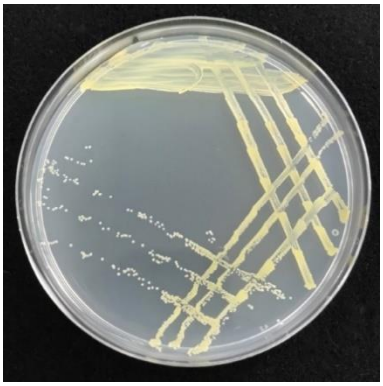

Figure 3.1 Streak-plate method used to obtain single colonies of bacteria.

To culture a bacterial species for experimental use, a loop of the required bacterium was aseptically inoculated into 100 mL of the required culture media for bacterial growth (Table 3.1). The inoculated culture media was then incubated under rotary conditions (120 rpm; C24 Incubator Shaker, New Brunswick Scientific, USA) at the appropriate temperature (Table 3.1) for 18-24 h to obtain a bacterial cell density of approximately 10^9 CFU mL^{-1}.

3.1.3 Re-Suspension and Serial Dilutions

Following bacterial cultivation, suspensions were centrifuged at 3939 × g for 10 min (Heraeus Labofuge 400R Centrifuge; Kendro Laboratory Products, UK). For experimental use, the supernatant was discarded and the bacterial pellet was re-suspended in 100 mL phosphate buffered saline (PBS; Oxoid Ltd, UK), providing a stock suspension of 10^9 CFU mL^{-1} which was then serially diluted (Figure 3.2), if required, to obtain the desired population density for experimental testing.

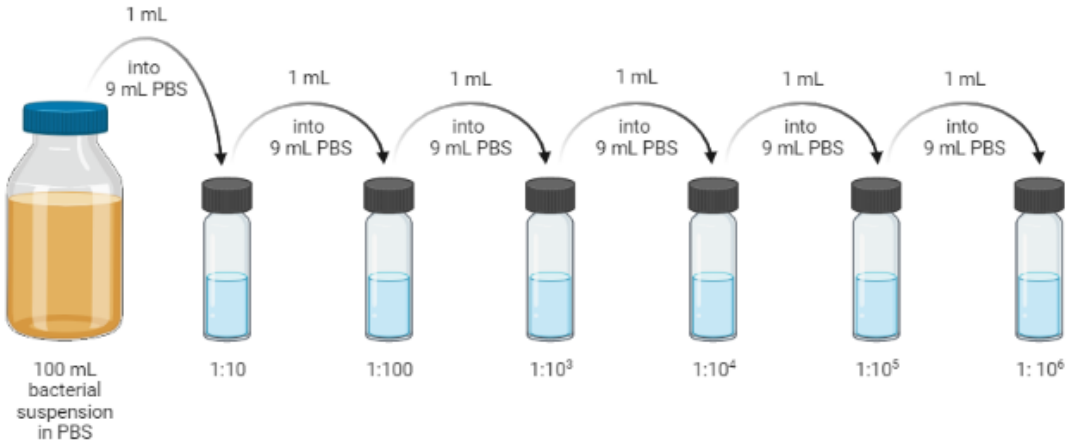

Figure 3.2 Serial dilution of a neat bacterial sample to obtain the required bacterial cell density for experimental use. Image created with BioRender.com.

3.1.4 Plating and Enumeration

To accurately determine bacterial populations before and after experimental treatments, samples were plated onto the appropriate agar medium and incubated to enable growth and enumeration.

For experiments which involved light treatment of agar-seeded bacterial samples, bacterial suspensions were spread plated onto agar plates. To do this, 100 µL samples were pipetted onto the agar plate, and manually spread using an L-shaped spreader to evenly distribute the sample across the plate surface.

For experiments which involved exposure of bacterial suspensions, following light-treatments, samples were plated using either the spread plate method (described above) or the drop plate method. If samples were estimated to be too numerous to count, they were serially diluted prior to plating. The drop plate technique was used in instances where multiple dilutions were required to be plated in order to determine bacterial populations. To do this, 10 µL droplets of bacterial sample were pipetted onto an agar plate,

and left to dry before incubating. Using this method, up to eight bacterial samples were plated onto a single agar plate, an example of which is shown in Figure 3.3.

Sample plates were incubated for 18-24 h at the appropriate growth temperature. Following incubation, bacterial colonies were enumerated using a colony counter (ThermoFisher Scientific, UK), with counts expressed as colony-forming units per millilitre (CFU mL^{-1}) for exposures conducted in liquid suspension, and CFU per plate (CFU $plate^{-1}$) or CFU per coupon for exposures on surfaces.

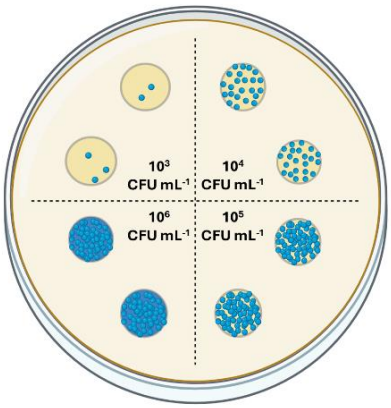

Figure 3.3 Drop plate technique for bacterial enumeration: 10 µL droplets of bacteria were pipetted onto an agar plate, left to dry and then incubated before subsequent enumeration. Image created with BioRender.com.

3.2 Bacteriophage Methodology

The bacteriophage studies conducted in Chapter 8 of this thesis utilised the bacteriophage phi6 and host bacterium *Pseudomonas syringae*. This section provides details of the methodology required for the cultivation and maintenance of both species, in addition to the methodology required for the preparation and enumeration of phi6 samples employed for experimental testing.

3.2.1 Cultivation and Maintenance of Host Bacterium Stock Populations

The host bacterium *P. syringae* (DSM 21482) was stored as detailed in Section 3.1.2. For experimental use, *P. syringae* was inoculated in 100 mL TSB and cultured at 25°C under rotary conditions (120 rpm) for 18-24 h, giving a bacterial cell density of approximately 1×10^9 CFU mL^{-1}.

3.2.2 Propagation and Maintenance of Bacteriophage Stock Populations

Bacteriophage phi6 (DSM 21518) was purchased as a 1 mL liquid suspension of bacteria-free lysates in the host's growth medium. Upon arrival, all bacterial cells and debris were eliminated from the liquid

suspension after lysis, by centrifugation and subsequent filtration through a single-use cellulose acetate membrane with a 0.2 µm pore size (Biomed Scientific). This size of filter was chosen to specifically allow passage of the bacteriophage and SM buffer whilst removing bacterial and cell debris.

The bacteriophage liquid suspension was propagated, and a high-titre phage stock solution was established through plate lysis and elution. For propagation, the bacteriophage liquid suspension was serially diluted in SM buffer (1:10 dilutions; 0.1 mL into 0.9 mL) and a 100 µL volume of each dilution was mixed with 100 µL of a *P. syringae* culture, which had been inoculated into TSB and incubated at 25°C for the 18-24 h prior. The bacteriophage-host bacterium solution was then incubated at 25°C for 10 min to allow bacteriophage attachment to bacterial cells. Following incubation, the solutions were mixed with 3 mL of enriched soft TSA and poured onto the centre of an enriched TSA plate. The plates were swirled to ensure even distribution across the surface and once solidified, were incubated for 18-24 h at 25°C. Post-incubation, 5 mL SM buffer was added to the plates which demonstrated confluent lysis and complete bacterial clearance, and these were then stored on a platform shaker for 40 min with slow agitation to allow elution to occur. Following this, the 5 mL liquid was transferred to a sterile tube and was filtered through a single-use 0.2 µm cellulose acetate membrane. This phage stock was then stored at 4°C for future experiments.

3.2.3 Assessment of Bacteriophage Stock Populations

Prior to commencing experimental work, the titre of the phage stock was regularly determined. To correctly determine population, the phage stock solution was first serially diluted in SM buffer (1:10 dilutions; 0.1 mL into 0.9 mL). A 100 µL volume of each dilution was then mixed with 100 µL of a *P. syringae* culture, which had been inoculated into TSB and incubated at 25°C for the 18-24 h prior. The bacteriophage-host bacterium solution was then incubated at 25°C for 10 min to allow attachment of the bacteriophage to the bacterial cells. Following incubation, the solutions were mixed with 4 mL molten enriched agar and poured onto the centre of an enriched TSB agar plate. The plates were swirled to ensure even distribution across the surface and once solidified, were incubated at 25°C for 18-24 h. Following incubation, the number of plaques formed in bacterial lawns were enumerated and, using the dilution factor associated with that given plate, the bacteriophage infectivity titre was calculated (Figure 3.4). This provided a bacteriophage concentration in plaque forming units per millilitre (PFU mL^{-1}).

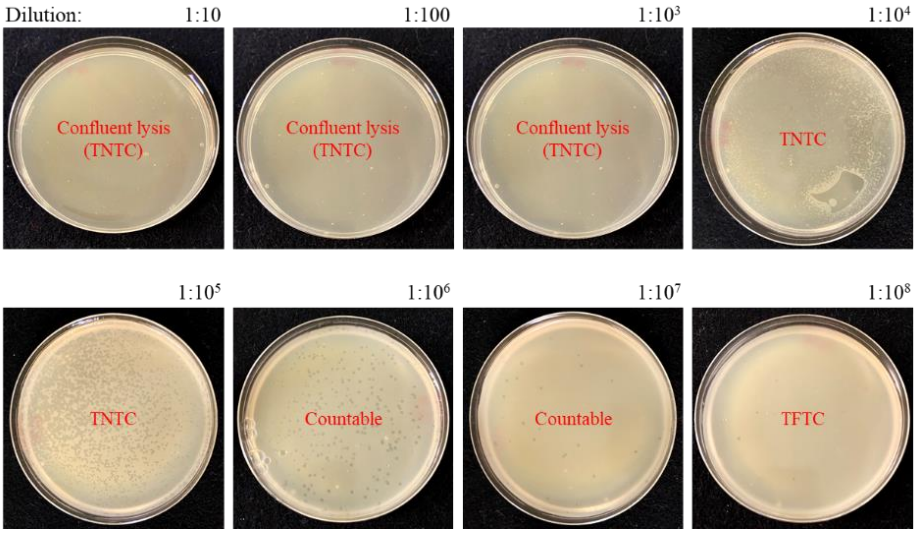

Figure 3.4 Appearance of phi6 plaques in *Pseudomonas syringae* lawns from serial dilutions (1:10) of the bacteriophage stock in SM buffer. [TNTC: too numerous to count; TFTC: too few to count].

3.2.4 Co-Incubation and Enumeration

The number of active bacteriophage in a given population post-exposure was determined via co-incubation with *P. syringae* through a double agar overlay plaque assay method, as shown in Figure 3.5. Briefly, a 100 µL bacteriophage sample (sequentially diluted in SM buffer if necessary) was added to 100 µL of an overnight *P. syringae* TSB culture and 3 mL enriched soft TSA. The solution was mixed and poured over the centre of a 90-mm enriched TSA plate, which was then swirled and left to dry. The plates were then co-incubated at 25°C for 18-24 h. Post-incubation, surviving bacteriophage populations were calculated through enumeration of plaques in the bacterial lawns and surviving phage load was expressed as PFU mL^{-1}.

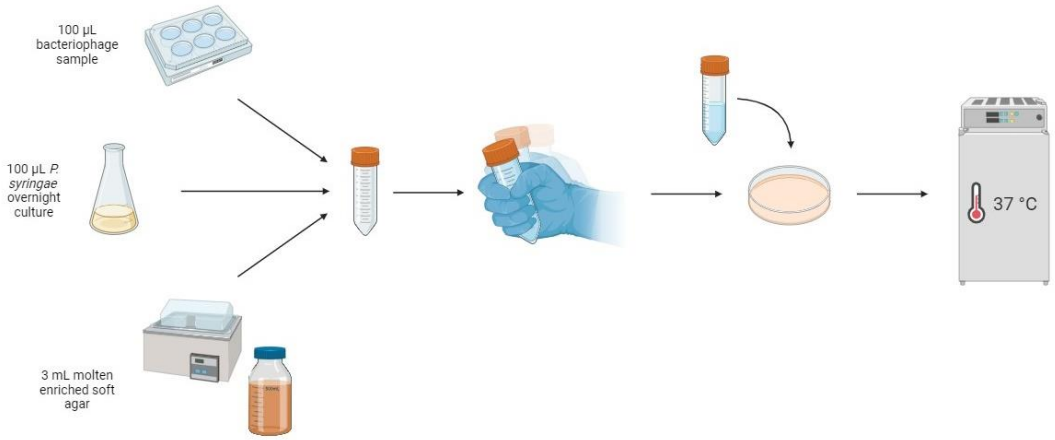

Figure 3.5 Double agar overlay plaque assay method for enumeration of phi6 bacteriophage populations in *Pseudomonas syringae* bacterial lawns. Image created on BioRender.com.

3.3 Media

This section details the specific culture and suspending media required throughout experimental testing.

The various media required for microbiological culture are detailed in Table 3.2. All media was prepared using distilled water in accordance with the manufacturer's instructions and was sterilised by autoclaving (Dixons, ST 2228) at 121°C for 15 min prior to use.

For some experiments in this thesis, bacteria/phage were light-exposed whilst suspended in different media. These suspension media are detailed in Table 3.3. PBS and SM buffer were employed as minimal suspension mediums for bacteria and bacteriophage populations, respectively. PBS was prepared using distilled water in accordance with the manufacturer's instructions. Both PBS and SM buffer were sterilised by autoclaving (Dixons, ST 2228) at 121°C for 15 min prior to use.

For experiments using organisms suspended in biologically-relevant media, artificial human saliva, defibrinated whole blood and artificial faeces were employed.

- **Artificial human saliva** was prepared based on the methodology used by Tomb (2017), which was a modified version of that used by Margomenou *et al*. (2000). Given the heat-sensitivity of various components within artificial human saliva, distilled water was sterilised prior to the aseptic addition of constituents. An artificial saliva-only control was prepared on each day of experiments to check for contamination. Once prepared, the artificial saliva media was adjusted to pH 7 (pH210 Microprocessor-based Bench pH/mV/°C meter, Hanna Instruments, UK) to replicate the typical conditions of human saliva. This media was prepared immediately prior to experimental use and was stored at 4°C between uses on the same day.
- **Defibrinated ovine whole blood** with 30% packed cell volume was obtained from E&O Laboratories Ltd, UK, and was stored at 4°C until required.
- **Artificial faecal samples** were prepared following the methodology used by Colón *et al*. (2015). To simulate real human faeces, inactivated *Saccharomyces cerevisiae* was used to represent bacterial debris, psyllium powder was used to represent carbohydrates, cellulose and oleic acid were used for fats, and miso paste was used to adjust nitrogen content (Colón *et al.*, 2015). Once prepared, artificial faeces samples were sterilised by autoclaving prior to use.

Table 3.2 Growth media and their constituents required for microbial cultivation.

Media	Constituents	Quantity Used	Manufacturer	Product Code
Nutrient Broth	N/A	13 g/L	Oxoid Ltd, UK	CM0001
Tryptone Soya Broth	N/A	30 g/L	Oxoid Ltd, UK	CM0876
Nutrient Agar	Nutrient Broth	13 g/L	Oxoid Ltd, UK	CM0001
	Agar Bacteriological	15 g/L	Oxoid Ltd, UK	LP0011
Tryptone Soya Agar	Tryptone Soya Broth	30 g/L	Oxoid Ltd, UK	CM0876
	Agar Bacteriological	15 g/L	Oxoid Ltd, UK	LP0011
Enriched Tryptone Soya Agar	Tryptone Soya Broth	30 g/L	Oxoid Ltd, UK	CM0876
	Agar Bacteriological	15 g/L	Oxoid Ltd, UK	LP0011
	5 mM Magnesium Sulfate ($MgSO_4$)	0.6 g/L	Acros Organics, UK	413485000
	5 mM Calcium Chloride ($CaCl_2$)	0.56 g/L	Thermo Scientific, UK	10515671
Enriched Soft Tryptone Soya Agar	Tryptone Soya Broth	30 g/L	Oxoid Ltd, UK	CM0876
	Agar Bacteriological	6 g/L	Oxoid Ltd, UK	LP0011
	5 mM Magnesium Sulfate ($MgSO_4$)	0.6 g/L	Acros Organics, UK	413485000
	5 mM Calcium Chloride ($CaCl_2$)	0.56 g/L	Thermo Scientific, UK	10515671

Table 3.3 Suspending media, and their constituents, used for experimental testing.

Suspension Media	Constituents	Quantity	Manufacturer/ Source	Product Code
PBS	N/A	10 tablet/L	Oxoid Ltd, UK	BR0014G
SM Buffer	N/A	N/A	G-Biosciences, USA	786-492
Artificial Human Saliva	$NAHCO_3$	5.29 g/L	Acros Organics, UK	AC217125000
	NaCl	0.88 g/L	VWR Chemicals, UK	27800.291
	K_2HPO_4	1.36 g/L	BDH Chemicals Ltd, UK	9266
	KCl	0.48 g/L	Sigma Aldrich, UK	208000
	α-Amylase	2000 IU	Sigma Aldrich, UK	A3176
	Mucin from Porcine Stomach	2 g/L	Sigma Aldrich, UK	M1778
Defibrinated Ovine Whole Blood	N/A	N/A	E&O Laboratories Ltd, UK	DSC050
Artificial Faeces	Distilled H_2O	800 g/L	N/A	N/A
	Dried Inactivated Yeast (*S. cerevisiae*)	60 g/L	Marigold, UK	N/A
	Psyllium Husk Powder	20 g/L	Whole Foods, UK	N/A
	Miso Paste	35 g/L	Yutaka, UK	YK70111A
	Cellulose	35 g/L	Sigma Aldrich, UK	435236
	Oleic Acid	40 g/L	Sigma Aldrich, UK	75096
	NaCl	4 g/L	Thermo Fisher Scientific, UK	10428420
	KCl	4 g/L	Sigma Aldrich, UK	208000
	$CaCl_2$	2 g/L	Sigma Aldrich, UK	746495

3.4 405-nm Light Exposure Systems

Three 405-nm light systems were employed to expose microbial samples throughout this thesis:

- a ceiling mounted 405-nm light EDS prototype system;
- a miniaturised 405-nm light EDS prototype system (for low irradiance bench-top testing); and,
- an ENFIS PhotonStar Innovate UNO 24 LED array (for high irradiance bench-top testing)

An overview of the light systems is provided in the following sections, with each system based on LED array(s) which emitted violet-blue light with a peak output at approximately 405-nm with bandwidths of 16-23 nm at full-width half-maximum (FWHM). Emission spectra data were captured using an HR4000 spectrometer (Ocean Optics, Germany) and Spectra Suite software version 2.0.151. The light source selected for experimental testing was based upon the irradiances required for microbial exposure and individual experimental demands. All irradiance readings were measured using a radiant power meter (Model 70260; L.O.T. Oriel Instruments Ltd, USA) and photodiode detector (Model IZ02413, L.O.T. Oriel Instruments Ltd, USA), and recorded in milliwatts per centimetre squared (mW cm^{-2}).

3.4.1 405-nm light EDS

The 405-nm light EDS is a prototype lighting unit developed at the University of Strathclyde (device patent numbers: EP2211914B1 (Europe) and US8398264B2 (USA)). These systems are designed to be retrofitted in place of a ceiling tile and emit low irradiance violet-blue light (typically <1 mW cm^{-2}) in order to provide continuous decontamination of the air and surfaces in the illuminated environment.

Two prototype devices with slightly differing light configurations were employed throughout this thesis: the first, which was used for optical characterisation experiments in Chapter 4, comprised four light apertures (configuration 1; Figure 3.7A) and the second, which was used for antimicrobial exposures to 405-nm light at irradiances of 0.021 - 1 mW cm^{-2} in Chapters 4-7, comprised three light apertures (configuration 2; Figure 3.7B). Despite the slightly different configurations, the systems were designed to provide the same optical output of approximately 0.5 mW cm^{-2} at a distance of 1.5 m from the source, providing comparable antimicrobial effects to that achieved within a typical room setting.

For operation, the 405-nm light EDS prototypes were driven by a low-voltage 270 W power supply (15 V at 18 A). The LED matrices of each aperture were covered by an optical lens system (Figure 3.6)

comprising a Fresnel lens and diffuser, which were positioned to aid in light distribution and scatter, respectively (Anderson *et al.*, 2008; Endarko, 2011); and a heat sink and fan for thermal management. Both prototypes were encased in a 59.2 × 59.2 cm square housing unit such that the systems could be retrofitted in place of a conventional ceiling tile.

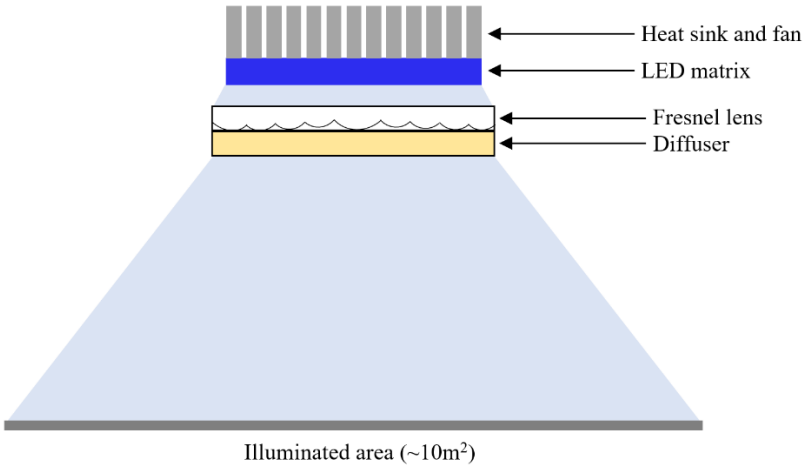

Figure 3.6 Design configuration of the 405-nm light EDS.

For clinical/commercial use as an overhead light source, the 405-nm light EDS includes both 405-nm LED arrays, for antimicrobial activity, and also white LEDs which produce illuminance of at least three times that of the 405-nm LEDs, for light blending. This results in a combined illumination output which is sufficient to inactivate microbial species, yet is predominantly white so to ensure blending with standard room lighting and ensure no visual disturbance to room occupants. As this thesis focused on antibacterial efficacy, all experimental testing was conducted with the systems operating in 'blue-only' mode: using only the 405-nm LEDs with the white LEDs disconnected (Figure 3.7C).

3.4.2 Miniaturised Bench-top 405-nm light EDS

The miniaturised 405-nm light EDS (Figure 3.8A) is a prototype lighting system designed, developed and built at the University of Strathclyde (Bradley, 2022). This light source was designed to miniaturise the original 405-nm light EDS prototype such that laboratory testing at the irradiance levels ordinarily produced by the original system within a typical 4 × 4 × 2 m room could be conducted on a smaller, bench-top scale. This light source, which was employed for antimicrobial exposures to irradiances ≤0.1 mW cm^{-2} in Chapter 5, was mounted on polyvinyl chloride (PVC) housing which held the array via a connecting metal pole above a base plate on which microbial samples were positioned (Figure 3.8B).

The light source delivered light to samples at a peak output of approximately 405 nm (21 nm FWHM (Figure 3.8C)). The design, build and optical profiling of this system is described in Chapter 6.

3.4.3 ENFIS PhotonStar Innovate UNO 24-LED array

The ENFIS PhotonStar Innovate UNO 24-LED array (PhotonStar Technologies, UK; Figure 3.9A) was employed in Chapters 6 and 7 for exposure of bacterial and bacteriophage samples, respectively, to irradiances in the range of 5 - 150 mW cm^{-2}. This single light array consisted of 24 violet-blue LEDs powered by a 62 V LED driver (Philips, Netherlands), which were connected to a heat sink and fan for thermal management. The system was mounted on a PVC housing which held the array via a connecting metal pole above a base plate on which microbial samples were positioned (Figure 3.9B). To fix the irradiance level for sample exposure, the distance between the array and the sample was adjusted, and the irradiance was measured. The light source delivered light to samples at a peak output of approximately 405 nm (16-nm FWHM, Figure 3.9C).

In all instances, the proportion of light in the optical emission spectrum of each light source recorded in the ranges of 440 nm and 460-480 nm, which, as discussed in Chapter 2, are known to negatively impact human health, were between 0-0.66% and 0-3.15%, respectively, and so can be considered to have negligible effects throughout the experiments performed in this thesis. Further, the proportion of light in the optical emission spectrum of each light source in the range of 420-430 nm, which is known to induce damage to viral structures (Richardson and Porter, 2005), was found to be 5.49-9.94% of all light output.

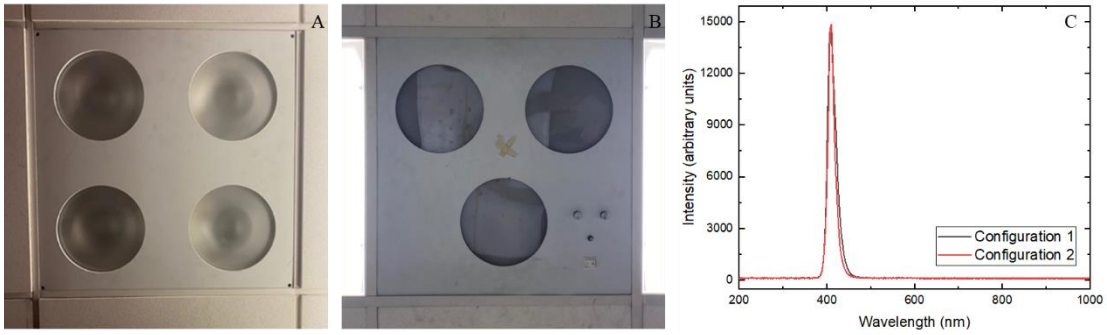

Figure 3.7 405-nm light EDS prototypes. Illustrating: (A) configuration 1 and (B) configuration 2 retrofitted in place of a ceiling tile for the purposes of environmental decontamination; and (C) the optical emission spectrum of each source measured in 'blue-only' mode, captured using an HR4000 spectrometer (Ocean Optics, Germany) and Spectra Suite software version 2.0.151.

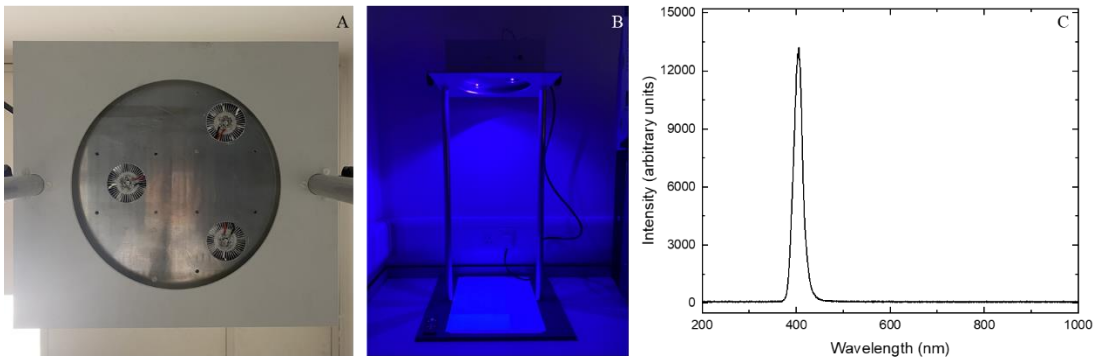

Figure 3.8 Miniaturised 405-nm light EDS. Illustrating: (A) LED arrays, (B) light source mounted on PVC housing at a variable height above a base plate for microbial positioning, and (C) optimal emission spectrum, captured using an HR400 spectrophotometer (Ocean Optics, Germany) and Spectra Suite software version 2.0.151.

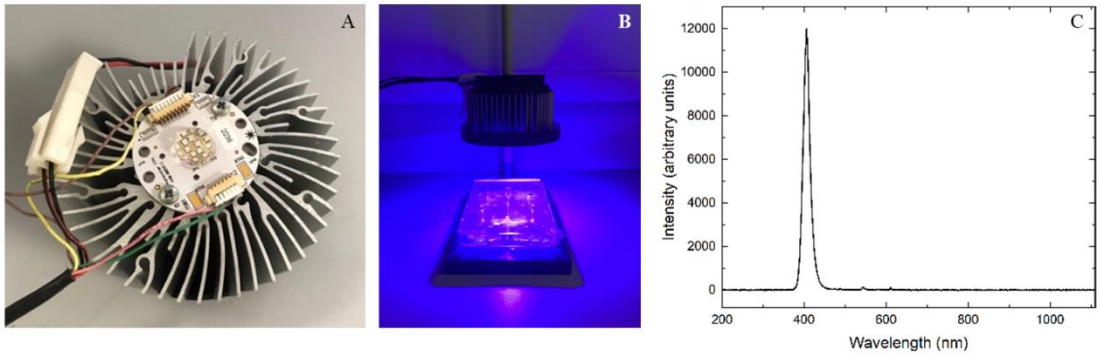

Figure 3.9 ENFIS PhotonStar Innovate UNO 24-LED array. Illustrating: (A) 24-LED array, (B) light source mounted on PVC housing at a variable height above a base plate for microbial positioning, and (C) optimal emission spectrum, captured using an HR400 spectrophotometer (Ocean Optics, Germany) and Spectra Suite software version 2.0.151.

3.5 Microbial Inactivation Data Analysis

3.5.1 Light Treatment Analysis

Throughout this thesis, microbial samples were exposed to 405-nm light at varying irradiances and exposure times. The applied dose of 405-nm light received by each sample was calculated using Equation (3.1):

$$Dose\ (J\ cm^{-2}) = Irradiance\ (Wcm^{-2}) \times Exposure\ Time\ (seconds) \tag{3.1}$$

Quantitative bacterial inactivation data is typically presented as either bacterial counts, the percentage surviving bacterial population in comparison to non-exposed equivalent control populations or reductions in $\log_{10}$ CFU mL^{-1} or CFU mL^{-1}, or as germicidal efficiency (GE) values. The presentation

of data as percentage surviving bacterial population in comparison to non-exposed equivalent control populations or as GE values was performed as a means to normalise datasets and enable more accurate comparisons to be made, as described in the relevant chapters.

GE is defined as the $\log_{10}$ reduction of a bacterial population by inactivation per unit dose in J cm^{-2} (Maclean *et al.,* 2009) and was calculated by $\log_{10}(N/N_0)$, where N_0 and N represent bacterial populations pre and post exposure, respectively, divided by the applied dose, in J cm^{-2}, required to achieve ≥95% inactivation, as presented in Equation (3.2):

$$Germicidal\ Efficiency = \frac{log_{10}(\frac{N}{N_0})}{Dose\ (J\ cm^{-2})_{\geq 95\%\ reduction}} \tag{3.2}$$

For analysis of low-density microbial populations exposed on surfaces (10^2 CFU $plate^{-1}$) and in liquid suspension (10^3 CFU mL^{-1}), complete/near-complete inactivation was considered as ≥95% reductions in 405-nm light exposed populations in comparison to non-exposed equivalent control populations.

In certain instances, enumerated bacterial samples were below the limit of detection (10 CFU mL^{-1}); however, this data has been included to demonstrate the complete or near-complete inactivation effect achieved.

3.5.2 Statistical Analysis

Experimental data points represent the mean values ± standard deviation (SD) of replicate independent experimental results, with the exact details for each experiment provided in the specific chapters.

All data storage, handling and calculations were performed using Microsoft Excel version 2021. All graphical data is presented using Origin 2022, with the exception of the 3D irradiance profile data included in Chapter 4 which was presented using MATLAB R2022b.

All statistical analysis was conducted using MINITAB Release 19. Significant differences ($P \leq 0.05$) between datasets were calculated at the 95% confidence level using either two sample t-tests or one-way ANOVA with Tukey post-hoc test, depending on the data being analysed. These significant differences are highlighted using an asterisk (*) in figures.

CHAPTER 4

Antibacterial Efficacy of the 405-nm light EDS

4.0 Overview

As discussed in Section 2.4.2, there are a number of publications demonstrating clinical efficacy of the 405 nm light EDS for decontamination of clinical environments (Maclean *et al.*, 2010, 2013a; Bache *et al.*, 2012a, 2018a; Murrell *et al.*, 2019), however it is important to build an understanding of the fundamental antimicrobial efficacy of the low irradiance light levels used in the system. This chapter aimed to demonstrate the broad-spectrum antibacterial efficacy of the 405-nm light EDS at heights typical of high-touch surfaces within occupied settings for a panel of key nosocomial bacteria. Additionally, antibacterial efficacy at various distances below the light source, and thus illumination levels, was evaluated. Findings provide fundamental evidence of the efficacy of low irradiance 405-nm light for bacterial inactivation, within a controlled laboratory setting.

4.1 Introduction

For use in occupied indoor environments, it is essential that the violet-blue light wavelengths employed by the 405-nm light EDS are delivered at sufficiently low irradiance (<1 mW cm^{-2}) such that they are within levels considered safe for continuous human exposure (ICNIRP, 2013). Much of the literature investigating the fundamental antimicrobial properties of violet-blue light have typically used considerably higher irradiance levels than that employed by the 405-nm light EDS (up to approximately 200 mW cm^{-2}) to achieve a rapid inactivation effect (Hamblin *et al.*, 2005; Guffey and Wilborn, 2006; Murdoch *et al.*, 2012; McKenzie *et al.*, 2014; Tomb *et al.*, 2014; Moorhead *et al.*, 2016b). Further, although clinical studies evaluating the performance of the 405-nm light EDS – as previously described in Section 2.4.2 (Maclean *et al.*, 2010, 2013a; Bache *et al.*, 2012a, 2018a; Murrell *et al.*, 2019) – established general reductions in bacterial contamination levels, it is difficult to accurately determine inactivation kinetics of individual bacterial species given the continuous generation of contamination

within dynamic healthcare environments, in addition to the variation in irradiance levels from the EDS at different positions in the room. The efficacy of such irradiances for the inactivation of individual bacterial pathogens is thus yet to be fully assessed.

Accordingly, the focus of the present chapter was to characterise the optical irradiance output profile of low irradiance 405-nm light systems within a typical room setting, and quantify, for the first time, the bactericidal effect of 405-nm light at these irradiances for the inactivation of low-density populations of surface-seeded nosocomial bacteria, comparable with typical contamination levels found on environmental surfaces, under controlled laboratory conditions. Differences in inactivation kinetics, and how bactericidal efficacy is affected spatially by varying irradiance exposures, was investigated, with particular focus on *S. aureus* and *P. aeruginosa*, selected due to their significance as causative agents of HAI, and to serve as a Gram-positive and Gram-negative bacterial representative, respectively. The findings of this chapter provide a comprehensive laboratory evaluation of 405-nm light systems for environmental decontamination and present evidence of its broad-spectrum antibacterial efficacy at the low irradiance levels which must be employed by 405-nm light EDS units in order for it to comply with exposure safety guidelines, such to build a better understanding of the exposure times required for inactivation of these bacterial pathogens when found contaminating healthcare environment, which will be essential in facilitating clinical translatability of the technology.

4.2 Optical Characterisation of the 405nm Light EDS

The aim of this section was to determine the typical irradiance levels produced by a 405-nm light EDS within an illuminated whole-room environment, such that the inactivation efficacy of these irradiance levels could be subsequently examined.

4.2.1 Methodology for the Optical Characterisation of the EDS

The EDS prototype used for the optical characterisation is detailed in Section 3.4.1 (configuration 1; Figure 3.7A). The irradiance output of each individual light aperture of the system was firstly established to ensure that an equal distribution of 405-nm light was produced from each. The 405-nm light EDS was switched on in ‘blue-only’ mode and, taking each aperture in turn, irradiance

measurements were taken from 0.2 m directly below the aperture, in approximately 0.1 m intervals, up to 1 m directly below the aperture, whilst the remaining three arrays were completely covered.

The 3D optical irradiance output profile of the full 405-nm light EDS was measured within a 4 × 4 × 2 m area in a vacant room in the Royal College Building of the University of Strathclyde, Glasgow, UK. The light source was retro-fitted in place of a ceiling tile in the centre of this room and an area of 16 m^2 (4 × 4 m) was measured on the floor, using the position directly underneath the 405-nm light EDS as a centre point, with markings in both X and Y directions placed at approximately 0.5 m intervals (Figure 4.1). Following this, approximate 0.5 m markings were placed vertically (in the Z direction), by attaching thin wire between the markings on the ground and the ceiling, and starting measurements from the ceiling and extending 2 m downwards. This provided a total area of 32 m^3 (4 × 4 × 2 m) for taking measurements (Figure 4.2A).

Irradiance measurements were taken at approximately 0.5 m intervals in X, Y and Z directions, with the light source used in 'blue-only' mode (Figure 4.2B) to ensure that the inactivation data gathered was accounted for solely by inactivation due to the antimicrobial blue lighting component only. Measurements were taken with the photodiode detector held parallel to the ceiling to represent the irradiance levels likely to illuminate surfaces at each particular measured area. These measurements were additionally repeated with the photodiode detector held angled towards the 405-nm light EDS to examine the irradiance levels likely to illuminate aerosolised matter in each particular area, with this additional data provided in Appendix A.

For further analysis of irradiance distribution, measured irradiance values were plotted as a function of both linear and angular displacement from the light source. The linear displacement (Δs; Figure 4.2B) of each measured point from the source was calculated by applying Pythagoras theorem, shown in Equation (4.1):

$$\Delta s = \sqrt{(distance \in X)^2 + (distance \in Y)^2 + (distance \in Z)^2} \tag{4.1}$$

The angular displacement (Δϴ; Figure 4.2B) of each measured point in X and Y directions from the light source was then calculated using the tangent trigonometric function given in Equation (4.2):

$$\Delta \emptyset = \tan^{-1}\left(\frac{distance \in X \text{ or } Y}{distance \in Z}\right) \tag{4.2}$$

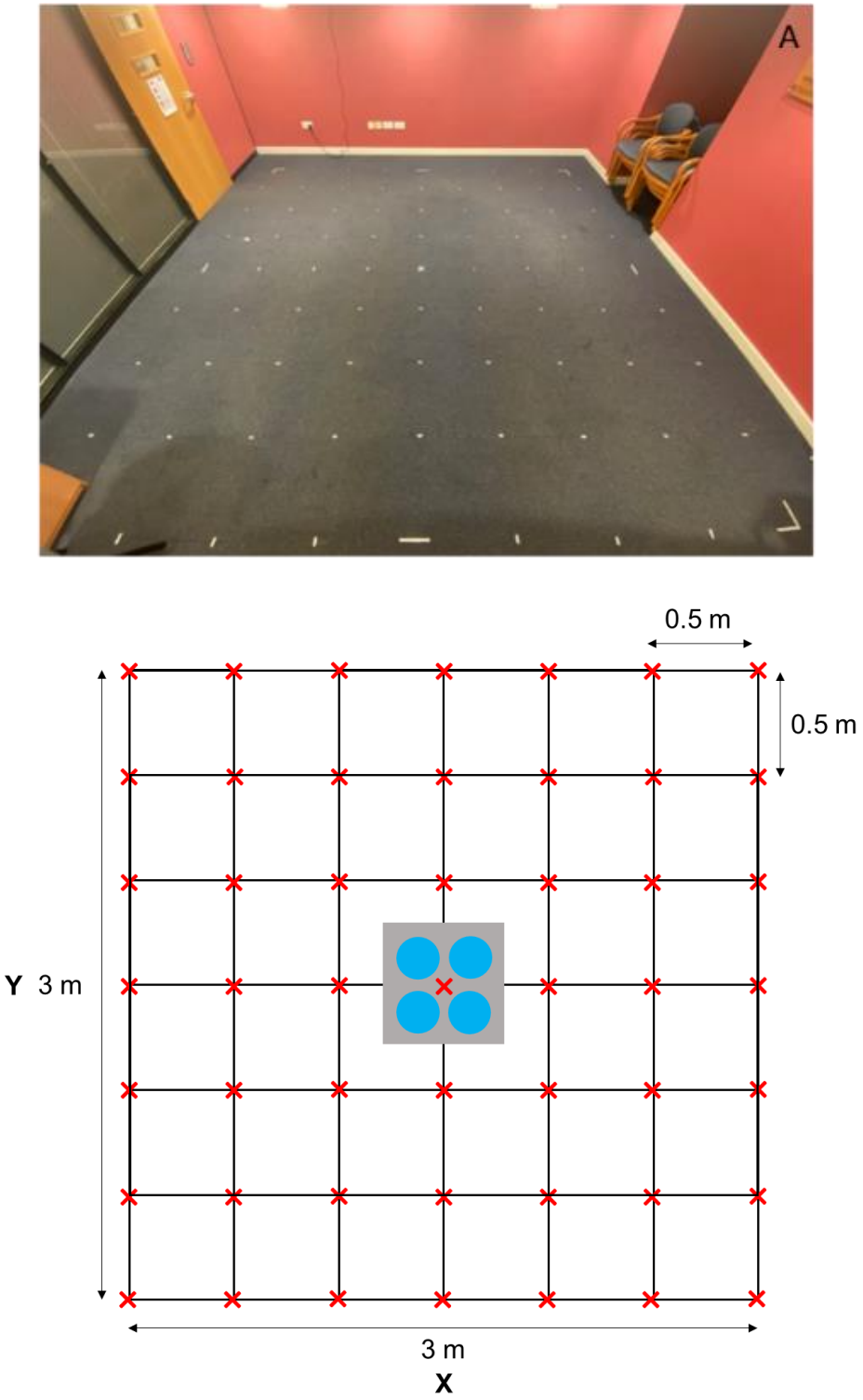

Figure 4.1 Floor markings placed in X and Y directions for irradiance profiling of 405-nm light EDS: (A) photograph and (B) diagrammatic representation.

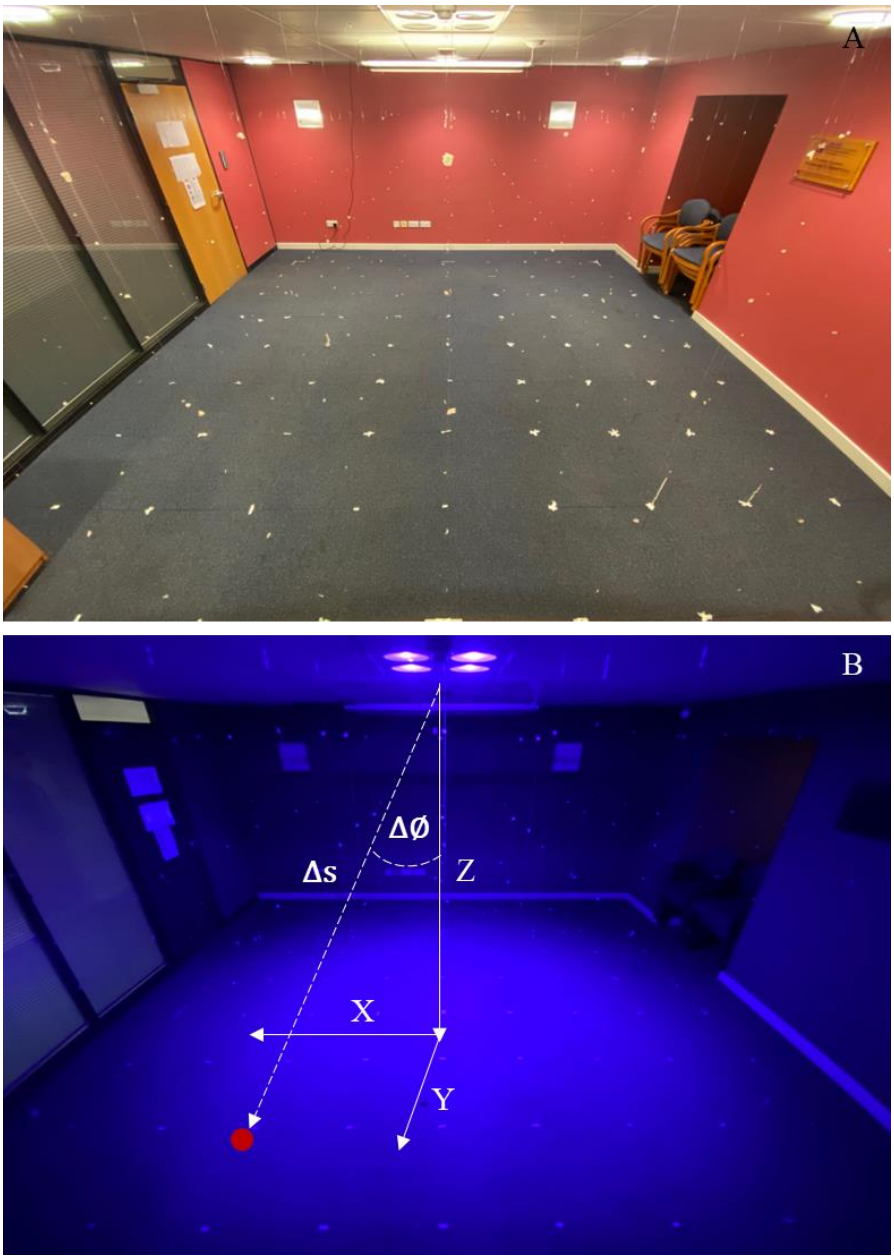

Figure 4.2 3D optical characterisation of the 405-nm light EDS: (A) the light source retrofitted in place of a ceiling tile in the centre of a 4 × 4 × 2 m sized room and (B) the light source operating in 'blue-only' mode with standard room lighting switched off for irradiance measurement. The associated parameters required to measure the linear (Δs) and angular (ΔΘ) displacement of a point of interest (indicated by the red circle) from the light source are indicated.

4.2.2 Results of the Optical Characterisation of the EDS

The irradiance output of each individual light array of the 405-nm light EDS is presented in Figure 4.3. Results indicate similar light levels produced by each individual array, with recorded irradiances of 3.04-3.24 mW cm^{-2} at a distance of 0.2 m from the source to 0.234-0.285 mW cm^{-2} at a distance of 1 m from the source. No significant difference between the levels of irradiance produced by each light array

was demonstrated (P=0.98), suggesting that an even distribution of light would be produced within the illuminated environment.

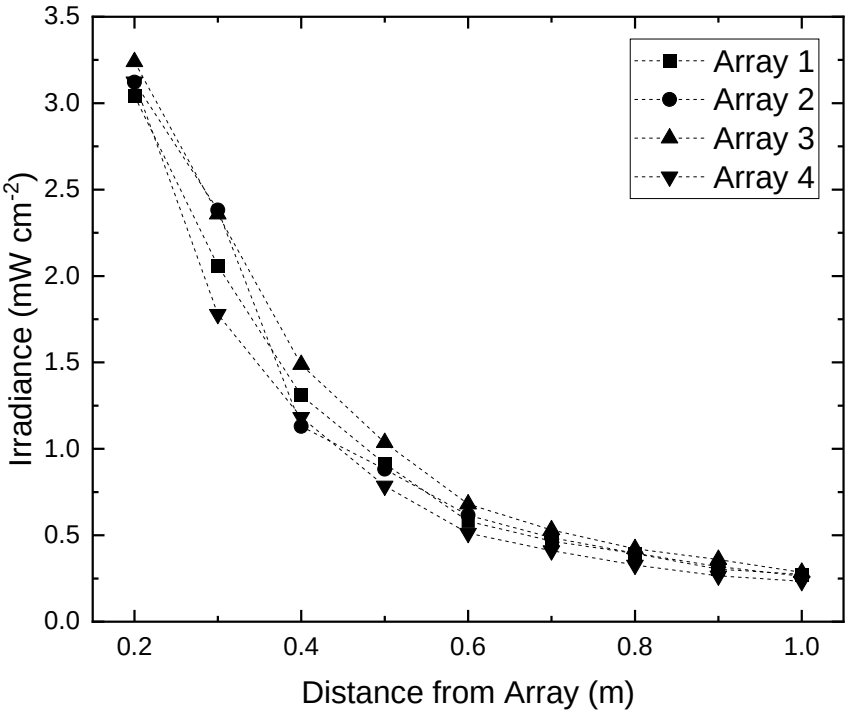

Figure 4.3 Irradiance output of each individual light array of the 405-nm light EDS.

The optical characterisation of the ceiling-mounted 405-nm light EDS within a vacant 4 × 4 × 2 m area produced a total of 324 readings. Irradiance measurements were modelled comprehensively using MATLAB R2022b (Figure 4.4) and on Origin as 2D slices at each distance measured in the Z direction (Figure 4.5). The 405-nm light EDS emitted irradiance values across the area ranging from 0.001-2.066 mW cm^{-2}. The highest irradiance values were collected at the closest measurements taken to the 405-nm light EDS (directly under the light source at a distance of 0.5 m) and the lowest irradiance values were generally collected at maximum distances in X and Y directions from the light source. The range of irradiance values collected was found to decrease as distance from the light source increased in the Z direction; highlighting, as expected, the uniformity of light distribution increases as distance from the light source increases. At a distance of 0.5 m from the light source in the Z direction, the range was found to be 2.066 mW cm^{-2}. This decreased to 0.899 mW cm^{-2} at a distance of 1 m, 0.454 mW cm^{-2} at a distance of 1.5 m and 0.258 mW cm^{-2} at a distance of 2 m. Interestingly, despite variations in light

distribution, there was no significant difference found (P=0.998) between the mean irradiance values at each distance in the Z direction (varied between 0.045-0.049 mW cm^{-2}).

For further analysis of irradiance distribution, the relationship between irradiance and both linear and angular displacement from the light source was determined and is presented in Figures 4.6A and B, respectively. Results in Figure 4.6A demonstrate a weak, yet significant (P<0.0001), negative linear relationship between irradiance levels and distance from the light source, confirmed by linear regression analysis indicating a Pearson's r value of -0.41285. General trends in Figure 4.6B indicate that the highest irradiance levels produced by the 405-nm light EDS were recorded when angular displacement from the light source in X and Y directions was minimal, with irradiance levels decreasing as angular displacement from the light source increased. No significant difference was found between the irradiance values measured at each angular displacement value for X and Y planes (P>0.05).

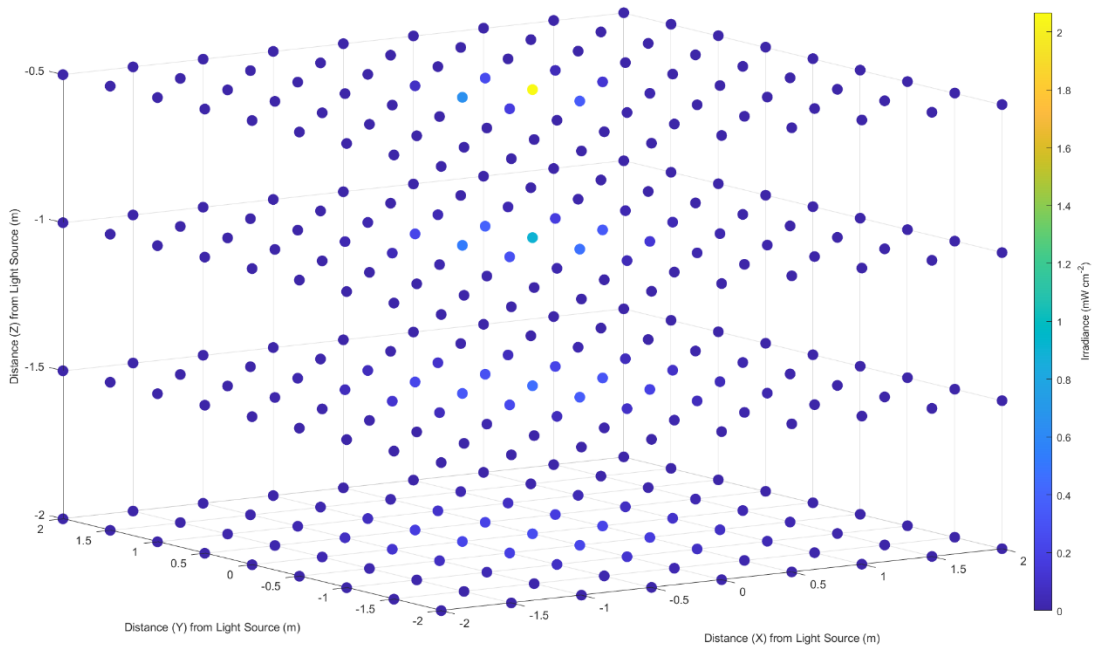

Figure 4.4 3D irradiance output profile of the ceiling-mounted 405-nm light EDS modelled on MATLAB R2022b. The ceiling-mounted 405-nm light EDS was installed at position (0,0,0), with X , Y and Z axes consistent with those outlined in Figure 4.2.

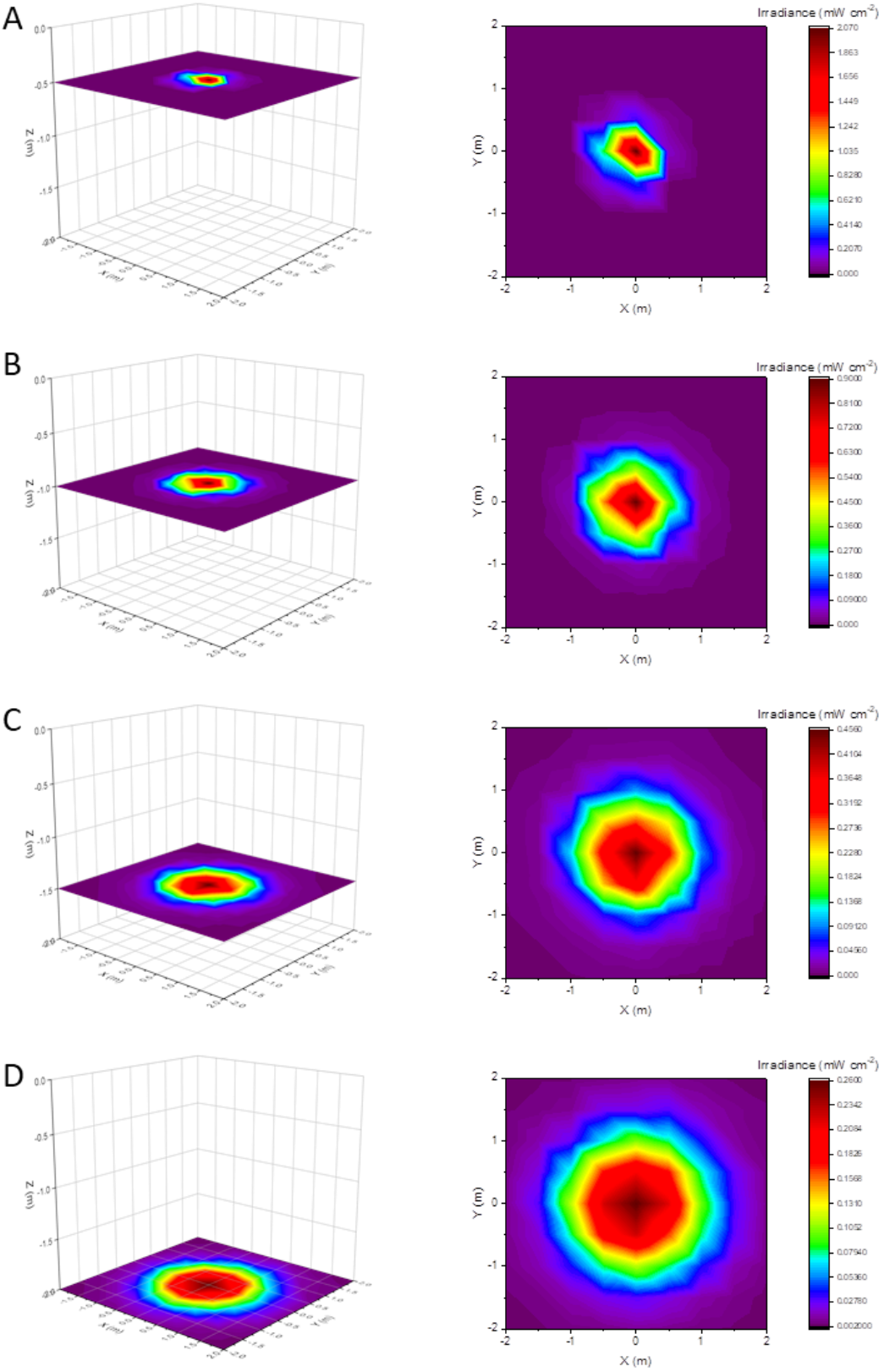

Figure 4.5 Irradiance distribution produced by ceiling-mounted low-irradiance 405-nm light EDS at distances of (A) 0.5 m, (B) 1 m, (C) 1.5 m and (D) 2 m in the Z direction, with measurements taken with the photodiode detector horizontal to the light source (please note that the scale is different for each graph).

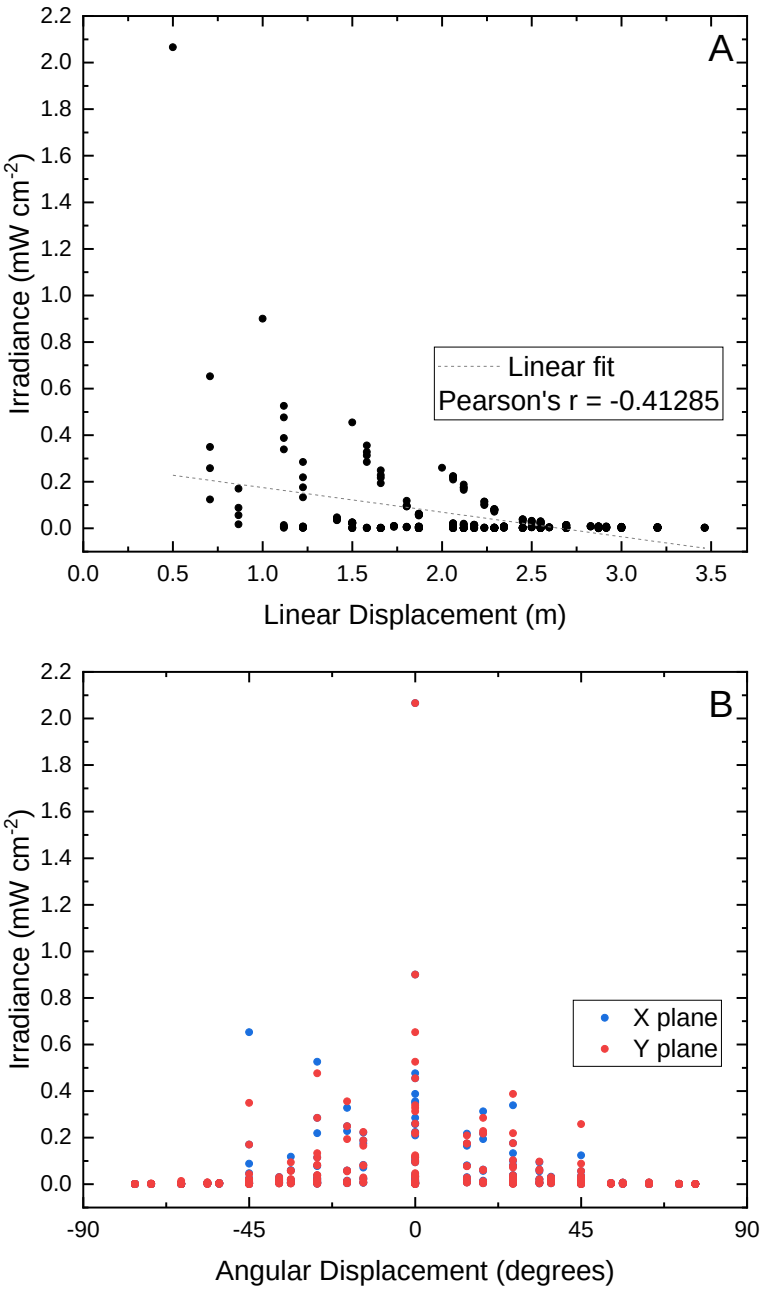

Figure 4.6 Irradiance distribution within 4× 4 × 2 m area plotted as a function of (A) linear displacement (Δs) and (B) angular displacement (ΔΘ) (in X and Y directions) from the ceiling-mounted 405-nm light EDS. In all instances, X, Y and Z axes are consistent with those outlined in Figure 4.2.

4.3 Inactivation Kinetics of Bacteria Exposed to 405-nm Light EDS

Based on the optical characterisation profile established, the next aim was to demonstrate the broad-spectrum bactericidal efficacy of the 405-nm light EDS at heights, and thus irradiance levels, typical of high-touch surfaces within occupied settings.

4.3.1 Methodology for Bacterial Exposures to the EDS

Antimicrobial testing was conducted using the EDS prototype described in Section 3.4.1 (configuration 2; Figure 3.7B). As previously described in Section 3.4.1, although two EDS prototypes with differing configurations were used in this thesis, both were designed to produce the same optical output. Bacterial suspensions of *A. baumannii, E. cloacae, E. coli, E. faecium*, *K. pneumoniae, P. aeruginosa*, *S. aureus* and *Y. enterocolitica* were prepared as described in Sections 3.1.2 and then serially diluted in PBS, as described in Section 3.1.3, to provide populations of 10^3 CFU mL^{-1} for experimental use. From these suspensions, 100 µL volumes were aseptically spread onto the surface of 90 mm diameter NA plates (or TSA plates in the case of *E. faecium*) to provide a starting population of approximately 100-300 CFU $plate^{-1}$ (1.6-4.7 CFU cm^{-2}) for each microorganism. Sample plates (with the lids removed) were exposed to increasing doses of 405-nm light for up to 16 h on a surface approximately 1.5 m directly below the light source; selected to represent the typical heights of high-touch surfaces within clinical and public areas (Figure 4.7). The irradiance produced at this distance was found to be 0.5 ± 0.02 mW cm^{-2}.

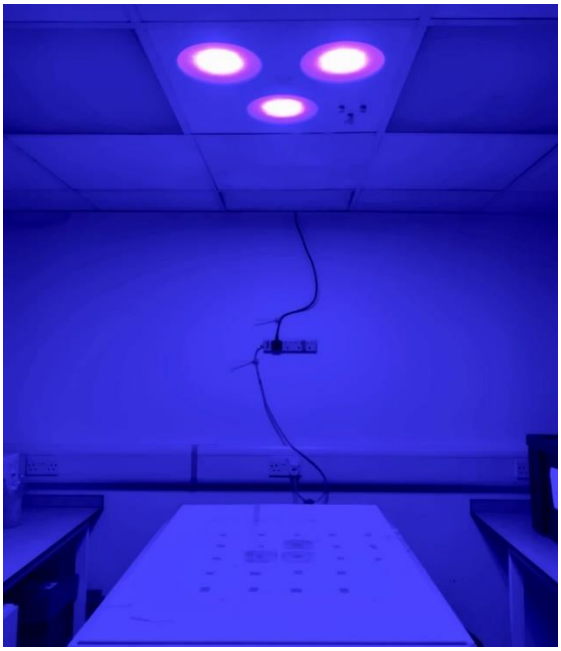

Figure 4.7 405-nm light EDS exposure of surface-seeded pathogens in 'blue-only' mode at a distance of ~1.5 metres from the light source, providing an irradiance at the sample surface of 0.5 mW cm^{-2}.

Control bacterial samples were prepared in an identical manner with the exception that they were exposed to standard laboratory lighting for equivalent durations. Post-exposure, the lids were replaced

and the seeded agar plates were incubated at 37°C for 18 h, before enumerating the viable bacterial CFU plate^{-1}. Results represent the mean values ± SD of triplicate replicates (n=3), and are reported as the percentage of surviving bacteria as compared to the equivalent non-exposed control samples.

4.3.2 Results for Bacterial Exposures to the EDS

Figure 4.8 displays the inactivation kinetics of eight nosocomial bacterial species each seeded onto agar surfaces at an initial population density of 10^2 CFU plate^{-1} and exposed to low irradiance 405-nm light at approximately 0.5 mW cm^{-2}. Results demonstrate ≥93.28% inactivation of all species, with general trends indicating that greater levels of inactivation were observed as exposure time increased. All bacteria collectively demonstrated broadly linear, and somewhat sigmoidal, inactivation curves with tailing observed.

Of the Gram-positive species investigated, *S. aureus* (Figure 4.8G) was found to be the most susceptible. The organism displayed exponentially decreasing inactivation kinetics with a significant 79.3% mean reduction (P=0.001) observed after 1 h/1.8 J cm^{-2} exposure, and near-complete inactivation (99.3%) achieved after 2 h/3.6 J cm^{-2} exposure. Results indicate *E. faecium* (Figure 4.8C) was the least susceptible Gram-positive species, requiring 16 h/28.8 J cm^{-2} to achieve similar levels of reduction (93.3%).

Collectively, the Gram-negative species, demonstrated similar patterns of inactivation. *A. baumannii* (Figure 4.9A) and *P. aeruginosa* (Figure 4.8F) were found to be the most susceptible, each requiring 2 h/3.6 J cm^{-2} exposure to achieve significant (P<0.0001) reductions of 86.5% and 93.4%, respectively. In contrast, *K. pneumoniae* (Figure 4.8E) was shown to be the least susceptible Gram-negative species, requiring 8 h/14.4 J cm^{-2} exposure to achieve a significant (P=0.004) 21.1% reduction, and 16 h/28.8 J cm^{-2} to achieve near-complete inactivation (97.4%).

In all cases, bacterial contamination in non-exposed control populations displayed no significant decay throughout the treatment duration (P>0.05).

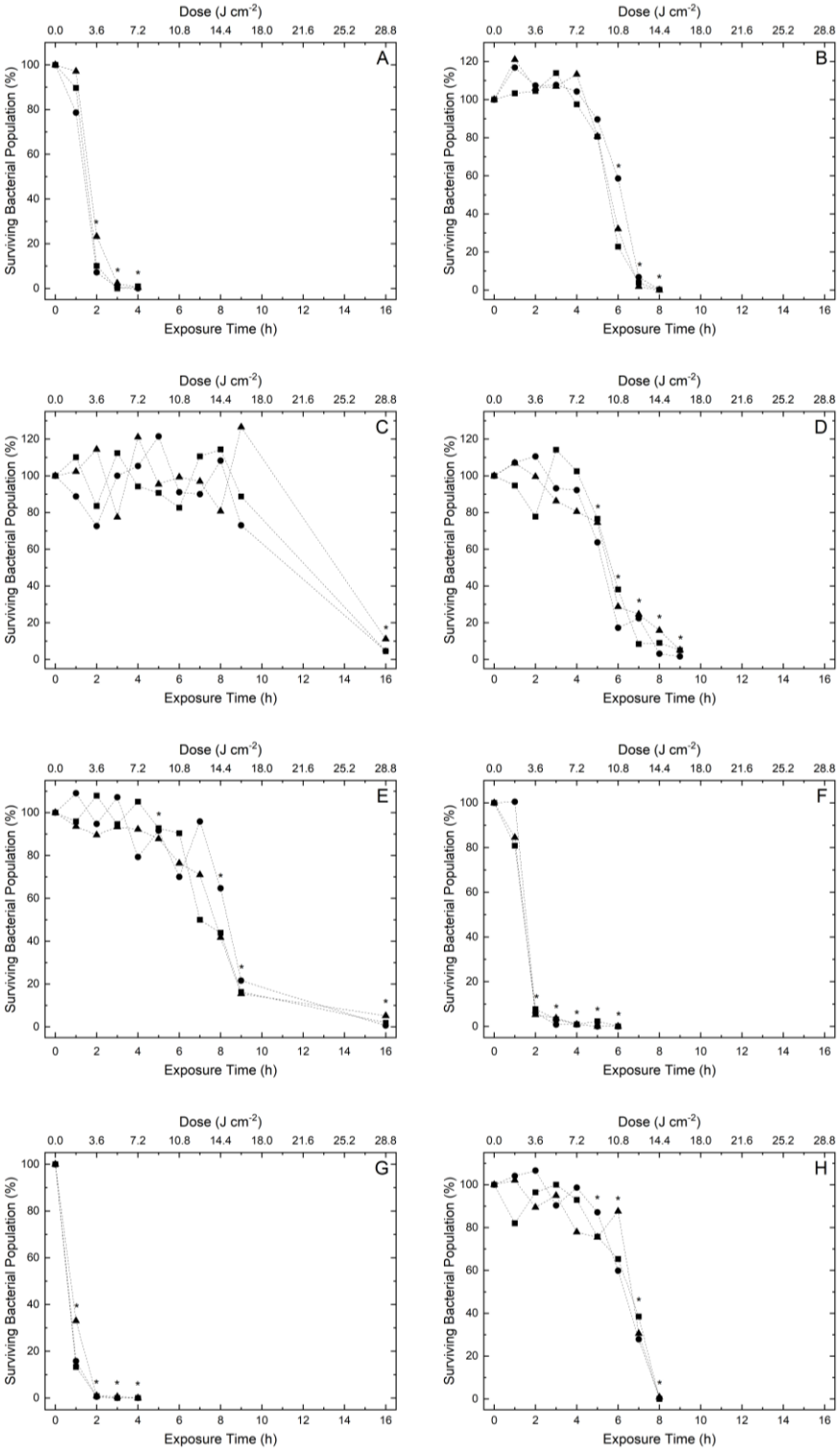

Figure 4.8 Inactivation of a range of bacterial pathogens associated with HAIs: (A) *Acinetobacter baumannii*, (B) *Enterobacter cloacae*, (C) *Enterococcus faecium*, (D) *Escherichia coli*, (E) *Klebsiella pneumoniae*, (F) *Pseudomonas aeruginosa*, (G) *Staphylococcus aureus* and (H) *Yersinia entercolitica*. Bacterial species were seeded onto agar surfaces and exposed to ~0.5 $mWcm^{-2}$ 405 nm light. Experiments were run in triplicate (● run 1; ■ run 2; ▲ run 3). Asterisks (*) represents points where the triplicate CFU $plate^{-1}$ counts were significantly different between test and control samples ($P<0.05$).

4.4 Effect of Irradiance and Exposure Distance on Inactivation Efficacy

In addition to its broad-spectrum efficacy at heights comparable with high-touch surfaces directly below the light source, it is also important to consider the efficacy of the 405-nm light EDS for the inactivation of bacterial contamination present at varying areas within the illuminated region. Using irradiance levels within the range gathered during the optical characterisation of the 405-nm light EDS, the aim of this section was to determine how irradiance and distance from the source affects bactericidal efficacy.

4.4.1 Methods for Assessing Effect of Irradiance and Exposure Distance on Inactivation Efficacy

To determine the effect of irradiance output of the 405-nm light EDS on bactericidal efficacy, inactivation kinetics of *S. aureus* and *P. aeruginosa* were established using irradiance levels ranging from 0.05-1 mW cm^{-2}. Seeded plates (with the lids removed) were prepared as described in Section 4.3.1, and positioned directly under the EDS light source and exposed to increasing doses of 405-nm light at approximate irradiances of 0.05, 0.15, 0.25, 0.5 and 1 mW cm^{-2} for up to 24 h.

To determine the effect of distance on bactericidal efficacy, inactivation kinetics of *S. aureus* and *P. aeruginosa* were established for exposures to the 405-nm light EDS across a radius of 2 m measured from the centre of the light source in the X direction. As shown in Figure 4.9, seeded plates (with the lids removed) were positioned approximately 1.6 m below the light source, and were situated in 0.1 m intervals from directly under the light source ($\Delta s = 1.6$ m; $\Delta\ \Theta = 0$) up to a distance of 2 m radially ($\Delta s = 2.56$ m; $\Delta\ \Theta = 51.3$), with irradiance measured at each fixed position. For each independent experiment, samples were exposed to the 405-nm light EDS for durations of 4, 8 and 24 h.

For both experiments, control bacterial samples were prepared in an identical manner with the exception that they were exposed to standard laboratory lighting for equivalent durations. Post-exposure, the lids were replaced and the seeded agar plates were incubated at 37°C for 18 h, before enumerating the viable bacterial CFU $plate^{-1}$. Results represent the mean values ± SD of triplicate replicates (n=3), and are reported as the percentage of surviving or reduced bacteria as compared to the equivalent non-exposed control samples.

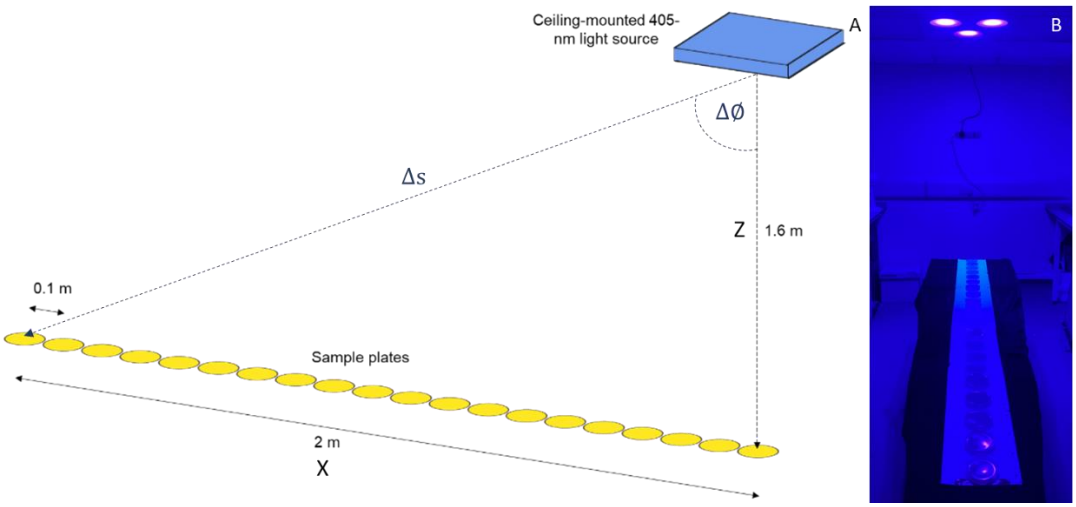

Figure 4.9 Experimental set-up to determine effect of distance from the source on bactericidal efficacy: (A) diagrammatic representation and (B) photograph.

4.4.2 Results for Assessing Effect of Irradiance and Exposure Distance on Inactivation Efficacy

Results in Figure 4.10A and B present the inactivation kinetics of *S. aureus* and *P. aeruginosa*, respectively, exposed on agar surfaces to the 405-nm light EDS at varying irradiances (0.05-1 mW cm^{-2}). Data presented for the inactivation of *S. aureus* (Figure 4.10A) was collected and provided by Laura Dougall (PhD student) for analysis. In all cases, a significant downward trend in the surviving bacterial populations was demonstrated as the exposure time increased, and non-exposed control samples showed no significant change throughout treatment ($P>0.05$). The only exception to this was that of the 5 h exposure of *P. aeruginosa* to 0.25 mW cm^{-2}, where controls were shown to be significantly lower than that of starting populations ($P=0.004$). This was thought to be the result of bacterial variability, and, given that no significant change was demonstrated following 6 and 18 h exposures to the same irradiance ($P=0.144$ and 0.322, respectively), and that the controls were still significantly higher than exposed values ($P<0.005$), this was considered negligible. Furthermore, general trends indicate that, to achieve significant levels of bacterial reduction, considerably shorter exposure times were required when exposed at higher irradiances; however, in some instances, less energy was required on a per unit dose basis when exposed at lower irradiances.

Considering the inactivation kinetics gathered for *S. aureus* (Figure 4.10A), exposure to the highest irradiance of 1 mW cm^{-2} for 1 h (3.6 J cm^{-2}) resulted in a significant 78.53% reduction in comparison

to non-exposed control populations (P=0.002). In contrast, when exposed at half this irradiance (0.5 mW cm^{-2}), double this exposure time (2 h; 3.6 J cm^{-2}) was required to achieve a significant reduction of 70.3% (P=0.008). Likewise, when exposed at the lowest irradiances of 0.15 and 0.05 mW cm^{-2}, greater exposure times of 4 h (2.16 J cm^{-2}) and 6 h (1.08 J cm^{-2}) were required to achieve significant reductions of 30.1% (P=0.025) and 15.2% (P=0.019), respectively. Furthermore, the exposure times required to achieve near-complete inactivation were shown to be significantly shorter when higher irradiance light sources were used (P≤0.05): 2 h (7.2 J cm^{-2}) was required to achieve a 99.0% reduction at the highest irradiance of 1 mW cm^{-2}; 4 h (7.2 J cm^{-2}) and 6 h (5.4 J cm^{-2}) were required to achieve similar reductions at irradiances of 0.5 and 0.25 mW cm^{-2}, respectively, and up to 18 h was required to achieve similar levels of reduction at the two lowest irradiances (0.15 and 0.05 mW cm^{-2}; equivalent to doses of 9.72 J cm^{-2} and 3.24 J cm^{-2}, respectively).

For *P. aeruginosa* (Figure 4.10B), inactivation kinetics demonstrate that, similar to *S. aureus*, 1 h exposure to the highest irradiance resulted in a significant 89.5% reduction compared to non-exposed control populations (P<0.005). When exposed at lower irradiances of 0.5 and 0.25 mW cm^{-2}, double this exposure time was required to achieve significant reductions of 93.7% (P<0.005) and 75.6% (P=0.03), respectively. Using the lowest irradiance of 0.05 mW cm^{-2}, a 24 h exposure was required to achieve a statistically significant 15% reduction in *P. aeruginosa* (P=0.022). Similar to *S. aureus*, the exposure times required to achieve complete/ near-complete (≥95%) inactivation of *P. aeruginosa* were shown to be significantly shorter when higher irradiance light sources were used (P≤0.05): 2 h (7.2 J cm^{-2}) was required to achieve a 99.7% reduction at the highest irradiance of 1 mW cm^{-2}; 3 h (5.4 J cm^{-2}) achieved similar reductions (97.5%) using 0.5 mW cm^{-2}; complete reductions were achieved between 6 and 18 h following exposures to 0.25 mW cm^{-2} (5.4-16.2 J cm^{-2}) and 0.15 mW cm^{-2} (3.24-9.72 J cm^{-2}); and complete reduction was not achieved using 0.05 mW cm^{-2} within the exposure times of this study (maximum reduction of 15% demonstrated following 24 h).

Table 4.1 presents a comparison of the doses required to achieve significant levels of reduction (P≤0.05) and complete/near-complete (≥95%) inactivation of both *S. aureus* and *P. aeruginosa* upon exposure to each irradiance application.

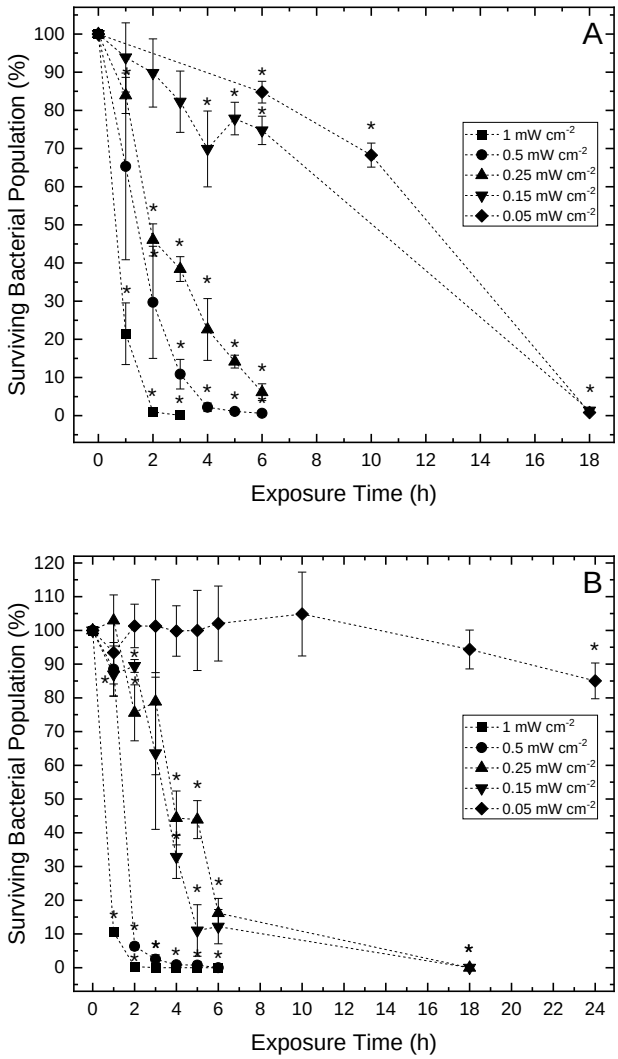

Figure 4.10 Inactivation kinetics of (A) *Staphylococcus aureus* and (B) *Pseudomonas aeruginosa* seeded on agar surfaces and exposed to 405-nm light at irradiances of 0.05, 0.15, 0.25, 0.5 and 1 mW cm^{-2}. Each data point represents the mean value ± SD (n = 3). Asterisks (*) represents points where the triplicate CFU plate^{-1} counts were significantly different between test and control samples (P≤0.05).

Table 4.1 Doses required to achieve significant reductions (P≤0.05) and complete/near-complete (≥95%) inactivation of *Staphylococcus aureus* and *Pseudomonas aeruginosa* upon exposure to each irradiance.

Irradiance (mW cm^{-2})	***S. aureus***		***P. aeruginosa***	
	Significant (P≤0.05) inactivation	**Complete (≥95%) inactivation**	**Significant (P≤0.05) inactivation**	**Complete (≥95%) inactivation**
0.05	6 h / 1.08 J cm^{-2}	18 h / 19.4 J cm^{-2}	18 h / 19.4 J cm^{-2}	N/A
0.15	4 h / 2.16 J cm^{-2}	18 h / 9.72 J cm^{-2}	1 h / 0.54 J cm^{-2}	18 h / 9.72 J cm^{-2}
0.25	1 h / 0.9 J cm^{-2}	6 h / 5.4 J cm^{-2}	2 h / 1.8 J cm^{-2}	18 h / 16.2 J cm^{-2}
0.5	2 h / 3.6 J cm^{-2}	4 h / 7.2 J cm^{-2}	2 h / 3.6 J cm^{-2}	3 h / 5.4 J cm^{-2}
1	1 h / 3.6 J cm^{-2}	1 h / 3.6 J cm^{-2}	1 h / 3.6 J cm^{-2}	2 h / 7.2 J cm^{-2}

Figures 4.11A and B present the inactivation kinetics of *S. aureus* and *P. aeruginosa*, respectively, on agar surfaces upon exposure to the 405-nm light EDS at varying radial distances (Δs = 1.6-2.56 m; ΔΘ = 0-51.3) for durations of 4, 8 or 24 h. Results comprehensively demonstrate that as the distance from the light source is increased, irradiance decreases, which in turn results in a decrease in the level of inactivation achieved. However, results also demonstrate that significantly greater bacterial reductions occurred as the exposure time to a particular irradiance increased ($P<0.05$).

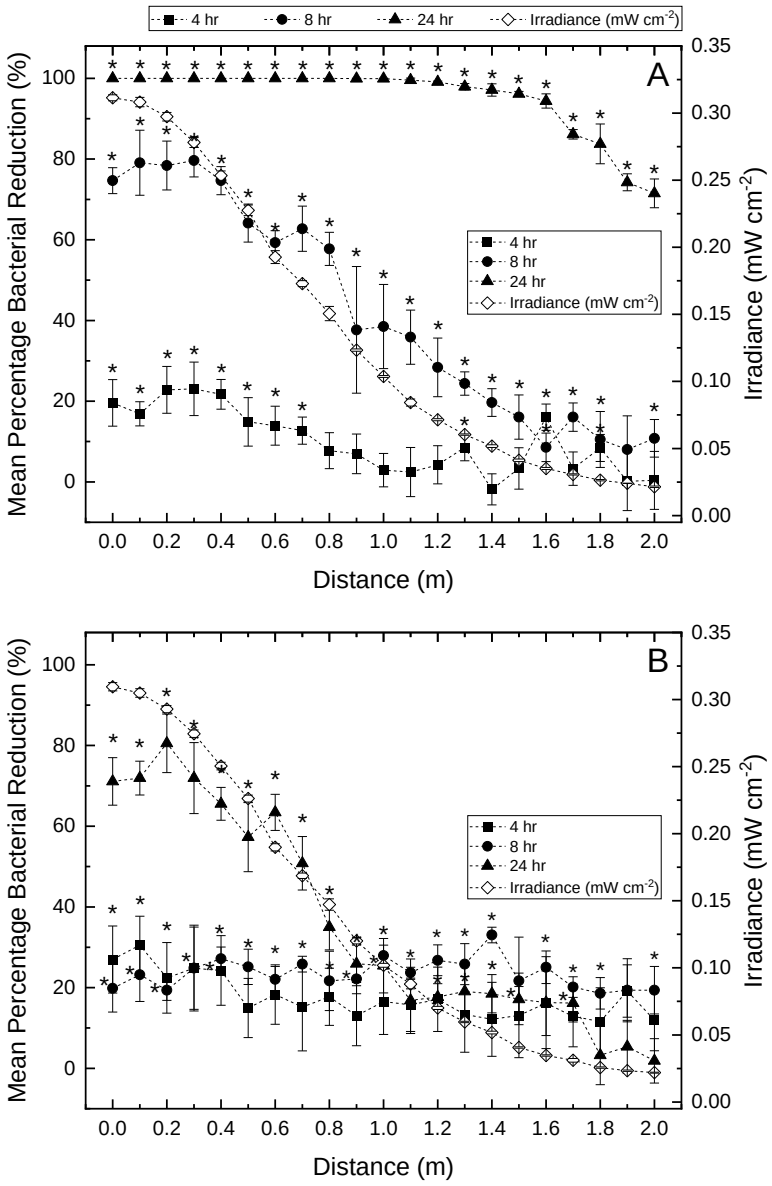

Figure 4.11 Inactivation kinetics of (A) *Staphylococcus aureus* and (B) *Pseudomonas aeruginosa* seeded on agar surfaces and exposed to a low irradiance 405-nm light source at distances ranging from directly below the light source (0 m) up to 2 m. Each data point represents the mean value ± SD (n = 6). Asterisks (*) represents points where the triplicate CFU plate^{-1} counts were significantly different between test and control samples ($P<0.05$).

When *S. aureus* samples (Figure 4.11A) were positioned directly below the light source (providing an approximate irradiance of 0.311 mW cm^{-2}), reductions of 19.6, 74.7 and 100% were achieved after exposure to the light source for 4, 8 and 24 h, respectively. In contrast, when the samples were positioned at this same distance of 1.6 m below the light source, but at 2 m off centre (providing an approximate irradiance of 0.021 mW cm^{-2}), reductions of 0.37, 10.79 and 71.51% were achieved after exposure to the light source for 4, 8 and 24 h, respectively. Following a 4 h exposure, results demonstrate that significant levels of inactivation (reductions ranging from 12.7-23.1%; $P<0.05$) were observed at distances ranging from directly below the light source to 0.7 m off centre, where samples were illuminated at irradiances ranging from 0.17-0.31 mW cm^{-2}. Exceeding this distance, where irradiances illuminating the samples were ≤0.15 mW cm^{-2}, no significant reductions in *S. aureus* populations were observed, with the exception of exposures at distances of 1.3, 1.6 and 1.8 m, where it is assumed that significant differences ($P=0.021$, 0.003 and 0.023, respectively) were obtained due to sample variability. When the exposure time was increased to 8 h, significant levels of inactivation (reductions ranging from 8.6-79.6%; $P<0.05$) were observed at all distances up to 1.7 m from the light source, whereby irradiances illuminating samples was as low as 0.03 mW cm^{-2}. Exposures at a distance of 1.8 and 1.9 m resulted in reductions of 10.52% ($P=0.085$) and 8.03% ($P=0.223$), respectively; however, exposure at a distance of 2 m resulted in a reduction of 10.8% which was found to be significantly different from the non-exposed control populations ($P=0.026$). Following the longest exposure time of 24 h, significant *S. aureus* reductions (71.5-100%; $P<0.0001$) were observed at all distances from the light source in comparison to non-exposed equivalent control populations.

The inactivation kinetics for *P. aeruginosa* (Figure 4.11A) demonstrated that when positioned directly below the light source (~0.311 mW cm^{-2}), reductions of 27, 19.8 and 71.1% were achieved following 4, 8 and 24 h exposure, respectively. In contrast, when the samples were positioned at this same distance of 1.6 m below the light source, but at 2 m off centre (~0.021 mW cm^{-2}), reductions of 11.9, 19.4 and 1.9% were achieved after exposure for 4, 8 and 24 h, respectively. Following a 4 h exposure, results demonstrate that significant levels of inactivation (reductions ranging from 22.4-30.5%; $P<0.05$) were observed at distances ranging from directly below the light source to 0.4 m off-centre, where samples were illuminated at irradiances ranging from 0.25-0.31 mW cm^{-2}. Exceeding this distance, where irradiances illuminating the samples were ≤0.23 mW cm^{-2}, no significant reductions were observed

(P>0.05). When exposed for a greater time of 8 h, significant reductions (18.6-27.9%; P<0.05) were observed at all distances from directly underneath to 2 m off centre from the light source. Exposed for the longest time of 24 h, significant levels of bacterial reduction (16.2-80.5%; P<0.05) were observed up to a distance of 1.7 m from the light source; beyond this distance, no significant reductions were observed (P=0.158-0.621).

4.5 Discussion

The experiments performed in this chapter were designed to provide a characterisation of the optical output profile of a ceiling-mounted low irradiance 405-nm light EDS within a typical room setting and demonstrate the broad-spectrum efficacy of 405-nm light employed at these low irradiance levels against a range of significant HAI-causing bacteria, at populations comparable with typical contamination levels found on indoor environmental surfaces.

It is widely acknowledged that bacterial contamination of environmental surfaces plays a significant role in the indirect transmission of infection within healthcare facilities (Kramer and Assadian, 2014). Physical cleaning within these environments is imperative, however, due to routine working practice, there is continual generation of environmental contamination in the air and on surfaces between cleans which can be further exacerbated by activities such as bed/dressing changes (Dougall *et al.*, 2019). As such, the ability to implement an infection control technology which addresses bacterial generation and dispersal in real-time is of significant interest. As discussed, recent publications have established the efficacy of 405-nm light EDS units to reduce bacterial contamination levels within clinical settings (Maclean *et al.*, 2010, 2013a; Bache *et al.*, 2012a, 2018a; Murrell *et al.*, 2019). These studies have successfully highlighted the practical efficacy of these systems within dynamic ward environments, where contamination levels are likely to vary with room activity (Dougall *et al.*, 2019) and the pathogenic potential of environmental bacteria is largely unknown. Full knowledge of the inactivation efficacy of the low irradiance 405-nm light ranges produced by these systems in whole-room environments, for the inactivation of key infection-inducing bacteria, however, is required. Accordingly, this chapter aimed to address this, using surface-seeded bacterial pathogens in a controlled laboratory setting.

The optical output profile of a 405-nm light EDS unit was initially characterised to enhance knowledge of the typical irradiance levels likely to illuminate surfaces and the air in the exposed environment. The dimensions of the profiled area were selected in accordance with Health Building Note 00-03, which advises that single-bed rooms, and each bed space in multi-bed rooms, within general NHS clinical spaces should be between 3-4 m in both length and diameter to enable adequate space for appropriate facilities and necessary room activities (Department of Health, 2013). Of the irradiance levels produced within this area (0.001-2.016 mW cm^{-2}), 88.2% of measurements were found to be <0.1 mW cm^{-2}, 4.6% were 0.1-0.2 mW cm^{-2}, 4.0% were 0.2-0.3 mW cm^{-2}, 2.2% were 0.3-0.4 mW cm^{-2} and 2.2% were >0.4 mW cm^{-2} (Figure 4.6). In all cases, irradiance levels were found to be highest in the areas directly underneath the light source, and lowest at the outermost points measured.

For further analysis, the relationship between irradiance and both linear and angular displacement from the light source was determined (Figures 4.6A and B, respectively). Results in Figure 4.6A indicate that irradiance output decreased linearly as linear displacement from the EDS increased. As demonstrated in Figure 4.6B, light irradiance distribution patterns are strongly influenced by angular displacement from the 405-nm light EDS, with general trends indicating a decrease in irradiance output as angular displacement from the unit increases in both X and Y directions. As previously mentioned, the LED matrices within 405-nm light EDS units are covered by an optical lens system, comprising a Fresnel lens and diffuser to aid in light distribution and scatter, respectively, which are designed to be a sufficient size to uniformly treat a surface area of approximately 10 m^2 at a distance of 2 m from the unit (Anderson *et al.*, 2008; Endarko, 2011). It may be the case that numerous light sources are required to achieve sufficient levels of decontamination across larger areas, however previous studies have reported comparable levels of reduction when using either one or two light sources, suggesting one 405-nm light EDS may be just as effective as two if used for a sufficient length of time (Maclean *et al.*, 2010; Bache *et al.*, 2012a, 2018a). It is important to consider the influence of both linear and angular displacement from the light source, however, as the relative decrease in bacterial bioburden has shown to be greater in areas closer to the light source (Maclean *et al.*, 2013a). In addition, only surfaces which are directly or reflectively illuminated by the 405-nm light EDS will be treated, and thus it is important to emphasise that this technology should be utilised as a complementary approach in conjunction with established cleaning procedures. Nevertheless, these findings provide an indication of the typical

irradiance levels produced spatially by these systems, and thus a greater understanding of the illumination that can be expected to expose pathogens within the environment.

To investigate the broad-spectrum bactericidal efficacy of the 405-nm light EDS, bacteria were exposed at a distance of approximately 1.5 m from the light source, which corresponded to an irradiance of 0.5 mW cm^{-2}. This was selected to represent the approximate distance between the room ceiling and frequently-touched, thus likely to be contaminated, surfaces within a typical room environment. Bacteria were exposed whilst seeded onto surfaces, rather than in liquid suspension, to mimic surface contamination within occupied environments. The ability of 405-nm light to successfully inactivate high microbial population densities in liquid suspension has previously been indicated in studies by Maclean *et al*. (2009), which showed a 9-log_{10} reduction of *S. aureus*, and Dai *et al*. (2013), which demonstrated an approximate 8-log_{10} reduction of *P. aeruginosa*; however, this study focussed on the inactivation of low-density bacterial populations (10^2 CFU $plate^{-1}$/2-5 CFU cm^{-2}) to replicate the typical levels of bacterial contamination likely to be found on environmental surfaces (Maclean *et al.*, 2013a). In addition, the current study employed low irradiance levels and long exposure times to reflect those used by 405-nm light EDS units within occupied settings to achieve a disinfection effect. As previously mentioned, 405-nm light EDS units are designed specifically for continuous use in the presence of people, and thus require low irradiance levels, in the region of those used in the present study, to be safely employed. A more rapid inactivation effect can be achieved with use of higher irradiances, as detailed in previous studies which use irradiances in the region of 10's – 100's mW cm^{-2} for bacterial inactivation (Hamblin *et al.*, 2005; Enwemeka *et al.*, 2008; Maclean *et al.*, 2009; Murdoch *et al.*, 2012; Wasson *et al.*, 2012). However, this study aimed to elucidate the efficacy of low irradiance (<1 mW cm^{-2}) 405-nm light under conditions representative of those used for whole-room decontamination.

Exposure conditions play a significant role in microbial susceptibility to 405-nm light treatment, with studies demonstrating an enhanced effect observed when exposed on inert surfaces, including PVC and acrylic, as opposed to nutritious agar surfaces (Murdoch *et al.*, 2012), and when exposed in biological media, including saliva, blood plasma and faeces, as opposed to minimal media (Tomb *et al.*, 2014, 2017b). The exposure conditions on indoor environmental surfaces are extremely variable, ranging from being completely clean to being contaminated with variable levels of organic and inorganic residues, and so this study utilised general purpose nutrient agar to establish a highly reproducible baseline of the

bacterial inactivation which can be achieved using the 405-nm light EDS. Although this media may contain photosensitive material which could augment the 405-nm light inactivation process, it also provides a more nutritious environment which supports the growth of a broad-spectrum of bacteria and so is likely to provide greater protection from oxidative stress than that of inert surfaces. Accordingly, it is expected that bacterial contamination, when present either on clean inert surfaces or in biological residues e.g. bacterial cells in saliva droplets, will demonstrate even greater susceptibility than that shown here, and so future work to assess this will be important to fully evaluate the efficacy of this technology.

Results in Figure 4.8 demonstrate that exposure to 405-nm light at an irradiance of ~0.5 mW cm^{-2} successfully inactivated all bacteria contaminated on agar surfaces, with ~2 log_{10} reductions (≥93.28% inactivation) achieved following delivered doses of 3.6-28.8 J cm^{-2}. The organisms selected in this study represent five of the twelve global WHO priority pathogens, including all of those appointed critical status, which together pose the greatest threat to human health and urgently require novel therapeutics (WHO, 2017). The findings of this study provide evidence to demonstrate the susceptibility of these key bacterial pathogens to inactivation by the 405-nm light EDS within practical exposure periods. The demonstration that low irradiance 405-nm light has wide antimicrobial activity against all tested organisms within a typical day of use indicates that, in addition to being applicable for environmental disinfection of clinical environments as shown previously (Maclean *et al.*, 2010, 2013a; Bache *et al.*, 2012a, 2018a; Murrell *et al.*, 2019), 405-nm light could also be employed for more widespread disinfection applications associated with environmental cleaning and public health (Kenall Manufacturing, 2017; Hubbell Lighting, 2020).

Comparatively, the Gram-positive and Gram-negative species investigated demonstrated relatively similar patterns of inactivation: for the Gram-positive bacteria, *S. aureus* required 2 h exposure for near-complete reductions (99.2%), whilst *E. faecium* required 16 h exposure for a 93.3% reduction; and the Gram-negative bacteria required 3-9 h to achieve near-complete reductions (≥96.1%), with the exception of *K. pneumoniae* which required 16 to achieve a similar reduction (97.5%). Interestingly, this contrasts with previous studies investigating 405-nm light susceptibility of high population bacterial densities (>10^5 CFU ml^{-1}) in liquid suspension, which reported an increase in the susceptibility of Gram-positive versus Gram-negative organisms (Maclean *et al.*, 2009; Murdoch *et al.*, 2012; McDonald *et al.*,

2013). However, in these previous studies bacteria were exposed at high irradiance levels in non-nutritious diluents for usually short exposure periods (min rather than h) whereas in the present study, low irradiances were used to inactivate low density populations, seeded onto nutritious surfaces and exposed over longer periods (up to 16 h in some cases). It is highly likely that such major differences in exposure conditions will have had metabolic and physiological effects on exposed bacteria and such factors might have affected the bacterial susceptibility to 405-nm light.

Differences in the inactivation achieved between species exposed under similar conditions is hypothesised to be due to variations in both the distribution and quantity of endogenous porphyrins produced by bacterial cells (Nitzan *et al.*, 2004). Coproporphyrin is believed to produce the majority of free radicals to actuate inactivation and *S. aureus* has previously been shown to produce coproporphyrin at 2-3 times the rate of *E. coli* (Nitzan *et al.*, 2004), which suggests that *S. aureus* may be more susceptible than *E. coli* to 405-nm light inactivation. Maclean *et al*. (2016) reported that the dose required to inactivate *E. coli* was 4 times greater than that of *S. aureus*, which is in agreement with findings in this study which demonstrated that 4.5 times less dose was required by *S. aureus* in comparison to *E. coli* to achieve near-complete reductions (≥96.1%). It should be noted, however, that other cellular factors, such as metallic bioburden, the presence and/or addition of a cell envelope and bacterial response to free radicals, are also likely to be effectual in the rate of bacterial inactivation (Murdoch *et al.*, 2012; Kumar *et al.*, 2015).

General trends indicate that *A. baumannii*, *S. aureus* and *P. aeruginosa* were the most susceptible to inactivation, each requiring 2-3 h exposure for a 1 $\log_{10}$ reduction, whilst *E. faecium* and *K. pneumoniae* were the least susceptible, each requiring longer 16 h exposures for similar reductions. These findings can be considered consistent with previous 405-nm light inactivation studies. Maclean *et al*. (2009) investigated the susceptibility of a range of medically important bacteria and found *S. aureus* the most susceptible to inactivation, with *K. pneumoniae*, *E. coli* and *E. faecalis* requiring higher doses for a 1 $\log_{10}$ reduction. Interestingly, in this previous study, *P. aeruginosa* was found to be one of the more resilient species to inactivation, but this was not the case in this present study, possibly due to differences in the exposure conditions. Interestingly, a more recent study by Hoenes *et al.* (2021) investigated the susceptibility of the ESKAPE pathogens in liquid suspension (10^7-10^8 CFU mL^{-1}) and found, similar to this present study, that *A. baumannii*, *S. aureus* and *P. aeruginosa* required the lowest doses to achieve

a 1 $\log_{10}$ reduction. Also, similar to the present study, the authors noted that *E. faecium* and *K. pneumoniae* were the least susceptible to treatment, and that *E. coli* was less susceptible than other strains (Hoenes *et al.*, 2021).

The aforementioned studies utilised higher irradiances than that employed here (10-71 mW cm^{-2} compared to 0.5 mW cm^{-2}), suggesting the comparative susceptibility of each species to light treatment is independent of light irradiance application. In addition to this, these studies required substantially higher doses than those utilised in the present study to achieve similar reductions. In this study, ~2 $\log_{10}$ reductions were achieved with doses as little as 3.6 J cm^{-2} (2 h exposure to 0.5 mW cm^{-2}). In contrast, Murdoch *et al*. (2012), who employed an irradiance of 71 mW cm^{-2} for low density surface-seeded populations, required doses in the region of 180-270 J cm^{-2} to achieve similar reductions. Although direct comparisons cannot be made between the results of this study and those of high-density liquid-suspended populations, it is worth noting that Maclean *et al*. (2009) required 27 J cm^{-2} for a 2 $\log_{10}$ reduction of *S. aureus*, whilst just 3.6 J cm^{-2} was required here, and Hoenes *et al*. (2021) required 525 J cm^{-2} for a 1 $\log_{10}$ reduction of *E. faecium*, whilst just 28.8 J cm^{-2} was required here; with both studies utilising 10 mW cm^{-2} for exposures compared to just 0.5 mW cm^{-2} used here.

Given that the irradiances produced across a standard room setting were shown to vary between 0.001-2.066 mW cm^{-2} (Figure 4.6), five light irradiances (0.05, 0.25, 0.5, 0.75 and 1 mW cm^{-2}) within this range were selected for exposure to determine the effects of varying low levels of irradiance on bacterial inactivation (Figure 4.10; Table 4.1). *S. aureus* and *P. aeruginosa* were again chosen as model organisms for this study due their frequency as surface contaminants in hospitals (Dancer, 2008; Sukhum *et al.*, 2022). Results demonstrate reductions of both species in all cases, with greater levels achieved as light dose was increased. Results for *S. aureus* (Figure 4.10A; Table 4.1) highlight that considerably shorter treatment times were required to achieve significant levels of bacterial reduction when exposed at higher irradiances: an initial significant degree of reduction and near-complete reduction took approximately 6 and 18 times longer, respectively, when exposed at the lowest irradiance (0.05 mW cm^{-2}) compared to the highest irradiance (1 mW cm^{-2}). Similarly, for *P. aeruginosa* (Figure 4.10B; Table 4.1), results also indicate that considerably shorter exposure times were required to achieve significant bacterial reductions when exposed at higher irradiances. In this case, approximately 18 times longer exposures were required to achieve an initial significant degree of reduction when exposed at the

lowest irradiance (0.05 mW cm^{-2}) compared to the highest irradiance (1 mW cm^{-2}). Complete/near-complete reductions took up to 9 times longer when exposed at 0.15 mW cm^{-2} compared to the highest irradiance (1 mW cm^{-2}), with complete/near-complete reductions not achieved within the 24 h sampling period when exposed at the lowest irradiance level (0.05 mW cm^{-2}; maximum reduction of 15% recorded). Interestingly, however, results in Figure 4.10 and Table 4.1 also demonstrate in some cases, per-unit-dose, an increased efficacy of inactivation when exposed at lower irradiances. For *S. aureus*, approximately 3.3 times lower dose (1.08 versus 3.6 J cm^{-2}) was required to achieve significant levels of reduction ($P \leq 0.05$) when exposed at the lowest irradiance (0.05 mW cm^{-2}) compared to the highest irradiance (1 mW cm^{-2}), respectively. Similar patterns were observed for *P. aeruginosa*, whereby, comparing 0.15 mW cm^{-2} and 1 mW cm^{-2} exposures, 6.6 times lower dose was required to achieve significant levels of reductions ($P \leq 0.05$) when exposed using the lower irradiance treatment (0.54 versus 3.6 J cm^{-2}, respectively).

On this basis, it is possible that lower irradiance 405-nm light, similar to that employed by the 405-nm light EDS, may be more efficient in comparison to that of higher irradiance exposures for the inactivation of bacteria on a per-unit-dose basis. It is possible that these differences may be due to the specific energy levels required to induce photoexcitation of porphyrin molecules within exposed bacterial cells, and that the use of higher irradiances may be inefficient due to the porphyrin photoexcitation pathway becoming saturated in the presence of excess photons which may not contribute to the inactivation process; whereas with lower irradiances the photons may be utilised more effectively with less photon wastage (Maclean *et al.*, 2016). This mechanism may also explain the less apparent differences in susceptibility between the Gram-positive and Gram-negative bacterial species tested in this study compared to previously published work which used higher irradiances (Maclean *et al.*, 2009; Murdoch *et al.*, 2012; McDonald *et al.*, 2013). Although beyond the scope of this chapter, the potential increase in inactivation efficacy per-unit-dose when using lower irradiance treatments, similar to that employed by the 405-nm light EDS, is of significant research interest, and will be investigated further in Chapter 6.

In addition to determining the broad-spectrum bactericidal efficacy of the 405-nm light EDS at a fixed position, this study evaluated bacterial inactivation kinetics at varying distances from the light source and at varying irradiances which could typically be expected at different positions within a whole-room

environment. *S. aureus* and *P. aeruginosa* were again chosen as model organisms for this study. Results in Figure 4.11 demonstrate that the irradiance decreased from approximately 0.310-0.311 mW cm^{-2} directly 1.6 m below the light source to 0.021-0.022 mW cm^{-2} when placed 2 m off centre (Δs=2.56 m). The extent of inactivation achieved per unit exposure time was also shown to decrease as distance from the centre of the light source increased. For *S. aureus* (Figure 4.11A), an initial exposure of 4 h demonstrated a 19.58% reduction directly underneath the light source (0.311 mW cm^{-2} irradiance) in comparison to just a 0.38% reduction underneath the light source at a distance of 2 m off-centre (0.021 mW cm^{-2} irradiance). A similar, although less pronounced, effect was demonstrated for *P. aeruginosa* (Figure 4.11B), where 4 h exposure demonstrated a 26.96% reduction directly underneath the light source (0.310 mW cm^{-2} irradiance) in comparison to a 11.93% reduction underneath the light source at a distance of 2 m off-centre (0.022 mW cm^{-2} irradiance). These results agree with previous work by this laboratory demonstrating that inactivation levels significantly decrease as distance from the 405-nm light source increases (Endarko, 2011). Results of this study do, however, also demonstrate that, regardless of distance from the light source, the level of inactivation achieved increases as the time of exposure is increased. Following an 8 h exposure of *S. aureus* (Figure 4.11A), significant bacterial reductions were achieved at distances approximately 2.6 times greater than that achieved after 4 h exposure (0.7 m off-centre in comparison to 1.8 m off-centre; $P<0.05$). When this was further increased to a 24 h exposure, significant bacterial reductions were demonstrated up to 2 m from the light source: 2.9 times greater than after the original 4 h exposure ($P<0.05$). For *P. aeruginosa* (Figure 4.11B), significantly greater reductions were achieved at distances up to five times greater when exposed for 8 and 24 h compared to 4 h (0.4 m off-centre in comparison to 2 and 1.7 m off-centre, respectively; $P<0.05$). A strong correlation between bacterial kill and exposure time to 405-nm light EDS units has previously been demonstrated on various surfaces within clinical settings (Maclean *et al.*, 2010; Bache *et al.*, 2018a) and this study confirms that pathogenic bacteria exposed under controlled laboratory conditions behave in a similar manner.

On comparison of the results in Figures 4.10 and 4.11, *P. aeruginosa* was shown to demonstrate lower susceptibility than that of *S. aureus* to 405-nm light when exposed at lower irradiance levels. The inactivation kinetics in Figure 4.10 show that, when exposed at the lowest irradiance of 0.05 mW cm^{-2}, an 18 h exposure resulted in 99.2% reduction for *S. aureus*, in comparison to just a 5.7% reduction for

P. aeruginosa. Similarly, for the results provided in Figure 4.11, 4 h exposure resulted in significant ($P<0.05$) bacterial reductions at distances approximately 1.75 times greater for *S. aureus* in comparison to *P. aeruginosa* (up to distances of 0.7 m compared to 0.4 m, respectively), and reductions following 24 h directly underneath the light source were 1.4 times greater for *S. aureus* (100% inactivation) in comparison to *P. aeruginosa* (71.1% inactivation). These findings are in agreement with the exposures conducted in Figure 4.8, where results showed that after 1 h exposure to 405-nm light at an irradiance of 0.5 mW cm^{-2}, *S. aureus* was reduced by 79.3% whilst *P. aeruginosa* was reduced by just 11.4%. These differences in inactivation observed for the two species may be due to variations in the distribution and quantity of endogenous porphyrins produced by bacterial cells, as previously discussed (Nitzan *et al.*, 2004).

Although collectively Figures 4.10 and 4.11 indicate that the treatment times required to achieve significant bacterial inactivation are prolonged at lower irradiance, results importantly also demonstrate that inactivation was still achievable at the lowest irradiances investigated and, given the continuous operational nature of the 405-nm light EDS, it is expected that sufficient inactivation would occur even at these lower irradiance exposures; further justifying the utilisation of the 405-nm light EDS for the decontamination of whole-room environments. Recent work by Bache *et al.* (2018) investigated the relationship between the bacterial inactivation achieved on surfaces around a hospital burns unit using a 405-nm light EDS and the irradiance received at each surface site and found that, following 7 consecutive days of use, there was no significant correlation. The authors sampled seventy sites, whereby incident irradiances ranged from 0.0023-0.2310 mW cm^{-2}, and observed consistent reductions regardless of the irradiance received at that site (Bache *et al.*, 2018). This was hypothesised to be due to the aerial decontamination effect: due to their closer proximity to the light source, airborne bacteria will be exposed to higher irradiances than that of surface-seeded bacteria, and therefore will be inactivated quicker – then, given they will be precipitated on surfaces at random, little correlation would be expected between inactivation and levels of irradiance received at the surface site (Bache *et al.*, 2018a). These results, coupled with those in Figures 4.10 and 4.11, further justify utilisation of the 405-nm light EDS for the decontamination of whole-room environments. Given its high safety profile, they can be installed as an overhead light source (Kenall Manufacturing, 2017) and utilised continuously

without posing a disturbance to room activity, with increased inactivation occurring as exposure time is increased (Maclean *et al.*, 2010, 2013a; Bache *et al.*, 2012a, 2018a; Murrell *et al.*, 2019).

It is important to mention that the inactivation kinetics presented in this study are representative of organisms which have been cultured under optimal conditions. Bacterial populations were cultured at 37°C in growth media and then exposed to the 405-nm light EDS on nutrient agar surfaces; cultivation and exposure conditions which exert minimal stress on the organisms. Importantly, laboratory studies have demonstrated that stressed organisms show increased susceptibility to 405-nm light inactivation (McKenzie *et al.*, 2014). Thus, when used practically for inactivation of bacterial contamination on environmental surfaces, such as in the case of hospital room disinfection (Maclean *et al.*, 2010, 2013a; Bache *et al.*, 2012a, 2018a; Murrell *et al.*, 2019), inactivation kinetics are likely to be enhanced. Organisms can remain on environmental surfaces for prolonged periods of time, with up to 90 days recorded previously in the case of staphylococci and enterococci (Neely and Maley, 2000), but these organisms will be stressed due to desiccation, starvation, and in some cases, sublethal exposure to disinfectants, and these concurrent stresses will likely increase microbial susceptibility to decontamination using 405-nm light. By exposing bacteria under controlled laboratory conditions with minimal stress factors, this study importantly demonstrates the likely exposure times required to inactivate key bacterial pathogens under 'worst-case scenario' conditions, with inactivation expected to be enhanced when used in practice.

Further considering the work of this study towards practical application in 'real' environments, it has been demonstrated here that bacterial contamination on surfaces – in this case, agar surfaces – can be effectively inactivated. However, it is also of interest to examine the efficacy of low irradiance 405-nm light for the inactivation of bacteria presented under conditions realistic to the healthcare environment. Previous publications have demonstrated that 405-nm light exposure, albeit at higher irradiance levels (110 mW cm^{-2}), is effective for the inactivation of bacteria on inert surfaces such as glass, acrylic and PVC (Murdoch *et al.*, 2012); and indeed the studies demonstrating the efficacy of low irradiance 405-nm light for disinfection of hospital isolation rooms collected samples from a wide range of surfaces and materials including door handles, table/locker surfaces, bed rails, computer keyboards/mouse and light switches (Maclean *et al.*, 2010, 2013a; Bache *et al.*, 2012a, 2018a; Murrell *et al.*, 2019). Developing an understanding of the efficacy of the 405-nm light EDS for the inactivation of bacteria

on common hospital surface materials, conducted under controlled laboratory conditions, is of significant research interest. Furthermore, the ability of 405-nm light to inactivate bacterial biofilm populations, which are of significant concern in the healthcare environment due to their persistence in the presence of thorough cleaning regimes, is an area of increasing research interest. McKenzie *et al*. (2013) previously reported successful reductions of *E. coli* biofilms on glass and acrylic surfaces using 405-nm light, with up to 7-$\log_{10}$ reductions observed following 1 h exposure to 140 mW cm^{-2}, however the ability of low irradiance 405-nm light, similar to that produced by the 405-nm light EDS, for the inactivation of bacterial biofilms remains broadly unknown. In addition, given current concerns associated with antimicrobial resistance, it is of interest to determine the susceptibility of MDR bacterial strains to 405-nm light inactivation. Maclean *et al.* (2009) successfully demonstrated the ability of 405-nm light (10 mW cm^{-2}) to inactivate MRSA, requiring just 1.25 times greater dose for a 5 $\log_{10}$ reduction than that of MSSA. Resistance development to 405-nm light is yet to be demonstrated, and it is believed to be unlikely due to its non-specific oxidative mechanism of inactivation and its vast array of cellular targets (Tomb *et al.*, 2017a). Regardless, an examination of the efficacy of the 405-nm light EDS to inactivate MDR strains, which are likely to be present within the hospital environment, is of significant interest. These areas of future study will be essential to further justify the prolonged use of these systems across the infection control sector, and thus some of these key consideratios will be investigated in greater detail in Chapter 5.

4.6 Conclusions

Overall, this chapter has successfully characterised the optical output and antibacterial efficacy of a low irradiance 405-nm light system designed for environmental decontamination applications under controlled laboratory conditions. Key findings associated with this chapter are detailed as follows:

- The optical output profile of a 405-nm light EDS was successfully characterised within a 4 × 4 × 2 m area, with the range of irradiances produced within this area found to be 0.001-2.016 mW cm^{-2}.
- The broad-spectrum antimicrobial efficacy of 405-nm light employed at a representative irradiance within this range (0.5 mW cm^{-2}) was demonstrated for the inactivation of low-

density populations of surface-seeded bacterial pathogens, known to be associated with HAIs, within exposure times realistic of those employed for whole-room decontamination (2-16 h).

- The effects of altering the distance of a surface-seeded bacterial samples from the light source, and thus the irradiance at which samples would be illuminated (0.021-1 mW cm^{-2}), were considered and, although differing levels of inactivation were demonstrated, complete (~2 log_{10}) reductions were still achievable, suggesting these factors will unlikely have a significant impact on the overall continuous decontamination effect achieved.

The irradiance levels (≤1 mW cm^{-2}) and large exposure distances (up to 2.56 m) used in this study, which are quite different to anything that has previously been described in the literature, have been used to provide a laboratory-based demonstration of the efficacy of 405-nm light for large scale environmental disinfection applications, as have been detailed by the previous studies carried out in the hospital environment (Maclean *et al.*, 2010, 2013a; Bache *et al.*, 2012a, 2018a; Murrell *et al.*, 2019). The findings of this chapter comprehensively advance knowledge of the 405-nm light EDS and its applicability for whole-room decontamination which, combined with its inherent safety benefits, furthers its widespread utilisation across the infection control sector.

CHAPTER 5

405-nm Light EDS Operational Considerations

5.0 Overview

This chapter builds upon the findings of the previous chapter by investigating the antibacterial efficacy of the 405-nm light EDS under various clinically-representative exposure conditions, with particular focus on spatial positioning and the surface presentation of exposed contamination.

5.1 Introduction

The ability of the 405-nm light EDS to reduce general contamination levels within clinical settings has been widely demonstrated (Maclean *et al.*, 2010, 2013a; Bache *et al.*, 2012a, 2018a; Murrell *et al.*, 2019), and findings in the previous chapter established its broad-spectrum bactericidal efficacy at irradiances typical of those illuminating high-touch surfaces within hospital rooms (0.5 mW cm^{-2}). For practical deployment, however, it is important to establish bacterial inactivation across a range of near-clinical exposure conditions.

In realistic settings, bacterial contaminants may be presented at varying distances from the light source, both on surfaces and in the air, and thus are likely to be illuminated by varying irradiances of 405-nm light (0.001-2.066 mW cm^{-2}; Chapter 4). It is therefore important to understand the bactericidal ability of the irradiances at the lower range of these values. Furthermore, although the exposures on agar surfaces performed in Chapter 4 provide a highly reproducible baseline of the bacterial inactivation which can be achieved using the 405-nm light EDS; in clinical environments, contamination will be present on inert surfaces which will likely exert substantially greater stress on the organisms. Previous studies have indicated an enhanced susceptibility of bacteria on inert versus agar surfaces to higher irradiances (~70 mW cm^{-2}) of 405-nm light inactivation (Murdoch *et al.*, 2012); however, this effect is yet to be established at lower irradiance applications. In addition, inert clinical surfaces are extremely

variable, ranging from being completely clean and dry, to soiled with variable levels of organic and inorganic residues. An enhancement in 405-nm light inactivation has been demonstrated in viruses exposed in biological media as opposed to minimal media (Tomb *et al.*, 2014, 2017b) – believed to be due to photosensitive components within such media acting as external photosensitisers and imparting local oxidative damage to the organisms – however, little is currently understood with respect to bacterial susceptibility under such conditions. Furthermore, bacterial biofilms – which are predominantly more resilient to disinfection than their planktonic counterparts (Maillard and Centeleghe, 2023) – are key drivers in HAI transmission (Vickery *et al.*, 2012; Costa *et al.*, 2019). They often reside in sinks, faucet aerators and shower heads; acting as microbial reservoirs which can disperse viable bacteria into the water stream and colonise patients, HCWs, environmental surfaces and medical equipment (Exner *et al.*, 2005). Exposure to higher irradiances (≥60 mW cm^{-2}) of violet-blue light has shown to successfully inactivate bacterial biofilms (McKenzie *et al.*, 2013; Soukos *et al.*, 2015; Wang *et al.*, 2016; Ferrer-Espada *et al.*, 2019, 2020); however, the efficacy of low irradiances, likely to be produced by the 405-nm light EDS for environmental decontamination, is widely unknown.

Given the diverse exposure conditions of indoor surfaces and their likely influence on microbial susceptibility to 405-nm light, this chapter evaluated the efficacy of the 405-nm light EDS for the inactivation of surface-seeded bacterial contamination under exposure contexts more representative of practical system deployment, as a means to further corroborate clinical efficacy and translatability. The experiments conducted in this chapter to fulfil these aims are as follows:

1. Design and implementation of a small-scale bench-top 405-nm light EDS prototype to enable exposure to irradiances within the range expected in a typical hospital isolation room which could be conducted practically at a distance of 0.5-1 m from the light source.

2. Establish the bactericidal efficacy of 405-nm light when employed at irradiances ≤0.1 mW cm^{-2} and determine, if any, a threshold irradiance below which no further inactivation occurs.

3. Establish inactivation efficacy of low irradiance (0.5 mW cm^{-2}) 405-nm light for bacteria suspended in minimal, organic and biologically-relevant media; and seeded on clinically-relevant surfaces.

4. Establish the efficacy of low irradiance (0.5 mW cm^{-2}) 405-nm light for inactivation, and inhibition of the development of, bacteria in monolayer and mature biofilms on microtiter plate wells and clinically relevant surfaces.

5.2 Miniaturisation of the 405-nm Light EDS for Bench-top Testing

An understanding of the efficacy of 405-nm light at the irradiance levels typically presented within an 32 m^2 standard isolation room (0.001-2.066 mW cm^{-2}; Chapter 4) is essential to comprehensively evaluate the performance of such systems. This, however, is challenging given the distances required to achieve such irradiances from the current 405-nm light EDS prototypes (up to 4.47 m; Chapter 4). To enable practical employment at bench-top level, a miniaturisation of the current 405-nm light EDS prototype, was developed.

5.2.1 Design Considerations of the Novel Unit

The purpose of this re-design was to enable laboratory testing of the 405-nm light EDS at the low irradiance levels ordinarily provided within a typical 32 m^3 room to be conducted at a smaller, bench-top scale. Towards achieving this, the following design criteria were appointed:

1. **Provision of light outputs ranging from 0.001-2.5 mW cm^{-2} at 0.5-1 m from the source.** This would enable antimicrobial testing at the irradiance levels ordinarily provided at much greater distances (≤4.47 m) by the original protype, to be conducted with greater ease at bench-top level.
2. **Reduction in overall system dimensions by 30-50%.** This would enable mounting on a bench-top test rig, and provide greater flexibility for transportation/use in various environments.
3. **Provision of lower power LED arrays than those currently employed with tuneable output irradiance via individual LED control through remote-control system and dimming function.** This would enable control of individual or combinational LED use, at varying brightness, thus maximising the range of irradiance levels which could be produced.
4. **Provision of uniform light spread across the testing area.** Given its smaller size, a uniform distribution of light across bacterial samples would be essential for inactivation data accuracy.

5.2.2 Build of the Miniaturised 405-nm Light EDS

The miniaturised 405-nm light EDS was designed and built by colleagues in the EEE workshop at the University of Strathclyde as part of an assignment for Design & Manufacture class E0400 (Bradley, 2022); considering the design criteria outlined in Section 5.2.1. The final design consisted of three 405-nm LED arrays (Mouser Electronics, UK) housed within a 30 × 30 cm aluminium plate – reducing overall unit size by 41% in comparison to previous prototypes – which were equally spaced by 15 cm in triangular formation; selected, based on pre-design irradiance scoping experiments, as the distance which provided the greatest uniformity of light distribution (Figure 5.1A). White LEDs, employed in the original 405-nm light EDS for aesthetic reasons, were not included in this prototype, as the focus of this study was to analyse antimicrobial capacity. Each array was driven by a 15V power supply (CPC Mean Well, UK) and contained a heat sink and fan (Novatech, UK) for thermal management, both driven by a PCB as opposed to drivers to conserve space in the housing (Figure 5.1B). A holographic light shaping diffuser (Luminit LLC, USA) with a 20° light shaping diffuser angle was used to cover the LED arrays to enhance light distribution across the testing area.

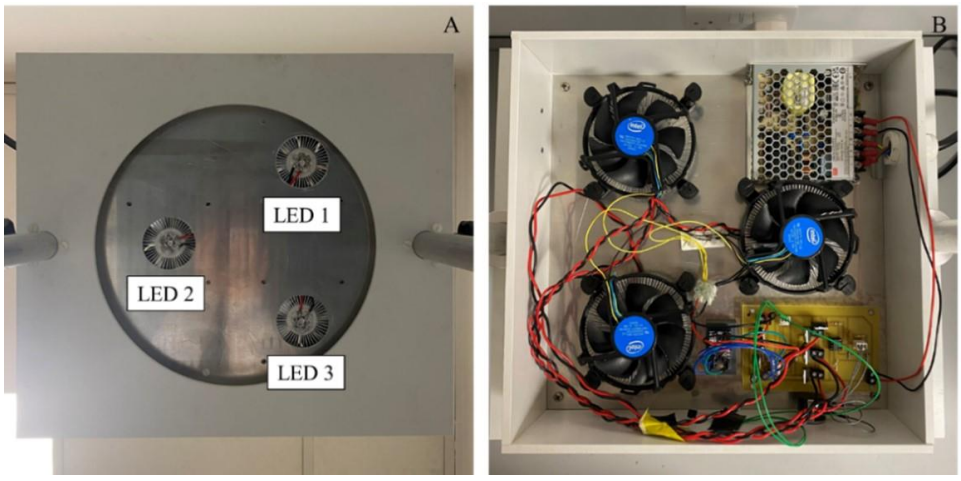

Figure 5.1 Miniaturised 405-nm light EDS: (A) Appearance of the lower side of the housing displaying the three LED arrays for exposure (LED 1, LED 2 and LED 3), and (B) appearance of the upper side of the housing displaying placement of the LEDs, fans, heatsinks, 15 V power supply, PCB and Arduino.

A remote control (Digi-Key, UK) was used to switch on either singular or multiple combinations of 405-nm LED arrays, as required, at any given time. The remote-control system was controlled by Arduino hardware and an infrared receiver contained within the system housing. The housing also contained a potentiometer for control of the dimming function. Collectively, LEDs could be dimmed

by turning the potentiometer by up to 10 turns, with 0 turns providing the lowest brightness setting (100% dimmed) and 10 turns providing the highest brightness setting (0% dimmed). The final configuration of the miniaturised EDS was then mounted using a testing rig above a 30 × 30 cm bench-top surface for antimicrobial testing (Figure 5.2). The distance between the light source and test surface could be increased up to a distance of 80 cm as required.

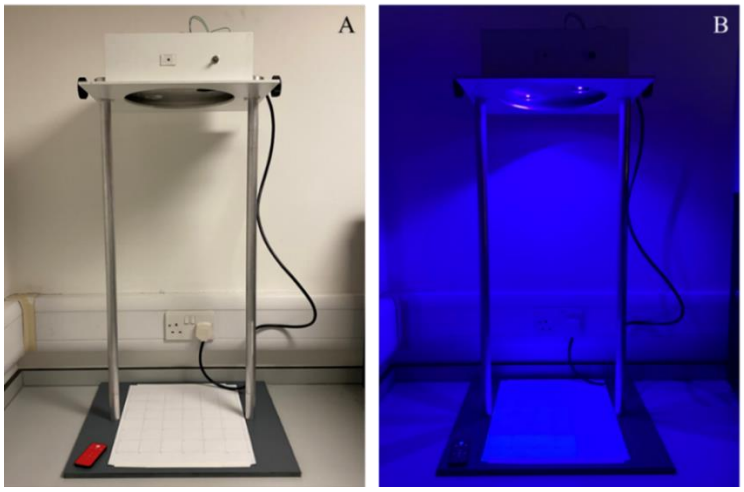

Figure 5.2 Miniaturised 405-nm light EDS mounted at a distance of 80 cm above a 30 × 30 cm surface for antimicrobial testing with (A) 405-nm LED arrays switched off and (B) 405-nm LED arrays switched on.

5.2.3 Optical Profiling of the 405-nm Light EDS

The irradiance distribution of the miniaturised 405-nm light EDS was characterised for individual and multiple LED usage, across the range of dimming settings provided, to determine the settings required for subsequent inactivation testing.

5.2.3.1 Methods: Optical Profiling of the 405-nm light EDS

The optical irradiance output profile was established with the light source mounted directly above the bench-top surface at the greatest achievable distance of 80 cm; providing the greatest uniformity of light distribution. Irradiance measurements were taken at approximately 5 cm intervals in X and Y directions across a 30 × 30 cm bench-top surface, positioned directly below the 30 × 30 cm system housing. Measurements were taken with all three LED arrays switched on and either 0, 50 or 100% dimmed, to establish maximum and minimum irradiance levels with all three LED arrays engaged; and with each LED array switched on individually whilst 100% dimmed, to determine the minimum irradiance levels of each individual array. Upon inspection, it was determined that the irradiance values gathered across

the 30 × 30 cm bench-top surface, even with singular 100% dimmed LED array use, were still higher than the lowest irradiance levels produced within the whole-room setting in Chapter 4. Accordingly, to mimic these levels, the bench-top testing surface was extended to 30 × 150 cm (Figure 5.3), and irradiance distribution for each individual LED array engaged whilst 100% dimmed was measured across this area.

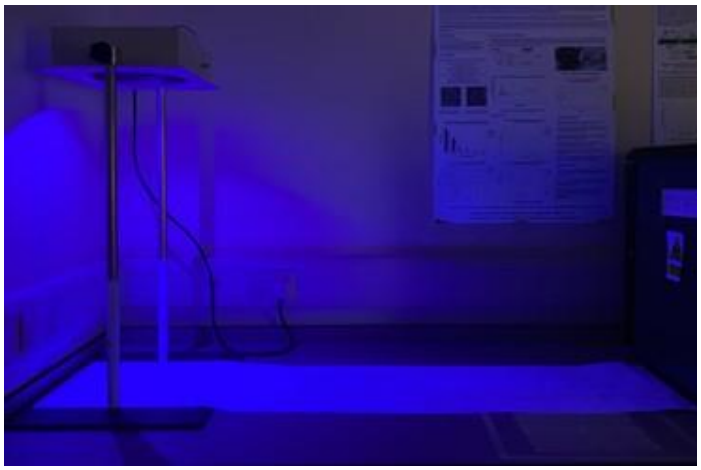

Figure 5.3 Miniaturised 405-nm light EDS mounted at a distance of 80 cm above a 150 × 30 cm surface for antimicrobial testing.

5.2.3.2 Results: Optical Profiling of the 405-nm Light EDS

The optical irradiance profile of the miniaturised EDS across a 30 × 30 cm testing surface positioned 80 cm directly below the source is presented in Figure 5.4. In this instance, all three LEDs were switched on with the potentiometer set at either 0% dimmed (Figure 5. 4A), 50% dimmed (Figure 5. 4B) or 100% dimmed (Figure 5.4C). The highest irradiance values produced by the EDS (0.934 mW cm^{-2}) were gathered directly underneath the light source when LEDs were 0% dimmed. At this setting, irradiance levels across the surface ranged by 0.159 mW cm^{-2}. As light intensity decreased between the three dimming settings, the range of irradiance levels also decreased ($P<0.001$), thus enhancing uniformity of light distribution: when 50% dimmed, this range was 0.034 mW cm^{-2}, and when 100% dimmed, this decreased further to 0.016 mW cm^{-2}. In the latter setting, the minimum irradiance level recorded was 0.092 mW cm^{-2}. By comparison, profiling of the full-scale prototype in Section 4.2 recorded irradiances as low as 0.001 mW cm^{-2} within a typical room setting.

To achieve these levels using the miniaturised 405-nm light EDS, the optical profile was then established across the 30 × 30 cm testing area for each LED array separately and 100% dimmed, with

results presented in Figure 5.5. Findings indicate similar levels of irradiance produced by each LED, despite LED 1 producing slightly higher irradiance output (P=0.004), with recorded maximum irradiances of 0.040-0.041 mW cm^{-2}, minimum irradiances of 0.031-0.032 mW cm^{-2}, and overall ranges of 0.008-0.011 mW cm^{-2}. Although promising, these irradiance levels were still higher than the lowest values obtained using the original full-scale 405-nm light EDS across a typical 4 × 4 × 2 m room setting, and so the testing surface was expanded (30 × 150 cm) and testing of each individual LED whilst 100% dimmed was repeated (Figure 5.6). Results again indicate similar irradiance levels produced by each LED (P=0.288), with maximum irradiance values of 0.04-0.042 mW cm^{-2} measured directly 80 cm underneath the centre of the light source and minimum irradiance values of 0.001 mW cm^{-2} measured 80 cm underneath the source at a radial distance of 135 cm. In this configuration, the miniaturised EDS was capable of illuminating the test area with the lowest irradiance levels (0.001 mW cm^{-2}) produced by the full-scale prototype centrally-installed within a typical room setting investigated in Chapter 4, in this case at much shorter distances from the light source (displacement of 1.7 m vs 4.47 m).

These results together confirmed its ability to expose a bench-top test surface with the range of irradiance levels established across a whole-room setting in Chapter 4, and as such, where required, the miniaturised EDS was employed for subsequent microbial inactivation testing in this chapter.

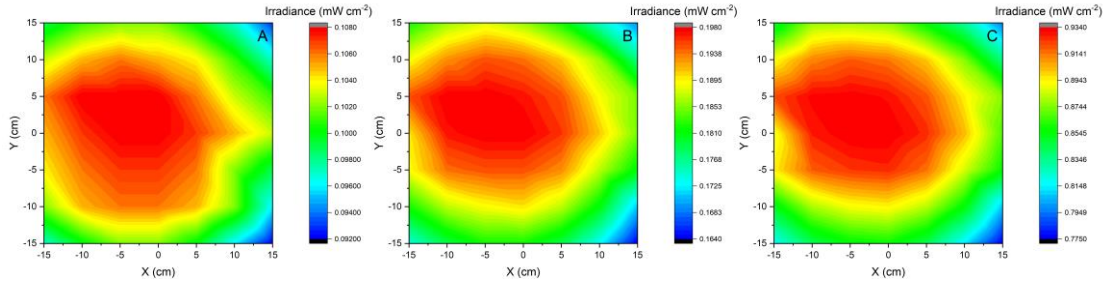

Figure 5.4 Irradiance distribution pattern of the miniaturised bench-top 405-nm light EDS at a distance of 80 cm from the sample surface when all 3 LEDs were on at (A) 0% dimmed, (B) 50% dimmed and (C) 100% dimmed.

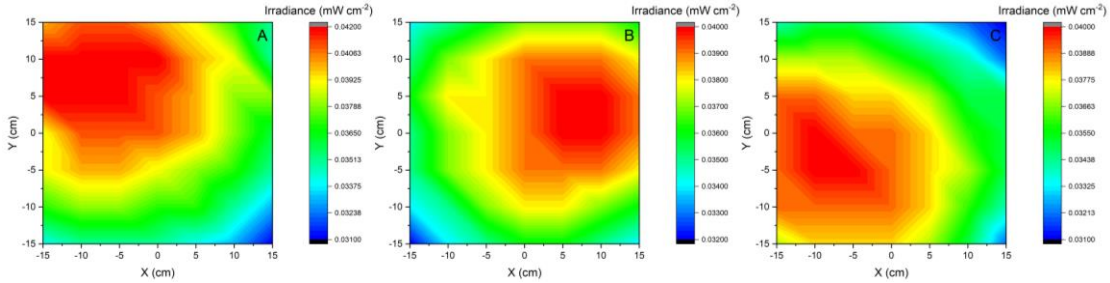

Figure 5.5 Irradiance distribution pattern of the miniaturised 405-nm light EDS at a distance of 80 cm from the sample surface with just (A) LED 1 on, (B) LED 2 on and (C) LED 3 on, at 100% dimmed setting in all cases.

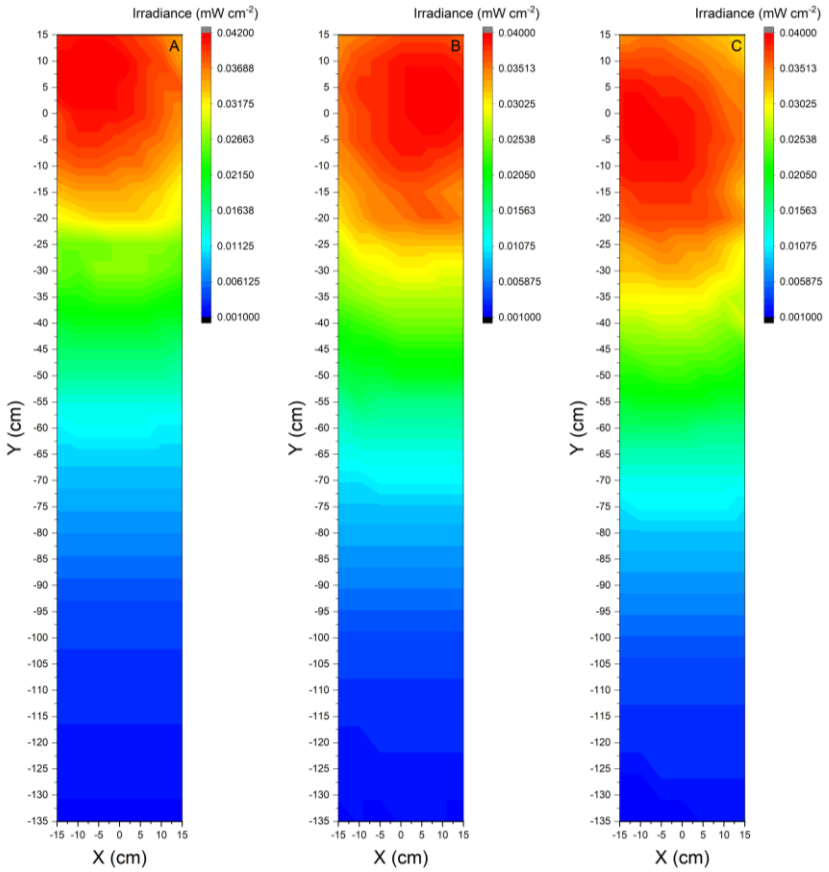

Figure 5.6 Irradiance distribution of the miniaturised bench-top 405-nm light EDS at a distance of 80 cm from the sample surface with just (A) LED 1 on, (B) LED 2 on and (C) LED 3 on, at 100% dimmed in all cases. The profiling area was extended an additional 120 cm.

5.3 Exposure to Low Irradiance Levels Produced within Whole-Room Settings

This section aimed to demonstrate the efficacy of lower irradiance 405-nm light exposures (at the lower range of those generated within a typical room setting; Chapter 4) for bacterial inactivation, and determine the minimum threshold of irradiance, if any, beyond which no further inactivation takes place.

5.3.1 Methods: Exposure to Low Irradiance Levels

To fulfil the aforementioned aims, *S. aureus*, chosen as a model organism, was initially exposed to 405-nm light for up to 72 h using a range of irradiances ≤0.1 mW cm^{-2}; which represents 88.2% of the irradiance levels produced by a single 405-nm light EDS installed in the centre of a 32 m^3 area (Figure 4.4; Chapter 4). Key irradiance levels within this range were then identified (0.1, 0.075, 0.5, 0.25, 0.1, 0.005 and 0.001 mW cm^{-2}) and *S. aureus* was exposed to each for up to 72 h. This latter study was conducted on both nutritious and non-nutritious agar surfaces, to evaluate its bactericidal impact.

5.3.1.1 Exposure to Low Irradiance Levels: Light Source

For experimental testing, the miniaturised EDS was mounted 80 cm from the sample surface and all three 405-nm LEDs were engaged and set to 10% brightness. As shown in Figure 5.7, the irradiance levels produced using this configuration decreased from approximately 0.1 mW cm^{-2} directly below the light source to approximately 0.003 mW cm^{-2} at a radial distance of 1.5 m from the light source.

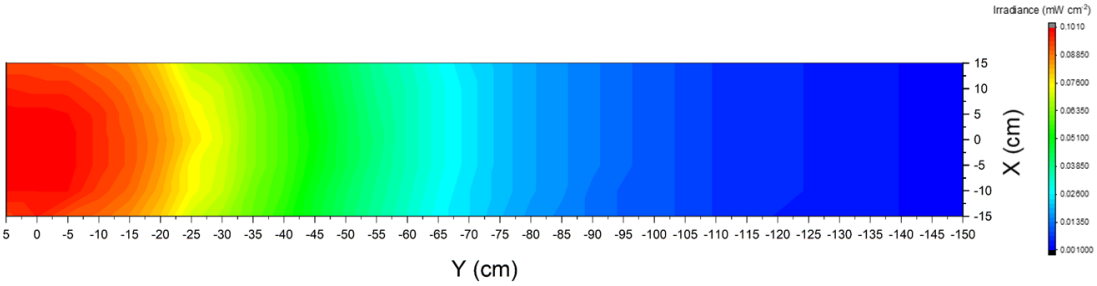

Figure 5.7 Irradiance distribution of the miniaturised 405-nm light EDS at a distance of 80 cm from testing surface and set to 10% brightness. The centre of the miniaturised EDS is aligned with co-ordinates (0,0).

5.3.1.2 Exposure to Low Irradiance Levels: Exposure Methodology

To determine system efficacy when using irradiance levels at the lower range of those produced within whole-room settings, inactivation kinetics of *S. aureus* upon exposure to 405-nm light at increasing distances from the source, equating to irradiances from 0.003-0.1 mW cm^{-2} were established.

S. aureus was seeded onto 90 mm diameter NA plates, to provide an initial population of 100-300 CFU $plate^{-1}$ (1.6-4.7 CFU cm^{-2}) (Section 3.1.2-3.1.3). Seeded NA plates (with lids on to prevent drying of agar) were positioned approximately 80 cm below the light source in 0.1 m intervals starting from directly underneath the light source (Δs = 0.8 m; $\Delta\Theta = 0^{o}$) up to a distance of 1.5 m radially (Δs = 1.7 m; $\Delta\Theta = 61.9^{o}$). For each independent experiment, samples were exposed for 24, 48 or 72 h. Control samples were prepared in an identical manner but were exposed to ambient laboratory lighting only.

To determine the minimum threshold of irradiance, if any, beyond which no further inactivation takes place, inactivation kinetics of *S. aureus* were established using key irradiances within this range. Seeded NA plates (with lids on) were positioned 80 cm below the light source and exposed to 405-nm light at irradiances of either 0.1, 0.075, 0.05, 0.025, 0.01, 0.005 or 0.001 mW cm^{-2} for up to 72 h, or until

complete inactivation was demonstrated. Control samples were prepared in an identical manner and exposed to ambient laboratory lighting only.

Post-exposure, the seeded agar plates were incubated at 37°C for 18-24 h, before enumerating the viable bacterial CFU plate^{-1}. Results represent the mean values ± SD of triplicate replicates (n=3), and are reported as the percentage of surviving or reduced bacteria as compared to the equivalent non-exposed control samples.

5.3.2 Results: Exposure to Low Irradiance Levels

Figure 5.8 presents the inactivation kinetics of *S. aureus* exposed on NA surfaces for up to 72 h at distances ranging from directly underneath the centre of the light source (Δs=0.8 m; $\Delta\Theta$=0º) up to 1.5 m (Δs=1.7 m; $\Delta\Theta$=61.9º); equating to exposures ranging from 0.01 to 0.0027 mW cm^{-2}, respectively. In all cases, non-exposed control populations, from which surviving populations were calculated, showed no significant change throughout treatment (P=0.088-0.894).

Findings comprehensively demonstrate that as the distance from the light source is increased, irradiance decreases, which in turn decreases the extent of inactivation achieved per unit time. Results do, however, also demonstrate significantly greater reductions as exposure time to a set irradiance increased, even at the lowest irradiance levels employed. Following 24 h exposure, significant levels of inactivation (reductions of 26.0-89.3% in comparison to non-exposed equivalent controls; P≤0.015) were achieved up to a radial distance of 0.9 m below the light source, where samples were illuminated at irradiances of 0.014-0.1 mW cm^{-2}. Beyond this distance, whereby samples were exposed to ≤0.011 mW cm^{-2}, no significant reductions were observed (P=0.067-0.894). Following 48 h exposure, results demonstrate significant levels of reduction (21.6-100%; P≤0.022) up to a radial distance of 1.1 m below the light source, where samples were illuminated at irradiances of 0.008-0.100 mW cm^{-2}. Beyond this distance, whereby samples were exposed at ≤0.006 mW cm^{-2}, no significant reductions were observed (P≥0.066), with the exception of exposure at a distance of 1.5 m radially from the light source, where a 20.4% reduction was observed (P=0.023). After 72 h, significant reductions (12.5-100%; P≤0.032) were observed up to a radial distance of 1.3 m below the light source, with samples in this range illuminated by 0.005-0.100 mW cm^{-2}. Beyond this distance (equating to exposures to ≤0.004 mW cm^{-2}) no significant reductions were observed (P≥0.105).

Results in Figure 5.9 present the inactivation kinetics of *S. aureus* seeded on NA surfaces and exposed to the miniaturised 405-nm light EDS at irradiances ranging from 0.001-0.100 mW cm^{-2}. In all cases, non-exposed control populations displayed no significant change throughout treatment (P=0.088-1.000). Results comprehensively demonstrate an increase in bacterial inactivation achieved as both irradiance and exposure time are increased. Exposed to 0.025-0.100 mW cm^{-2}, significant bacterial reductions were demonstrated following 24 h exposure (40.1-89.3%; P≤0.003), with the extent of inactivation achieved by the highest irradiance (0.1 mW cm^{-2}; 89.3% reduction) shown to be significantly greater than that achieved by 0.05 and 0.075 mW cm^{-2} (71.2-76.4% reductions; P<0.001), which were both significantly greater than that achieved by 0.025 mW cm^{-2} exposures (40.1% reduction; P<0.001). When exposed to a lower irradiance of 0.01 mW cm^{-2}, a greater exposure of 48 h was required to demonstrate significant bacterial inactivation (28.5% reduction; P=0.015), and when exposed at an even lower irradiance of 0.005 mW cm^{-2}, 72 h exposure was required to achieve significant bacterial inactivation (12.5% reduction; P=0.032). No significant bacterial inactivation was demonstrated throughout the treatment duration for bacterial samples exposed to 0.001 mW cm^{-2} (P=0.935-1.000).

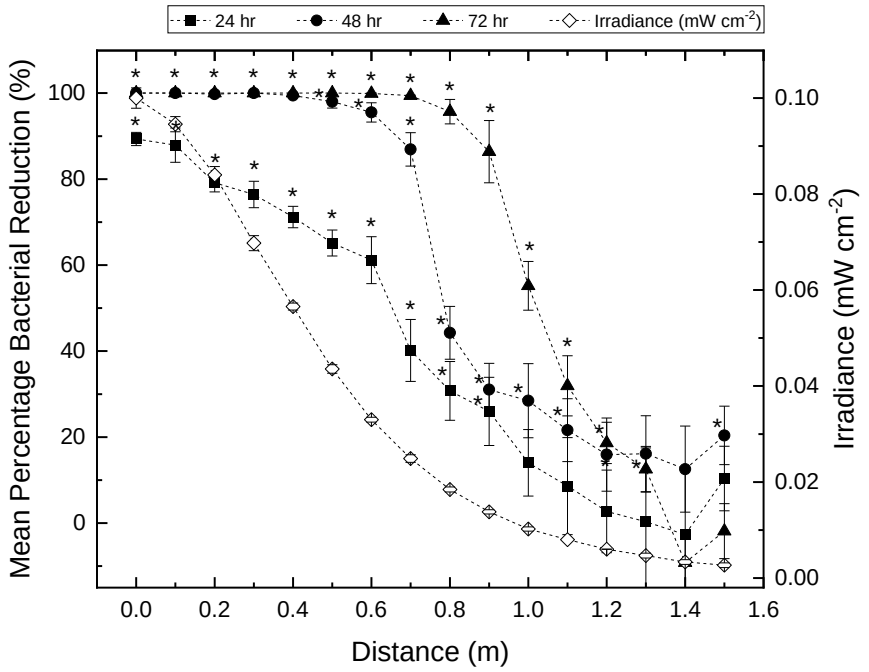

Figure 5.8 Inactivation kinetics of *Staphylococcus aureus* seeded on nutrient agar surfaces and exposed to low irradiance 405-nm light at distances ranging from 0.8 m directly below the light source (Δs=0.8 m; ΔΘ=0º) up to 1.5 m radially (Δs=1.7 m; ΔΘ=61.9º); equating to light intensities of 0.1 mW cm^{-2} down to 0.0027 mW cm^{-2}, respectively, in comparison to that of equivalent non-exposed controls. Each data point represents the mean value ± SD (n=3). Asterisks (*) represent data points where 405-nm light exposed triplicate CFU $plate^{-1}$ counts were significantly lower than equivalent control counts (P<0.05).

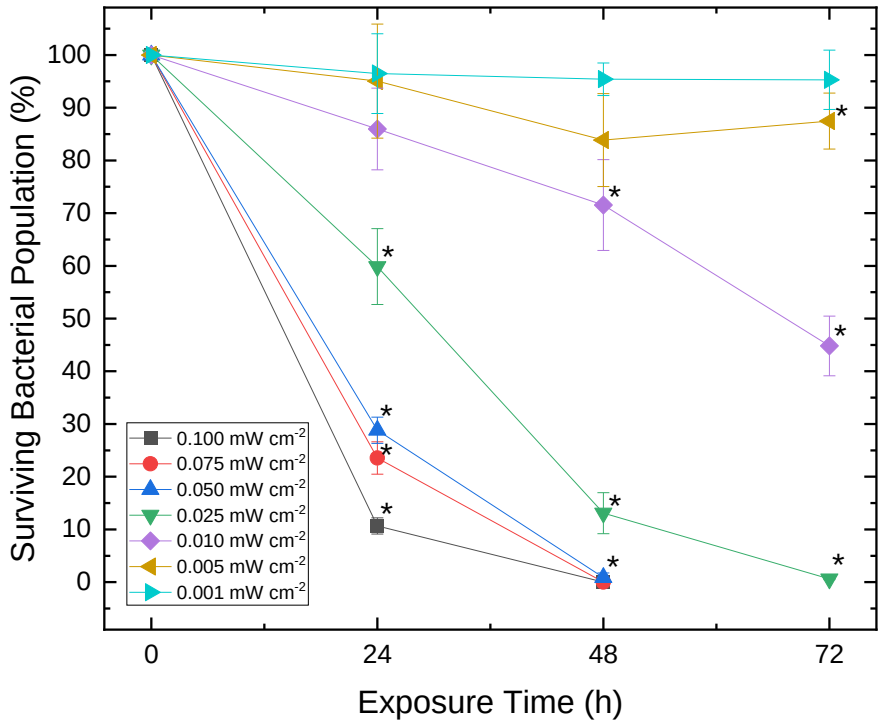

Figure 5.9 Inactivation kinetics of *Staphylococcus aureus* seeded on NA surfaces and exposed to 405-nm light at irradiance ranging from 0.001-0.100 mW cm^{-2} in comparison to that of equivalent non-exposed populations. Each data point represents the mean value ± SD (n=3). Asterisks (*) represent data points where the 405-nm light exposed triplicate CFU plate^{-1} counts were significantly lower than that of equivalent control counts (P<0.05).

5.4 Effect of Suspension Media and Fomite Material on Bacterial Inactivation

This section examined the efficacy of low irradiance 405-nm light for inactivation of surface-seeded *S. aureus* when exposed firstly, in various nutritious and non-nutritious suspension media, and secondly, when dried onto various clinically-relevant surfaces; to better depict system efficacy in dynamic clinical environments.

5.4.1 Effect of Suspension Media on Bacterial Inactivation Efficacy

This study assessed the comparative efficacy of 405-nm light for inactivation of bacteria seeded on agar whilst in the presence of non-nutritious (PBS) or nutritious biological media (saliva, blood and faeces).

5.4.1.1 Methods: Effect of Suspension Media on Bactericidal Efficacy

5.4.1.1.1 Effect of Suspension Media on Bactericidal Efficacy: Light Source

The light source used was the original 405-nm light EDS prototype (configuration 2; Section 3.4.1). This was selected, as opposed to the miniaturised 405-nm light EDS, to provide a greater surface area

for exposures of multiple 90 mm agar plates. For experimental testing, the ceiling-mounted light source was positioned directly above a surface for exposure at a distance of approximately 1.5 m. The irradiance produced at this distance was found to be 0.5 ± 0.02 mW cm^{-2} for all bacterial samples.

5.4.1.1.2 Effect of Suspension Media on Bactericidal Efficacy: Sample Preparation

The suspension media employed for bacterial exposures in this study was PBS, artificial human saliva, defibrinated ovine whole blood and artificial faeces; which were sourced and prepared as described in Section 3.3. For experimental use, the prepared suspension of artificial faeces (Section 3.3) was extremely viscous, and thus was diluted (1:100; 1 mL into 99 mL) in distilled water to enable experimental testing (Figure 5.10), and to better depict conditions of faecal transmission within hospital wastewater. Once prepared, the diluted samples were sterilised by autoclaving prior to use. *S. aureus* was then seeded into the suspending media to provide a 10^3 CFU mL^{-1} population (Section 3.1.2-3.1.3). For each bacterial suspension, 100 µL volumes were then spread plated onto NA to provide an initial population of ~100-300 CFU $plate^{-1}$ (1.6-4.7 CFU cm^{-2}).

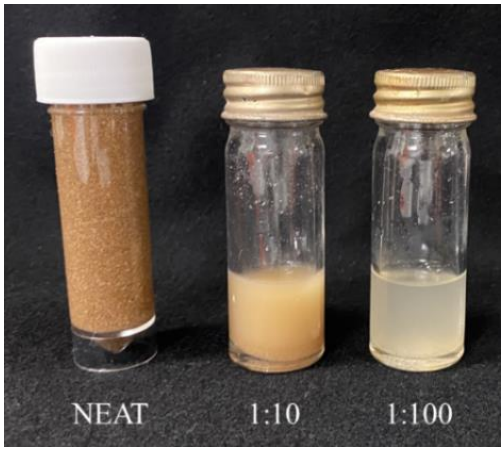

Figure 5.10 Artificial faeces preparation and serial dilutions performed in distilled water (1:100 dilution was employed for experimental testing).

5.4.1.1.3 Effect of Suspension Media on Bactericidal Efficacy: Exposure Methodology

Inactivation kinetics of *S. aureus* in either PBS, saliva, whole blood or artificial faeces and seeded onto NA plates were established upon exposure to an increasing dose of 405-nm light. Seeded plates (with lids off) were positioned approximately 1.5 m below the light source, providing an irradiance of ~0.5 mW cm^{-2} at the plate surface, and were exposed for up to 4 h. Following exposure, agar plates were incubated at 37 ºC for 18-24 h, before enumerating the viable bacterial CFU $plate^{-1}$. In all cases, control

samples were prepared in an identical manner and were exposed to ambient laboratory lighting only. Results represent the mean values ± SD of triplicate replicates (n=3), and are reported as the percentage of surviving bacteria as compared to the equivalent non-exposed control samples.

5.4.1.1.4 Effect of Suspension Media on Bactericidal Efficacy: Light Transmissibility

The transmissibility and photosensitivity of the suspending media (PBS, saliva, blood and faeces) was assessed to indicate its potential effect on bacterial susceptibility.

Firstly, the ability of 405-nm light to transmit through freshly prepared media samples seeded onto agar plates was determined (Figure 5.11). NA plates of identical depth were prepared by pipetting 10 mL molten NA into sterile petri dishes. Once dried, the plates were positioned directly underneath the miniaturised 405-nm light EDS, with the photodiode detector held directly underneath the plate. The light output was adjusted until ~0.5 mW cm^{-2} was detected. Following this, 100 µL of each sample was individually pipetted and evenly spread across the surface of the plates (Figure 5.12). Irradiance was then recorded using the same method as described for pre-seeded plates (n=6).

Secondly, to indicate the presence of porphyrins or other components with the ability to absorb 405-nm light and emit fluorescence, thus potentially able to aid in the photoinactivation effect, fluorescence measurements were taken between 400-700 nm of freshly prepared PBS, artificial saliva, artificial faeces and ovine whole blood when excited at 405-nm using an RF-531 PC spectrophotometer (Shimadzu, USA).

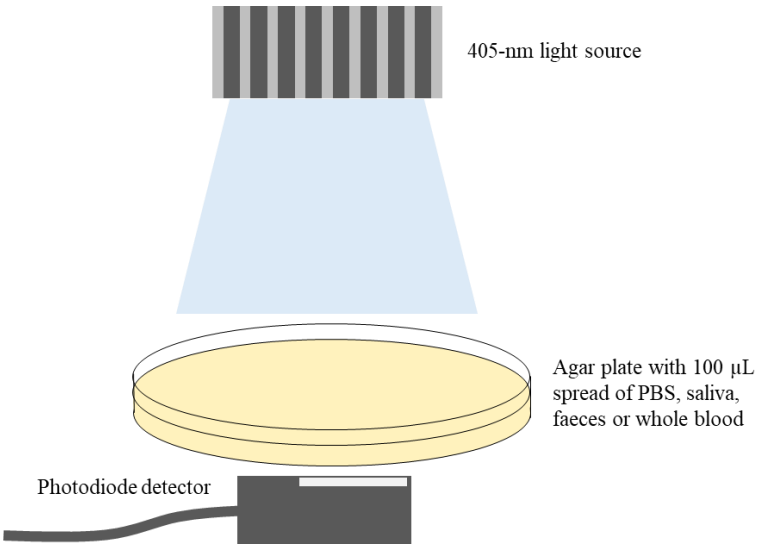

Figure 5.11 Experimental set-up to measure loss of light transmission through surface-seeded bacterial samples.

Figure 5.12 Nutrient agar plates seeded with 100 µL, from left to right: PBS, artificial saliva, artificial faeces (1:1000 dilution) and ovine whole blood.

5.4.1.2 Results: Effect of Suspension Media on Bactericidal Efficacy

Figure 5.13 presents inactivation kinetics of *S. aureus* seeded on NA in the presence of PBS, artificial saliva, blood or artificial faeces, upon exposure to increasing doses of 0.5 mW cm^{-2}. In all cases, a significant downward trend in surviving populations was demonstrated upon increasing exposure time ($P<0.05$). Control populations showed no significant change throughout treatment ($P\geq0.057$); excluding artificial faeces samples, which significantly decreased after 4 h ($P=0.014$).

When suspended in non-nutritious media, i.e. PBS, a significant 24.6% reduction was demonstrated after just 1 h exposure ($P=0.016$), with 76.6% reductions achieved after 4 h ($P<0.001$). By comparison, reductions in nutritious media were variable. In saliva, a 56.5% reduction was demonstrated after just 1 h ($P=0.001$); which increased to a 93.7% reduction following 4 h ($P<0.001$). Excluding measurements after 2 h, where similar inactivation occurred (57.5-63.1% inactivation; $P=0.209$), inactivation achieved at all other time points were shown to be significantly greater for bacteria suspended in saliva as opposed to PBS ($P<0.001$). Exposures in faeces similarly achieved significant reductions following 1 h (14.1% reduction; $P=0.017$); however, this was significantly lower than equivalent reductions in PBS ($P=0.009$) and saliva ($P<0.001$). Following 4 h, reductions of 64.4% were demonstrated; which again were significantly lower than reductions achieved by this time point in both PBS ($P<0.001$) and saliva ($P<0.001$). Bacteria suspended in blood were the least susceptible to treatment, with no significant reductions observed until 4 h exposure (9.4% reduction; $P=0.034$); which was significantly lower than reductions achieved by all other media at this time point sampled ($P<0.001$).

The intensity of 405-nm light passing through each suspension media is presented in Table 5.1. As demonstrated, the highest intensity of light passing occurred in PBS (100%), which was statistically similar ($P=0.235$) to that recorded for artificial saliva (99.9%) and artificial faeces (99.5%). The lowest

intensity of light passing was demonstrated through whole blood (23.5%), which was significantly lower than that demonstrated for all other suspending media investigated ($P<0.001$). The fluorescence emission spectra of each suspension media when excited at 405-nm is presented in Figure 5.14. As shown, am emission peak was demonstrated at 468 nm for artificial saliva and artificial faeces, with the latter also presenting a second, smaller peak at 495 nm. No emission peaks were observed in whole blood.

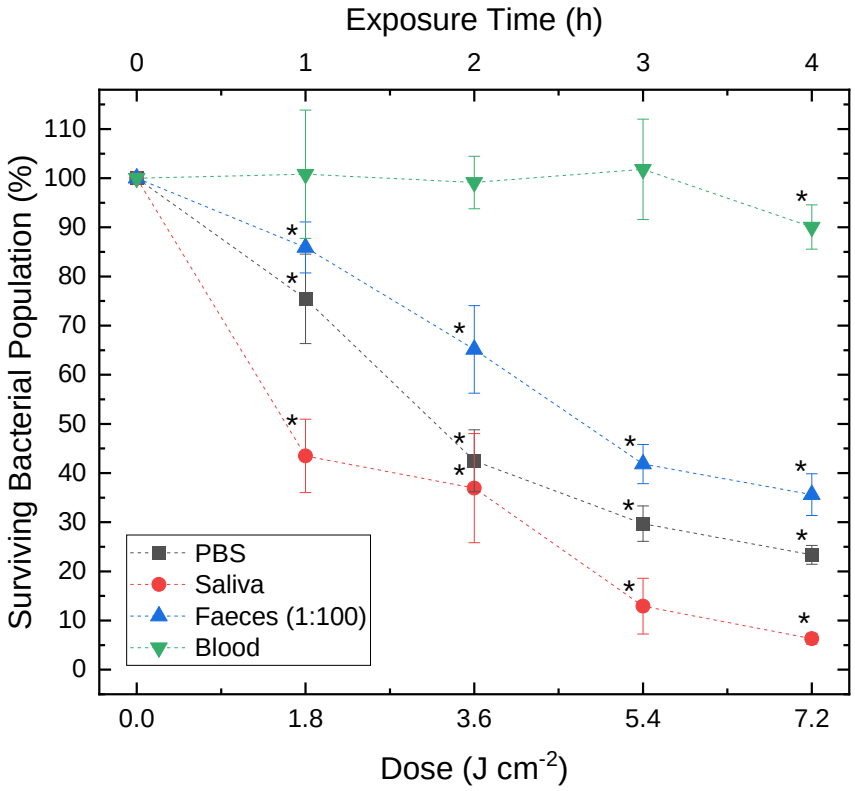

Figure 5.13 Inactivation kinetics of *Staphylococcus aureus*, seeded on agar surfaces in the presence of PBS, saliva, artificial faeces or blood, upon exposure to 405-nm light at an irradiance of ~0.5 mW cm^{-2}. Each data point represents the mean value ± SD (n = 6). Asterisks (*) represent points where the triplicate CFU $plate^{-1}$ counts were significantly different between test and control samples ($P \leq 0.05$).

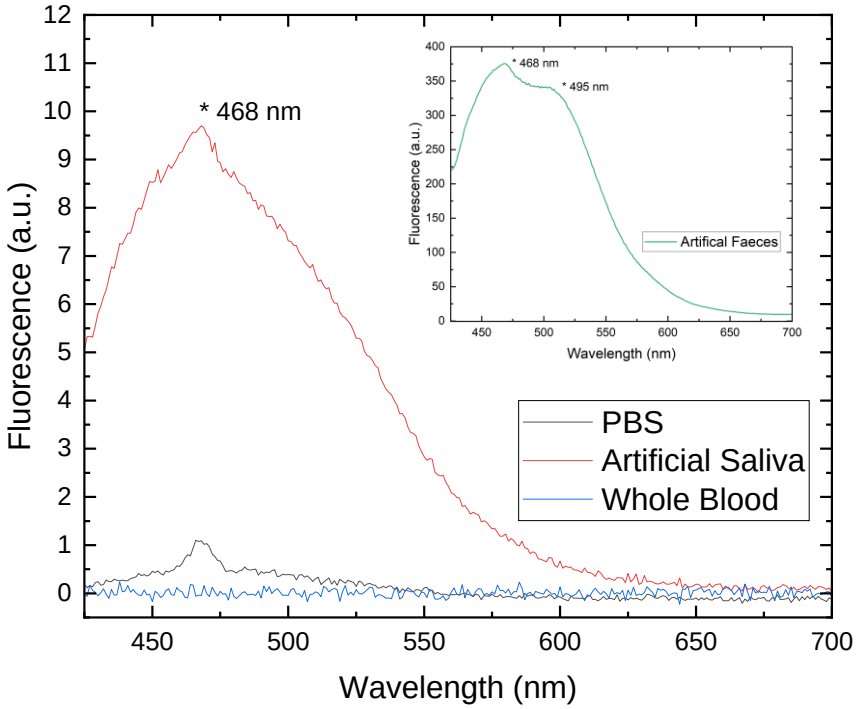

Figure 5.14 Fluorescence emission spectra of various suspension media (PBS, artificial saliva, artificial faeces and whole blood) upon excitation at 405-nm wavelengths. Asterisks (*) indicate the peak emission wavelengths for each media.

Table 5.1 Percentage of 405-nm light passing through varying suspension media seeded (100 µL) and spread onto NA plates of identical depth. 405-nm light irradiance was measured through the smear and agar using a photodiode detector.

Medium	**PBS**	**Saliva**	**Faeces (1:100)**	**Blood**
Light Passage (%)	100	99.9	99.5	23.5

5.4.2 Effect of Fomite Material on Bacterial Inactivation Efficacy

This study assessed the efficacy of the 405-nm light EDS to inactivate *S. aureus* when dried onto four fomites (PVC, stainless steel, glass and vinyl), which represent common healthcare surfaces.

5.4.2.1 Methods: Effect of Fomite Material on Bactericidal Efficacy

5.4.2.1.1 Effect of Fomite Material on Bactericidal Efficacy: Light Source

The light source used was the miniaturised 405-nm light EDS (Sections 3.4.2 and 5.2); mounted 80 cm from the sample surface with all three 405-nm LED apertures engaged and set to 95% brightness. This provided sufficient area for samples to receive ~0.5 mW cm^{-2} for experimental testing (Figure 5.15).

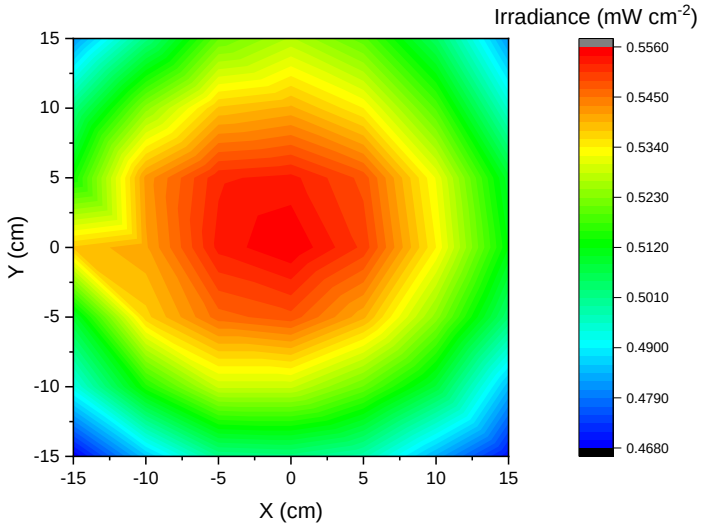

Figure 5.15 Irradiance distribution pattern of the miniaturised 405-nm light EDS at a distance of 80 cm from the testing surface with all three LED apertures switched on and 5% dimmed.

5.4.2.1.2 Effect of Fomite Material on Bactericidal Efficacy: Surface Preparation and Seeding

Four materials – PVC, stainless steel, glass and vinyl (2000 Pur, Polyflur Ltd, UK) – were prepared as 15 × 15 mm coupons (Figure 5.16). Immediately prior to experiments, coupons were cleaned with 70% ethanol to sterilise and remove grease from the materials. Coupons were then immersed in 10 mL 10^7 CFU mL^{-1} bacterial suspensions (prepared as per Section 3.1.2-3.1.3) for 30 min at room temperature under rotary conditions (120 rpm). Coupons were then aseptically removed from suspensions and transferred to sterile 90-mm petri dishes which were placed in a laminar flow cabinet for 20 min to dry. This methodology was adapted from McKenzie (2014) and Buchovec *et al.* (2010).

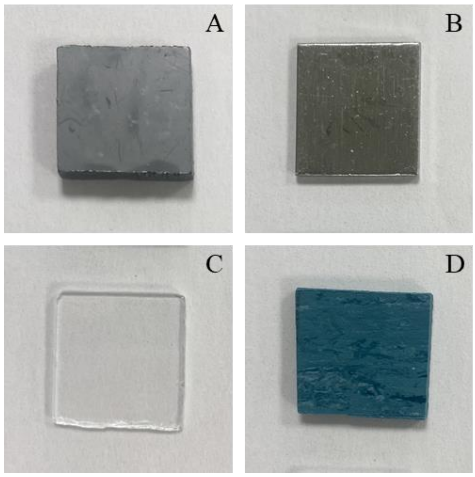

Figure 5.16 Surface coupons (15 × 15 mm) employed to represent common healthcare fomite materials to assess surface decontamination efficacy using the 405-nm light EDS: (A) PVC, (B), stainless steel, (C) glass and (D) Vinyl (2000Pur).

5.4.2.1.3 Effect of Fomite Material on Bactericidal Efficacy: Exposure Methodology and Bacterial Recovery

Seeded coupons were positioned 80 cm below the light source (Figure 5.17) and exposed to 405-nm light at ~0.5 mW cm^{-2} for either 4 or 24 h. Following exposure, surviving bacteria were recovered into a 10 mL volume containing 9 mL PBS + 1 mL 3% Tween-80 suspension using a swabbing method adapted from McKenzie (2014). Briefly, the light-exposed surface of each coupon was swabbed continuously for 2 min, to ensure maximum recovery of bacteria, using a sterile cotton-tipped swab moistened in the 10 mL (9 mL PBS + 1 mL 3% Tween-80) recovery solution. The swab was then immersed in the 10 mL recovery solution and vortexed for 1 min to resuspend bacteria from the swab into solution. For enumeration of total viable bacterial counts from each sample, recovered solutions were serially diluted, where necessary, in PBS and plated onto NA plates using the drop plate method described in Section 3.1.4. Agar plates were then incubated at 37 °C for 18-24 h, before enumerating viable bacterial CFU $plate^{-1}$, and calculating viable bacterial CFU per coupon. In all cases, control coupons were prepared and treated in an identical manner, and exposed to ambient laboratory lighting. Results represent the mean values ± SD of triplicate replicates measured in duplicate (n=6), and are reported as the mean viable $\log_{10}$ bacterial counts in CFU per coupon.

Figure 5.17 Experimental set-up for exposure of seeded surface coupons using miniaturised 405-nm light EDS.

5.4.2.1.4 Effect of Fomite Material on Bactericidal Efficacy: Surface Characterisation

To determine the wettability of each surface coupon, contact angles were determined by pipetting 2 µL deionised water and TSB droplets onto each surface and then imaging using a smartphone with microlens attachment. Images were analysed using ImageJ software with the 'drop_analysis' plug-in

and LB-ADSA method. Results represent the mean values ± SD of triplicate replicates measured in duplicate for each inert surface (n=6).

5.4.2.2 Results: Effect of Fomite Material on Bactericidal Efficacy

Contact angle measurements, as a means of assessing surface wettability, are presented in Table 5.2 and Figure 5.18. PVC was shown to produce the highest contact angles (water: 71.65° and TSB: 69.29°); and stainless steel was found to produce the lowest (water: 18.43° and TSB: 28.32°). Analysis of the data found that deionised water deposited on stainless steel was significantly more hydrophilic than glass, which together were significantly more hydrophilic than vinyl, which together were significantly more hydrophilic than PVC ($P<0.001$). Similar results were demonstrated using TSB: stainless steel and glass were together significantly more hydrophilic than vinyl, which together were significantly more hydrophilic than PVC ($P<0.001$). No significant differences were demonstrated between the contact angles made with water and TSB ($P=0.392$-0.816), with the exception of stainless steel ($P<0.001$), which is likely the result of its surface roughness influencing droplet attachment.

Table 5.2 Contact angle of deionised water and tryptone soya broth with PVC, stainless steel, glass and vinyl.

Material	PVC	Stainless steel	Glass	Vinyl
Water Contact Angle (°)	71.65 ± 4.68	18.43 ± 2.60	30.33 ± 1.08	48.06 ± 6.15
TSB Contact Angle (°)	69.29 ± 4.45	28.32 ± 0.77	30.51 ± 1.54	48.94 ± 6.64

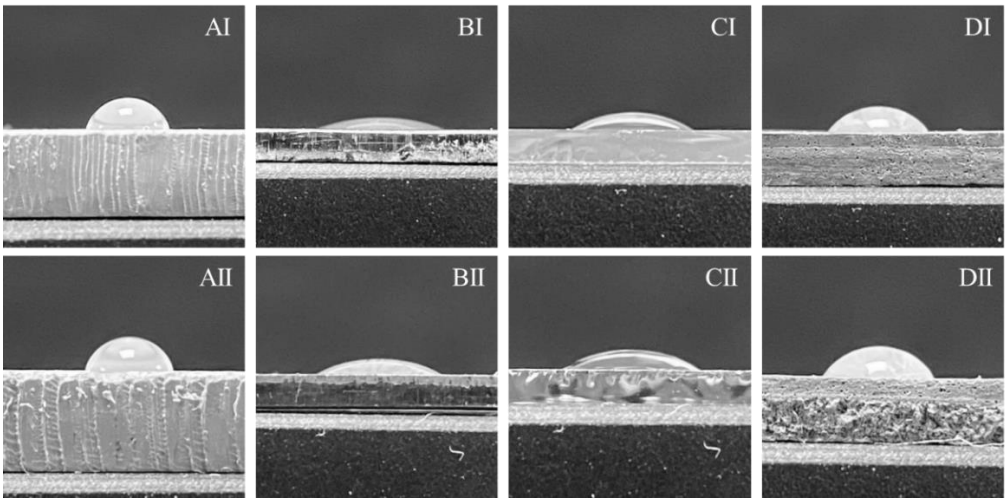

Figure 5.18 Contact angles of 10 µL of (I) water and (II) tryptone soya broth on coupons of (A) PVC, (B) stainless steel, (C) glass and (D) vinyl.

Inactivation of *S. aureus* dried onto surface coupons and exposed to 405-nm light at ~0.5 mW cm^{-2} for either 4 or 24 h is presented in Figure 5.19. Exposed for 4 h (7.2 J cm^{-2}), bacterial inactivation was shown to be greatest on vinyl (0.59 log_{10} CFU per coupon (72.9%) reduction; P<0.001). Reductions of 0.27 (7.8%) and 0.06 (3.4%) log_{10} CFU per coupon were demonstrated on glass and stainless steel, respectively (P=0.27-0.535), and no reductions were demonstrated on PVC (P=0.458). Seeded bacterial levels pre-treatment were significantly lower on vinyl compared to all other materials (P<0.001), however, which may have accounted for these findings. On vinyl and stainless steel, no significant reductions were presented for control populations following 4 h (P≥0.127); however, reductions of 0.54 and 0.41 log_{10} CFU per coupon reduction were noted on PVC and glass, respectively (P=0.003).

Exposed for 24 h (43.2 J cm^{-2}), reductions were again greatest on vinyl (2.03 log_{10} CFU per coupon (98.8%) reduction; P<0.001); with 1.93 (98.4%), 1.68 (97.8%) and 1.66 (97.0%) log_{10} CFU per coupon reductions demonstrated on stainless steel, glass and PVC, respectively (P<0.001). No significant difference in seeded bacteria levels was demonstrated across all materials prior to exposure (P=0.658); however, following 24 h, control populations decreased on PVC, glass and vinyl (0.20-0.45 log_{10} CFU per coupon reductions; P=0.013-0.043), whilst no significant reductions were demonstrated on stainless steel (P=0.448). Regardless, in all cases, significant reductions were indicated between non-exposed and exposed samples. Across all exposures, bacterial levels seeded onto coupons prior to exposure ranged from 5.43-6.07 log_{10} CFU per coupon, and although variation was demonstrated between materials (P<0.001), no significant differences between counts on each individual material prior to each exposure was presented (P>0.05). As expected, as exposure time, and thus dose, was increased, *S. aureus* levels on all materials was significantly reduced (P<0.001).

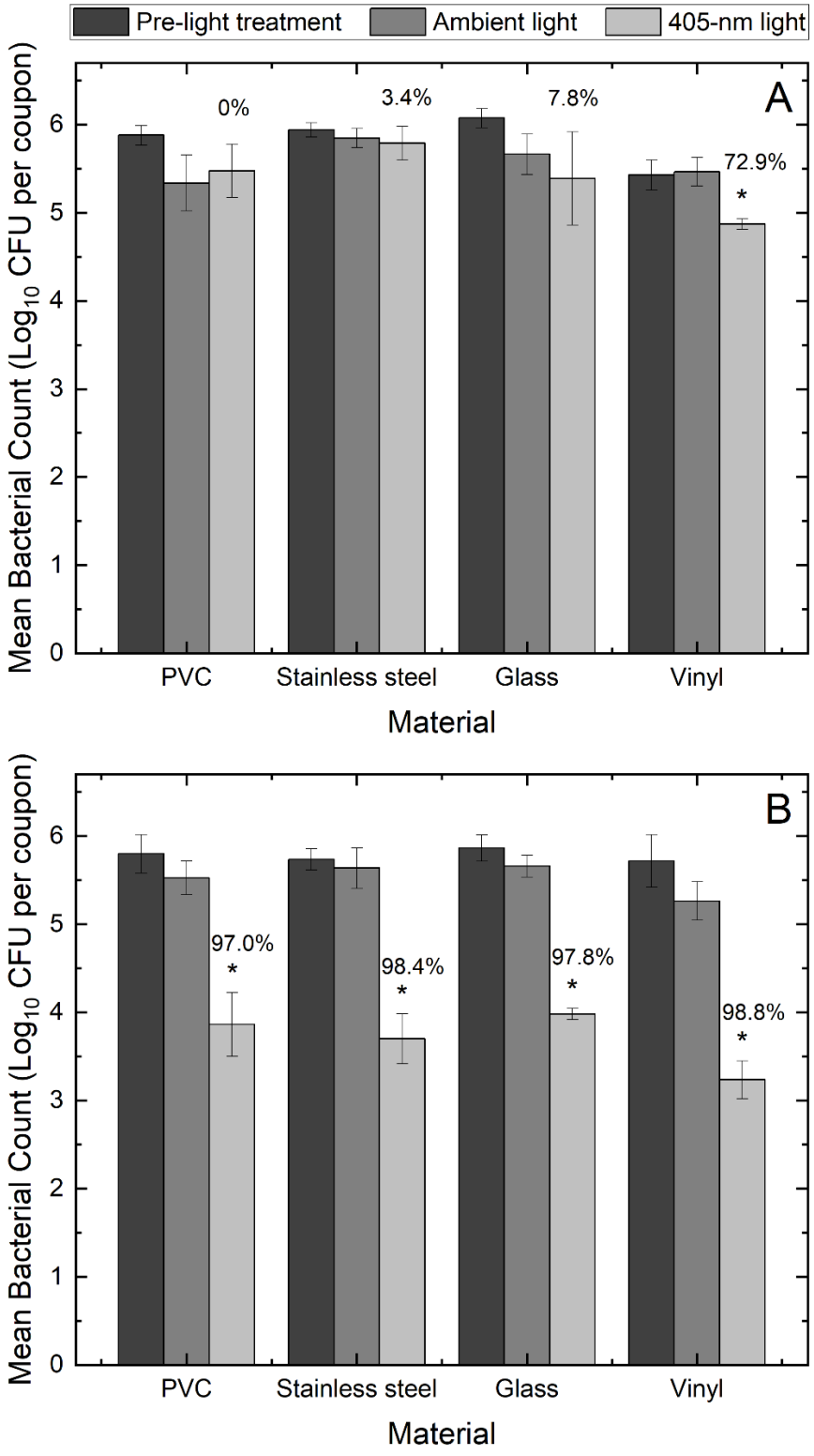

Figure 5.19 Mean *Staphylococcus aureus* counts recovered from PVC, stainless steel, glass and vinyl surface coupons following (A) 4h and (B) 24 h exposure to either ambient light or 405-nm light at an irradiance of ~0.5 mW cm^{-2} (n=6±SD). Mean percentage bacterial reductions in comparison to equivalent ambient light exposed control samples are presented above 405-nm light exposed samples. Asterisks (*) represent materials in which the 405-nm light exposed samples were significantly lower than the equivalent ambient light exposed samples ($P \leq 0.05$).

5.5 Low Irradiance 405-nm Light Inactivation of Biofilms

Clinical contamination of high-touch surfaces with nosocomial biofilms has been widely reported (Bhatta *et al.*, 2018; Ledwoch *et al.*, 2018; Costa *et al.*, 2019). Bacteria embedded within biofilms are substantially more resilient than their planktonic counterparts to common surface disinfectants (Bridier *et al.*, 2011) and thus present a major healthcare challenge. These studies aimed to assess the efficacy of low irradiance 405-nm light to inhibit the formation of, and inactivate, monolayer and mature *S. aureus* biofilms, on microplate wells and common healthcare surfaces.

5.5.1 Methods: Low Irradiance 405-nm Light Inactivation of Biofilms

The efficacy of 405-nm light for biofilm inhibition and inactivation were quantified by two procedures: a crystal violet assay method was used to quantity biofilm biomass on microplate wells; and a swabbing method was used to assess viable cell counts on surfaces coupons.

5.5.1.1 Low Irradiance 405-nm Light Inactivation of Biofilms: Light Source

The light source used for experiments was the miniaturised 405-nm light EDS (Sections 3.4.2 and 5.2); mounted 80 cm from the test surface with all three 405-nm light apertures engaged and set to 95% brightness, as employed in Section 5.4. The resulting irradiance distribution (Figure 5.15) provided sufficient area across the test surface for samples to receive ~0.5 mW cm^{-2}.

5.5.1.2 Low Irradiance 405-nm Light Inactivation of Biofilms: Assessment of Biofilm Formation on Plates using Crystal Violet Assay

To assess the ability of low irradiance 405-nm light to inhibit the formation of *S. aureus* biofilms within microplate wells over a 24 h exposure period, 1 mL 10^3 and 10^6 CFU mL^{-1} bacterial suspensions (prepared as per Sections 3.1.2-3.1.3) were dispensed into individual wells of a sterile polystyrene 24-well microplate (Corning™ Costar™, Fisher Scientific, UK), and the plates were then positioned directly under the EDS at ~0.5 mW cm^{-2} and left for 24 h (at room temperature). In all cases, control coupons were prepared and treated in an identical manner, and exposed to ambient laboratory lighting. A sterile media control was included for both ambient and 405-nm light exposed samples.

The quantity of biofilm present following light treatments was assessed using a crystal violet biofilm assay method adapted from Robertson *et al*. (2017). To execute this, a 0.1% w/v crystal violet solution

(Acros Organics, UK) was prepared in distilled water. Following 24 h exposure to light treatments, the growth media supernatants from each test and control well were aspirated and each was washed twice in distilled water to remove non-adherent bacteria. A 1 mL volume of 0.1% w/v crystal violet was then added to each well and samples were incubated at room temperature for 15 min. Following incubation, excess crystal violet was removed by washing in distilled water until subsequent washes did not visually remove any further excess staining (typically around 4-5 washes). A 2 mL volume of 80% v/v methanol was then added to each sample well before gently agitating (60 rpm) at room temperature for 15 min to fully desaturate the biofilm. This process was conducted for all exposed and non-exposed samples, a media-only control and a methanol-only control. 250 µL volumes of de-stained solutions were then transferred to a 96-well plate and the optical density at 595 nm was read using a MultiSkan GO™ microplate spectrophotometer (Thermo Scientific, UK). Results represent the mean values ± SD of triplicate replicates measured in duplicate (n=6), and are reported as the absorbance at 595 nm, which directly correlated with the biomass present.

5.5.1.3 Low Irradiance 405-nm Light Inactivation of Biofilms: Assessment of Biofilm Formation on Inert Surfaces using Swabbing

To further the work conducted in Section 5.5.1.2, this section quantitatively assessed the ability of the 405-nm light EDS to both (i) inhibit the formation of monolayer and mature biofilms and (ii) inactivate established monolayer and mature biofilms; in both instances on clinically-relevant surfaces (Section 5.4.2). The steps followed to conduct this testing are presented in Figure 5.20. Briefly, biofilms were prepared on 15 × 15 mm inert coupons manufactured from PVC, stainless steel, glass and vinyl (2000 Pur, Polyflur Ltd, UK; Figure 5.16). Immediately prior to experiments, coupons were cleaned in 70% ethanol to sterilise and remove grease. Coupons were then immersed in 10^6 CFU mL^{-1} bacterial suspensions for 1 h to facilitate initial attachment. Following this, bacterial solutions were discarded and coupons were transferred to wells within a 6-well microplate and immersed in 3 mL sterile TSB.

To determine the ability of the 405-nm light EDS to inhibit biofilm formation, coupons in TSB suspensions were then left for either 4 h (to enable monolayer biofilm formation) or 24 h (to enable mature biofilm formation) directly under the light source (~0.5 mW cm^{-2}) at room temperature. Control

coupons were prepared in an identical manner but were exposed to ambient lighting for equivalent durations.

To determine the ability of the 405-nm light EDS to inactivate established biofilms, after coupons were left for 1 h to facilitate initial attachment, they were transferred into fresh TSB and left at room temperature under ambient laboratory lighting for either 4 h (to enable monolayer biofilm formation) or 24 h (to enable mature biofilm formation). Following these incubations periods, coupons were removed from the TSB suspensions, washed once in PBS to remove any non-adherent bacteria, and placed in a sterile petri dish where they were left to dry for 10 min. Coupons were then positioned directly under the light source (~0.5 mW cm^{-2}) for 24 h at room temperature. Control coupons were prepared in an identical manner but were exposed to ambient lighting for the equivalent duration.

Post-exposure in all instances, surviving bacterial colonies were recovered from the exposed side of individual coupons using the swabbing method previously described in Section 5.4.2.1.3 (McKenzie, 2014). Recovered solutions were then serially diluted, where necessary, in PBS and plates onto TSA plates using the drop plate method described in Section 3.1.4. Agar plates were then incubated at 37 °C for 18-24 h, before enumerating the viable bacterial CFU $plate^{-1}$, and then calculating the viable bacterial CFU per coupon. Results represent the mean values ± SD of triplicate replicates measured in duplicate (n=6), and are reported as either mean bacterial counts or the reduction in mean bacterial counts between ambient light and 405-nm light exposed samples, in $\log_{10}$ CFU per coupon.

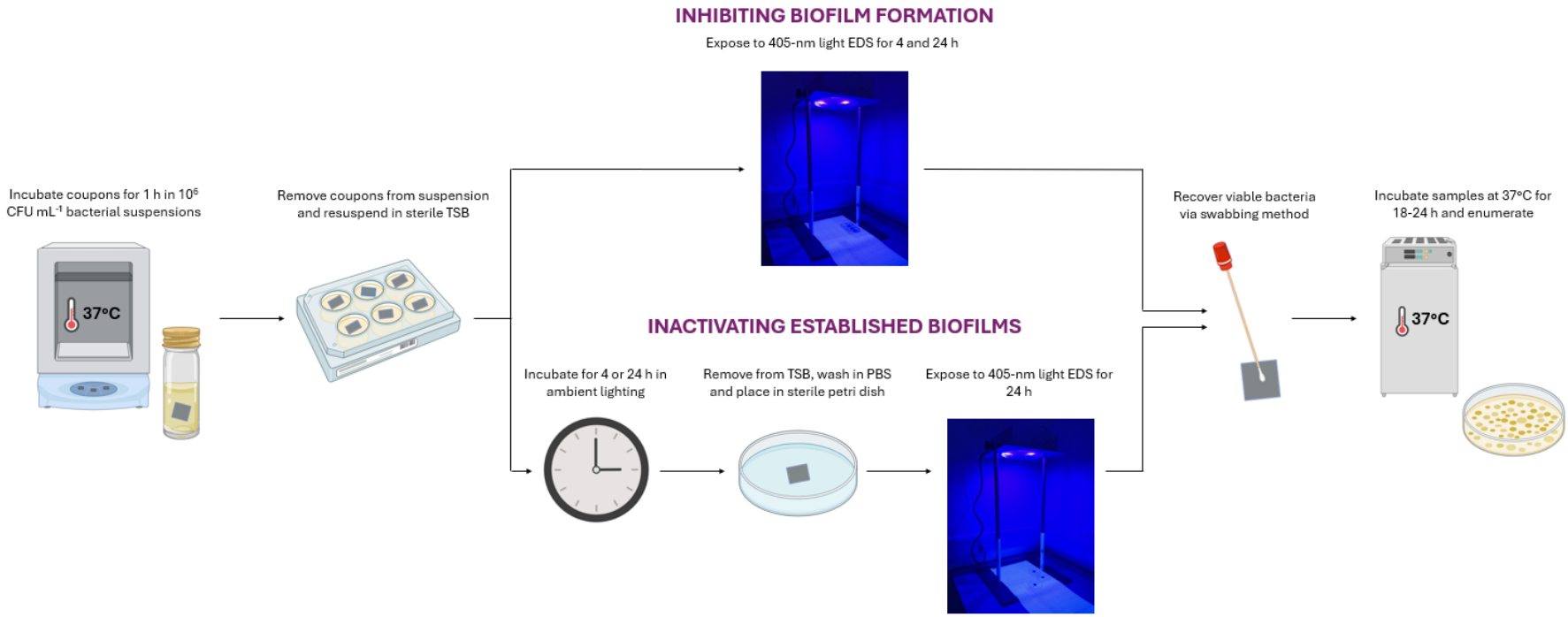

Figure 5.20 Experimental methodology for assessing biofilm formation on inert surface coupons.

5.5.2 Results: Low Irradiance 405-nm Light Inactivation of Biofilms

5.5.2.1 Low Irradiance 405-nm Light Inactivation of Biofilms: Inhibition of the Development of Monolayer and Mature Biofilms

Biofilm biomass formed on the surface of wells in a 24-well microplate, upon exposure to 0.5 mW cm^{-2} 405-nm light for 24 h, is presented in Figure 5.21. Significant reductions in biomass were observed following 405-nm light exposure, in the case of both 10^3 and 10^6 $CFUml^{-1}$ seeding densities ($P<0.001$). In 10^3 CFU mL^{-1} populations, $OD_{595\ nm}$ in ambient lighting was 0.066; whilst values of only 0.026 were reached when exposed to 405-nm lighting ($P<0.001$). Similarly, when immersed in 10^6 CFU mL^{-1} populations, the $OD_{595\ nm}$ of samples exposed in ambient lighting was 0.122; in comparison to just 0.041 when exposed to 405-nm lighting ($P<0.001$). These results indicate the inhibitory effect of 405-nm light in the formation of mature *S. aureus* biofilms over a 24 h period. It was, however, of interest to further this work by assessing total viable counts on clinical surfaces in response to 405-nm light treatment, and thus the swabbing quantification method was employed.

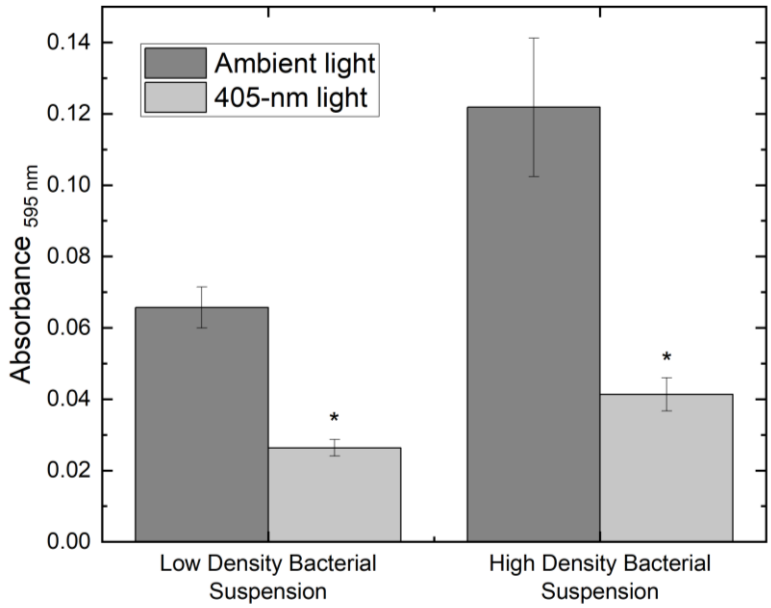

Figure 5.21 Comparison of biofilm formation following 24 h exposure of low density (10^3 CU mL^{-1}) and high density (10^6 CFU mL^{-1}) *Staphylococcus aureus* suspensions to ambient laboratory lighting or 405-nm lighting (~0.5 mW cm^{-2}). Data points represent the mean ±SD (n=6). Asterisks (*) represent a statistically significant difference between levels of biofilm developed for ambient and 405-nm light exposed samples ($P \leq 0.05$).

Results in Figures 5.22-5.23 demonstrate the ability of low irradiance (0.5 mW cm^{-2}) 405-nm light to inhibit the development of both monolayer and mature *S. aureus* biofilms on a range of clinical surfaces.

Figure 5.22 presents the populations of monolayer and mature *S. aureus* biofilms following 4 and 24 h development, respectively, in both ambient and 405-nm lighting conditions at room temperature. When incubated for 4 h under 405-nm lighting conditions, biofilms reached 5.59, 5.47, 5.47 and 5.30 $\log_{10}$ CFU per coupon on PVC, stainless steel, glass and vinyl, respectively; which, in all cases, were significantly lower than those developed in ambient lighting (5.94, 5.96, 6.30 and 6.26 $\log_{10}$ CFU per coupon, respectively; $P \leq 0.002$). When incubated for 24 h, biofilms reached 8.69, 9.08, 9.10 and 8.63 $\log_{10}$ CFU per coupon on PVC, stainless steel, glass and vinyl, respectively, when exposed to ambient lighting; with levels significantly greater on stainless steel and glass in comparison to PVC and vinyl ($P<0.001$). By comparison, biofilms formed after 24 h exposure to 405-nm lighting were significantly lower ($P<0.01$), with mean levels recorded as 5.18, 5.27, 4.53 and 5.88 $\log_{10}$ CFU per coupon on PVC, stainless steel, glass and vinyl, respectively. Together, these findings, consistent with results in Figure 5.21, indicate the inhibitory effect of 405-nm light on the development of both monolayer and mature *S. aureus* biofilms.

Results in Figure 5.23 present the mean $\log_{10}$ reductions in biofilm levels formed on each surface following 4 and 24 h exposure to 405-nm lighting compared to ambient lighting at room temperature. In all cases, reductions in biofilm development were significantly greater upon 405-nm light for 24 h compared to 4 h ($P<0.001$); likely due to the significantly larger quantities of biofilm formed with increasing incubations ($P<0.001$). After 4 h incubation in broth suspensions, significantly greater biofilm inhibition was shown on glass and vinyl compared to PVC and stainless steel ($P<0.001$); however, this is likely accounted for, at least in part, by the significantly higher quantities of biofilms formed amongst control populations on these materials ($P<0.001$). After 24 h incubation, the greatest inhibition of biofilm development was demonstrated on glass, which was significantly greater than that of stainless steel and PVC ($P<0.001$), which were again significantly greater than that of vinyl ($P<0.001$). Significantly greater levels of biofilms were formed amongst control populations on glass and stainless steel, however, in comparison to that of PVC and vinyl ($P<0.001$), which again could have, at least in part, accounted for this difference. Regardless, findings overall indicate that low levels of 405-nm light can inhibit biofilm development on common hospital surfaces over time as biofilm populations continue to increase.

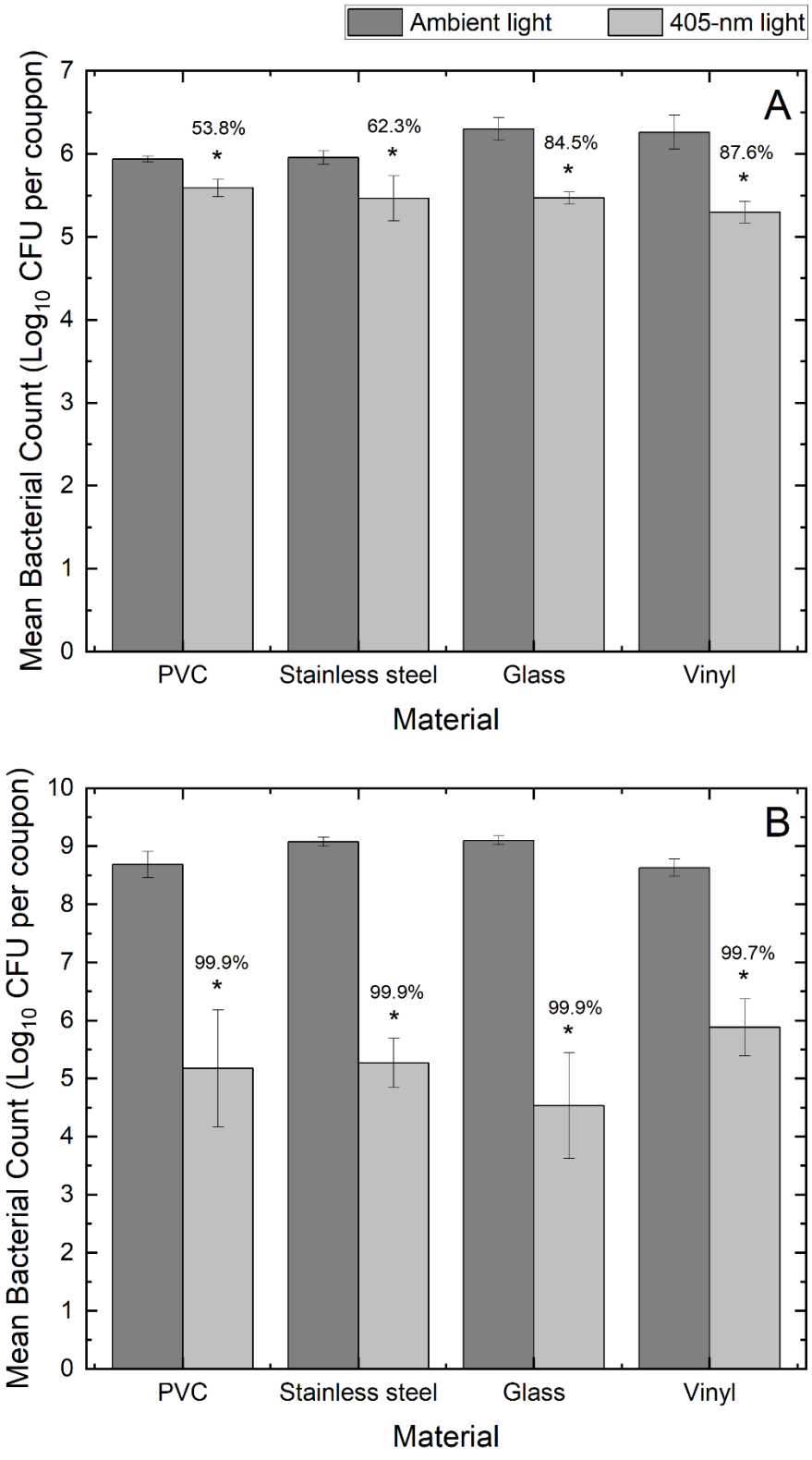

Figure 5.22 Levels of *Staphylococcus aureus* biofilms developed on PVC, stainless steel, glass and vinyl surfaces following (A) 4 h and (B) 24 h exposed to either ambient light or 405-nm light at an irradiance of ~0.5 mW cm^{-2}. Data points represent the mean ± SD (n=6). Mean percentage reductions in biofilms in comparison to equivalent ambient light exposed control samples are presented above 405-nm light exposure samples. Asterisks (*) represent a statistically significant difference between the levels of biofilm developed for ambient and 405-nm light exposed samples ($P \leq 0.05$).

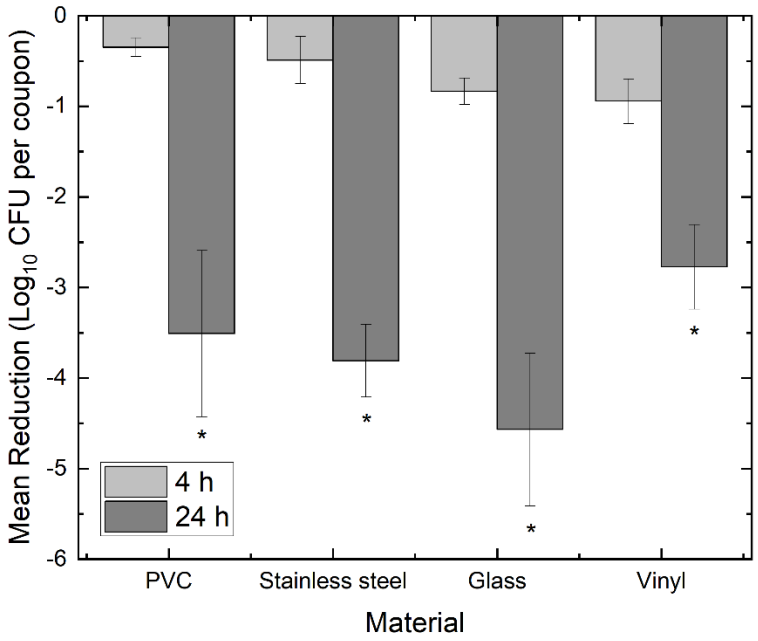

Figure 5.23 Reduction of *Staphylococcus aureus* biofilms developed on PVC, stainless steel, glass and vinyl surfaces following either 4 h or 24 h exposure to 405-nm light at an irradiance of ~0.5 mW cm^{-2} in comparison to ambient light. Data points represent the mean ± SD (n=6). Asterisks (*) represent significantly greater reductions in biofilm levels achieved for samples exposed for 24 h in comparison to 4 h ($P \leq 0.05$).

5.5.2.2 Low Irradiance 405-nm Light Inactivation of Biofilms: Inactivation of Established Monolayer and Mature Biofilms

Results in Figures 5.24-5.25 demonstrate the ability of low irradiance (0.5 mW cm^{-2}) 405-nm light to inactivate established monolayer and mature biofilms on clinically relevant surfaces.

Figure 5.24 presents the log_{10} populations of (A) monolayer and (B) mature biofilms following 4 and 24 h development, respectively, and then exposed to either ambient or 405-nm lighting for 24 h. When incubated in broth solutions for 4 h, bacterial biofilm populations of 5.26, 4.97, 5.35 and 4.58 CFU per coupon were recorded on PVC, stainless steel, glass and vinyl, respectively; with biofilm levels developed on glass and PVC significantly greater than those on vinyl ($P<0.001$), and no significant difference demonstrated between that developed on stainless steel compared to all other material ($P>0.05$). When incubated in broth solutions for 24 h, biofilm populations reached 7.86, 7.46, 7.34 and 6.91 CFU per coupon on PVC, stainless steel, glass and vinyl, respectively; which, in all cases, were significantly higher than those developed after 4 h ($P<0.001$). Biofilm development following 24 h incubation in broth solutions on PVC coupons were significantly greater than that on stainless steel and glass, which were together significantly greater than that on vinyl ($P<0.001$).

In all cases, control populations of monolayer ($P \leq 0.006$) and mature ($P < 0.001$) biofilms significantly reduced following 24 h exposure to ambient light, compared to levels measured immediately following the drying process: monolayer biofilm populations reduced by 9.9-17.0% and mature biofilm populations reduced by 14.7-23.4%. No significant difference ($P > 0.05$) was demonstrated between reductions observed on monolayer and mature biofilms, excluding on stainless steel where significantly greater reductions were observed in mature biofilms ($P = 0.005$). In all cases, both monolayer ($P \leq 0.032$) and mature ($P \leq 0.022$) *S. aureus* biofilms decreased when exposed to 405-nm light, compared to ambient light, for 24 h. Monolayer biofilm populations recorded on PVC, stainless steel, glass and vinyl following 405-nm light exposure were 3.31, 3.55, 2.91 and 2.41 $\log_{10}$ CFU per coupon, respectively; compared to 4.36, 4.47, 4.62 and 3.84 $\log_{10}$ CFU per coupon, respectively, for those exposed to ambient light (reductions of 93.0, 85.5, 96.7 and 66.6%, respectively). Mature biofilm populations recorded on PVC, stainless steel, glass and vinyl following exposure 405-nm light exposure were 5.55, 4.33, 3.85 and 4.05 $\log_{10}$ CFU per coupon, respectively; compared to 6.02, 5.90, 6.26 and 5.49 log10 CFU per coupon, respectively, when exposed to ambient light (reductions of 61.2, 96.7, 99.4 and 95.7%, respectively).

Figure 5.25 present the mean $\log_{10}$ reductions in monolayer and mature biofilms following 24 h exposure to 405-nm light compared to ambient light. For stainless steel and glass, reductions were significantly greater in mature versus monolayer biofilms: 1.58 vs 0.92 $\log_{10}$ CFU per coupon on stainless steel ($P < 0.001$) and 2.41 vs 1.71 $\log_{10}$ CFU per coupon on glass ($P < 0.001$). However, on PVC, reductions were significantly greater in monolayer biofilms (1.34 vs 0.78 $\log_{10}$ CFU per coupon; $P < 0.001$) and on vinyl, no significant difference was determined between reductions of monolayer and mature biofilms (1.43 vs 1.44 $\log_{10}$ CFU per coupon; $P = 0.959$). For monolayer biofilms, reductions observed on glass and vinyl were significantly greater than on stainless steel ($P < 0.001$), with no significant difference demonstrated between reductions on PVC and all other surfaces ($P > 0.05$). For mature biofilms, reductions observed on glass were significantly greater than on stainless steel and vinyl, which together were significantly greater than reductions on PVC ($P < 0.001$). Regardless, findings overall indicate that low levels of 405-nm light (0.5 mW cm^{-2}; 43.2 J cm^{-2}) can inactivate *S. aureus* biofilms of varying complexity from common hospital surfaces.

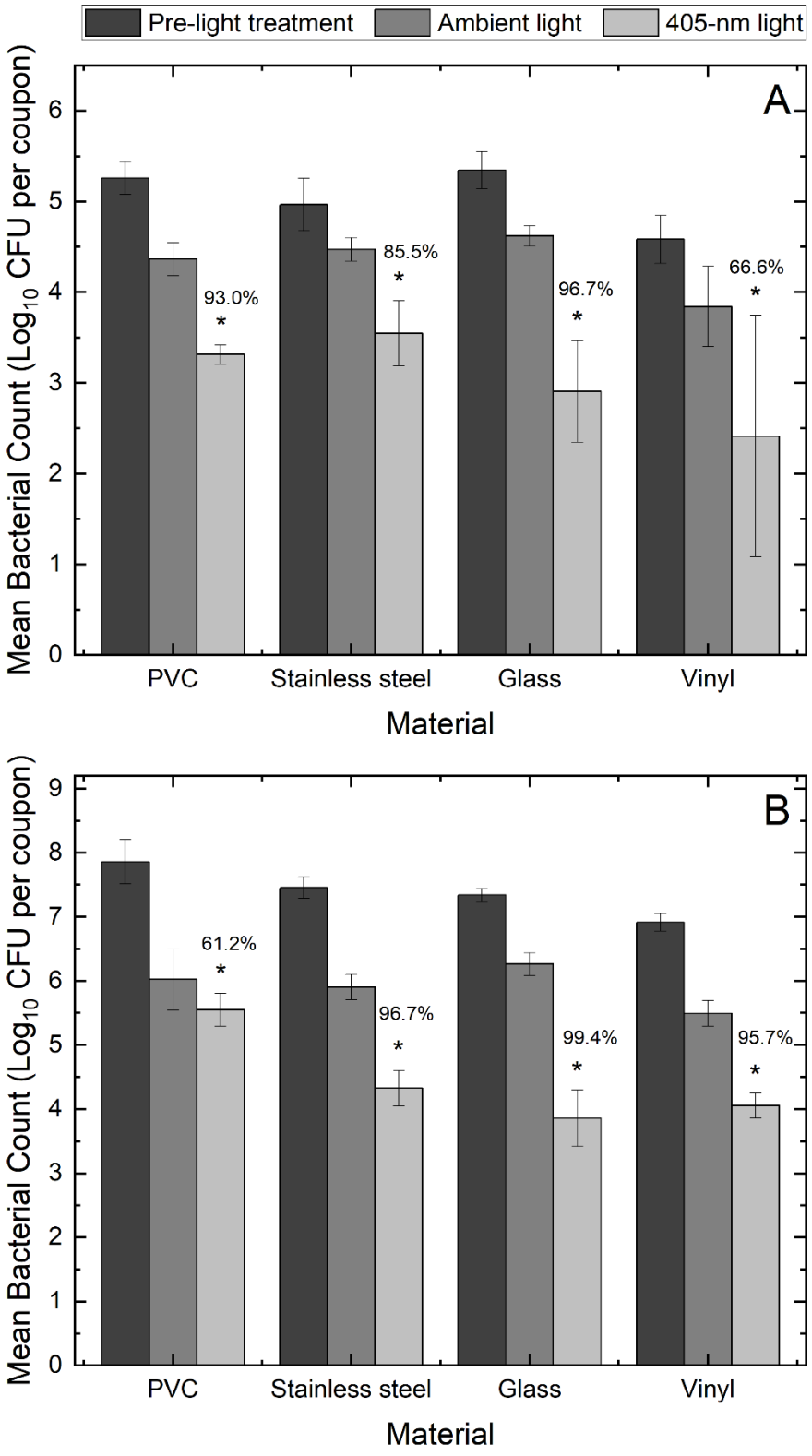

Figure 5.24 Levels of *Staphylococcus aureus* biofilms developed for either (A) 4 h or (B) 24 h on PVC, stainless steel, glass and vinyl and then exposed to either ambient light or 405-nm light at an irradiance of ~0.5 mW cm^{-2} for 24 h. Data points represent the mean ± SD (n=6). Mean percentage reductions in biofilms in comparison to equivalent ambient light exposed control samples are presented above 405-nm light exposure samples. Asterisks (*) represent a statistically significant difference between biofilm levels present following exposure to ambient and 405-nm light ($P \leq 0.05$).

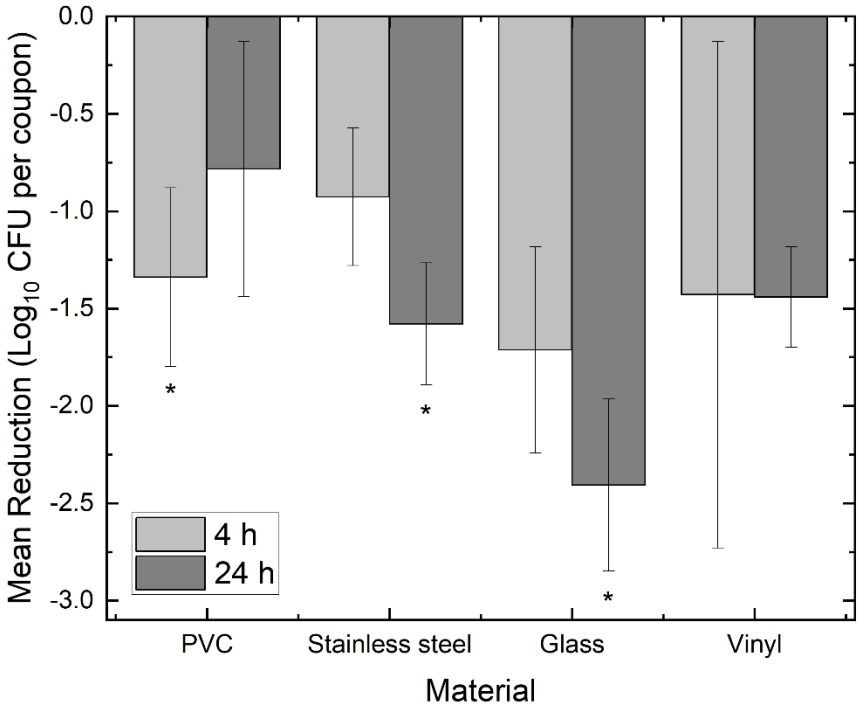

Figure 5.25 Reduction of *Staphylococcus aureus* biofilms developed on PVC, stainless steel, glass and vinyl surfaces following either 4 h or 24 h exposure to 405-nm light at an irradiance of ~0.5 mW cm^{-2} in comparison to ambient light. Data points represent the mean ± SD (n=6). Asterisks (*) represent significantly greater reductions in biofilm levels achieved in comparison to the alternative time period for that material ($P \leq 0.05$).

5.6 Discussion

The studies performed in this chapter address key operational considerations associated with clinical implementation of the 405-nm light EDS for surface decontamination, and the following sections will discuss key findings associated with this work.

5.6.1 Exposure to Low Irradiance Levels Produced within Whole-Room Settings

By assessing efficacy for bacterial inactivation when employed at the lowest range of irradiances expected to illuminate surfaces within a typical room setting, valuable findings were provided regarding the levels of inactivation, and the timescales required to achieve this, which could be expected within a typical hospital room, in addition to providing insight into the minimum threshold irradiance levels required for inactivation to occur.

Bacterial contamination has been indicated on various surfaces within hospital isolation rooms, including hospital beds, sinks, furniture, floors, walls and medical equipment (Chaoui *et al.*, 2019).

When practically deployed, the 405-nm light EDS will likely be positioned at varying distances from these surfaces, and thus each will likely be illuminated at varying irradiance levels, potentially lower than those used in Chapter 4 to model the illumination of high-touch surfaces (~0.5 mW cm^{-2}). Additionally, surfaces may be occluded or shaded from illumination, thus hindering irradiance received. It is indubitable that contaminant position, and potential obstruction from direct illumination, will impact inactivation capacity and are common limitations associated with 405-nm light EDS studies. This chapter aimed to address these considerations by investigating the antibacterial efficacy of 405-nm light at the lower range of irradiance levels produced within a whole room setting. The irradiance levels employed (≤0.31 mW cm^{-2} in Figure 5.8 and ≤0.1 mW cm^{-2} in Figure 5.9) account for 96.3 and 85.8%, respectively, of irradiances measured within the profiling established in Section 4.2, and were thus considered an adequate representation of the levels likely to illuminate healthcare surfaces.

Promisingly, with the exception of exposures to 0.001 mW cm^{-2}, bacterial inactivation was shown to significantly increase upon longer exposure to, and thus higher doses of, 405-nm light (Figures 5.8-5.9; P≤0.032). For practical deployment, the 405-nm light EDS is designed to be used continuously during daylight hours, or ceaselessly in instances where light would not pose disturbance. As such, results here imply the ability of the system to maintain low levels of contamination throughout a typical room environment. Clinical studies investigating the 405-nm light EDS have demonstrated similar effects: evidencing increased reductions in viable bacterial counts on various surfaces positioned at varying distances from the light source including door handles, table/locker surfaces, bed rails, computer keyboard/mouse and light switches, with increasing exposure (Maclean *et al.*, 2010; Bache *et al.*, 2012a; Murrell *et al.*, 2019). Results here corroborate these findings, and provide fundamental laboratory-controlled inactivation kinetics of known contaminants exposed to known irradiance levels.

Given no significant reductions were demonstrated within 72 h exposure to 0.001 mW cm^{-2} (Figure 5.9; P=0.935-1.000), exposure to this particular irradiance was extended for up to 7 days; however, no significant inactivation was demonstrated within this period (P≥0.089). In this instance, there likely exists a minimum threshold irradiance level for antimicrobial activity of 405-nm light between 0.001 and 0.005 mW cm^{-2}. It is possible that, below this level, any low levels of ROS produced as a result of these low-level light exposures are within levels capable of being detoxified by bacterial antioxidant defence mechanisms. Bacterial populations of 10^2 CFU $plate^{-1}$ were selected to replicate typical levels

of contamination likely to be found on healthcare environmental surfaces (Maclean *et al.*, 2013a); however, it is important to note that, on inert clinical surfaces, organisms will be under greater stress due to the risk of desiccation, and thus are likely to demonstrate greater susceptibility than that established here. Findings in this instance indicate the presence of a threshold level of irradiance, however this is likely to differ depending on the organism and its exposure conditions.

5.6.2 Effect of Suspension Media and Fomite Material on Bacterial Inactivation

To emulate realistic environmental conditions, studies in this chapter examined the efficacy of the EDS for inactivation of bacterial contamination presented in various organic, inorganic and biological suspension media; and bacterial contamination deposited on various inert clinical surfaces. Whilst contaminating the healthcare settings, bacteria are often suspended within biological fluids, smears or matter, which may influence their susceptibility to light inactivation. Biological matter may contain photosensitive media that could enhance ROS generation and cellular inactivation, coupled with the fact that microbial contamination in the environment will be stressed due to starvation or desiccation, which will likely make them more susceptible to inactivation. Conversely, the biological matter (such as saliva, faeces or blood) surrounding the microbial contamination may reduce light penetration to the cells, affecting inactivation efficacy. Establishing inactivation kinetics under such conditions was considered a key area of study in better understanding efficacy of the 405-nm light EDS.

Microorganisms can be transmitted from infected patients to the environment via various corporeal fluids including expectorate drops, blood, fluid from exposed wounds, excrement and urine (Bonadonna *et al.*, 2017). These fluids can be deposited onto inanimate objects via either direct contact with an infected individual or indirect contact with medical personnel, where they can survive for months and serve as HAI transmission vectors (Kramer *et al.*, 2006; Bonadonna *et al.*, 2017). For implementation within clinical settings, whereby surfaces may be contaminated with both pathogens and bodily secretions, it was considered essential to comparatively assess the efficacy of low irradiance 405-nm light for inactivation of microbes suspended in both minimal and biologically relevant media.

Viral inactivation by 405-nm light has previously shown to be enhanced when exposed in nutritious media, with findings demonstrating enhanced inactivation of bacteriophage ΦC31 when exposed in NB suspensions as opposed to PBS, with up to nine times greater inactivation demonstrated (Tomb *et al.*,

2014); and enhanced inactivation of feline calicivirus when exposed in biologically-relevant media suspensions, including blood plasma, artificial saliva and artificial faeces, and other organically-rich media, as opposed to PBS, reporting 50-85% less dose required to achieve equivalent inactivation (Tomb *et al.*, 2017b). The authors hypothesised this was likely due to the presence of photosensitive components within organically-rich and biologically-relevant media which are predisposed to 405-nm light sensitisation and thus could potentially act as exogenous photosensitisers; eliciting damage via ROS or other toxic photoproducts upon 405-nm light exposure to adjacent viral particles in suspension (Tomb *et al.*, 2014, 2017b). While this effect is less thoroughly demonstrated for bacteria, Meurle *et al*. (2021) recently demonstrated an enhancement in the 405-nm light inactivation of *Staphylococcus carnosus* – employed as a non-pathogenic surrogate for *S. aureus* – in an endotracheal model when exposed in artificial saliva as opposed to PBS, hypothesising that the unfavourable conditions of the saliva suspension – most notable the higher salt concentrations– could weaken the bacterial cells capability to withstand or repair damage caused by 405-nm light photoinactivation.

Results of this study indicate enhanced inactivation when suspended in saliva compared to PBS, demonstrating over two times greater reductions following just 1 h exposure (56.5 vs 24.6%, respectively; $P<0.001$). From data in Figure 5.14, the artificial saliva employed was shown to demonstrate strong fluorescence emission peaks at 468 nm upon 405-nm light exposure – whilst minimal fluorescent activity was shown for PBS – thus suggesting the presence of components in saliva, likely mucins as discussed by Tomb (2017), which are predisposed to 405-nm light photosensitisation and thus could act as exogenous photosensitisers to elicit inactivation in a similar mechanism to that previously described for viruses (Tomb *et al.*, 2014, 2017b). Further, mucins present within human saliva are considered host-defence proteins, known to exhibit antimicrobial properties via their ability to bind with, agglutinate and clear microorganisms (Gorr, 2009), and so this will likely have also contributed to the observed effects. Meurle *et al*. (2021) employed an artificial saliva which lacked any components known to elicit antimicrobial effects and yet enhancement was still demonstrated, suggesting it is likely the unfavourable conditions presented by saliva which will predominantly have caused this inactivation effect.

This hypothesis may explain why when suspended in artificial faeces, also known to contain photosensitive components (Figure 5.14), bacteria demonstrated lower susceptibility to 405-nm light

inactivation than in PBS. The human gut microbiome is one of the most densely populated microbial communities known to exist, characterised by stability and resilience (Rinninella *et al.*, 2019). There is therefore potential for this media to support bacterial survival – more so than saliva suspensions – thus hampering 405-nm light inactivation effects. As discussed, inactivated *Saccharomyces cerevisiae,* psyllium powder, cellulose, oleic acid and miso paste were employed to simulate the typical composition of bacterial debris, carbohydrates, fibre, fats and nitrogen within real human faeces (Colón *et al.*, 2015). Quantities of each will realistically be variable, however: individual gut microbiomes are extremely diverse as a result of environmental factors, health conditions and alimentary habits (Aranda-Michel and Giannella, 1999; Rapozo *et al.*, 2017). Alterations to this composition can affect host immunity (Rapozo *et al.*, 2017), thus potentially impacting the efficacy of 405-nm light inactivation. Further, albeit insignificant, the transmission of 405-nm light through artificial faeces suspensions was shown to be reduced compared to that of PBS and saliva (Table 5.1). Regardless, significant levels of inactivation were still achieved at all measured time points ($P \leq 0.017$), with up to 64.4% reductions demonstrated following 4 h, indicating the antibacterial efficacy of the 405-nm light EDS when presented in such mediums.

These findings differ to that demonstrated previously for viral inactivation, which was significantly enhanced in both saliva and faeces compared to minimal media (Tomb *et al.*, 2017b). It may be the case that, given their lack of endogenous porphyrins, viral inactivation by 405-nm light is more heavily influenced by photosensitisation of the suspension media in comparison to that of bacterial cells, which contain both intracellular porphyrins and more established host defence mechanisms to protect from oxidative stress. It is thus hypothesised that, for bacterial inactivation, a dynamic balance may exist where nutrient rich suspension media can potentially induce secondary antimicrobial effects through 405-nm light photosensitisation, thereby enhancing bacterial inactivation; whilst also potentially providing adequate nutrition to aid survival and defend against oxidative damage. Further investigation to elucidate the stimulatory or inhibitory effects of suspension media on 405-nm light bacterial inactivation is necessary, given its importance when considering the likely exposure conditions of bacteria in practical settings.

Despite differences in susceptibility, *S. aureus* inactivation was successfully demonstrated in both saliva and faecal suspensions, with a likelihood that populations would continue to decrease upon increasing

exposure time based on the demonstrated trajectories of inactivation. When exposed in whole blood, however, no significant bacterial reductions were demonstrated (≤0.87% reductions; P=0.816-0.981) until 4 h (9.94% reduction; P=0.034). This is likely due to the limited ability of 405-nm light to penetrate through, and thus excite photosensitive components within, the media, as indicated by the loss in transmission of 405-nm light and fluorescence emission data in Table 5.1 and Figure 5.14, respectively. Results in Table 5.1 demonstrated a 76.5% loss of light transmission through whole blood samples – whilst minimal loss (0-0.5%) was demonstrated for all other tested media – and it is therefore expected that this will have significantly hampered the ability of 405-nm light photons to adequately reach bacterial contaminants within blood samples, in comparison to that of the other media investigated. Given components of whole blood have previously shown to be predisposed to 405-nm light photosensitisation (Tomb, 2017), and its demonstrated trajectory of inactivation, it is of interest to establish if longer exposures could warrant greater levels of inactivation. Multiple studies have demonstrated the ability to inactivate microorganisms using 405-nm light when exposed in human plasma and platelet concentrates (Tomb *et al.*, 2017b; Maclean *et al.*, 2020); however, there is limited evidence to demonstrate its capacity for inactivation in whole blood, which is a more likely environmental contaminant media than that of individual blood components. Although its opacity was shown to hamper inactivation effects; this contaminant is more noticeable on surfaces than that of translucent biological mediums, and thus would likely be adequately removed by manual cleaning and disinfection protocols.

As previously discussed, the persistence of nosocomial agents on hospital surfaces plays a significant role in the transmission of HAIs (Kramer *et al*., 2006). Given its broad-spectrum efficacy and favourable safety profile, 405-nm light technology has recently been implicated for safe, unobtrusive and continuous decontamination of occupied environments. Various studies have substantiated its ability to reduce bacterial levels from surfaces within hospital settings (Maclean *et al.*, 2010, 2013a; Bache *et al.*, 2012a, 2018a; Murrell *et al.*, 2019); however, a comprehensive understanding of its antimicrobial capabilities on a range of common healthcare surfaces is relatively unknown. Experiments in this chapter therefore sought to assess the comparative efficacy of low irradiance 405-nm light for the inactivation of *S. aureus* seeded onto PVC, stainless steel, glass and vinyl coupons. These were selected to represent common materials employed, and thus likely to become contaminated, within healthcare

settings: due to its versatility and affordability, PVC is commonly used for manufacture of medical devices and hospital interiors (ECVM, 2023); due to its strength and durability, stainless steel is a common choice for medical devices and equipment, furniture and structural elements (Essentra Components, 2023); International Health Facility Guidelines recommend that the floors and walls of hospital areas, which are likely to come into direct contact with patients or other bodily fluids, are surfaced with smooth, impermeable and seamless materials such as vinyl (International Health Facility Guidelines, 2022); whilst window fixtures and wall dividers are primarily manufactured from glass.

Bacterial adhesion to, and thus subsequent survival on, surfaces is considerably influenced by wettability (Yang *et al.*, 2022), and so this was an important consideration during experimental testing. Despite significant differences between the wettability of each material, data in Figure 5.19 indicated similar levels of *S. aureus* attachment onto each surface following 30 min immersion in bacterial solutions (P=0.568) – with the exception of vinyl surfaces for 4 h exposures (Figure 5.19A), which demonstrated significantly lower bacterial attachment than that of the other materials investigated (5.43 $\log_{10}$ CFU per coupon versus 5.88-6.07 $\log_{10}$ CFU per coupon; P<0.001) – suggesting, in this instance, wettability had minimal influence on initial bacterial attachment; thus implying an equal likelihood of *S. aureus* contamination on such surfaces in clinical settings. Surface wettability was, however, somewhat influential on the extent of bacterial inactivation achieved following 405-nm light exposure (Figure 5.19). Following 4 h, no bacterial reductions on PVC – which showed the lowest wetting (69.29-71.65°) – were demonstrated (P=0.458). These findings align with recent work by Chen *et al*. (2023), which indicated the effectiveness of 405-nm light for surface-seeded bacterial inactivation depends on contact angles made with the surface: reporting greater $\log_{10}$ reductions on surfaces with higher hydrophilicity, and lower reductions on surface with contact angles >65º, which are considered hydrophobic (Vogler, 1998). Kim & Kang (2020) similarly found that surface hydrophobicity affects UV-C inactivation of bacteria on materials, reporting increasing reductions with decreasing water contact angles. The authors attributed these variations to be due to differences in bacterial aggregation tendencies on the surfaces (Chen *et al*., 2023; Kim & Kang, 2020). In the present study, it is possible that the hydrophobicity of PVC caused the bacterial inoculum to assemble in a smaller area, resulting in the development of dense longitudinal stacking structure of cells and undesirable shading from light exposure (Kim & Kang, 2020). In contrast, it is likely that the hydrophilicity of the other materials

investigated encouraged the spread of bacteria over a larger surface area, suggesting less bacterial stacking and thus greater overall light exposure (Kim & Kang, 2020), which may explain the greater inactivation observed. Similar reductions were observed on stainless steel (0.06 $\log_{10}$ CFU per coupon reductions; P=0.127), however, which demonstrated the highest wettability of all materials. Further, the greatest bacterial reductions were observed on vinyl (0.59 $\log_{10}$ CFU per coupon reductions; P<0.001), which exhibited contact angles in the mid-range amongst those tested. These findings suggest alternative surface characteristics are also likely influential on the bactericidal efficacy of 405-nm light.

Kim & Kang (2020) established a correlation between surface roughness and bacterial inactivation by UV light exposure, demonstrating lower reductions of *E. coli*, *S. typhimurium* and *Listeria monocytogenes* when seeded onto stainless steel and PVC versus glass, with the latter demonstrating significantly lower surface roughness (P<0.05). Surfaces with imperfections, such as the stainless steel used in this thesis, contain peaks and crevices which can both shield from light exposure and retain bacteria with stronger adhesion due to the greater surface area for contact (Chen *et al.*, 2023). If both surface wettability and roughness are considered, this could explain the similarly low bacterial reductions observed on both PVC and stainless steel in Figure 5.20. Additional surface characteristics which can influence microbial inactivation include the zeta potential and porosity of materials (Bernady and Malley, 2023). Further, if surfaces are reflective, inactivation efficacy will likely be enhanced, given that photons which do not directly illuminate microbial cells can be reflected and potentially absorbed by nearby microbial cells, rather than being adsorbed by the material. The balance between these factors may explain the differing antimicrobial patterns demonstrated following 24 h exposure; however, further work is required to comprehensively profile the surface characteristics of each coupon and their influence on inactivation.

Control populations (Figure 5.19) were shown to vary throughout treatment, and thus it is difficult to directly compare bacterial reductions. Following 4 h exposure to ambient lighting, bacterial levels on both PVC and glass significantly reduced compared to pre-exposure levels (0.54 and 0.28 $\log_{10}$ CFU per coupon reductions, respectively; P=0.003); whilst no significant reductions were demonstrated on stainless steel and vinyl (P=0.127-0.707). Following 24 h exposure to ambient lighting, bacterial levels on all materials significantly reduced (0.20-0.45 $\log_{10}$ reductions; P=0.013-0.043) with the exception of stainless steel (P=0.448). Given stainless steel demonstrated greater hydrophilicity and surface

roughness, these findings suggest the potential influence of wetting and roughness on bacterial survival for extended periods of time, regardless of light exposure.

Findings in Figure 5.13 indicate that, for *S. aureus* suspended in PBS and seeded onto nutrient agar surfaces, a dose of 7.2 J cm^{-2} achieved 0.63 log_{10} reductions. Exposure of *S. aureus* on inert surface coupons (Figure 5.19) to this same dose achieved 0-0.59 log_{10} reductions which, although can be considered somewhat similar, cannot be accurately compared given that the latter were seeded at substantially higher densities (~10^2 CFU $plate^{-1}$ vs 10^{5-6} CFU per coupon) to enable enumeration, which was likely influential on inactivation efficacy. Murdoch *et al*. (2012) found *L. monocytogenes* to be more susceptible to 405-nm light inactivation when exposed on PVC and acrylic surfaces as opposed to agar surfaces: using 71-110 mW cm^{-2}, 0.93 and 0.22 log_{10} reductions were achieved on PVC and acrylic, respectively, following 30 J cm^{-2}; whilst just 0.07 log_{10} reductions were achieved on agar surfaces following double this dose (60 J cm^{-2}). It is therefore likely that bacteria seeded onto inert clinical surfaces, which are likely pre-disposed to greater environmental stress, will demonstrate greater susceptibility to 405-nm light inactivation than that of agar surfaces.

This study used similar seeding methodology to that of McKenzie (2014), who examined the ability of 405-nm light at ~60 mW cm^{-2} to inactivate *E. coli* seeded onto various surface coupons. Comparing the two common materials investigated – glass and vinyl – initial bacterial levels were found to be substantially higher in this study than that of McKenzie (2014): 5.07 vs 4.61 log_{10} CFU mL^{-1} for glass and 5.42 vs 4.66 log_{10} CFU mL^{-1} for vinyl. This is likely due to the different species employed and their varying affinities for surface attachment, with previous work by Oh *et al*. (2018) establishing that the time constant of bacterial-substrate adhesion is 2-4 times greater for *E. coli* than *S. aureus*, meaning a greater quantity of *S. aureus* colonies will likely have attached during the 30 min incubation of the coupons in bacterial suspension, as demonstrated. McKenzie (2014) demonstrated 4.61 and 4.45 log_{10} reductions on glass and vinyl, respectively, following 36 J cm^{-2}; whilst in this study, equivalent reductions of 1.68 and 2.03 log_{10} reductions were observed, respectively. Although direct comparisons cannot be made, findings together suggest *S. aureus* is potentially less susceptible than *E. coli* when dried on surfaces to 405-nm light inactivation; or that the dose delivery regime employed by McKenzie *et al.* (60 mW cm^{-2} for 10 min) was more effective for inactivation of *E. coli* in that instance in comparison to the regime employed here for *S. aureus* inactivation (0.5 mW cm^{-2} for 24 h). Regardless,

findings of this study overall indicate the ability of low irradiance 405-nm light to inactivate bacterial contaminants on various healthcare-associated surfaces; advancing knowledge on the effectiveness of the 405-nm light EDS, and provide an indication of the potential exposures times likely required to inactivate microbial contamination within the healthcare setting.

5.6.3 Low Irradiance 405-nm Light Inactivation of Biofilms

This chapter successfully demonstrated the ability of 405-nm light to inhibit the development of and inactivate established bacterial biofilms on microplate wells and inert clinical surfaces. It is widely acknowledged that hospital surface contamination contributes greatly to the transmission of HAI-inducing pathogens, and that bacteria contained within biofilms significantly heighten this risk, given the majority of nosocomial microbial and chronic infections are associated with biofilm formation (Jamal *et al.*, 2018). As discussed, inactivation of bacteria presented in biofilms using blue light has previously been indicated (McKenzie *et al.*, 2013; Soukos *et al.,* 2015; Wang *et al.,* 2016; Li *et al.*, 2018; Ferrer-Espada *et al.*, 2019, 2020; Gomez *et al.*, 2019; Tsutsumi-Arai *et al.*, 2019, 2022; Blee *et al.*, 2020; McMullan *et al.*, 2022; Maknuna *et al.*, 2023); however, these studies have primarily been conducted at higher irradiances (13-300 mW cm^{-2}), and so its capacity under conditions representative of environmental decontamination applications is yet to be fully established. As such, this study sought to examine the ability of low irradiance (0.5 mW cm^{-2}) 405-nm light to inhibit the formation of, and inactivate, monolayer and mature biofilms on common healthcare surfaces – namely PVC, stainless steel, glass and vinyl – as a means of further establishing efficacy of the technology for practical applications.

The ability of low irradiance 405-nm light to inhibit the formation of mature biofilms on surfaces was first examined using a crystal violet staining assay. Results of this assay (Figure 5.21) indicated that, for both low (10^3 CFU mL^{-1}) and high (10^6 CFU mL^{-1}) seeding densities, biofilm production was significantly inhibited ($P<0.001$) upon exposure to low irradiance (0.5 mW cm^{-2}) 405-nm light for 24 h, with 60.1 and 66.4% lower biomass presented, respectively, compared to controls; and significantly greater inhibition demonstrated for those generated in high versus low density bacterial populations ($P<0.001$). These findings suggest the potential ability for low intensity exposures to continually inhibit biofilm growth, thus maintain low levels of contamination, within clinical settings.

Crystal violet assays have been widely used in PDT studies (Misba *et al.*, 2016, 2019; Güzel Tunccan *et al.*, 2018; Pourhajibagher *et al.*, 2018; Banerjee *et al.*, 2020; Akhtar *et al.*, 2021; He *et al.*, 2022) and are considered the most widely used quantification technique in microtiter plate assays (Azeredo *et al.*, 2017). However, few studies have used the technique to specifically examine biomass inhibition upon 405-nm light exposure. McMullan *et al*. (2022) recently used a crystal violet assay to demonstrate blue light (2.78 mW cm^{-2} for 24 h) was sufficient to destroy the extracellular biofilm architecture of four MDR organisms; proposing the technology as a wearable device for continuous ambulatory wound treatment. Results presented in this study, to the best of the author's knowledge, present, for the first time, the potential ability of 405-nm light to inhibit the formation of biofilms in the context of environmental decontamination.

Although results using the crystal violet assay are indicative of reductions in biofilm mass upon light exposure, it was not possible to determine corresponding cell viability as a result of these treatments. As such, a direct method of biofilm quantification was employed to determine viable bacterial counts pre- and post-exposure. A swabbing and conventional culture plating method was chosen in this instance, given it represents a common biofilm enumeration method in healthcare and laboratory settings (McKenzie *et al.*, 2013; Johani *et al.*, 2018; Ledwoch *et al.*, 2018; Redanz *et al.*, 2021). Biofilm inhibition was measured on the four surface coupons employed in Section 5.4.2, and thus the wettability results in Section 5.4.2.2 also apply here. Results in Figure 5.22 and 5.23 indicate that biofilm growth in ambient lighting was significantly greater on glass and vinyl compared to PVC and stainless steel after 4 h ($P<0.001$); and on glass and stainless steel compared to PVC and vinyl after 24 h ($P<0.001$). Given that, with TSB droplets, glass and stainless steel demonstrated the highest hydrophilicity and PVC the lowest ($P<0.001$), and that stainless has previously shown to be associated with higher surface roughness than glass and PVC (Kim & Kang, 2020), these findings align with the hypothesis discussed in Section 5.4.2.2, which suggests surface wetting and roughness are key characteristics in the affinity of microbial attachment; proposing a possible explanation for the differences in biofilm growth rates observed, and in biofilm inhibition demonstrated upon 405-nm light exposure. Figures 5.22 and 5.23 demonstrate inhibition of both monolayer and mature biofilms, respectively, was greatest on glass surfaces ($P<0.001$); which demonstrated higher hydrophilicity amongst the materials investigated ($P<0.001$). Regardless of these differing levels, however, results together demonstrate that development

of monolayer and mature biofilms in all instances was significantly inhibited when exposed to low irradiance (0.5 mW cm^{-2}) 405-nm lighting, and that greater reductions were demonstrated for biofilms of greater size ($P<0.001$); highlighting the potential ability of the 405-nm light EDS to continuously minimise development of environmental biofilms, and thus infection spread, within healthcare settings.

By comparison, results from the crystal violet assay demonstrated the quantity of biomass formed on microplate wells upon incubation with *S. aureus* (10^6 CFU mL^{-1}) was 66.4% lower following 24 h exposure to 405-nm lighting compared to ambient lighting; whilst, from the swabbing method, viable biofilm cell counts formed on surface coupons upon incubation with this same population were 99.70-99.99% lower following the same exposures. Although results cannot be directly compared, it is interesting to note the substantially larger reductions recorded using the swabbing method. These findings potentially suggest either the mass of *S. aureus* biofilms is of a substantial size even at low densities; or that a number of non-viable or planktonic bacteria were quantified by the crystal violet assay results, which, as discussed, has previously been reported as a limitation of the technique (Latka and Drulis-Kawa, 2020; Amador *et al.*, 2021). The washing step following initial suspension in bacterial solutions should, however, have minimised likelihood of the latter.

It is important to also highlight that variations in room temperature may have influenced the levels of biofilm growth in each instance. In the studies performed in this chapter, biofilm growth was conducted at room temperature, as a means to mimic typical environmental conditions. However, slight changes in temperature may have enhanced/hampered growth rates, and so this should be considered when evaluating the data. To minimise these effects where possible, all control and test data were conducted during the same time period, and the testing of each inert surface was conducted within the same week, to ensure temperatures were as consistent as possible.

Biofilms can demonstrate a 100-1000-fold increase in antimicrobial tolerance compared to planktonic cells (Ceri *et al.*, 1999), and thus are extremely difficult to eradicate. Results in Figures 5.24 and 5.25 demonstrated the ability of low irradiance (0.5 mW cm^{-2}; 43.2 J cm^{-2}) 405-nm light to inactivate previously formed monolayer and mature biofilms, respectively, from various surfaces commonly found within healthcare settings. The greatest monolayer biofilm reductions were demonstrated on glass, vinyl and PVC (1.71, 14.3 and 1.34 log_{10} CFU per coupon reductions, respectively), which were

statistically higher (with the exception of PVC) than that on stainless steel (0.93 $\log_{10}$ CFU per coupon reduction; $P<0.001$); suggesting that the roughness of stainless steel may in this case have caused a shadowing effect and limited the absorption of 405-nm light in comparison to the other surfaces employed. However, for mature biofilms, reductions observed on glass were significantly greater than on stainless steel and vinyl, which together were significantly greater than that on PVC ($P<0.001$); suggesting other surface characteristics will likely have impacted bacterial inactivation in this instance. It is important to note, however, that it is somewhat difficult to make direct comparisons between the reductions demonstrated on each surface given the differences in starting populations presented on coupons prior to exposure which, as previously discussed, is likely due to differences in the affinity of each material for bacterial attachment. Further, results indicated that, once removed from suspension, dried, and exposed to ambient lighting for a further 24 h, biomass in all instances significantly decreased ($P\leq0.006$); suggesting viable bacteria recoverable from these surfaces will decrease over time, regardless of biofilm complexity and material characteristics. Considering each material individually, however, the extent of bacterial reductions within 24 h were variable, with greater reductions shown on stainless steel and glass for mature biofilms ($P<0.001$), and on PVC for monolayer biofilms ($P<0.001$), with no significant difference shown on vinyl for reductions of monolayer and mature biofilms ($P=0.959$). This suggests 405-nm light inactivation of biofilms may be possible regardless of biofilm complexity, which is promising considering the dynamic nature of the healthcare setting and the potential for biofilms to be presented on surfaces at varying degrees of structural integrity.

The methodology used to develop monolayer and mature biofilms in this study was based on that used by McKenzie *et al*. (2013), who demonstrated, for the first time, the 405-nm light inactivation of monolayer (4 h developed) and mature (24, 48, 72 h developed) *E. coli* biofilms on glass and acrylic surfaces, and also the 405-nm light inactivation of *P. aeruginosa*, *L. monocytogenes* and *S. aureus* monolayer (4 h developed) biofilms. Upon comparison of *S. aureus* biofilms formed on glass surfaces, McKenzie *et al*. (2013) demonstrated a 1.87 $\log_{10}$ reduction upon exposure to 84 J cm^{-2}; whilst in this study, similar reductions (1.71 $\log_{10}$) were presented upon exposure to 43.2 J cm^{-2}. Although higher populations of bacteria were initially seeded on glass by McKenzie *et al*. (2013) compared to this study (5.89 versus 3.61 $\log_{10}$ CFU mL_{-1}), it is interesting to highlight that McKenzie *et al.* utilised a differing dose delivery regime to that employed here (140 mW cm^{-2} for 10 min versus 0.5 mW cm^{-2} for 24 h),

suggesting, as previously implicated for planktonic bacteria, the efficacy of 405-nm light may be enhanced, on a per unit dose basis, for inactivation of bacterial biofilms when lower irradiance light sources are employed. For mature *E. coli* biofilms developed over 24 h on glass, McKenzie *et al*. (2013) demonstrated ~2.27 $\log_{10}$ reductions following 168 J cm^{-2} (140 mW cm^{-2} for 20 min). In this study, mature *S. aureus* biofilms also developed for 24 h on glass showed similar reductions (2.41 $\log_{10}$ reductions) using 43.2 J cm^{-2}. These findings may indicate the enhanced susceptibility of *S. aureus* biofilms, compared to *E. coli* biofilms, to 405-nm light inactivation. Gram-negative bacteria have previously been implicated as less susceptible than Gram-positive bacteria to 405-nm light inactivation (Maclean *et al.*, 2009; Murdoch *et al.*, 2012; McDonald *et al.*, 2013). Although different species are not directly comparable and, again, differences in starting populations were noted between McKenzie *et al*. (2013) and this study (5.7 vs 5.26 $\log_{10}$ CFU mL^{-1}), these differences may also be due to the differing dose regimes employed, necessitating future study into the effects of dose application on biofilm inactivation.

Previous studies have suggested that inactivation of bacterial biofilms upon 405-nm light stimulation may be primarily attributed to cellular membrane damage, which in turn will disrupt biofilm integrity and reduce affinity for bacterial surface attachment (Novo *et al.*, 1999; McKenzie *et al.*, 2016; Biener *et al.*, 2017; Kim and Yuk, 2017). Whilst much is known about the damaging effects of ROS on microbial cells and the ROS defence mechanisms employed by microbial cells, little is currently understood regarding the interplay between these factors; and further study is recommended to fully elucidate this effect. Various studies have investigated the efficacy of blue light wavelengths for inactivation of bacterial biofilms (McKenzie *et al.*, 2013; Soukos *et al.,* 2015; Wang *et al.,* 2016; Li *et al.*, 2018; Ferrer-Espada *et al.*, 2019, 2020; Gomez *et al.*, 2019; Tsutsumi-Arai *et al.*, 2019, 2022; Blee *et al.*, 2020; McMullan *et al.*, 2022; Maknuna *et al.*, 2023), however the majority have used higher irradiance exposures to demonstrate this effect (13-300 mW cm^{-2}). Recent work by Blee *et al*. (2020), however, provided evidence suggesting ROS produced upon low irradiance (0.07-0.75 mW cm^{-2}) 405-nm light exposure results in hyperpolarisation of membrane potentials and dispersal of both Gram-positive and Gram-negative bacteria from surfaces at all stages of biofilm formation; with this dispersal shown to be much quicker in Gram-positive versus Gram-negative species. Results also suggested that the dispersal mechanism is activated above a certain ROS threshold and is associated with a

corresponding lag time (Blee *et al.*, 2020), which may also explain the potential increased efficacy when applying doses at lower intensity over an extended time.

It is essential that future research is conducted to fully comprehend the mechanisms associated with this inactivation mechanism. It will be important to establish the efficacy of low irradiance 405-nm light to inactivate other biofilm species which, given differences in morphology and size due to species-specific factors (Coraça-Huber *et al.*, 2020), will likely have differing susceptibilities to treatment. Further, it is important to establish its ability to inactivate polymicrobial biofilms as, clinically, biofilm matrices often constitute various pathogens (Schapira *et al.*, 2023). Previous work has established its ability to do this (McKenzie, 2014; Soukos *et al.*, 2015; Wang *et al.*, 2016; Ferrer-Espada *et al.*, 2019); however, as with previous findings, much of these studies have utilised high irradiance light sources to achieve this effect (~60-140 mW cm^{-2}). Assessing compatibility in the context of environmental decontamination will be crucial in furthering implementing this technology clinically.

Considering experimental work in this chapter comprehensively, it is notable that all bacterial inactivation studies were conducted using *S. aureus* as a model organism due to its significance as a causative agent of HAIs (Cairns *et al.*, 2018). As previously discussed, it is recognised that bacterial responses to 405-nm light exposure are variable, and thus it is essential that these studies are expanded to determine broad-spectrum inactivation efficacy of the system.

5.7 Conclusions

Overall, findings of this chapter provide an enhanced depiction of the efficacy of low irradiance 405-nm light systems under more tangible conditions realistic to healthcare settings. Key findings associated with this chapter are detailed as follows:

- A miniaturised 405-nm light EDS was designed to enable antimicrobial testing at the irradiance levels ordinarily provided by the 405-nm light EDS within a typical 32 m^3 room to be conducted on a smaller, laboratory bench-top scale. The designed prototype was found to be

capable of illuminating surfaces at levels as low as 0.001 mW cm^{-2} at much shorter distances than that of the full-scale 405-nm light EDS (displacement of 1.70 vs 4.47 m).

- The bactericidal efficacy of 405-nm light when employed at irradiances ≤0.1 mW cm^{-2} was demonstrated for the inactivation of *S. aureus*, with significant reductions achieved as low as 0.005 mW cm^{-2}, with this likely being the threshold irradiance level for antimicrobial activity in this instance.
- Comparisons indicated that 405-nm light inactivation of *S. aureus* is possible in both minimal and organically-rich media, with inactivation shown to be enhanced in the presence of photosensitive components within the suspension media and hampered by a decrease in the degree of light transmissibility through the suspension media.
- The efficacy of 405-nm light for the inactivation of *S. aureus* seeded onto clinically-relevant surfaces was established, with up to 2.03 log_{10} CFU per coupon reductions demonstrated within 24 h exposure to 0.5 mW cm^{-2}. Comparisons indicated that the surface wetting profile of each material may be influential in the extent of inactivation achieved, along with potentially other surface characteristics.
- The efficacy of low irradiance (0.5 mW cm^{-2}) 405-nm light for the inactivation of *S. aureus* biofilms was demonstrated, with reductions in the development of, and formed, monolayer and mature biofilms (up to 4.6 log_{10} reductions) within 24 h exposure on both microplate wells and clinically relevant surfaces.

Given the degree of unpredictability associated with the presentation of microbial contaminants within dynamic clinical environments, there are many factors to consider when evaluating the efficacy of the 405-nm light EDS to reduce environmental pathogen contamination, and consequently, HAI transmission. This chapter provides greater insight into these areas, further justifying its implementation as a complementary decontamination technology across the infection control sector.

CHAPTER 6

Bactericidal Efficacy and Energy Efficiency of Low Irradiance 405-nm Light

6.0 Overview

This chapter aims to investigate the broad-spectrum bactericidal efficacy and energy efficiency of low irradiance 405-nm light, in comparison to higher irradiance exposures, for the inactivation of ESKAPE pathogens. Based on these findings, associated damage mechanisms elicited in response to such exposures, namely ROS generation and membrane damage, were examined. These findings together provide fundamental evidence of the enhanced susceptibility of nosocomial bacteria to low irradiance 405-nm light, further supporting its implementation in decontamination applications.

6.1 Introduction

Owed to its inherent antimicrobial profile (Tomb *et al.*, 2018) at exposure levels safe for mammalian cells (Ramakrishnan *et al.*, 2014), there has been interest in violet-blue light for infection control applications which involve exposure of sensitive tissues or materials, including decontamination of occupied clinical environments (Maclean *et al.*, 2010, 2013a; Bache *et al.*, 2012b, 2018b; Murrell *et al.*, 2019) and wound decontamination (Dai, *et al*., 2013a; Dai, *et al*., 2013b; McDonald *et al*., 2011). To ensure compatibility in such instances, light irradiances of <20 mW cm^{-2} have generally been used. This can differ from studies solely investigating the fundamental antimicrobial properties of violet-blue light, which can use considerably higher irradiances (typically up to ~200 $mWcm^{-2}$) to achieve rapid disinfection (Hamblin *et al.*, 2005; Guffey and Wilborn, 2006; Murdoch *et al.*, 2012; McKenzie *et al.*, 2014; Tomb *et al.*, 2014; Moorhead *et al.*, 2016b).

Additionally, there is currently little evidence to demonstrate the inactivation efficacy of low irradiance 405-nm light, on a per-unit-dose basis, in comparison to that of the higher irradiances typically studied

in literature. Results in Chapter 4 demonstrated the broad-spectrum antibacterial efficacy of low irradiance (<1 $mWcm^{-2}$) 405-nm light for the inactivation of key nosocomial bacterial pathogens, and highlighted that low irradiance exposures may be more efficient, per-unit-dose, for inactivation than higher irradiance exposures; however, this observation is yet to be fully elucidated. Further, although various cellular targets of the 405-nm light oxidative burst have previously been identified (McKenzie *et al.*, 2016; Biener *et al.*, 2017; Bumah *et al.*, 2017; Fila *et al.*, 2017; Kim and Yuk, 2017), a comparative investigation into the cellular targets and damage mechanisms induced by 405-nm light exposure, and how these may vary when exposed to a fixed dose using varying light delivery regimes, i.e. high intensity/short duration or low intensity/long duration, is yet to be established.

Accordingly, the present chapter aimed to expand knowledge about the GE of low versus high irradiance 405-nm light, on a per-unit-dose basis. Experiments investigated the inactivation of ESKAPE pathogens at various population densities upon exposure to fixed light doses using varying irradiances, to determine the impact of bacterial load and illumination intensity on inactivation efficacy. Such exposures were initially conducted on agar surfaces, to provide indication of environmental surface decontamination; however, these were expanded to include exposures in liquid suspension, to comprehensively indicate bactericidal efficacy. Further, preliminary experiments assessed bacterial responses – specifically intracellular ROS production and membrane integrity – upon exposure to a fixed dose using differing light delivery regimes. A greater understanding of these fundamental principles will be crucial in the development and optimisation of low-power energy efficient antimicrobial light sources.

6.2 Low versus High Irradiance for Inactivation of Surface-Seeded Bacteria

The present study aimed to establish influence of irradiance on the 405-nm light inactivation of surface-seeded ESKAPE bacteria, by exposing each to a fixed dose of 405-nm light using three distinct irradiance applications (0.5, 5 and 50 mW cm^{-2}) and comparing susceptibility at equivalent light doses.

6.2.1 Methods: Low versus High Irradiance Inactivation of Surface-Seeded Bacteria

6.2.1.1 Bacterial Preparation

Suspensions of *E. faecium*, *S. aureus*, *K. pneumoniae*, *A. baumannii*, *P. aeruginosa* and *E. cloacae* were prepared (Section 3.1.2) and serially diluted in PBS to provide a population density of 10^3 CFU mL^{-1} (Section 3.1.3). Samples were then seeded onto 50 mm agar plates at a density of 10^2 CFU $plate^{-1}$.

6.2.1.2 Light Source

Two light sources were employed for experimental testing in this experiment: the ENFIS PhotonStar Innovate UNO 24-LED array (Section 3.4.3; Figure 6.1A) was mounted above bacterial samples at a distance of either 24.8 or 8.0 cm, providing irradiances of 5 and 50 $mWcm^{-2}$ at the sample surface, and the 405-nm light EDS (Section 3.4.1; Figure 6.1B) was positioned approximately 140 cm above a surface on which samples were exposed, providing ~0.5 mW cm^{-2} at the sample surface.

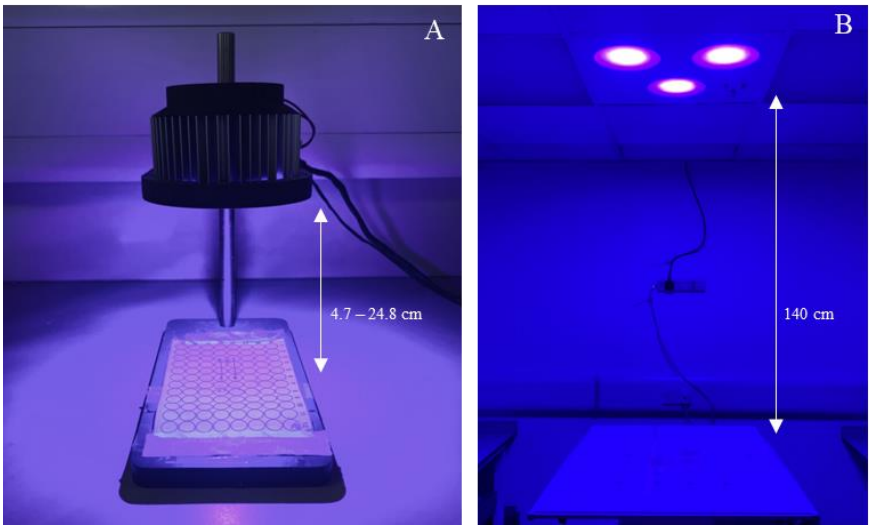

Figure 6.1. Experimental set-up for exposure of bacterial pathogens to 405-nm light using (A) ENFIS PhotonStar Innovate UNO 24 LED array and (B) 405-nm light EDS.

6.2.1.3 Exposure Methodology

Seeded plates with the lids removed (n=3) were exposed to increasing durations of light treatment at three irradiance levels, 0.5, 5 and 50 $mWcm^{-2}$, with exposure times selected to ensure equivalent light doses (3 – 90 Jcm^{-2}) were delivered to samples (Equation 3.1; Table 6.1). Control samples were prepared in an identical manner but exposed to ambient laboratory lighting only. Following light treatment, sample plates were incubated at 37°C for 18-24 h and surviving bacterial colonies were enumerated and

recorded as CFU plate^{-1}. Results represent the mean values ± SD of triplicate replicates (n=3), and are reported as the percentage of surviving bacteria as compared to the equivalent non-exposed control samples, or as GE values (Section 3.5.1).

Table 6.1 405-nm light treatments of surface-seeded bacterial samples (10^2 CFU plate^{-1}).

Irradiance (mWcm^{-2})	**0.5**	**5**	**50**	**Dose Delivered (Jcm^{-2})**
Exposure Time (min)	50	-	-	**1.5**
	100	10	1	**3**
	150	-	-	**4.5**
	200	20	2	**6**
	250	-	-	**7.5**
	300	30	3	**9**
	350	-	-	**10.5**
	400	40	4	**12**
	450	-	-	**13.5**
	500	50	5	**15**
	1000	100	10	**30**
	1500	150	15	**45**
	2000	200	20	**60**
	2500	250	25	**75**
	3000	300	30	**90**

6.2.2 Results: High versus Low Irradiance Inactivation of Surface-Seeded Bacteria

Inactivation kinetics of ESKAPE bacteria (10^2 CFU plate^{-1}) following exposure to increasing doses of 405-nm visible light at three independent irradiance regimes are presented in Figure 6.2. Results demonstrate a significant downward trend in surviving bacterial populations for all organisms when light dose was increased, and non-exposed control samples showed no change throughout ($P>0.05$).

Inactivation was significantly enhanced for all organisms when the dose was delivered at lower irradiance. Exposed to the highest irradiance of 50 mWcm^{-2}, ESKAPE pathogens collectively required 9-75 J cm^{-2} (3-25 min) to achieve a significant degree of inactivation (19-68.3% reductions) in comparison to non-exposed populations ($P<0.05$). At this same irradiance, doses of 45-150 J cm^{-2} (15-50 min) were required to achieve complete or near-complete (≥96.73%) inactivation. Exposed at 5 mWcm^{-2}, all species collectively required lower dose applications of 6-30 Jcm^{-2} (20 min–1 h 40 min)

to achieve a significant degree of inactivation (29.3-69.9% reductions) compared to controls ($P<0.05$). Complete or near-complete inactivation (≥95.47%) was achieved by all species at this same irradiance following exposure to 15-60 Jcm^{-2} (50 min – 3 h 20 min). When exposed to 0.5 mW cm^{-2}, ESKAPE pathogens collectively required just 3-30 Jcm^{-2} (1 h 40 min – 16 h 40 min) to achieve a significant degree of inactivation (14.8-96.6% reductions) compared to controls ($P<0.05$), with 6-30 Jcm^{-2} (3 h 20 min – 16 h 40 min) required to achieve complete or near-complete (≥96%) inactivation.

Differences were demonstrated in the susceptibility of each ESKAPE pathogen at each irradiance application. Exposed at the lowest irradiance of 0.5 $mWcm^{-2}$, *S. aureus*, *A. baumannii* and *P. aeruginosa* proved most susceptible to treatment, collectively requiring ≤9 J cm^{-2} to achieve complete or near-complete inactivation, which was 1.5-3.3 times less than that required by other species. Exposed at the highest irradiance of 50 $mWcm^{-2}$, *E. faecium*, *A. baumannii* and *P. aeruginosa* were most susceptible, requiring 45 J cm^{-2} for complete/ near-complete inactivation, whereas *K. pneumoniae* and *E. cloacae*, which were least susceptible, required much greater doses of 150 Jcm^{-2} to achieve similar reductions.

The mean GE for near-complete (≥95.6%) 405-nm light inactivation of surface-seeded ESKAPE bacteria upon these exposures is presented in Figure 6.3. Results demonstrate enhanced GE for inactivation of all ESKAPE pathogens when exposed at 0.5 $mWcm^{-2}$: values ranged from 0.05-0.29, which were significantly greater ($P\leq0.05$) than exposures to both 5 and 50 $mWcm^{-2}$ (ranging from 0.03-0.22 and 0.01-0.05, respectively). Overall, GE for inactivation was approximately 3.1-8.1 times greater when exposed using 0.5 $mWcm^{-2}$ compared to 50 $mWcm^{-2}$; of which, the greatest difference was demonstrated by *E. cloacae* (0.10 versus 0.01).

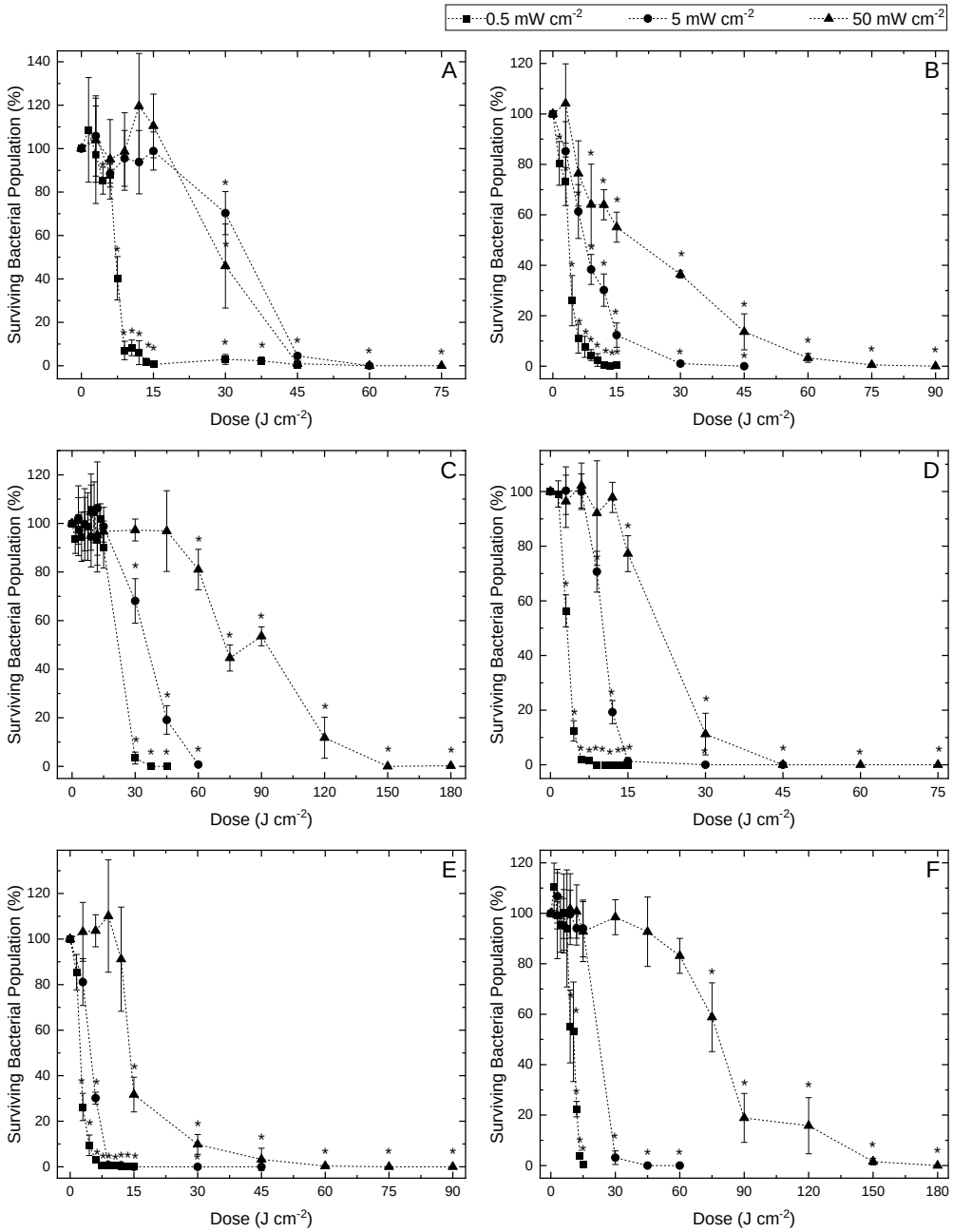

Figure 6.2 Inactivation of surface-seeded ESKAPE pathogens, (A) *Enterococcus faecium*, (B) *Staphylococcus aureus*, (C) *Klebsiella pneumoniae*, (D) *Acinetobacter baumannii*, (E) *Pseudomonas aeruginosa* and (F) *Enterobacter cloacae*, upon exposure to increasing doses of 405-nm light at irradiances of 0.5, 5 and 50 mWcm^{-2}. Surviving bacterial populations are presented as percentages with respect to equivalent non-exposed control populations. Each data point represents the mean value ± SD (n = 3). Asterisks (*) represent data points in which there was a significant reduction in the surviving bacterial population in comparison to the equivalent non-exposed control population (P≤0.05).

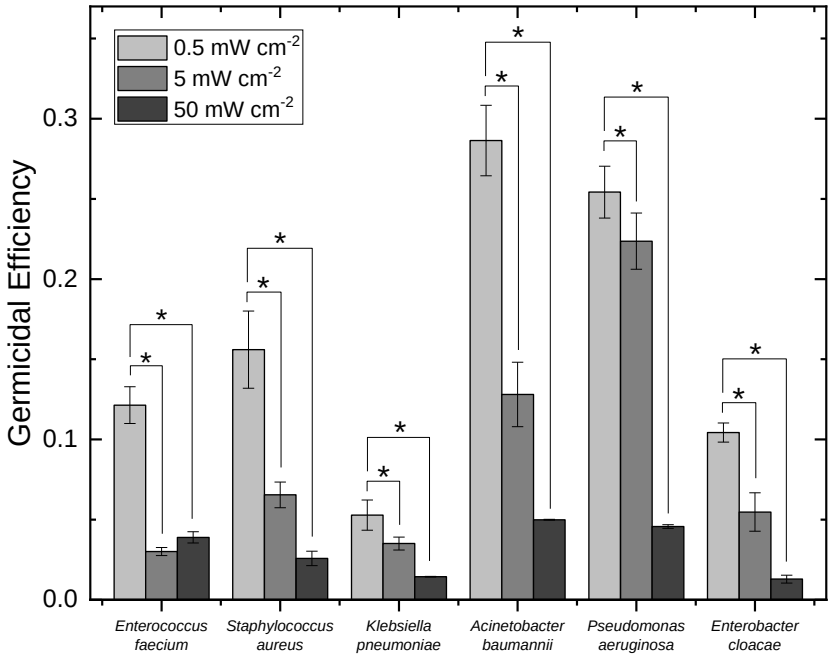

Figure 6.3 GE for the complete/near-complete (≥95%) inactivation of surface-seeded ESKAPE pathogens (10^2 CFU plate^{-1}) upon exposure to identical doses of 405-nm light using irradiances ranging from 0.5-50 mW cm^{-2}. Each data point represents the mean value ± SD (n = 3). For each data point, GE was calculated at the dose at which complete or near-complete (≥95%) inactivation was achieved. Asterisks (*) represent significant differences between the GE values gathered from each independent irradiance exposure (P≤0.05).

6.3 Low versus High Irradiance for Inactivation of Suspended Bacteria

The following set of experiments aimed to establish the influence of irradiance application on the 405-nm light inactivation of *S. aureus* and *P. aeruginosa* suspensions – selected as Gram-positive and Gram-negative representative species, respectively – by exposing each to increasing doses of light using five irradiance applications (5-150 mW cm^{-2}) and comparing susceptibility at equivalent light doses.

6.3.1 Methods: Low versus High Irradiance Exposure for Inactivation of Suspended Bacteria

6.3.1.1 Bacterial Preparation

S. aureus and *P. aeruginosa* were each prepared as described in Section 3.1.2 and serially diluted in PBS to provide a population density of 10^3 CFU mL^{-1} for experiments (Section 3.1.3).

6.3.1.2 Light Source

The ENFIS PhotonStar Innovate UNO 24-LED array (Figure 6.1A) was used for all bacterial exposures. The distance between the light source and bacterial samples was adjusted to achieve the required

irradiances for exposures as follows: 5 $mWcm^{-2}$ – 24.8 cm; 10 $mWcm^{-2}$ – 17.5 cm; 50 $mWcm^{-2}$ – 8.0 cm; 100 $mWcm^{-2}$ – 5.7 cm; 150 $mWcm^{-2}$ – 4.7 cm.

6.3.1.3 Exposure Methodology

Bacterial suspensions were exposed to increasing durations of light treatment at irradiances of either 5, 10, 50, 100 and 150 $mWcm^{-2}$. Following preparation of 10^3 CFU mL^{-1} suspensions, 250 µL volumes of each were held in a 96-well plate (providing a sample depth of 7.8 mm) covered by an adhesive plate seal (Thermo Scientific, UK) to prevent evaporation, and positioned below the light source. To ensure any light adsorption by the adhesive plate seal was accounted for, irradiance measurements were taken through the material, and the height of the light source was adjusted accordingly to ensure the desired irradiance reached bacterial samples. Exposure times were selected to ensure equivalent light doses (22.5 – 180 Jcm^{-2}) were delivered to samples (Equation 3.1; Table 6.2). Control samples were prepared in an identical manner but were exposed to ambient laboratory lighting only. The temperature of microbial suspensions was monitored prior and post light treatments using a Kane May KM340 thermocouple (Comark Instruments, UK) to ensure inactivation was the result of light exposure and not heat effects. Following light treatment, two 100 µL aliquots from each sample were spread plated and incubated at 37°C for 18-24 h. After incubation, colonies were enumerated with results reported as surviving bacterial load in CFU mL^{-1}. Results represent the mean values ± SDof triplicate replicates measured in duplicate (n=6), and are reported as the percentage of surviving bacteria as compared to the equivalent non-exposed control samples, or as GE values (Section 3.5.1).

Table 6.2 405-nm light treatments of liquid-suspended bacterial samples (10^3 CFU mL^{-1}).

Irradiance ($mWcm^{-2}$)	**5**	**10**	**50**	**100**	**150**	**Dose Delivered (Jcm^{-2})**
Exposure Time (min)	75	37.5	7.5	3.75	2.5	**22.5**
	150	75	15	7.5	5	**45**
	225	112.5	22.5	11.25	7.5	**67.5**
	300	150	30	15	10	**90**
	450	225	45	22.5	15	**135**
	600	300	60	30	20	**180**

6.3.2 Results: Low versus High Irradiance Exposure for Inactivation of Suspended Bacteria

Figure 6.4 presents the inactivation kinetics of *S. aureus* and *P. aeruginosa* (10^3 CFU mL^{-1}) suspensions exposed to increasing doses of 405-nm light at five independent irradiances. In all cases, a downward trend in surviving populations was demonstrated when light dose increased, and no significant changes were observed in non-exposed control populations throughout ($P \leq 0.05$). At all irradiances, complete/ near-complete inactivation (≥98.6%) of both species was achieved following 90 Jcm^{-2}; however, general trends indicate an enhanced susceptibility to inactivation when exposed using lower irradiances.

When *S. aureus* (Figure 6.4A) was exposed using 100 and 150 $mWcm^{-2}$, a dose of 67.5 Jcm^{-2} (11.25 and 7.5 min, respectively) was required to achieve significant inactivation (82.6% and 84.6% reductions, respectively) compared to equivalent non-exposed controls ($P \leq 0.05$). Using 50 $mWcm^{-2}$, a lower dose of 45 Jcm^{-2} (15 min) achieved a significant 35.9% reduction ($P \leq 0.05$), and using the lowest irradiances of 5 and 10 $mWcm^{-2}$, a dose of just 22.5 Jcm^{-2} (1.25 and 0.625 h, respectively) was required to achieve significant reductions of 62.1% and 82.1%, respectively ($P \leq 0.05$). The dose required for complete/near-complete (≥99.7%) *S. aureus* inactivation was significantly lower when exposed at lower irradiances ($P \leq 0.05$): 45 Jcm^{-2} using 5 and 10 $mWcm^{-2}$ compared to double this energy (90 Jcm^{-2}) using 50, 100 and 150 $mWcm^{-2}$.

P. aeruginosa similarly demonstrated increased susceptibility when exposed at lower irradiance (Figure 6.4B). Exposed to 150 $mWcm^{-2}$, the dose required to achieve significant reductions (68.7%) was 67.5 J cm^{-2} (7.5 min; $P \leq 0.05$). Using 10, 50 and 100 $mWcm^{-2}$, a smaller dose of 45 Jcm^{-2} (1.25 h, 15 min and 7.5 min, respectively) was required to achieve significant reductions of 99.7%, 36.1% and 61.7%, respectively ($P \leq 0.05$). Using 5 $mWcm^{-2}$, just 22.5 Jcm^{-2} (1.25 h) was required to achieve a significant 94.6% reduction ($P \leq 0.05$) and, at this dose, inactivation was significantly greater when exposed at 5 $mWcm^{-2}$ in comparison to all other irradiances ($P \leq 0.05$). Following 45 J cm^{-2}, inactivation was significantly greater when exposed at 5 and 10 $mWcm^{-2}$ in comparison to all other irradiances ($P \leq 0.05$). Complete/ near-complete (≥99.1%) inactivation was achieved using ≤2 times less dose at low irradiance compared to higher irradiances: 45 Jcm^{-2} was required for 5 and 10 $mWcm^{-2}$ exposures, compared to 67.5 Jcm^{-2} for 100 $mWcm^{-2}$ exposures and 90 Jcm^{-2} for both 50 and 150 $mWcm^{-2}$ exposures.

The mean GE for the 405-nm light inactivation of both species across the range of irradiances investigated is presented in Figure 6.5. Results demonstrate significant ($P<0.001$) enhancement in GE for inactivation of both species when exposed at 5 and 10 $mWcm^{-2}$ (values of 0.06-0.07) compared to 50-150 mW cm^{-2} (values of 0.02-0.04). For both species, no signficant difference was demonstrated between GE values upon exposures to 5 and 10 mW cm^{-2} ($P>0.05$) and exposures to 50, 100 and 150 mW cm^{-2} ($P>0.05$), with the exception of GE values for *S. aureus* upon exposure to 100 and 150 mW cm^{-2}, which were significantly different ($P<0.001$). Overall, GE was approximately 2.1 - 3 times greater when exposed using 5 $mWcm^{-2}$ compared to 150 $mWcm^{-2}$; of which, the greatest difference was demonstrated by *S. aureus* (0.65 versus 0.02).

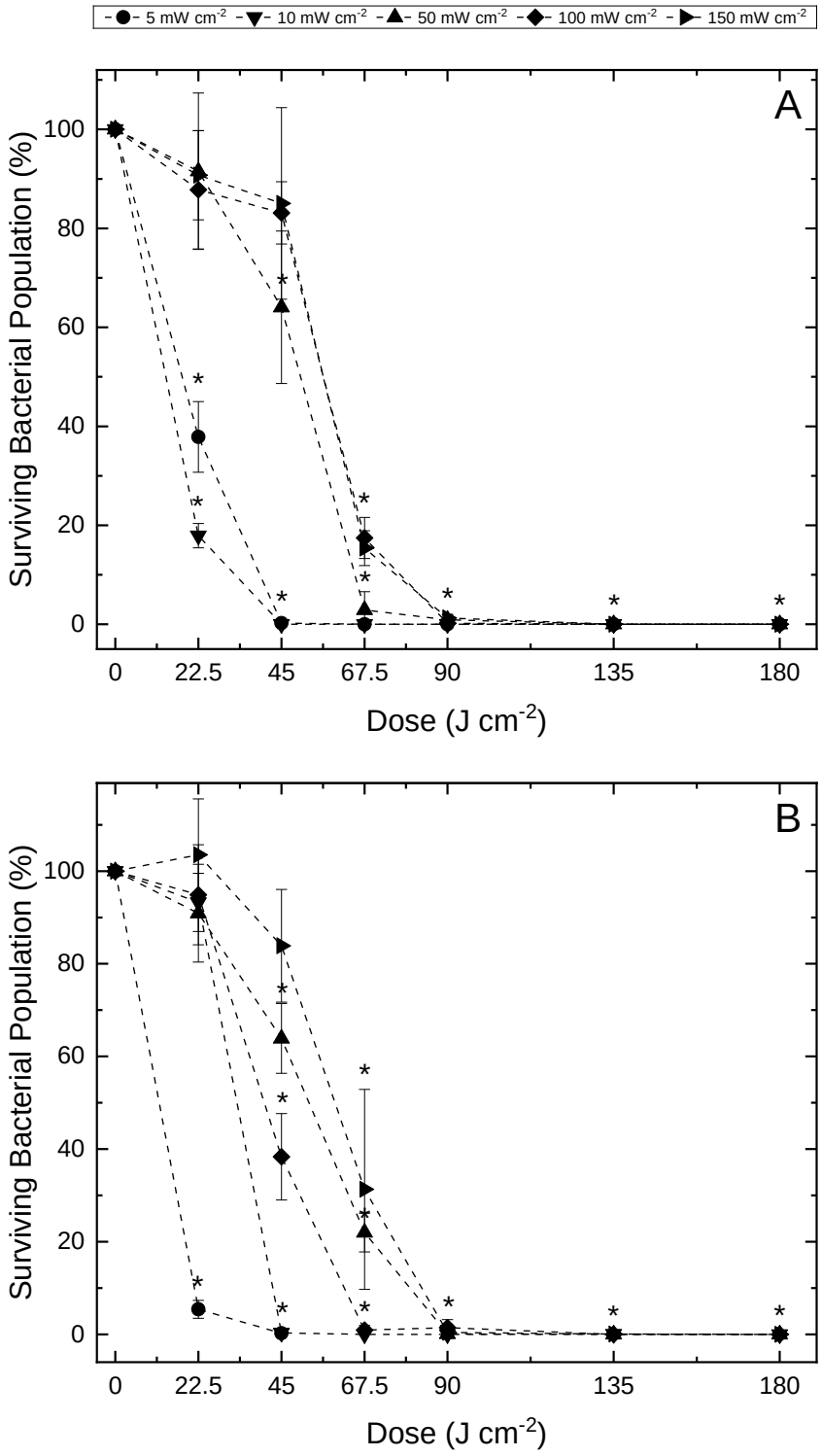

Figure 6.4 Inactivation of (A) *Staphylococcus aureus* and (B) *Pseudomonas aeruginosa* suspended in PBS upon exposure to 405-nm light up to a dose of 180 Jcm^{-2} at irradiances of 5, 10, 50, 100 and 150 mW cm^{-2}. Surviving bacterial populations are presented as percentages with respect to equivalent non-exposed controls. Each data point represents the mean value ± SD (n=6). Asterisks (*) represent data points in which there was a significant reduction in surviving bacterial populations compared to equivalent non-exposed control populations ($P \leq 0.05$).

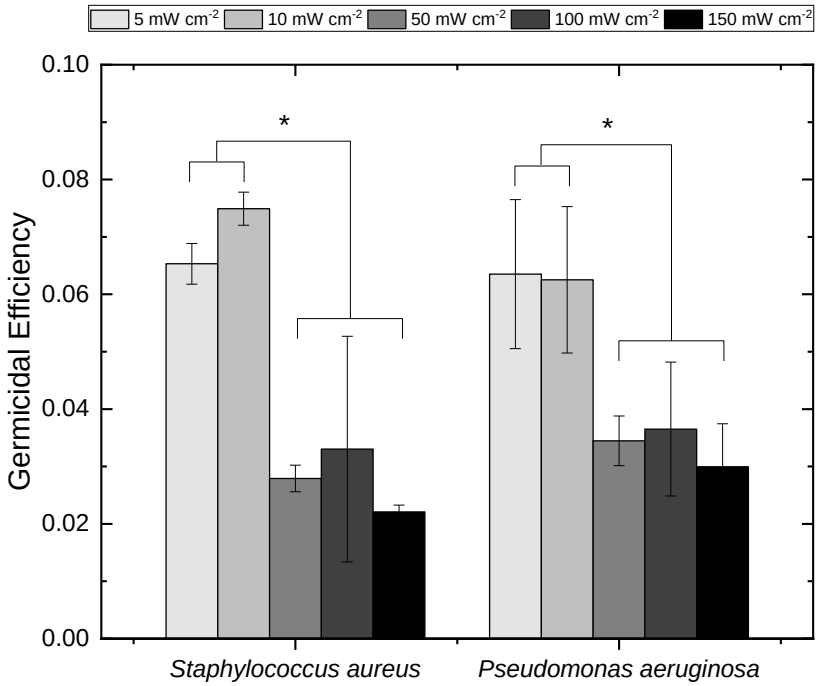

Figure 6.5 GE for the complete/near-complete (≥95%) inactivation of *Staphylococcus aureus* and *Pseudomonas aeruginosa* suspensions (10^3 CFU plate^{-1}) upon exposure to identical doses of 405-nm light using irradiances ranging from 5-150 mW cm^{-2}. Each data point represents the mean value ± SD (n = 3). For each data point, GE was calculated at the dose at which complete or near-complete (≥95%) inactivation was achieved. Asterisks (*) represent significant differences between GE values gathered from independent irradiance exposures (P≤0.05).

6.4 Effect of Bacterial Bioburden on Low Irradiance 405-nm Light Inactivation

For applications involving sensitive material or tissue exposure, bacterial contamination levels may vary. For environmental decontamination, low bacterial populations (~10^2 CFU cm^{-2}) are typically expected (Maclean *et al.*, 2014); whilst for wound decontamination, a microbial load of >10^5 CFU g^{-1} is typically considered the threshold for infection diagnosis (Gardner and Frantz, 2008). The present study aimed to establish the influence of bacterial population density on the efficacy of low irradiance 405-nm light exposure, and how it compares to higher irradiance exposures on a per-unit-dose basis.

6.4.1 Methods: Effect of Bacterial Bioburden on Low Irradiance 405-nm Light Inactivation

6.4.1.1 Bacterial Preparation

Suspensions of *E. faecium*, *S. aureus*, *K. pneumoniae*, *A. baumannii*, *P. aeruginosa* and *E. cloacae* were prepared and serially diluted in PBS to the required population density for exposure (Sections 3.1.2-3.1.3).

6.4.1.2 Light Source

The ENFIS PhotonStar Innovate UNO 24-LED array was employed for exposures to 5 – 150 $mWcm^{-2}$, whilst the 405-nm light EDS was employed for exposures to ~0.5 mW cm^{-2} (Section 6.2.1.2).

6.4.1.3 Surface-Seeded Bacterial Exposure

To establish the influence of bacterial bioburden on the efficacy of low irradiance 405-nm light for surface decontamination, ESKAPE bacteria were seeded onto 50 mm agar plates at densities of 10^1-10^8 CFU $plate^{-1}$ and exposed to 0.5 $mWcm^{-2}$ 405-nm light for 16 h (28.8 Jcm^{-2}) and 24 h (43.2 Jcm^{-2}) with plate lids removed. Following light treatment, the lids were replaced, and plates were incubated at 37°C for 18-24 h. Following incubation, plates were photographed for qualitative analysis, with results compared to control samples held under ambient room lighting conditions.

6.4.1.4 Liquid-Suspended Bacterial Exposure

To establish the influence of population density on the efficacy of 405-nm light for inactivation of liquid-suspended bacteria, 3 mL volumes of *S. aureus* and *P. aeruginosa* at densities of 10^3-10^9 CFU mL^{-1} were transferred to a 6-well plate, providing a sample depth of 3.2 mm, and exposed to increasing doses of 405-nm light at irradiances of 5, 50 and 150 $mWcm^{-2}$. Exposure times were selected to ensure equivalent light doses (36 – 288 Jcm^{-2}) were delivered to samples (Equation 3.1; Table 6.3). All 6-well plates were covered with an adhesive plate seal to prevent evaporation, and so irradiance measurements were taken through the material as described in Section 6.3.1.3 to ensure the desired irradiance reached bacterial samples. Control samples were prepared in an identical manner but were exposed to ambient laboratory lighting only. The temperature of microbial samples was monitored immediately prior and post light treatment (Kane May KM340 thermocouple; Comark Instruments, UK). Post-treatment, 100 µL samples (n=2) were plated onto agar and incubated at 37°C for 18-24 h. Following incubation, colonies were enumerated and susceptibility at equivalent light doses compared. Results represent the mean values ± SD of triplicate replicates measured in duplicate (n=6), and are reported as percentage of surviving bacteria compared to equivalent non-exposed controls, bacterial counts in log_{10} CFU mL^{-1}, and GE values (Section 3.5.1).

A key consideration when exposing bacterial suspensions of differing population density is the ability for the light treatment to transmit through the suspension and interact with the suspended cell. To

investigate this, the transmission of 405-nm light through suspensions of *S. aureus* and *P. aeruginosa* at populations of 10^3-10^9 CFU mL^{-1} was measured using a Biomate 5-UV-Vis spectrophotometer (Fisher Scientific, UK). Additionally, it was of interest to determine the loss of light intensity through the 3.2 mm depth of the 3 ml samples held in the 6-well plate in the experimental set-up. To do this, the photodiode detector was used to take irradiance measurements through the base of the 6 well-plate, with 3 ml samples of bacterial suspensions at the differing population densities aliquoted into the appropriate well and exposed to the ENFIS PhotonStar Innovate UNO 24 LED array (Figure 6.6). The loss of 405-nm light irradiance through the bacterial samples was then calculated as a percentage in comparison to PBS alone. Results represent the mean values ± SD of triplicate replicates (n=3), and are reported as the percentage of light passage through bacterial suspensions as compared to PBS suspensions.

Table 6.3 405-nm light treatments of bacterial samples suspended in PBS (10^{3-9} CFU mL^{-1}).

Irradiance ($mWcm^{-2}$)	**5**	**50**	**150**	**Dose Delivered (Jcm^{-2})**
Exposure Time (min)	120	12	4	**36**
	240	24	8	**72**
	360	36	12	**108**
	480	48	16	**144**
	720	72	24	**216**
	960	96	32	**288**

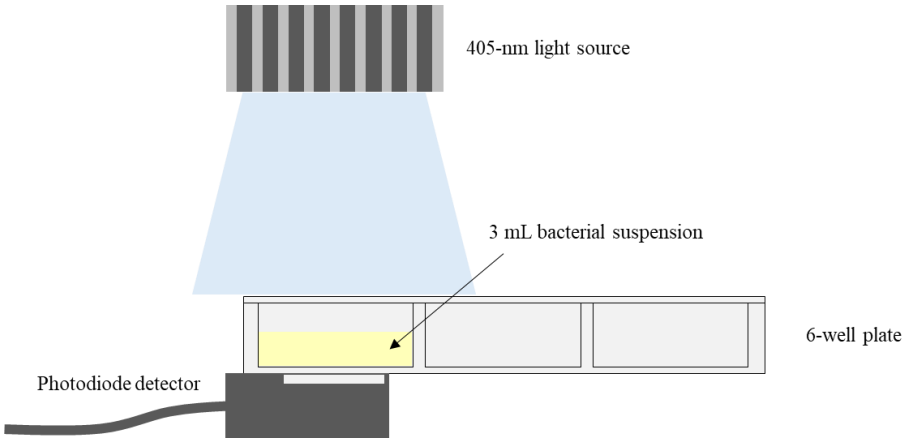

Figure 6.6 Experimental set-up to measure loss of 405-nm light transmission through bacterial samples.

6.4.2 Results: Exposure of Surface-Seeded Bacteria

Figure 6.7 displays agar plates seeded with *S. aureus* and *P. aeruginosa* at population densities of 10^1-10^8 CFU $plate^{-1}$ and exposed to 0.5 $mWcm^{-2}$ for 16 h (28.8 Jcm^{-2}) and 24 h (43.4 Jcm^{-2}). Results for the

other four bacterial species are shown in Appendix B. General trends indicate that the susceptibility of surface-seeded bacteria to low irradiance 405-nm light inactivation is similar regardless of initial population density. Similar $\log_{10}$ reductions were demonstrated at each initial seeding density as the light dose was increased, with results indicating that all bacteria presented at high surface population densities can be reduced by low irradiance 405-nm light exposure as the duration of exposure, and thus applied dose, is increased. By comparison of the two representative species presented in Figure 6.7, *S. aureus* appears to demonstrate greater susceptibility than that of *P. aeruginosa*, with 24 h exposure resulting in complete elimination of 10^7 CFU plate^{-1} *S. aureus* populations in comparison to just 10^5 CFU plate^{-1} *P. aeruginosa* populations, respectively. Nevertheless, results overall demonstrate successful inactivation of all ESKAPE pathogens at contamination levels (10^2 CFU plate^{-1}) likely to typically occur within occupied environments (Maclean *et al.*, 2013a), and even at potentially much higher levels should these occur, using low irradiance (0.5 mW cm^{-2}) light.

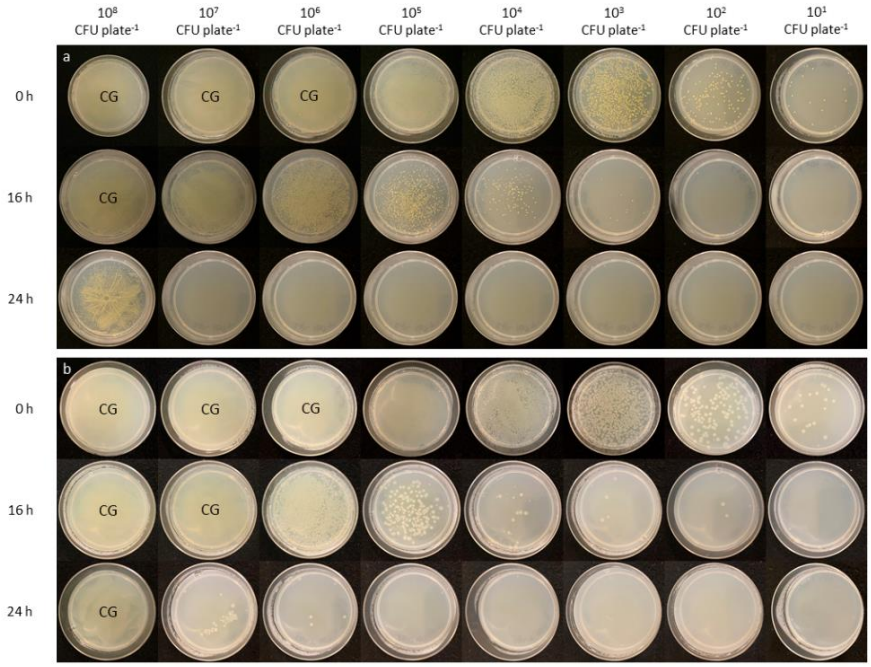

Figure 6.7 Appearance of (a) *Staphylococcus aureus* and (b) *Pseudomonas aeruginosa* at 10^8 – 10^1 CFU plate^{-1}, upon exposure to 0.5 mWcm^{-2} 405-nm light for 16 and 24 h (28.8 and 43.4 J cm^{-2}, respectively). [CG: confluent growth of bacteria].

6.4.3 Results: Inactivation of Bacterial Suspensions

Inactivation kinetics of *S. aureus* and *P. aeruginosa* suspensions, at initial densities of $10^{3\text{-}9}$ CFU mL^{-1}, upon exposure to increasing doses of 405-nm light at three independent irradiances are presented in

Figures 6.8 and 6.9, respectively. For each population density, results are presented as both counts (log_{10} CFU mL^{-1}) and surviving populations compared to non-exposed equivalent controls (%). Results for *S. aureus* (Figure 6.8) demonstrate a significant enhancement in susceptibility to 405-nm light inactivation when using low irradiance at population densities of $\leq 10^7$ CFUmL^{-1} and, conversely, when using higher irradiance at a population density of 10^9 CFUmL^{-1} ($P \leq 0.05$). At 10^3 CFUmL^{-1}, log_{10} bacterial counts (Figure 6.8A) were significantly lower upon exposure to 5 mW cm^{-2} compared to both 50 and 150 mW cm^{-2} ($P<0.001$) at all light doses measured. Upon exposure to an initial dose of 36 J cm^{-2}, an approximate 2.46 log_{10} CFU mL^{-1} reduction was demonstrated using 5 mW cm^{-2}; compared to just 0.04-0.16 log_{10} CFU mL^{-1} reductions using 50-150 mW cm^{-2}. Further, complete reduction was achieved upon 72 J cm^{-2} using 5 mW cm^{-2}; whilst three times this dose (216 J cm^{-2}) was required when using 50-150 mW cm^{-2}. Similarly, the percentage surviving 10^3 CFU mL^{-1} populations (Figure 6.8B) were significantly lower at all doses when exposed to 5 mW cm^{-2} compared to higher irradiances ($P<0.001$). Approximately 4-6 times less dose was required to achieve near-complete inactivation (≥96.4%) at this density when exposed at the lowest irradiance: 36 Jcm^{-2} at 5 $mWcm^{-2}$ versus 144 Jcm^{-2} at 50 $mWcm^{-2}$ and 216 Jcm^{-2} at 150 $mWcm^{-2}$. Similar patterns were observed for 10^5 CFU mL^{-1} (Figure 6.8C and D) and 10^7 CFU mL^{-1} (Figure 6.8E and F) populations. In both cases, exposure to initial doses of 36 and 72 J cm^{-2} resulted in significantly lower bacterial counts when exposed at 5 mW cm^{-2} compared to 50 and 150 mW cm^{-2} ($P<0.001$): reductions of up to 3.88 and 5.35 log_{10} CFU mL^{-1} in 10^5 and 10^7 CFU mL^{-1} populations, respectively, using 5 mW cm^{-2}; compared to reductions of 0.62-0.72 and 0.39-1.55 log_{10} CFU mL^{-1}, respectively, using 50-150 mW cm^{-2} (Figure 6.8 C and E). Both 10^5 and 10^7 CFU mL^{-1} populations required 2-4 times less dose to achieve complete/near-complete reductions (≥95.1%) using 5 mW cm^{-2} compared to 150 mW cm^{-2}. When exposed at 10^8 CFU mL^{-1}, however, no significant difference was demonstrated in the inactivation efficacy of each irradiance application ($P \geq 0.58$; Figure 6.8G and H). The only exception was by 144 J cm^{-2}, where bacterial levels illuminated using 5 mW cm^{-2} were significantly lower than that achieved by other irradiances ($P=0.014$). It should be noted, however, that the percentage reduction upon exposure to this irradiance at this same dose was statistically similar to that achieved using 150 mW cm^{-2} ($P>0.05$). Discordantly, when exposed at 10^9 CFU mL^{-1}, although no significant difference was demonstrated between bacterial counts upon exposure to each irradiance ($P \geq 0.081$; Figure 6.8I), higher irradiances were found to achieve

significantly greater percentage reductions per-unit-dose: 36 Jcm^{-2} achieved a 72.9% reduction using 150 $mWcm^{-2}$, which was significantly greater ($P<0.001$) than the 55.6 and 48.0% reductions recorded using 50 and 5 $mWcm^{-2}$, respectively (Figure 6.8J). Non-exposed log_{10} *S. aureus* control populations were shown in some cases to significantly decrease throughout treatment ($P\leq0.05$; Figure 6.8); however, in all cases, 405-nm light exposed populations were significantly lower ($P\leq0.01$), with the exception of 10^5 CFU mL^{-1} *S. aureus* exposures to 150 mW cm^{-2}, in which significant reductions were noted from 72 J cm^{-2} onwards ($P<0.001$).

Results for *P. aeruginosa* (Figure 6.9) indicate a significant enhancement in inactivation with lower irradiance exposures at all population densities ($P\leq0.05$). At 10^3 CFUmL^{-1}, log_{10} bacterial counts were found to be significantly lower upon exposure to doses of 36, 72 and 144 J cm^{-2} when 5 mW cm^{-2} was used compared with all other irradiances ($P\leq0.027$; Figure 6.9A). Exposure to 36 Jcm^{-2}, for example, resulted in a 0.82 log_{10} CFU mL^{-1} reduction (59.8% reduction) when illuminated at 5 mW cm^{-2}, significantly greater than the 0.07 log_{10} CFU mL^{-1} (11.0%) reduction using 150 $mWcm^{-2}$ ($P<0.001$), or 0.13 log_{10} CFU mL^{-1} (27.8%) reduction when using 50 mW cm^{-2} ($P<0.001$) (Figure 6.9A). Similar results were obtained using a 10^5 CFU mL^{-1} population, whereby inactivation was significantly enhanced upon exposure to initial doses of 36 and 72 J cm^{-2} using the lowest irradiance compared to higher irradiances ($P<0.001$): exposure to 36 J cm^{-2} using 5 mW cm^{-2} resulted in reductions of ~0.71 log_{10} CFU mL^{-1} (64.8%); compared to reductions of 0.06-0.28 log_{10} CFU mL^{-1} (12.5-18.6%) when exposed using 50-150 mW cm^{-2} (Figure 6.9C and D). For 10^7 CFUmL^{-1} populations (Figure 6.9E and F), both 5 and 50 mW cm^{-2} irradiances were shown to be significantly more effective for inactivation than 150 mW cm^{-2} up to a dose of 144 J cm^{-2} ($P\leq0.006$). Exposure to 36 J cm^{-2} using 5 mW cm^{-2} resulted in significantly greater bacterial reductions ($P<0.001$) than that of exposures using 50-150 mW cm^{-2} (0.96 versus 0.06-0.54 log_{10} CFU mL^{-1} reductions; Figure 6.9E), and two times less dose was shown to be required for near-complete inactivation (≥97.3%) when exposed using the two lower irradiances (108 J cm^{-2}) compared to the highest (216 Jcm^{-2}; Figure 6.9F). In contrast to *S. aureus*, inactivation of 10^9 CFU mL^{-1} *P. aeruginosa* populations (Figure 6.9G and H) was shown to be enhanced using lower irradiance: log_{10} bacterial counts were significantly lower ($P<0.001$) upon doses of 72-144 J cm^{-2}, with up to 3.92 log_{10} bacterial reductions noted using 5 mW cm^{-2} compared to 1.52-1.89 log_{10} CFU mL^{-1} reductions using 50-150 mW cm^{-2}; and percentage surviving bacterial counts were

significantly lower using 5 mW cm^{-2} compared to 150 mW cm^{-2} up to 108 J cm^{-2} ($P \leq 0.002$), with 2-3 times less dose required for near-complete inactivation (≥98.0%) when exposed at 5 $mWcm^{-2}$ (72 Jcm^{-2}) in comparison to 50 $mWcm^{-2}$ (144 Jcm^{-2}) and 150 $mWcm^{-2}$ (216 Jcm^{-2}). Similar to *S. aureus* (Figure 6.8), non-exposed log_{10} *P. aeruginosa* control populations were shown, in some cases, to significantly decrease throughout treatment duration ($P \leq 0.05$; Figure 6.9). However, in all cases, 405-nm light exposed populations were significantly lower in comparison to non-exposed controls from an initial dose of 36 J cm^{-2} onwards ($P \leq 0.01$), with the exception of 10^3 CFU mL^{-1} exposures to 150 mW cm^{-2}, in which significant reductions were initially noted following 72 J cm^{-2} ($P<0.001$), and 10^5 CFU mL^{-1} exposures to 50 and 150 mW cm^{-2}, in which significant reductions were initially noted following 72 J cm^{-2} ($P<0.001$ and $P=0.038$, respectively).

The mean GE for the 405-nm light inactivation of bacterial suspensions investigated in this section are presented in Figure 6.10. For *S. aureus* (Figure 6.10A), GE values for inactivation of initial densities of 10^3-10^7 CFU mL^{-1} were significantly greater when 0.5 $mWcm^{-2}$ was used in comparison to that of higher irradiances ($P \leq 0.001$): GE values for *S. aureus* inactivation using 5 mW cm^{-2} compared to 150 mW cm^{-2} were ~4.1 times greater when exposing 10^3 CFU mL^{-1} populations, ~1.5 times greater when exposing 10^5 CFU mL^{-1} populations and ~1.6 times greater when exposing 10^7 CFU mL^{-1} populations. GE values for inactivation of 10^8 CFU mL^{-1} *S. aureus* suspensions, however, were relatively similar (0.022-0.025), with significantly greater values demonstrated for exposures to 50 mW cm^{-2} compared to 5 mW cm^{-2} ($P=0.035$). At the highest density (10^9 CFU mL^{-1}), GE values, although again similar (0.015-0.019), were significantly lower for exposure to 5 mW cm^{-2} compared to both higher irradiance exposures ($P=0.001$). GE values for *S. aureus* inactivation using 5 mW cm^{-2}, unlike higher irradiances, were shown to significantly decrease as population density increased until 10^8 CFU mL^{-1} ($P<0.001$), with no signficanty difference demonstrated between values for 10^8 and 10^9 CFU mL^{-1} inactivation.

For *P. aeruginosa* (Figure 6.10B), GE values at each irradiance were fairly comparable. For 10^3 CFU mL^{-1} populations, GE values were similar (0.019-0.022; $P=0.339$), with no key patterns demonstrated between irradiance application and the efficacy of 405-nm light inactivation. For higher populations, greater values were presented at lower irradiances: at 10^5 CFU mL^{-1}, GE values for 5 and 50 mW cm^{-2} exposures were higher than 150 mW cm^{-2}, however only values from 50 mW cm^{-2} exposures were significantly higher ($P=0.002$); at 10^7 CFU mL^{-1}, values obtained using both 5 and 50 mW cm^{-2} were

significantly higher, and approximately 1.5-1.8 times that achieved using 150 mW cm^{-2} ($P<0.001$); and at 10^9 CFU mL^{-1}, exposures using 5 mW cm^{-2} were found to be associated with significantly higher GE values, approximately 2.4-2.5 times that, of 50 and 150 mW cm^{-2} exposures ($P<0.001$).

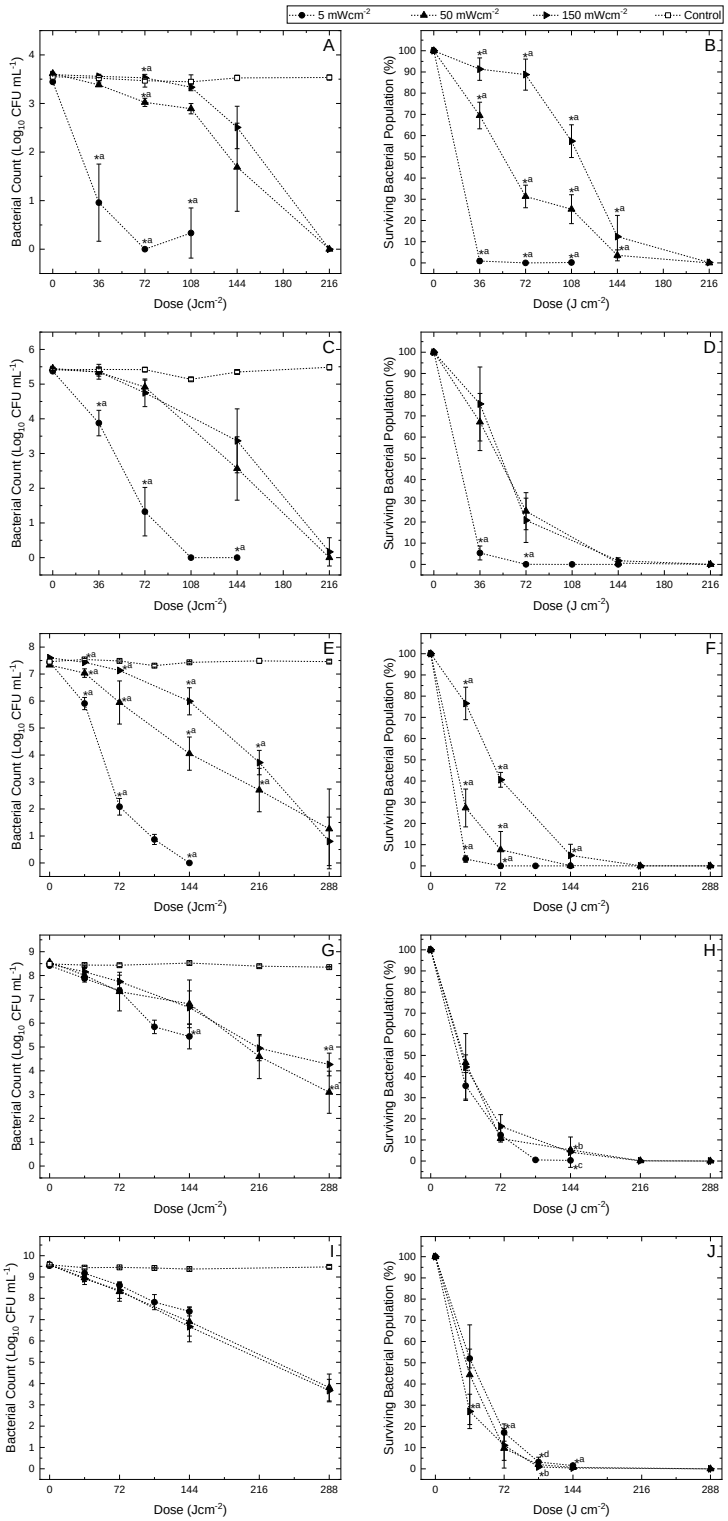

Figure 6.8 Inactivation kinetics of *Staphylococcus aureus* suspended in PBS at initial population densities of (A-B) 10^3 CFU mL^{-1}, (C-D) 10^5 CFU mL^{-1}, (E-F) 10^7 CFU mL^{-1}, (G-H) 10^8 CFU mL^{-1} and (I-J) 10^9 CFU mL^{-1}, upon exposure to increasing doses of 405-nm light at irradiances of 5, 50 and 150 mW cm^{-2}. Results are presented as both bacterial counts in $\log_{10}$ CFU mL^{-1} (A, C, E, G and I) and percentage surviving bacterial populations with respect to equivalent non-exposed control populations (B, D, G, H and J). Each data point represents the mean value ± SD (n = 3). Asterisks (*) represents levels of inactivation significantly different to other irradiances at a particular applied dose (P≤0.05): *a, significantly different to all other irradiances; *b, significantly different to 5 mW cm^{-2}; *c, significantly different to 50 mW cm^{-2} and *d, significantly different to 150 mW cm^{-2}.

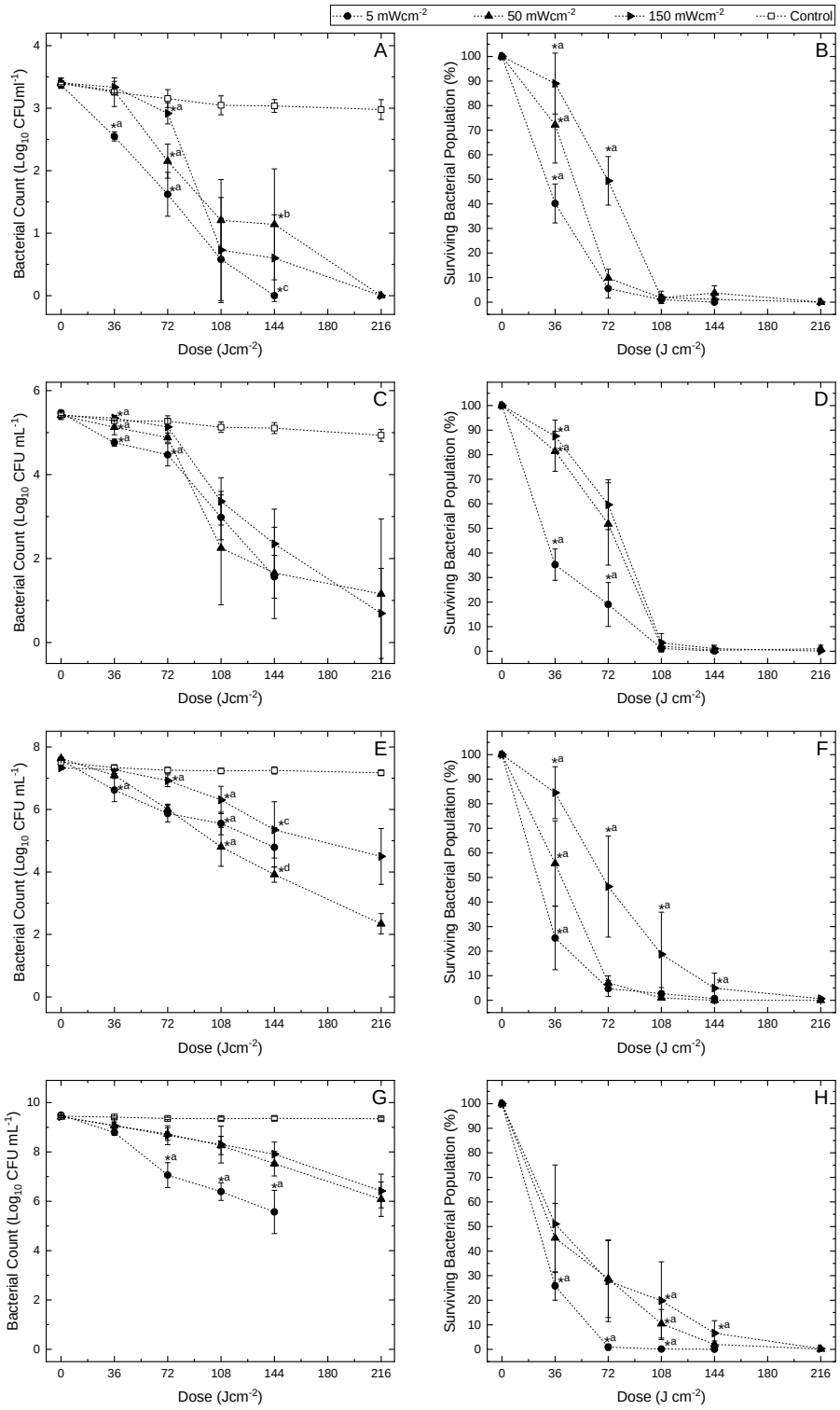

Figure 6.9 Inactivation kinetics of *Pseudomonas aeruginosa* suspended in PBS at initial population densities of (A-B) 10^3 CFU mL^{-1}, (C-D) 10^5 CFU mL^{-1}, (E-F) 10^7 CFU mL^{-1} and (G-H) 10^9 CFU mL^{-1}, upon exposure to increasing doses of 405-nm light at irradiances of 5, 50 and 150 mW cm^{-2}. Results are presented as both bacterial counts in $\log_{10}$ CFU mL^{-1} (A, C, E and G) and percentage surviving bacterial populations with respect to equivalent non-exposed control populations (B, D, G and H). Each data point represents the mean value ± SD (n = 3). Asterisks (*) represents levels of inactivation significantly different to other irradiances at a particular applied dose (P≤0.05): *a, significantly different to all other irradiances; *b, significantly different to 5 mW cm^{-2}; *c, significantly different to 50 mW cm^{-2} and *d, significantly different to 150 mW cm^{-2}.

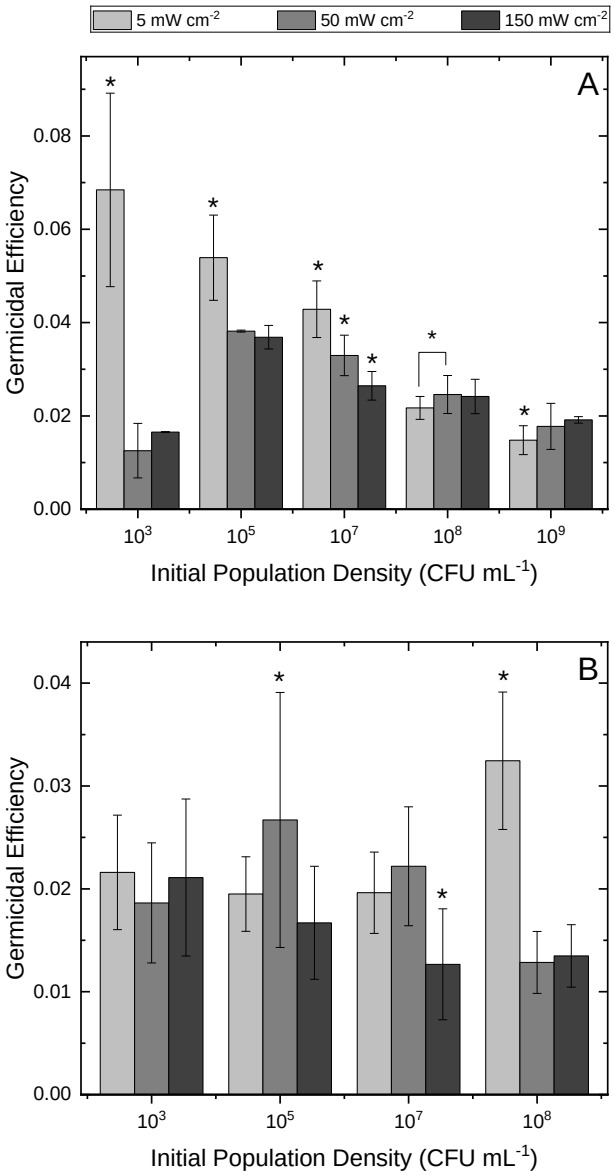

Figure 6.10 GE for complete/near-complete (≥95%) inactivation of liquid-suspended (A) *Staphylococcus aureus* and (B) *Pseudomonas aeruginosa* (10^3-10^9 CFU mL^{-1}; 3 mL) upon exposure to identical doses of 405-nm light using irradiances of 5-150 mW cm^{-2}. Each data point represents the mean value ± SD (n = 3). For each data point, GE was calculated at the dose at which complete or near-complete (≥95%) inactivation was achieved. Asterisks (*) represent irradiance exposures which had a significantly different GE value from that of all other irradiance exposures (P≤0.05).

Figure 6.11 presents the transmission of 405-nm light through bacterial suspensions at varying cell densities ($10^{3\text{-}9}$ CFU mL^{-1}). Results measured via UV-Vis spectrophotometry (Figure 6.11A) indicate that 405-nm light transmission was fairly consistent for both bacteria until 10^6 CFU mL^{-1} (95.5-99.6% and 96.3-100%, respectively). Beyond which, transmission steadily decreased with increasing population density, with 405-nm light transmission reduced to just 1.8 and 2.5% for 10^9 CFU mL^{-1}

populations of *S. aureus* and *P. aeruginosa*, respectively. To mimic the light treatment conditions used in the tests, the loss of light through the 3.2 mm depth in the test plate was measured (Figure 6.11B). For both bacteria, no significant difference was demonstrated between transmission through PBS and that of suspensions $\leq 10^8$ CFU mL^{-1} ($P \geq 0.132$); however, transmission through 10^9 CFU mL^{-1} suspensions were found to be significantly lower than that of PBS ($P < 0.001$), and all other suspensions ($P < 0.001$). Comparatively, transmission through *S. aureus* and *P. aeruginosa* was shown to be statistically similar for all population densities ($P \geq 0.079$), with the exception of 10^9 CFU mL^{-1} suspensions, in which transmission was significantly greater through *P. aeruginosa* suspensions compared to that of *S. aureus* ($P = 0.008$).

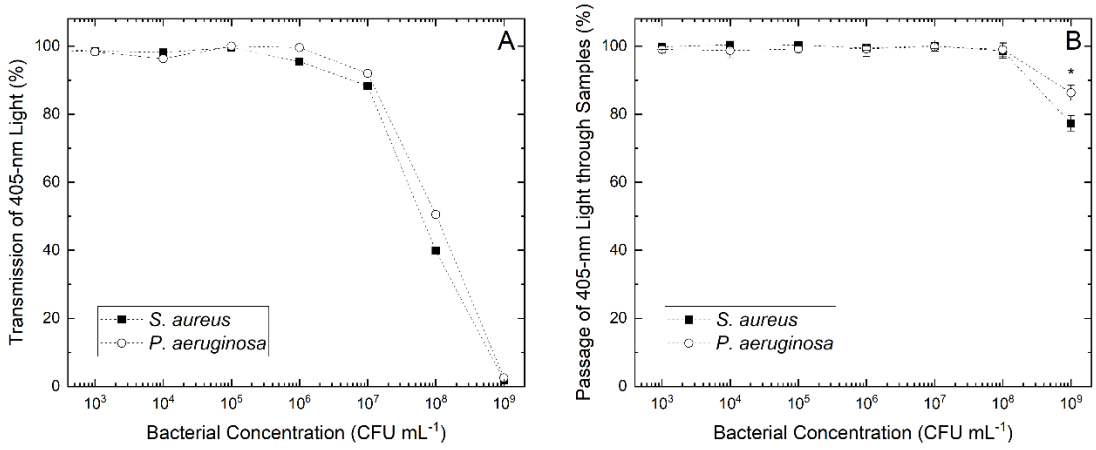

Figure 6.11 405-nm light transmission through suspensions of *Staphylococcus aureus* and *Pseudomonas aeruginosa* at population densities of $10^{3\text{-}9}$ CFU mL^{-1} measured using (A) standard UV-Vis spectrophotometry and (B) a power meter and photodiode detector, through the 3.2 mm depth of the test set-up (n=3). Asterisks (*) represent bacterial concentrations in which there was a significant difference in the % transmission of 405-nm light through different bacteria.

6.5 Bacterial Cell Damage by Low versus High Irradiance 405-nm Light

Based on findings in Sections 6.2-6.4, this section aimed to determine the differences, if any, in cellular cytotoxic responses – namely, intracellular ROS production and membrane damage – of *S. aureus* and *P. aeruginosa* upon exposure to identical doses of 405-nm light using different irradiance regimes.

6.5.1 Methods: Bacterial Cell Damage by Low versus High Irradiance Exposures

6.5.1.1 Bacterial Light Treatment

To determine the influence of irradiance application on cellular cytotoxic responses to 405-nm light, suspensions of *S. aureus* and *P. aeruginosa* were firstly exposed to light treatment using a similar methodology to that implemented in Section 6.4.1.4. For these test protocols, high density 10^9 CFU mL^{-1} population densities were required to be used. Briefly, 3 mL volumes of *S. aureus* and *P. aeruginosa* were transferred to a 6-well microplate (providing a sample depth of 3.2 mm) and exposed to increasing doses of 405-nm light at irradiances of 5, 50 and 150 $mWcm^{-2}$. Exposure times were selected to ensure equivalent light doses (36 – 144 Jcm^{-2}) were delivered to samples (Equation 3.1). All 6-well plates were covered with an adhesive plate seal to prevent evaporation, and so irradiance measurements were taken through the material as described in Section 6.3.1.3 to ensure the desired irradiance reached bacterial samples. The light treatments delivered to samples are presented in Table 6.4. Control samples were prepared in an identical manner but were exposed to ambient laboratory lighting only. Post-exposure, samples were processed following the steps outlined in Sections 6.5.1.2-6.5.1.4.

Table 6.4 405-nm light treatments of 10^9 CFU mL^{-1} bacterial suspensions.

Irradiance ($mWcm^{-2}$)	**5**	**50**	**150**	**Dose Delivered ($J\ cm^{-2}$)**
Exposure Time (minutes)	120	12	4	**36**
	240	24	8	**72**
	360	36	12	**108**
	480	48	16	**144**

6.5.1.2 Inactivation Kinetics

To determine the bacterial inactivation kinetics of 10^9 CFUmL^{-1} populations, following exposure to the light treatments outlined in Section 6.5.1.1, 100 µL samples (n=2) were plated onto agar and incubated at 37°C for 18-24 h. Following incubation, colonies were enumerated. Results represent the mean values ± SD of triplicate replicates measured in duplicate (n=6), and are reported as bacterial reductions as compared to the equivalent non-exposed control samples in $\log_{10}$ CFU mL^{-1}.

6.5.1.3 ROS Detection and Measurement

The detection and measurement of intracellular ROS production was conducted using 6-carboxy-2',7'-dichlorodihydrofluorescein diacetate (carboxy-H_2DCFDA). Carboxy-H_2DCFDA is a chemically reduced, acetylated form of fluorescein often used as an indicator of ROS in various cell types including bacteria, cancers, neutrophils and phagocytes. This non-fluorescent molecule is readily converted to a green fluorescent form when acetate groups are removed by intracellular esterases and oxidation, via ROS activity, occurs within the cell (Thermo Fisher Scientific, 2023). The generation of green fluorescence from carboxy-H_2DCFDA is therefore indicative of the presence of intracellular oxidative stress. This dye has previously been used to detect ROS generated in response to 405-nm light exposure in bacteria in literature (Ramakrishnan *et al.*, 2016; Minor and Sabillón, 2023), and the methodology used was adapted from Ramakrishnan *et al*. (2016). Following exposure to light treatments described in Section 6.5.1.1, all exposed and non-exposed samples were centrifuged at 4036 × g for 15 min (GT1 centrifuge) to achieve a cell pellet. The supernatant was discarded and 300 µL 25 µM carboxy-H_2DCFDA (C400; Thermo Fisher Scientific, UK) was then added to the pellet, vortexed and incubated in the dark for 30 min at room temperature to allow the probe to accumulate within cells. Post-incubation, suspensions were made up to 3 mL with PBS, and fluorescence was measured immediately using an RF-5001PC spectroflurophotometer at an excitation wavelength of 495 nm and emission wavelength of 525 nm. Results represent the mean values ± SD of triplicate replicates (n=3), and are reported as the percentage increase in green fluorescence intensity generated from carboxy-H_2CDFDA, as an indicator of ROS production, as compared to the equivalent non-exposed control samples. For this experiment, the initial three dose points were selected for analysis (36, 72 and 108 J cm^{-2}).

6.5.1.4 Membrane Integrity Assessment

To assess the integrity of bacterial cell membranes in response to light treatments, the leakage of intracellular nucleic acids into the extracellular matrix was quantified using spectrophotometric analysis. The methodology employed was adapted from McKenzie *et al*. (2016). Following exposure to light treatments described in Section 6.5.1.1, all exposed and non-exposed samples were centrifuged at 3939 × g for 5 min (Heraeus Labofuge 400R; Kendro Laboratory Products, UK). The supernatant was extracted and analysed using a Biomate 5-UV-Vis spectrophotometer (Fisher Scientific, UK), with

absorbance measured at 260 nm to indicate the presence of leaked nucleic acids. Results represent the mean values ± SD of triplicate replicates (n=3), and are reported as the percentage increase in absorbance at 260 nm, as an indicator for the leakage of nucleic acid material, as compared to the equivalent non-exposed control samples.

6.5.2 Results: Bacterial Cell Damage by Low versus High Irradiance Exposures

6.5.2.1 Inactivation Kinetics

Figure 6.12 presents the reductions of (A) *S. aureus* and (B) *P. aeruginosa* upon exposure to increasing doses of 405-nm light using 5, 50 and 150 mW cm^{-2}. Surviving counts of all 405-nm light exposed samples were significantly lower than that of non-exposed controls ($P \leq 0.002$): following a final dose of 144 J cm^{-2}, *S. aureus* counts reduced from 9.23 to 7.38 log_{10} CFU mL^{-1} using 5 mW cm^{-2}, 9.51 to 6.91 log_{10} CFU mL^{-1} using 50 mW cm^{-2}, and 9.47 to 6.67 log_{10} CFU mL^{-1} using 150 mW cm^{-2}; whilst *P. aeruginosa* counts reduced from 9.43 to 5.57 log_{10} CFU mL^{-1} using 5 mW cm^{-2}, 9.38 to 7.53 log_{10} CFU mL^{-1} using 50 mW cm^{-2}, and 9.27 to 7.91 log_{10} CFU mL^{-1} using 150 mW cm^{-2}.

For exposures of *S. aureus* (Figure 6.12A) to 36 J cm^{-2}, reductions achieved using 150 mW cm^{-2} were significantly greater than that achieved using 5 mW cm^{-2} (0.58 versus 0.28 log_{10} CFU mL^{-1} reductions; $P=0.001$); with no significant difference demonstrated between that of 50 mW cm^{-2} and other irradiances (0.45 log_{10} CFU mL^{-1} reductions; $P \geq 0.05$). At higher dose applications, the two higher irradiances achieved greater reductions: by 72 J cm^{-2}, 50 and 150 mW cm^{-2} achieved 1.07-1.22 log_{10} CFU mL^{-1} reductions, which was significantly greater than the 0.78 log_{10} CFU mL^{-1} reductions achieved using 5 mW cm^{-2} ($P<0.001$); by 108 J cm^{-2}, reductions of 1.92-2.07 log_{10} CFU mL^{-1} were achieved using 50-150 mW cm^{-2}, which was significantly greater than that of 5 mW cm^{-2} (1.60 log_{10} CFU mL^{-1} reductions; $P<0.001$); and following 144 J cm^{-2}, reductions of 2.61-2.81 log_{10} CFU mL^{-1} were achieved using 50-150 mW cm^{-2}, which was significantly greater than that of 5 mW cm^{-2} (1.85 log_{10} CFU mL^{-1} reductions; $P<0.001$). Contrastingly, results for *P. aeruginosa* (Figure 6.12B) demonstrate, for all dose applications, significantly greater reductions upon exposure to 5 mW cm^{-2} compared to 50-150 mW cm^{-2}: reductions of 0.60 log_{10} CFU mL^{-1} versus 0.35-0.36 log_{10} CFU mL^{-1}, respectively, were observed following 36 J cm^{-2} ($P=0.003$); reductions of 2.34 log_{10} CFU mL^{-1} versus 0.60-0.67 log_{10} CFU mL^{-1}, respectively, were observed following 72 J cm^{-2} ($P<0.001$); reductions of 3.01 log_{10} CFU mL^{-1} versus 1.01-

1.07 log_{10} CFU mL^{-1}, respectively, were observed following 108 J cm^{-2} (P<0.001); and reductions of 3.86 log_{10} CFU mL^{-1} versus 1.37-1.85 log_{10} CFU mL^{-1}, respectively, were observed following 144 J cm^{-2} (P<0.001). Comparing the two species, significantly greater reductions were demonstrated by *P. aeruginosa* compared to *S. aureus* at all doses using 5 mW cm^{-2} (reductions of ≤3.87 versus ≤1.85 log_{10} CFU mL^{-1}, respectively; P<0.001); whilst significantly greater reductions were achieved by *S. aureus* compared to *P. aeruginosa* when exposed to all doses using 50 and 150 mW cm^{-2} (reductions of ≤2.61-2.81 log_{10} CFU mL^{-1} compared to ≤1.37-1.85 log_{10} CFU mL^{-1}, respectively; P≤0.002), with the exception of exposures to 36 J cm^{-2} using 50 mW cm^{-2}, whereby no significant difference was demonstrated (0.45 and 0.36 log_{10} CFU mL^{-1} reductions, respectively; P=0.317).

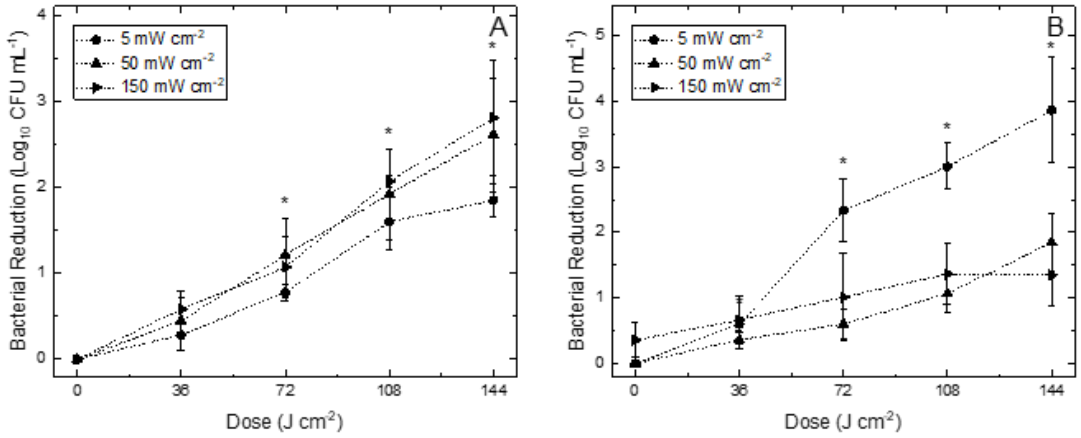

Figure 6.12 Reductions of (A) *Staphylococcus aureus* and (B) *Pseudomonas aeruginosa* suspensions (10^9 CFU mL^{-1}) upon exposure to increasing doses of 405-nm light at irradiances of 5, 50 and 150 mW cm^{-2}. Data points are presented as log_{10} bacterial reductions in comparison to non-exposed equivalent controls and represent the mean value ± SD (n=6). Asterisks (*) represent data points where log_{10} reductions achieved by exposure to 5 mW cm^{-2} were significantly different to that of 50 and 150 mW cm^{-2} exposures (P≤0.05).

6.5.2.2 ROS Detection and Measurement

Figure 6.13 presents the percentage increase in green fluorescence detected from carboxy H_2-DCFDA upon exposure of (A) *S. aureus* and (B) *P. aeruginosa* to increasing doses of 405-nm light at irradiances of 5-150 mW cm^{-2}. Results for *S. aureus* (Figure 6.13A) indicate no significant increase in the green fluorescence detected in light-exposed samples compared to equivalent non-exposed controls across all delivery regimes (P≥0.096). Although insignificant, small increases in fluorescence compared to equivalent controls were detected when exposed to 405-nm light using 5 and 150 mW cm^{-2} (maximum increases of 9.62 and 8.85%, respectively); whilst no increase was demonstrated using 50 mW cm^{-2}. No significant difference was demonstrated between the increases in fluorescence detected as treatment

progressed for each irradiance (P=0.615-0.848) and further, no significant difference was demonstrated between the fluorescence intensity between each irradiance across all doses (P=0.322-0.683). Results for *P. aeruginosa* (Figure 6.13B) similarly demonstrate no significant increase in fluorescence detected in light-exposed samples compared to equivalent non-exposed controls across all irradiances (P=0.110-0.690), with the exception of 5 mW cm^{-2} exposures to 72 J cm^{-2}, in which fluorescence levels were significantly higher in exposed versus non-exposed samples (41.96 versus 26.25, respectively; P=0.011). Although insignificant (P=0.169-0.890), an upward trend was demonstrated in fluorescence intensity, for all light irradiance regimes, as treatment time, and thus dose, increased. The percentage increase compared to controls using 5 mW cm^{-2} was 57.4% upon an initial dose of 36 J cm^{-2}, which increased to 121.5% following 108 J cm^{-2}; using 50 mW cm^{-2}, no percentage increase was demonstrated after 36 J cm^{-2}; however, a 17.1% increase was demonstrated after 108 J cm^{-2}; and using 150 mW cm^{-2}, a 14.9% increase was demonstrated following 36 J cm^{-2}, which increased to 30.3% following 108 J cm^{-2}. No significant differences were observed in fluorescence intensity upon exposure to each irradiance at each dose (P=0.231-0.764), however, greater levels were demonstrated at the lowest irradiance, with 4-7 times greater fluorescence detected by 108 J cm^{-2} using 5 mW cm^{-2} compared to higher irradiances. Comparatively, greater fluorescence was detected upon all exposures for *P. aeruginosa* compared to *S. aureus*, however only levels observed upon 36 J cm^{-2} using 5 mW cm^{-2} and 72 and 108 J cm^{-2} using 150 mW cm^{-2} were statistically significant (P=0.002-0.033).

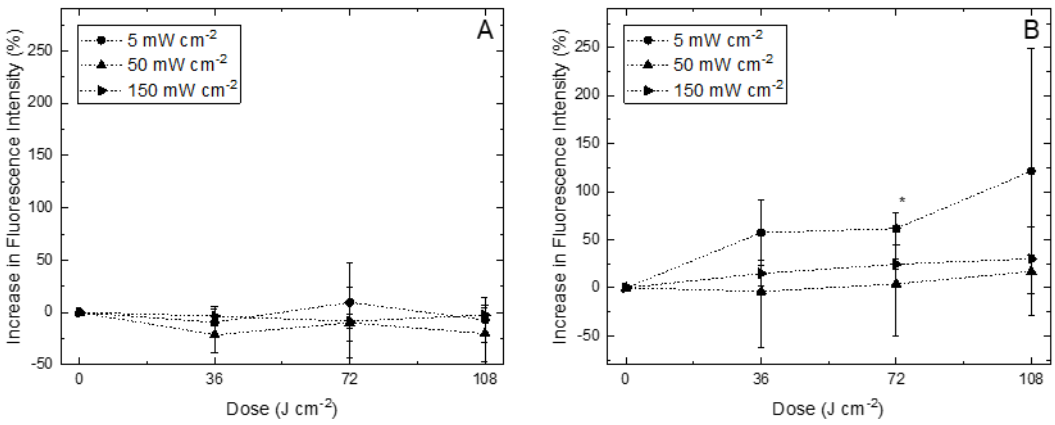

Figure 6.13 ROS fluorescence intensity in (A) *Staphylococcus aureus* and (B) *Pseudomonas aeruginosa* cells upon exposure to increasing doses of 405-nm light at irradiances of 5-150 mW cm^{-2}, measured through incubation with carboxy-H_2DCFDA and spectrophotometric measurement at an excitation wavelength of 495 nm and an emission wavelength of 525 nm (n=3±SD). Asterisks (*) represent data points in which there was a significant difference (P≤0.05) between exposed and non-exposed control samples.

6.5.2.3 Membrane Integrity Assessment

Figure 6.14 presents the comparative increase in absorbance at 260 nm of (A) *S. aureus* and (B) *P. aeruginosa* upon exposure to increasing doses of 405-nm light using irradiances of 5-150 mW cm^{-2} compared to equivalent non-exposed controls. In all cases, absorbance at 260 nm was greater upon 405-nm light exposure compared to non-exposed controls ($P \leq 0.045$ in all cases up to 108 J cm^{-2}), with an upward trend in absorbance at 260 nm demonstrated as exposure time, and thus dose, increased: by 108 J cm^{-2} in all cases, absorbance readings were significantly greater than starting values ($P \leq 0.092$).

For *S. aureus* (Figure 6.14A), values were statistically similar across all irradiances (P=0.358-0.851), with the exception of exposures to 144 J cm^{-2}, whereby the increase in absorbance using 50 mW cm^{-2} was significantly greater than that of 5 and 150 mW cm^{-2} (0.28 versus 0.16-0.18, respectively; P=0.001). Although insignificant, the increase in absorbance upon exposure to 5 mW cm^{-2} was lower than that of higher irradiances upon ≥72 J cm^{-2}: values of 0.15 compared to 0.17-0.19 at 72 J cm^{-2}; 0.17 compared to 0.20 at 108 J cm^{-2} and 0.16 compared to 0.19-0.28 at 144 J cm^{-2}. For *P. aeruginosa* (Figure 6.14B), values were significantly higher upon higher irradiance exposure (P=0.001-0.033). The increase in absorbance at 260 nm upon 36 J cm^{-2} using 150 mW cm^{-2} was significantly higher than 5 mW cm^{-2} (0.41 versus 0.02; P=0.033), with no significant difference between 50 mW cm^{-2} and other irradiances (0.26; P>0.05). Upon ≥72 J cm^{-2}, values were significantly higher using 50-150 mW cm^{-2} compared to 5 mW cm^{-2}: 0.26-0.41 versus 0.07 at 72 J cm^{-2} (P=0.001); 0.50-0.52 versus 0.17 at 108 J cm^{-2} (P=0.013); and 0.64 versus 0.23 at 144 J cm^{-2} (P=0.003).

Comparatively, the increase in absorbance at 260 nm upon exposure to 5 mW cm^{-2} was statistically similar for both *S. aureus* and *P. aeruginosa* up to 108 J cm^{-2} (P=0.076-0.933); beyond which, values for *P. aeruginosa* were significantly greater than *S. aureus* (0.23 versus 0.16; P=0.033). Using 50 mW cm^{-2}, values were statistically similar at 36 J cm^{-2} (P=0.364); beyond which, values for *P. aeruginosa* were significantly greater than *S. aureus*: 0.58 versus 0.17 at 72 J cm^{-2} (P=0.002), 0.52 versus 0.20 at 108 J cm^{-2} (P=0.013) and 0.64 versus 0.28 at 144 J cm^{-2} (P=0.012). Using 150 mW cm^{-2}, values were significantly greater, in all cases, *for P. aeruginosa* compared to *S. aureus*: 0.41 versus 0.13 at 36 J cm^{-2} (P=0.033), 0.61 versus 0.19 at 72 J cm^{-2} (P=0.004), 0.50 versus 0.20 at 108 J cm^{-2} (P=0.009) and 0.64 versus 0.18 at 144 J cm^{-2} (P=0.001).

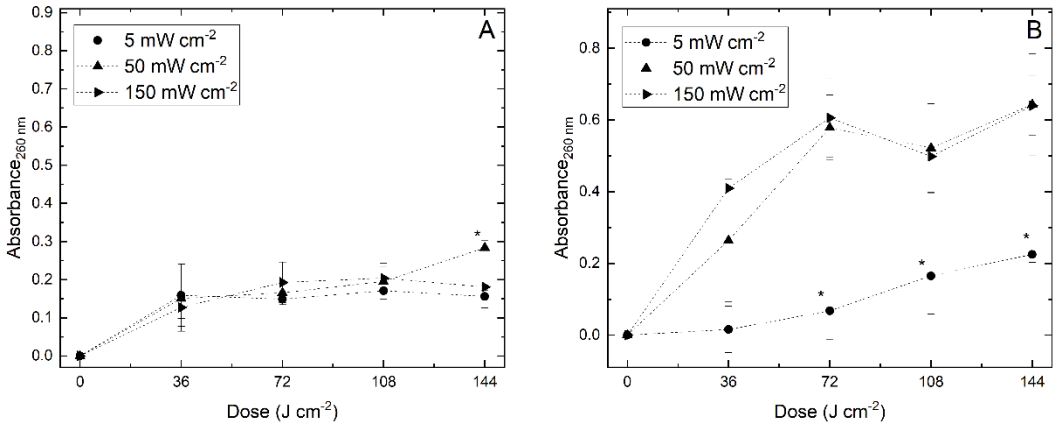

Figure 6.14 Comparison of the difference in absorbance measurements of exposed and non-exposed (A) *Staphylococcus aureus* and (B) *Pseudomonas aeruginosa* cell supernatants at 260 nm upon exposure to an increasing dose of 405-nm light at irradiances of 5, 50 and 150 mW cm^{-2}. Each data point represents the mean value ± SD (n=3±SD). Asterisks (*) represent data points which are significantly different to all other irradiances (P≤0.05).

6.6 Discussion

This chapter has successfully demonstrated the efficacy of lower irradiance 405-nm light for the inactivation of key nosocomial bacteria presented at various population densities on surfaces and in liquid suspension, and has additionally highlighted the enhanced susceptibility of bacteria to inactivation when exposed to a fixed dose of 405-nm light using lower irradiances compared to higher irradiances. Further, preliminary investigations into oxidative stress produced by bacterial cells in response to such exposures has provided indication of the potential mechanisms of damage and cellular targets associated with 405-nm light inactivation of bacteria.

As mentioned, given its increased safety profile over UV light, there is interest in the development of antimicrobial violet-blue light for infection control applications which require exposure of sensitive materials or occupied environments, whereby lower irradiances are generally used to ensure compatibility with such applications. For environmental decontamination, violet-blue light is typically employed at levels <1 mWcm^{-2} to ensure the safety of exposed room occupants (ICNIRP, 2013). An irradiance of 0.5 mWcm^{-2} was selected for surface-seeded bacterial exposures in this chapter to represent the typical level used to illuminate high-touch surfaces when the technology is employed in a room environment (Chapter 4). It is recognised that irradiance levels will vary depending on the distance of the contaminated surface from the location of the light source, however, findings in the previous

chapter demonstrated that a range of irradiance levels <1 $mWcm^{-2}$ can achieve bacterial inactivation, and so this particular irradiance was selected as a representative 'low' level. Results in Figures 6.2, 6.7 and Appendix B, indicate that all surface-exposed ESKAPE pathogens (10^1-10^8 CFU $plate^{-1}$) were reduced by exposure to 0.5 $mWcm^{-2}$, with greater levels of inactivation achieved as light dose was increased. When exposed to this irradiance at 10^2 CFU $plate^{-1}$, which was chosen to represent the typical upper levels of contamination reported within hospital isolation rooms (Maclean *et al.*, 2013a), the susceptibility of each ESKAPE pathogen was variable, however, complete/ near-complete (≥96.6%) inactivation of each species individually was achieved using 6-30 Jcm^{-2} (3.3-16.6 h) (Figure 6.2). Comparative exposures of bacterial suspensions to 0.5 mW cm^{-2} could not be conducted due to the limited viability of bacteria whilst suspended for lengthy periods in PBS. Alternatively, an irradiance level of 5 $mWcm^{-2}$ was selected, with this irradiance being in the region of those suggested for wound disinfection applications (5-20 mW cm^{-2}) (McDonald *et al.*, 2011; Dai *et al.*, 2013a, 2013b). Use of 5 $mWcm^{-2}$ was shown to successfully reduce suspended *S. aureus* and *P. aeruginosa* (selected as Gram-positive and Gram-negative representatives, respectively), with near-complete (≥99.7%) inactivation achieved for both species with a dose of 45 Jcm^{-2} (2.5 h; Figure 6.4).

In addition to comparing the bactericidal efficacy of different doses of 405-nm light, this chapter has also provided novel information on the comparative bactericidal efficacy of 405-nm light when the same dose of light is applied at different irradiation levels. The results provide key evidence to demonstrate the enhanced bactericidal efficacy of low irradiance 405-nm light in comparison to that of higher irradiance exposures, per-unit-dose. Results in Figure 6.2 indicate all surface-seeded ESKAPE bacteria (10^2 CFU $plate^{-1}$) required a significantly ($P<0.05$) lower dose to achieve complete/near-complete (≥95.47%) inactivation when exposed using lower irradiance levels: exposures to 0.5 $mWcm^{-2}$ required 1.5-3.3 times less energy that than required by exposures to 5 $mWcm^{-2}$, and 3.3-11.1 less energy than that required by exposures to 50 $mWcm^{-2}$. Although all employed irradiance levels achieved significant levels of inactivation, the dose required for a 1 log_{10} reduction was significantly less ($P\leq0.05$) for all species when exposed using 0.5 $mWcm^{-2}$ (6-30 Jcm^{-2}) in comparison to both 5 $mWcm^{-2}$ (9-60 J cm^{-2}) and 50 $mWcm^{-2}$ (30-150 J cm^{-2}). The GE for inactivation of each ESKAPE pathogen (Figure 6.3) was also shown to be significantly higher ($P\leq0.05$) when exposed using the lowest irradiance (ranging from 0.05-0.29) in comparison to higher irradiances (ranging from 0.03-0.22 for 5 mW cm^{-2} and 0.01-0.05

for 50 mW cm^{-2}). Similarly, results in Figure 6.4 suggest *S. aureus* and *P. aeruginosa* in suspension also required lower doses to achieve significant levels of inactivation when exposed using lower irradiance levels: both species required 3 times less energy when exposed using 5 $mWcm^{-2}$ compared to 150 $mWcm^{-2}$ (22.5 versus 67.5 J cm^{-2}; $P \leq 0.05$). Similarly, although all exposures did induce complete/near-complete (≥99.74%) inactivation, significantly lower doses ($P<0.05$) were required to achieve this when exposed using lower irradiance levels: two times less energy was required when exposed using 5 $mWcm^{-2}$ compared to 150 $mWcm^{-2}$ (45 versus 90 J cm^{-2}; $P \leq 0.05$). Comparison of exposures over the initial dose range of 0-45 Jcm^{-2} further highlights this difference in efficacy: following 45 Jcm^{-2}, log_{10} reductions of 2.94 and 3.37 were observed for *S. aureus* exposed at 5 and 10$mWcm^{-2}$, respectively; in comparison to just 0.21, 0.08 and 0.08 log_{10} reductions when exposed at 50, 100 and 150 $mWcm^{-2}$, respectively. Similarly, at this same application of dose, log_{10} reductions of 2.86 and 2.81 were observed for *P. aeruginosa* exposed at 5 and 10 $mWcm^{-2}$, respectively; in comparison to just 1.25, 0.43 and 0.08 log_{10} reductions when exposed at 50, 100 and 150 $mWcm^{-2}$, respectively. The GE for inactivation at this initial population density of 10^3 CFU mL^{-1} (Figure 6.5) was significantly greater ($P<0.001$) for both *S. aureus* and *P. aeruginosa* when exposed to ≤10 mW cm^{-2} compared to ≥50 $mWcm^{-2}$, further demonstrating the bactericidal energy efficiency of using low irradiance levels.

Interestingly, these findings can be considered to conflict with previous studies which depicted a dose-dependency associated with 405-nm light exposure, which suggest inactivation increases with applied dose, irrespective of the light delivery regime (high intensity/short duration or low intensity/long duration) (Endarko *et al.*, 2012; Murdoch *et al.*, 2012; Barneck *et al.*, 2016). It is important to consider, however, that these studies compared exposures to irradiances within the same order of magnitude, and thus it is possible that light intensity may have a greater influence on inactivation efficacy when irradiances of varying orders of magnitude are compared. Murdoch *et al*. (2012), for example, exposed suspensions of *L. monocytogenes* to 108 Jcm^{-2} of 405-light using irradiances of 10-30 $mWcm^{-2}$ and found, although the log_{10} reduction achieved was slightly greater at lower intensity, there was no significant difference in the level of inactivation achieved at the different irradiance exposures. Similarly, Barneck *et al*. (2016) investigated equivalent 405-nm light dose exposures using irradiances of 2.38-2.89 and 8.85-9.71 $mWcm^{-2}$ on surface-seeded *S. aureus*, *S. pneumoniae*, *E. coli* and *P.*

aeruginosa, and demonstrated similar log_{10} reductions for both equivalent radiant exposures. The authors did note, however, that from the appearance of growth distribution patterns on treated culture plates, low intensity/long duration exposure regimes may provide a superior bactericidal effect due to the continuous nature of treatment (Barneck *et al.*, 2016).

The concept that differences in inactivation efficacy may become increasingly evident when comparing irradiance applications of greater orders of magnitude is further supported by Endarko *et al.* (2012), who found no significant difference ($P>0.05$) in the 405-nm light inactivation rate of *L. monocytogenes* when exposed to a constant dose using irradiances ranging from 44-85.6 $mWcm^{-2}$ but did demonstrate significantly greater inactivation when exposed to a constant dose using 8.6 $mWcm^{-2}$ in comparison to 85.6 $mWcm^{-2}$. Further, in Chapter 4, whilst evaluating broad-spectrum antibacterial efficacy of the 405-nm light EDS for surface-simulated decontamination, an enhancement in the inactivation of *S. aureus* was observed on a per-unit-dose basis when lower irradiance light sources were employed (Figure 4.10; Table 4.1); suggesting that low irradiance 405-nm light exposure, at levels similar to that employed for environmental decontamination, may be more efficient for bacterial inactivation than that of higher irradiance light sources on a per-unit-dose basis.

These findings provide key evidence to indicate the application of 405-nm light dose has an important role in the mechanisms of microbial inactivation. This improvement in bactericidal efficacy demonstrated at lower irradiance exposures may be due to specific levels of energy required for microbial inactivation, and it is possible that bacteria may adopt different response mechanisms when exposed to high intensity/short duration regimes in comparison to low intensity/long duration regimes. It has previously been identified that, when light irradiance is increased, there is the potential for photoinactivation to be limited by a depletion in oxygen supplies (Moseley *et al.*, 2006; Rogers, 2012) or saturation of the electronic absorption of porphyrins (Maclean *et al.*, 2016), which could result in a surplus of excited porphyrin molecules which are unable to participate in the photoinactivation process. However, in this study, the light irradiances used were substantially lower than the irradiance levels which could instigate saturation of the electronic absorption of porphyrins, and the inactivation kinetics of *S. aureus* at an initial density of 10^9 CFU mL^{-1} shown in Figure 6.8 indicate that oxygen is not lacking at the higher irradiances employed in this study. A possible explanation for the observed effects could be the result of bacterial responses to a relatively gentle oxidative stress for a prolonged period of time,

as opposed to a higher oxidative stress for a much shorter period of time. Whilst much is known about the damaging effects of ROS on microbial cells and cellular ROS defence mechanisms, there is relatively little understanding of how the interplay between these factors affects microbial populations in different environments (Imlay, 2019). High levels of ROS within the cell can induce genomic mutations, and particularly RNA damage (Seixas *et al.*, 2022), as well as oxidative modification of proteins, lipids and glycans which can lead to metabolic malfunction and cell death; whilst, conversely, low levels of local ROS play an important role within the cell both as redox-signalling molecules in a wide spectrum of pathways involved in the maintenance of cellular homeostasis and regulating key transcription factors (Schieber and Chandel, 2014; Fasnacht and Polacek, 2021). It is clear that ROS can induce a variety of both beneficial and detrimental effects on microbial cell survival, and the results of the present study, demonstrating greater GE when exposed using 405-nm light at relatively low irradiance levels over an extended period compared with a higher irradiance over a shorter period, further adds to this body of knowledge. A plausible explanation is that such low-level exposure over a prolonged period is in some way more damaging to the cell but alternatively it could be that ROS cellular defences are less effective under these conditions, or that the study results reflect some combination of enhanced lethality and impaired defence associated with prolonged exposure to low level 405 nm light.

To better comprehend the interplay between applied 405-nm light dose and irradiance, and the extent to which it affects 405-nm light inactivation, an assessment of the potential for a threshold level of irradiance to exist, whereby beyond which no further inactivation takes place, regardless of increasing dose, is an important area of future study. To do this, a panel of bacterial species could be exposed for a fixed time to 405-nm light at increasing irradiances, and thus doses. If inactivation levels were to plateau at a particular irradiance level, this may indicate a limit in the dose-dependent nature of 405-nm light exposure, potentially as a result of a depletion in oxygen supplies and thus a surplus of excited porphyrin molecules unable to participate in the photoinactivation process. These findings may help to explain why the efficacy of 405-nm light bacterial inactivation is variable depending on the mode of light delivery, and a better understanding of this fundamental concept could assist in the optimisation of low power, energy efficient antimicrobial lighting systems.

In terms of the comparative susceptibility of ESKAPE pathogens, results in Figure 6.2 indicate surface-seeded *S. aureus*, *A. baumannii* and *P. aeruginosa* were most susceptible to 0.5 mW cm^{-2}; collectively

requiring doses ≤ 6 J cm^{-2} to achieve 1 log_{10} reductions, in comparison to *E. faecium*, *K. pneumoniae* and *E. cloacae*, which required doses of 9, 30 and 13.5 J cm^{-2}, respectively. These results reflect those of Hoenes *et al*. (2021), who similarly found that *A. baumannii*, *S. aureus* and *P. aeruginosa* required lower doses of 405-nm light than that of other ESKAPE pathogens to achieve a 1 log_{10} reduction. The authors exposed ESKAPE pathogens at a higher irradiance (20 mW cm^{-2}) than employed in this study (Hoenes *et al.*, 2021), suggesting the comparative susceptibility of each species to treatment is independent of light irradiance application. This is corroborated by exposures to 50 $mWcm^{-2}$ shown in Figure 6.2, which demonstrated similar patterns of susceptibility. The species-specific differences in susceptibility observed in this study are likely due to differences in both the distribution and quantity of endogenous porphyrins produced by different bacterial cells (Nitzan *et al.*, 2004; Maclean *et al.*, 2009; Kumar *et al.*, 2015). Regardless, complete/near-complete (≥96.6%) inactivation of all species was demonstrated using low irradiance 405-nm light, similar to that employed for whole-room decontamination, within realistic exposure times for system use (16.6 h). These findings support those of Chapter 4, which similarly demonstrated that 0.5 $mWcm^{-2}$ 405-nm light could successfully inactivate a range of nosocomial and foodborne pathogens, with complete reductions of each species demonstrated in 2-16 h.

When exposed on surfaces, the qualitative data in Figure 6.7 and Appendix B indicates that low irradiance (0.5 $mWcm^{-2}$) 405-nm light could inactivate increasingly high bacterial population densities as the time of exposure, and thus applied dose, was increased. It is important to note that the high surface population densities employed in this study were used to provide insight into the mechanisms of 405-nm light inactivation and are significantly higher than typical contamination levels expected within healthcare settings (Maclean *et al.*, 2013a). Bacteria in this study were exposed on a nutritious medium, as a means to provide highly reproducible inactivation kinetics within the healthcare setting, and, although it may contain photosensitive components capable of enhancing the 405-nm light inactivation process, it also supports the growth and survival of a broad-spectrum of bacterial species and so will likely offer greater protection from oxidative stress than that of inert environmental surfaces (Murdoch *et al.*, 2012). It is therefore expected that bacteria present on inert environmental surfaces or suspended in the air would demonstrate even greater susceptibility to 405-nm light inactivation than that shown here. The demonstration of successful bacterial inactivation using low irradiance 405-nm light on

nutritious media and at population densities which significantly exceed that expected of contaminant levels within healthcare settings further supports the suitability of this technology for environmental decontamination.

Similar to the results reported for surface exposed bacteria, this chapter also demonstrated the GE of low irradiance 405-nm light when bacterial populations are treated in liquid suspension. The temperature of liquid samples was also monitored for all treatments, with the greatest temperature increase observed with the longest exposures at highest irradiance (10^9 CFU mL^{-1}; 150 mW cm^{-2}; ≥24 min; up to 42 ºC from 21 ºC). Despite this, regimes applied using lower irradiances were still found to achieve greater inactivation on a per unit dose basis, indicating that temperature had minimal effect. Results in Figures 6.8-6.10 demonstrate that the enhancement in inactivation efficacy observed for lower irradiance exposures is apparent for various bacterial population densities in suspension. For *S. aureus* with initial population densities of 10^3-10^7 CFUmL^{-1}, the dose required for an approximate 1 log_{10} reduction (Figure 6.8A, C and E) was up to 4 times lower using 5 mWcm^{-2} compared to higher irradiances, with corresponding GE values (Figure 6.10A) significantly greater for 5 mWcm^{-2} exposures compared to all other regimes (P≤0.001). When exposed at an initial population density of 10^8 CFUmL^{-1}, the dose required for an approximate 1 log_{10} reduction (Figure 6.8G) was the same for both 5 and 50 mW cm^{-2} exposures (72 J cm^{-2}), which was half of that required when exposed using 150 mW cm^{-2} (144 J cm^{-2}); however, corresponding GE values (Figure 6.10A) were significantly greater for 50 mW cm^{-2} compared to 5 mW cm^{-2} (P=0.035). By contrast, when exposed at an initial density of 10^9 CFUmL^{-1}, the dose required for an approximate 1 log_{10} reduction (Figure 6.8I) was the same for all irradiance exposures (72 J cm^{-2}), and GE values (Figure 6.10A), although similar across all irradiance exposures (0.015-0.019), were significantly lower at 5 mWcm^{-2} compared to all other irradiances (P=0.001). These results for *S. aureus* exposed at an initial density of 10^9 CFU mL^{-1} deviate from the overall findings of this study for reasons that are not yet fully understood. As previously discussed, this observation is likely due to differences in the species-specific response of bacteria to relatively gentle oxidative stress for prolonged periods, compared to higher oxidative stress for shorter periods, however further investigation is necessary to fully elucidate the mechanisms responsible.

Results for *P. aeruginosa* (Figure 6.9) demonstrate an enhancement in the efficacy of low irradiance 405-nm light for inactivation regardless of initial population density. When exposed at an initial density

of 10^3 CFU mL^{-1}, the dose required for an approximate 1 log_{10} reduction (Figure 6.9A) was 1.5 times greater when exposed using 150 mW cm^{-2} compared with lower irradiances. When exposed at an initial density of 10^5 CFU mL^{-1}, the same dose was required for an approximate 1 log_{10} reduction at all seeding densities (108 Jcm^{-2}; $P>0.05$). However, over this initial 1 log_{10} reduction, the efficacy of inactivation was shown to be significantly greater at lower irradiance: an initial dose of 36 Jcm^{-2} achieved 64.8% reductions using 5 mW cm^{-2}; 18.6% reductions using 50 mW cm^{-2}; and 12.5% reductions using 150 mW cm^{-2} ($P\leq0.05$). At initial densities of 10^7 and 10^9 CFU mL^{-1}, the dose required for an approximate 1 log_{10} reduction was 1.5-2 times lower when exposed using 5 $mWcm^{-2}$ compared to 150 mW cm^{-2}, with corresponding GE values significantly greater for 5 $mWcm^{-2}$ exposures compared to 150 $mWcm^{-2}$ ($P<0.001$; Figure 6.10B). Whilst the enhancement in GE observed for liquid-suspended bacteria (Figure 6.9) was not as definite as that observed for surface-seeded bacteria (Figure 6.3), it is worth noting that this may be due to the higher irradiances employed for liquid-suspended bacterial exposures: bacteria have limited viability in PBS over extended time periods, and thus this study was unable to expose suspensions to same irradiances employed for surface exposures, as previously discussed. The current results provide key evidence regarding the fundamentals of 405-nm light inactivation of liquid-suspended bacteria; however, for environmental decontamination purposes, it is important to consider efficacy under other conditions representative of practical system deployment, such as, as investigated in the previous chapter, efficacy for inactivation of bacteria exposed whilst suspended in biological media and dried on inert surfaces (Figure 5.12).

These species-specific differences in inactivation kinetics may be accounted for by the differences in light transmission through bacterial suspensions of varying density as shown in Figure 6.11. Results collected using the photodiode detector (Figure 6.11B) indicated minimal irradiance loss through both bacterial suspensions up to 10^8 CFU mL^{-1} ($P\geq0.132$); beyond which, irradiance loss significantly increased ($P<0.001$), with loss significantly greater through *S. aureus* suspensions compared to *P. aeruginosa* ($P=0.008$). Similar patterns were also demonstrated for spectrophotometric data (Figure 6.11A). These findings suggest irradiance penetration is unlikely to have influenced inactivation at exposure levels $\leq10^8$ CFU mL^{-1}; however, the limited light transmission demonstrated through 10^9 CFU mL^{-1} *S. aureus* samples, in comparison to equivalent *P. aeruginosa* and PBS samples, may explain why the inactivation kinetics of *S. aureus* exposed at this density deviated from overall findings of the study.

It is possible that the thicker layers of peptidoglycan surrounding this Gram-positive bacterium may increase 405-nm light attenuation, limiting inactivation as cell density increases, or that other factors, such as cellular production of light absorbing pigments, e.g. *S. aureus* carotenoids, may affect light penetration through dense populations. Further, at the higher cell densities investigated in this study, it is likely that bacterial clumping will result in shading effects which will likely influence light penetration through suspensions. These hypotheses align with a recent systemised review of current findings regarding microbial inactivation by violet-blue light exposure, which demonstrated a slight increase in the dose requirements for a 1 $\log_{10}$ reduction in bacteria upon increasing population density (Tomb *et al.* 2018). Further, Bumah et al. (2013) previously demonstrated that the bactericidal effect is not influenced by population density; however, reduced light penetration through suspensions will be limiting. Although contamination is unlikely to be presented at these higher densities, this study sought to examine how bacterial density, and thus shading, may affect 405-nm light inactivation. It is important to consider, however, only one Gram-positive and Gram-negative representative species were investigated here, and further study into the comparative interactions of 405-nm light with various Gram-positive and Gram-negative bacteria is essential.

The differing extents of bacterial reduction demonstrated in these studies following exposure to a common dose using different light delivery regimes suggests that the mechanism of 405-nm light photoinactivation, or its cellular targets, may vary depending on how light dose is delivered. To better comprehend the oxidative stress induced in the bacteria investigated in this chapter to low irradiance 405-nm light, and how it compares to that of higher irradiance exposures, two indicators of cellular damage – intracellular ROS production and membrane integrity – were assessed and compared.

Produced in excess, ROS can induce oxidative stress at levels sufficient to overwhelm cellular antioxidant defence systems and instigate lethal cellular damage (Ray *et al.*, 2012; Vatansever *et al.*, 2013), and previous studies have indicated that the bactericidal mechanism of 405-nm light inactivation is attributable to oxidative damage as a result of an overproduction of ROS within the cell (Ramakrishnan *et al.*, 2016). Experiments in this chapter assessed levels of ROS in bacteria upon exposure to a fixed dose of 405-nm light using different delivery regimes, to evaluate the influence of irradiance application on ROS generation. For both bacteria (Figure 6.13), no significant increase in fluorescence was detected in light-exposed samples ($P \geq 0.096$), however, in *P. aeruginosa* (Figure

6.13B), an upward trend was demonstrated as dose increased: 4-7 times greater levels of fluorescence were detected when exposed to 144 J cm^{-2} using 5 mW cm^{-2} compared to higher irradiances (P=0.231-0.764). Comparing these findings for *P. aeruginosa* with the inactivation kinetics presented in Figure 6.12 – whereby an upward trend in inactivation was demonstrated over time, and exposure to this same dose (144 J cm^{-2}) achieved 2.1-2.8 times greater log_{10} reductions when exposed to 5 mW cm^{-2} compared to higher irradiances – it is suggested that, as expected, 405-nm light inactivation of bacteria is the result of an overproduction of ROS with higher levels of ROS generated upon increasing doses; but also, importantly, the greater inactivation efficacy of lower irradiance exposures on a per-unit-dose basis likely arises from greater levels of intracellular ROS produced in response to such illumination.

It is important to highlight that the insignificance of these increases in fluorescence measured here warrants further study to substantiate the aforementioned hypothesis. Ramakrishnan *et al*. (2016) previously investigated green fluorescence generation from carboxy-H_2DCFDA upon incubation with *S. epidermidis* exposed to 405-nm light using 15 mW cm^{-2} for ≤6 h (≤324 J cm^{-2}) and, although results demonstrated a significant increase in fluorescence for exposures up to 3 h (P≤0.05), levels significantly reduced following 6 h exposure (P≤0.05). The authors attributed this to the high levels of dying cells at that stage, which would likely have damaged membranes: this may lead to leakage of intracellular esterases from the cell, thus implying less deacetylation of the non-fluorescent dye molecule (Ramakrishnan *et al.*, 2016). This hypothesis may also explain why minimal levels of ROS were detected for *S. aureus* exposures in this study: corresponding inactivation kinetics in Figure 6.12 demonstrate 48.0-72.9% reductions following 36 J cm^{-2}, and thus there is potential that from this exposure level onwards, cell membranes will have been sufficiently damaged to the extent that the majority of the dye – either acetylated or deacetylated – will have leaked from the cells prior to subsequent assessment. Ramakrishnan *et al*. (2016) also suggested that the lower fluorescence demonstrated after 3 h in their study could be due to an ability of cells to upregulate their intrinsic antioxidant capacities to counteract the increased ROS formation over time. However, similar to that concluded by Ramakrishnan *et al*. (2016), given the significant bacterial reductions demonstrated following all light exposures investigated in this study (Figure 6.12), it is likely that the limited fluorescence detected was due to the former hypothesis. *P. aeruginosa* demonstrated similar reductions following 36 J cm^{-2} (54.2-73.7%), so this hypothesis could also explain the insignificant and variable

fluorescence levels detected for this bacterium. Further, the half-life of ROS is extremely short (typically seconds; (Griendling *et al.*, 2016)) and it is therefore possible that the discrete measurements collected in this study over, by comparison, substantially greater exposure times (up to 6 h), will not be indicative of the full extent to which ROS is produced in response to such exposures. Findings in this chapter provide a snapshot of ROS levels at the given time of measurement, and it is likely that ROS produced prior will have decayed after a short time and thus be no longer detectable. Although indicating potential differences in species-specific oxidative stress in response to 405-nm light, results highlight the necessity to further investigate oxidative stress production in bacteria to better depict the effects of varying 405-nm light delivery, with particular interest in measuring cumulative ROS levels over an extended exposure period.

To assess the impact of differing 405-nm light delivery regimes on cellular damage, experiments in this chapter assessed and compared the extent to which the cell membrane is a favourable target of 405-nm light induced oxidative stress when exposed to a fixed dose using differing methods of light delivery, i.e. high intensity/short duration or low intensity/long duration. It is important to note that, as discussed, all cellular macromolecules – including lipids, proteins and nucleic acids – can be damaged by ROS (Devasagayam *et al.*, 2004), and thus various cellular components – including the cell membrane, DNA and virulence factors (McKenzie *et al.*, 2016; Biener *et al.*, 2017; Bumah *et al.*, 2017; Fila *et al.*, 2017; Kim and Yuk, 2017) – could be a target of the 405-nm light-induced oxidative burst. In this instance, cell membrane integrity was selected as a representative cellular structure for investigation due its relevance as a key damage indicator of 405-nm light exposure (Dai *et al.*, 2013b; McKenzie *et al.*, 2016). Future study to assess damage inflicted on other key cellular components, however, is essential to provide a broader understanding of the mechanisms of 405-nm light inactivation.

Results for both *S. aureus* and *P. aeruginosa* (Figure 6.14) demonstrate that exposure to increasing doses of 405-nm light increased absorbance readings at 260 nm, indicating an upward trend in the release of nucleic acids from light-damaged cells and thus increasing damage to cell membrane integrity. These findings correlate with the inactivation kinetics presented in Figure 6.12, and also previous findings by McKenzie *et al.* (2016), who investigated absorbance at 260 nm for both *E. coli* and *S. aureus* upon exposure to 405-nm light using 65 mW cm^{-2} for ≤180 min (≤702 J cm^{-2}) and similarly reported an increase in absorbance with increasing dose and inactivation levels.

Interestingly, when comparing the absorbance readings of this study on a per-unit-dose basis, discernibly different patterns were demonstrated for each bacterial species. For *S. aureus* (Figure 6.14A), no significant difference was demonstrated between the increase in absorbance upon exposure to each light intensity (P=0.358-0.851) – with the exception of exposures to 144 J cm^{-2}, where significantly greater increases were demonstrated using 50 mW cm^{-2} (P=0.001) – and, although statistically insignificant, lower increases in absorbance were demonstrated for 5 mW cm^{-2} compared to all other irradiances for exposures to ≥72 J cm^{-2}. These findings can be considered to correlate with the inactivation kinetics presented in Figure 6.12, whereby no significant differences were demonstrated between the surviving log_{10} counts of *S. aureus* upon exposure to these same irradiances (P≥0.081), but exposures to 5 mW cm^{-2} achieved significantly lower log_{10} reductions compared to both higher irradiances for exposures to ≥72 J cm^{-2}. Together, these findings suggest that the greater bacterial reductions demonstrated upon exposure to a fixed dose using 50-150 mW cm^{-2} compared to 5 mW cm^{-2} is possibly attributable to the greater extent of membrane damage inflicted upon exposure to the former. It is important to emphasise, however, the lack of statistical significance in these results, and thus further study would be required to fully support this hypothesis.

For *P. aeruginosa* (Figure 6.14B), greater increases in absorbance at 260 nm were observed when higher irradiances were used – with values shown to be significantly greater at all doses investigated when exposed using 150 mW cm^{-2} versus 5 mW cm^{-2} (P=0.01-0.033) – indicating greater leakage of nucleic acid material, and thus greater extents of membrane damage, when exposed to a fixed dose using higher irradiances. These findings conflict, however, with the inactivation kinetics presented in Figure 6.12, which demonstrate significantly greater inactivation per-unit-dose, in all cases, when exposed to 5 mW cm^{-2} compared to higher irradiances (P≤0.003). Together, these findings suggest that the cell membrane may not be the primary target of low irradiance 405-nm light inactivation, and damage to other cellular targets may be responsible for the greater inactivation demonstrated. Biener *et al*. (2017) previously observed that, for MRSA exposure to 405-nm light (135 mW cm^{-2} for ≤30 min), the damage induced on cellular membranes occurred drastically within the first 5 min, continuing slowly as exposure time increased. It is therefore possible that this immediate damage effect was similarly demonstrated here upon exposure to the higher irradiances (50-150 mW cm^{-2}), and that exposure to lower intensities over a longer exposure period, compared to higher intensities over a shorter exposure

period, may have produced a different damage response. As discussed in Chapter 2, the mechanism of 405-nm light inactivation is the result of widespread oxidative damage to various cellular targets within microbial cells; however, these studies suggest that the rate at which ROS is produced may influence the primary targets of damage. The studies performed in this chapter provide a preliminary indication of bacterial stress responses to low irradiance 405-nm light exposure, and how it compares to that of higher irradiance exposures; however, to comprehensively understand the underlying mechanisms responsible for these findings, it is essential that further investigation is conducted, particularly to assess the cumulative leakage of materials from cells over time.

It is also important to highlight that, to quantify the two cytotoxic parameters investigated in this study, bacterial populations were required to be exposed to light treatments at population densities of 10^9 CFU mL^{-1}. As demonstrated in Figure 6.12 and discussed previously, inactivation kinetics of *S. aureus* at this density followed a different trend to that demonstrated at all other population densities and for all other investigated bacteria. Further, these densities are substantially higher than levels that would be expected to contaminate healthcare surfaces, and so do not accurately depict cellular responses in those settings. It is possible that different results would be gathered when examining intracellular ROS production and membrane integrity of bacteria exposed at lower densities, and thus findings are likely limited by this.

6.7 Conclusions

Overall, this chapter has successfully demonstrated the broad-spectrum antimicrobial efficacy and enhanced GE of low irradiance 405-nm light for the treatment of a panel of key nosocomial pathogens. The experiments performed within this chapter were conducted using bacteria seeded on agar, to represent contamination on environmental surfaces; however, work was also expanded to include bacteria in suspension, to comprehensively indicate the effects of 405-nm light exposure on bactericidal efficacy. Key findings associated with this chapter are detailed as follows:

- Significant inactivation of ESKAPE pathogens was achieved at a range of bacterial cell densities with complete/near-complete (≥96%) inactivation demonstrated in all cases for lower irradiance (≤5 mW cm^{-2}) 405-nm light exposures.

- Comparisons indicated, on a per-unit-dose basis, significantly lower doses were required to achieve significant reductions of all species when exposed at lower irradiances, with the exception of *S. aureus* suspended at high cell density, suggesting that bacterial density, at normally occurring environmental levels, has minimal influence on decontamination efficacy.
- Preliminary investigations into the associated damage mechanisms and cellular targets of such exposures suggests that, for *P. aeruginosa*, this enhanced inactivation efficacy demonstrated at lower irradiances is associated with higher intracellular oxidative stress levels and lower levels of cellular membrane damage. Results for *S. aureus* were less conclusive, with experimental testing limited by the necessity to expose populations at higher bacterial densities. Further work to elucidate the photoinactivation mechanism associated with this species is therefore recommended.

This chapter provides fundamental evidence of the susceptibility of ESKAPE pathogens to low irradiance 405-nm light exposure, which, in conjunction with its established safety benefits, further supporting its use for infection control applications involving decontamination of occupied environments, or for treatments involving mammalian cell/tissue exposure.

CHAPTER 7

Antiviral Efficacy of Low Irradiance 405-nm Light

7.0 Overview

The recent COVID-19 pandemic has considerably heightened the necessity for novel strategies to safely decontaminate communal areas. As previously discussed, low irradiance 405-nm light has been shown to effectively provide safe and continuous decontamination of occupied room settings, and so may offer a potential means of controlling SARS-CoV-2 spread within the environment. This chapter establishes the antiviral efficacy of low irradiance 405-nm light for the inactivation of a SARS-CoV-2 surrogate, bacteriophage phi6. The susceptibility of phi6 to low irradiance 405-nm light was investigated at both low and high seeding densities and when suspended in both minimal and biologically-relevant suspension media, to additionally determine the influence of population and suspension media on viral susceptibility. Preliminary data demonstrating the susceptibility of phi6 to high irradiance 405-nm light were also conducted for comparative purposes. The findings in this chapter provide the first evidence to demonstrate the efficacy of low irradiance 405-nm light systems for the inactivation of a SARS-CoV-2 surrogate employed using parameters (irradiance and treatment distance) representative of practical system deployment.

7.1 Introduction

SARS-CoV-2 is a novel RNA coronavirus which instigated the ongoing COVID-19 pandemic and has caused, at the time of writing, over 578 million infections and 6.4 million deaths worldwide (WHO, 2022b); the highest number of global deaths in comparison to all other pandemics in the last century (Wilder-Smith, 2021).

SARS-CoV-2 is a positive-sense single-stranded enveloped RNA virus of the *Coronaviridae* family. The virus is approximately 0.1 μm in diameter with 80% resemblance to the phylogenetic identity of

SARS-CoV and 50% resemblance to Middle East respiratory syndrome coronavirus (Muralidar *et al.*, 2020; Laue *et al.*, 2021). The virus encodes four structural proteins (nucleocapsid protein, spike protein, membrane protein and envelope protein), sixteen non-structural proteins (nsp1-16) and additional accessory proteins (Wang *et al.*, 2020). The structural proteins, in combination with a lipid bilayer derived from the host cell, form the envelope and are responsible for delivering viral genomic RNA into the cell (Lamers and Haagmans, 2022). The non-structural proteins primarily mediate RNA processing, replication and transcription; and the accessory proteins often have immunoevasive properties (Lamers and Haagmans, 2022).

The virus is believed to have initially emerged in the city of Wuhan, China, in December 2019 (WHO, 2020a). The disease spread rapidly, being declared an international public health emergency by 30th January; the sixth outbreak to ever be classified in this manner (Eurosurveillance Editorial Team, 2020). On 11th March 2020, COVID-19 was declared a global pandemic, with over 118,000 deaths across 113 countries (WHO, 2020b). By 2020 year-end, an estimated 8 and 30% of HICs and LMICs government resources, respectively, were diverted to the COVID-19 response; resulting in overall diagnostic/ treatment delays and deteriorations in patient care (Bell *et al.*, 2022).

The disease is highly contagious (Hu *et al.*, 2021) and person-to-person transmission is believed to occur predominantly through contact with oral-nasal respiratory secretions and airborne droplets generated from infected individuals (Bak *et al.*, 2021; Zhou *et al.*, 2021). Consequently, it is well-recognised that poorly ventilated indoor communal spaces provide a significant risk of SARS-CoV-2 transmission (WHO, 2021b) and multiple COVID-19 outbreaks have been reported within crowded closed settings in which people are in close proximity for extended periods of time (Peng *et al.*, 2022). In addition, the virus has been shown to survive and remain viable in the environment for multiple days, and in some cases weeks, on various surfaces and fomites (Riddell *et al.*, 2020; van Doremalen *et al.*, 2020; Kasloff *et al.*, 2021), with the risk of exposure substantially increased at higher viral loads (King *et al.*, 2022). The disease can be presented asymptomatically, to mild illness in the form of a fever, cough and/or loss of taste and smell, to critical illness in the form of respiratory failure, septic shock and/or multiple organ dysfunction (National Institutes of Health, 2023). Recent findings have demonstrated that over half of transmission events occur in asymptomatic or pre-symptomatic individuals (Viana Martins *et al.*, 2022).

An enhanced understanding of the role of closed communal environments as a source of SARS-CoV-2 transmission has focussed attention on the importance of environmental cleaning and disinfection as a means of reducing disease spread. Established techniques for whole-room decontamination of public environments such as UV light has demonstrated sufficient efficacy towards the disinfection of SARS-CoV-2 (Heilingloh *et al.*, 2020; Inagaki *et al.*, 2020; Lorca-Oró *et al.*, 2022; Olagüe *et al.*, 2022), however, they are broadly limited to infrequent use in unoccupied and sealed environments due to their harmful radiation effects and long-term material degradation upon repeated exposure, as discussed in Section 2.3.3.6 (Matsumura and Ananthaswamy, 2004; Teska *et al.*, 2020).

Consequently, novel methods of environmental decontamination to augment current SARS-CoV-2 infection control procedures are continuously being sought. As discussed in Section 2.4, violet-blue 405-nm light technology offers a potential novel solution to enhance current environmental decontamination protocols, due to its ability to be applied at levels which can sufficiently decontaminate environments whilst also remaining safe for human exposure (Maclean *et al.*, 2010, 2014). The bactericidal efficacy of the 405-nm light EDS is well established, however, by comparison, the viricidal properties of the 405-nm EDS are less understood. Tomb *et al*. (2018) previously demonstrated that inactivation of non-enveloped viruses is possible in the absence of photosensitisers, but at much higher doses than that required by bacteria (approximately 10 times greater doses required for a 1 $\log_{10}$ reduction), suggesting the inactivation effect observed is possibly due to exposure to the low-level UV-A photon output (380-390 nm) at the tail-end of the 405-nm LED emission spectrum (Tomb *et al.*, 2014, 2017b). The authors additionally noted that viral susceptibility can be increased when suspended in photosensitive media including artificial saliva (Tomb *et al.*, 2014, 2017b); which was further corroborated by Kingsley *et al*. (2017), who demonstrated greater inactivation of non-enveloped Tulane virus when exposed in the presence of singlet oxygen enhancers.

Given the global impact of the COVID-19 pandemic, establishing the efficacy of 405-nm light for the inactivation of SARS-CoV-2 is of significant research interest. Rathnasinghe *et al*. (2021) recently demonstrated successful reductions of SARS-COV-2 upon exposure to low irradiance (0.035-0.6 mW cm^{-2}) 405-nm light, and additionally highlighted the increased susceptibility of lipid-enveloped viruses in comparison to non-enveloped viruses (identical irradiations achieved 2.3 $\log_{10}$ reductions in SARS-COV-2 after 8 hr and just 0.1 $\log_{10}$ reductions in a non-enveloped RNA virus after 24 hr);

suggesting the lipid envelope itself may instigate ROS production. Other studies have similarly demonstrated the susceptibility of SARS-CoV-2, or an appropriate surrogate, to 405-nm light inactivation when present on surfaces and in liquid media, both in the presence and absence of photosensitisers (Biasin *et al.*, 2021; Enwemeka *et al.*, 2021; Gardner *et al.*, 2021; Lau *et al.*, 2021; Vatter *et al.*, 2021). Although highly encouraging, these studies have primarily demonstrated inactivation using 405-nm light at high irradiances (≥78.6 mW cm^{-2}) or at low irradiances delivered at a very short distance (~2.3-25.4 cm) from the sample surface (Biasin *et al.*, 2021; Enwemeka *et al.*, 2021; Gardner *et al.*, 2021; Lau *et al.*, 2021; Rathnasinghe *et al.*, 2021; Vatter *et al.*, 2021), however, it is of great importance to determine if inactivation of SARS-CoV-2 can be achieved under conditions which more accurately represent those which would be safely and practically implemented for environmental decontamination of communal areas.

The aims of this chapter were therefore to investigate the antiviral efficacy of 405-nm light for the inactivation of SARS-CoV-2 under conditions representative of those implemented for whole-room decontamination of occupied environments. Based on the Hazard Group classification of SARS-CoV-2 (HG3) and the containment level of the laboratory utilised (BSL2), experimental testing on SARS-CoV-2 was not possible and so bacteriophage phi6 was instead employed as a coronavirus surrogate. Phi6 is a double stranded RNA lytic bacteriophage of the Cystoviridae virus family which infects *Pseudomonas* bacteria (Vidaver *et al.*, 1973; Yang *et al.*, 2016). It possesses similarities to that of coronaviruses (Figure 7.1), namely, it is of similar size, has spike proteins and is enveloped by a lipid membrane (Vidaver *et al.*, 1973; Yang *et al.*, 2016; Fedorenko *et al.*, 2020), and thus has been suggested and utilised as a surrogate for the study of SARS-CoV-2 in multiple publications (Fedorenko *et al.*, 2020; Rockey *et al.*, 2020; Bangiyev *et al.*, 2021; Ordon *et al.*, 2021; Vatter *et al.*, 2021; Ahuja *et al.*, 2022; Baker *et al.*, 2022; Dey *et al.*, 2022; Gomes *et al.*, 2022; Karaböce *et al.*, 2022; Zargar *et al.*, 2022).

In this chapter, the 405-nm light EDS was used to illuminate samples of bacteriophage phi6 as a surrogate for SARS-CoV-2 using low irradiance 405-nm light (0.5 mW cm^{-2}) at a distance of 1.5 metres, representative of the typical irradiance levels and distance of samples from the light source within occupied settings. Inactivation kinetics were established with the phage suspended in minimal media, to evaluate the effect of direct interaction between the light and the phage, and also, with the phage

suspended in artificial saliva in order to better replicate how the phage would interact with the light treatment when within respiratory secretions and droplets, as would likely be the case with clinical transmission. Inactivation kinetics were additionally established at two seeding densities representative of viral loads at two distinct sampling times from the onset of SARS-CoV-2 symptoms, to establish the impact of population density on inactivation efficacy. Comparison of the antiviral efficacy and GE of higher irradiance (50 mW cm^{-2}) 405-nm light sources for the inactivation of phi6 is also provided for comparison. The results of this chapter provide a means of evaluating the potential of this environmental decontamination technology to be used as a method of controlling transmission of SARS-CoV-2 within occupied healthcare settings and other public areas.

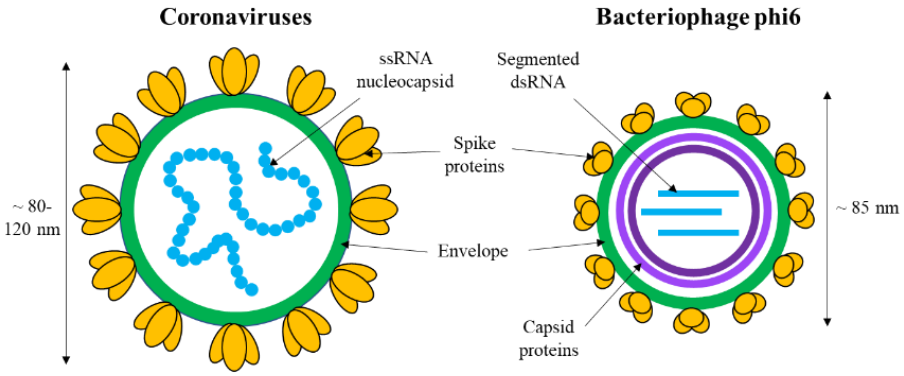

Figure 7.1 Structure of SARS-CoV-2, and comparison to its surrogate, bacteriophage phi6.

7.2 Methods

7.2.1 Bacteriophage and Host Bacterium

Bacteriophage phi6 (DSM 21518) and its host bacterium *P. syringae* (DSM 21482), both purchased from the Leibniz-Institute DSMZ German Collection of Microorganisms and Cell Cultures GmbH (Braunschweig, Germany), were used for experiments in this chapter. The propagation and cultivation of the bacteriophage and host bacterium, respectively, maintenance of stock populations and co-incubation and enumeration techniques required to conduct experiments using these microorganisms is detailed in Section 3.2. For experimental testing, phi6 populations were prepared and then serially diluted in SM buffer, as described in Sections 3.2.2-3.2.3, with the last dilution being in either SM buffer or artificial saliva, to provide starting populations of either 10^{3-4} PFU mL^{-1} or 10^{7-8} PFU mL^{-1}.

7.2.2 Media

For experimental testing, the bacteriophage was suspended in either minimal or organically-rich biological media. For the minimal media, SM buffer (G-Biosciences), consisting of 50mM Tris.HCl (pH 7.5), 100mM NaCl, 8mM $MgSO_4$ and 0.01% gelatin, was used. For the organically-rich biological media, artificial saliva was prepared as described in Section 3.3.

7.2.3 405-nm Light Source

The light sources used for bacteriophage exposures were the 405-nm light EDS (configuration 2; Figure 7.2A) and the ENFIS PhotonStar Innovate UNO 24-LED array (Figure 7.2D), as previously described in Sections 3.4.1 and 3.4.3, respectively. The 405-nm light EDS was mounted in place of a ceiling tile (Figure 7.2B) and the single 405-nm LED array was mounted on PVC housing (Figure 7.2E), both positioned directly above a surface for sample placement.

7.2.4 Exposure of Bacteriophage to 405-nm Light

For exposure, 3 mL suspensions of bacteriophage phi6, suspended at low (~$10^{3\text{-}4}$ PFU mL^{-1}) and high (~$10^{7\text{-}8}$ PFU mL^{-1}) seeding densities in SM buffer and artificial human saliva, were aliquoted into individual wells of a 6-well plate and positioned either 1.5 m below the 405-nm light EDS (Figure 7.2B), giving an incident irradiance of approximately 0.5 mW cm^{-2} at the sample surface, or 8.3 cm below the ENFIS PhotonStar Innovate UNO 24-LED array (Figure 7.2E), giving an incident irradiance of approximately 50 mW cm^{-2} at the sample surface. All 6-well plates were covered with an adhesive plate seal to prevent evaporation, and so irradiance measurements were taken through the material as described in Section 6.3.1.3 to ensure the desired irradiance reached bacterial samples. Samples were exposed to increasing doses of 405-nm light, with control samples held under standard laboratory lighting for equivalent exposure durations (‘ambient light controls’). To comparatively assess the impact of ambient light exposure on bacteriophage survival, additional control samples were held in complete darkness for the maximum duration of 405-nm light exposures (‘dark controls’). The temperature of microbial suspensions was monitored immediately prior and post light treatments (Kane May KM340 thermocouple; Comark Instruments, UK) to ensure inactivation was the result of light exposure and not heat effects. No significant increase in sample temperature was recorded with either high or low irradiance exposure.

Following exposure, the number of active phage in each sample were determined via co-incubation with *P. syringae* through the double agar overlay plaque assay method described in Section 3.2.4. The plates were then co-incubated at 25°C for 18-24 h, with surviving bacteriophage populations then calculated through enumeration of plaques in the bacterial lawns and expressed as PFU mL^{-1}. Results represent the mean values ± SD of a minimum of duplicate replicates measured in duplicate ($n \geq 4$), and are reported as bacteriophage load (log_{10} PFU mL^{-1}), bacteriophage reductions as compared to the equivalent non-exposed control samples (log_{10} PFU mL^{-1}) or GE values (Section 3.5.1).

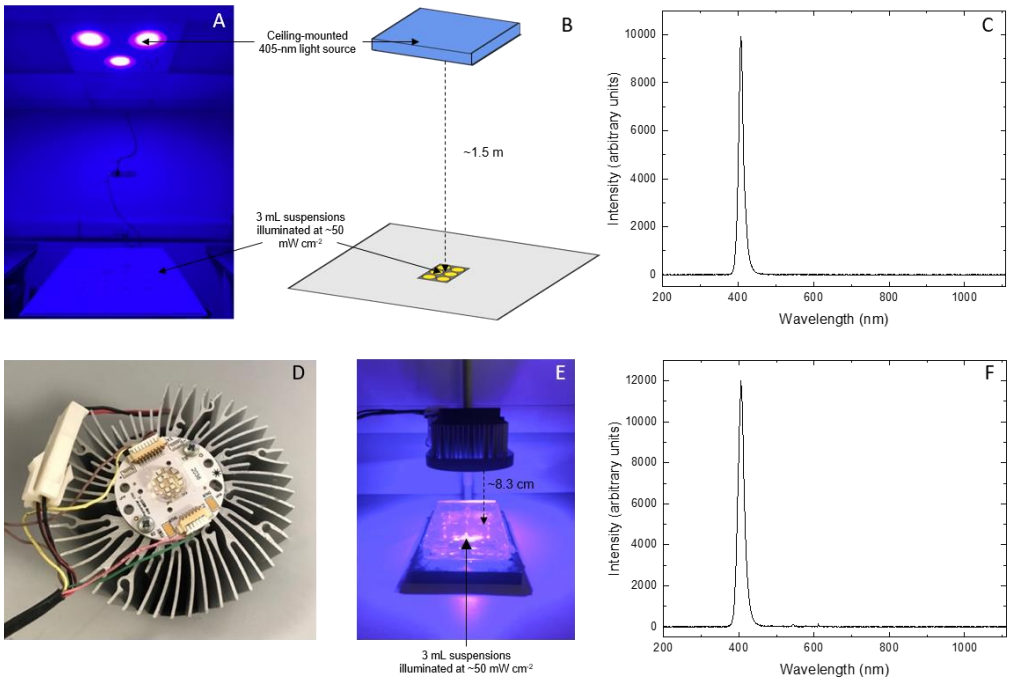

Figure 7.2 Light sources for exposure of bacteriophage phi6: (A) 405-nm EDS using in 'blue-only' mode, (B) diagrammatic representation of experimental arrangement and (C) emission spectra of the 405-nm output of the EDS; (D) single 405-nm LED array, (E) experimental arrangement and (C) emission spectra of the 405-nm output of the single LED array. All emission spectra data were captured using an HR4000 spectrometer (Ocean Optics, Germany) and Spectra Suite software version 2.0.151.

7.3 Results

The antiviral efficacy of low-irradiance 405-nm light for the inactivation of a SARS-CoV-2 surrogate presented in both minimal and biologically-relevant media, and comparative exposures to high irradiance 405-nm light, are provided in the following sections.

7.3.1 Inactivation of a SARS-CoV-2 Surrogate in Minimal and Biologically-Relevant Media using Low-Irradiance 405-nm Light

Results for the inactivation of low- and high-density populations of bacteriophage phi6 using 405-nm light at an irradiance of 0.5 mW cm^{-2} when exposed in both SM buffer and artificial saliva are presented in Figures 7.3 and 7.4, respectively. In all cases, significant inactivation was demonstrated ($P<0.05$).

At both low and high seeding densities, susceptibility was shown to be significantly enhanced when bacteriophage populations were exposed whilst suspended in artificial saliva compared to SM buffer ($P\leq0.05$). At low-density, exposure to 43.2 J cm^{-2} resulted in a maximum 2.41 log_{10} reduction in artificial saliva, compared to just 0.06 log_{10} reduction in SM buffer. For exposures in SM buffer, a greater dose of 172.8 J cm^{-2} was required to achieve a maximum 3.05 log_{10} reduction. Similarly, at high-density, a dose of 97.2 J cm^{-2} achieved a maximum 6.18 log_{10} reduction in artificial saliva, whereas a greater dose of 259.2 J cm^{-2} was required to achieve a maximum 6.28 log_{10} reduction in SM buffer. Collectively, results demonstrate that 405-nm light inactivation was 2.6-4 times more effective when the bacteriophage was suspended in saliva compared to SM buffer.

As hypothesised, the doses/treatment durations required to achieve complete/near-complete inactivation (approximately ≤1 log_{10} populations remaining) of phi6 populations were greater when exposed at high-density as opposed to low-density, however, results indicate that the dose required to achieve an approximate 1 log_{10} reduction in artificial saliva was the same when exposed at both low and high seeding densities (21.6 J cm^{-2}; 12 h). This differed when exposed in minimal SM buffer media, with an approximate 1 log_{10} reduction being achieved with 43.2 J cm^{-2} (24 h) in high density populations, but requiring >129.6 J cm^{-2} (>72 h) in low-density populations.

With regards to controls held in ambient lighting, natural decay of populations was evident over the extended exposure times for all phage suspensions ($P\leq0.05$), with reductions in saliva more apparent: at low density, a 0.38 log_{10} reduction was observed following 96 h in SM buffer, compared to a 0.61 log_{10} reduction after just 24 h in saliva and similarly, at high density, a 1.10 log_{10} reduction was observed after 144 h in SM buffer, compared to a 1.70 log_{10} reduction after 54 h in saliva. Compared to starting concentrations, controls demonstrated significant reductions ($P\leq0.05$) following 9 and 12 h of ambient light exposure for low- and high-density populations in saliva, respectively. Control populations in SM

buffer, by comparison, showed less variation ($P>0.05$), with significant reductions only observed following 96 h exposure to ambient light for low-density populations at 48 h, and again at 144 h for high-density populations ($P\leq0.05$). In contrast, control populations held in complete darkness demonstrated no significant decay over the extended durations in SM buffer ($P>0.05$) and, although decay was demonstrated in saliva ($P\leq0.05$), reductions were still significantly lower than that observed for samples held in ambient lighting. Following 24 h for low-density populations and 54 h for high-density populations, 0.61 and 1.70 $\log_{10}$ reductions were demonstrated in ambient lighting, respectively, compared to 0.60 and 0.51 $\log_{10}$ reductions demonstrated in complete darkness, respectively ($P\leq0.05$).

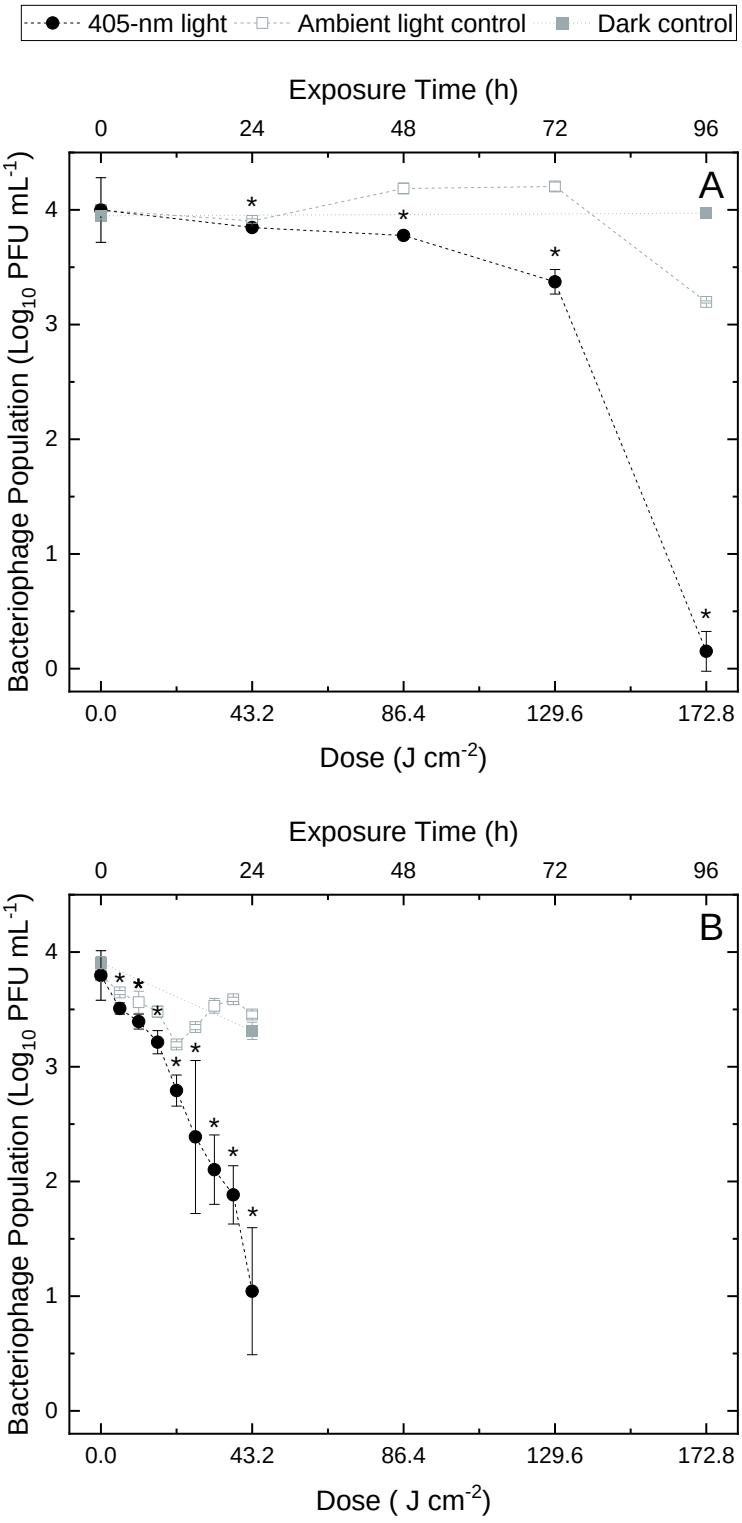

Figure 7.3 Inactivation of bacteriophage phi6 suspended in (A) SM buffer and (B) artificial human saliva at population densities of 10^{3-4} PFU mL^{-1} upon exposure to increasing doses of 405-nm light at an irradiance of ~0.5 mW cm^{-2}. Each data point represents the mean value ± SD ($n \geq 4$). Asterisks (*) indicate significant differences between exposed and non-exposed phi6 populations (two sample t-test; $P \leq 0.05$, Minitab Statistical Software v19).

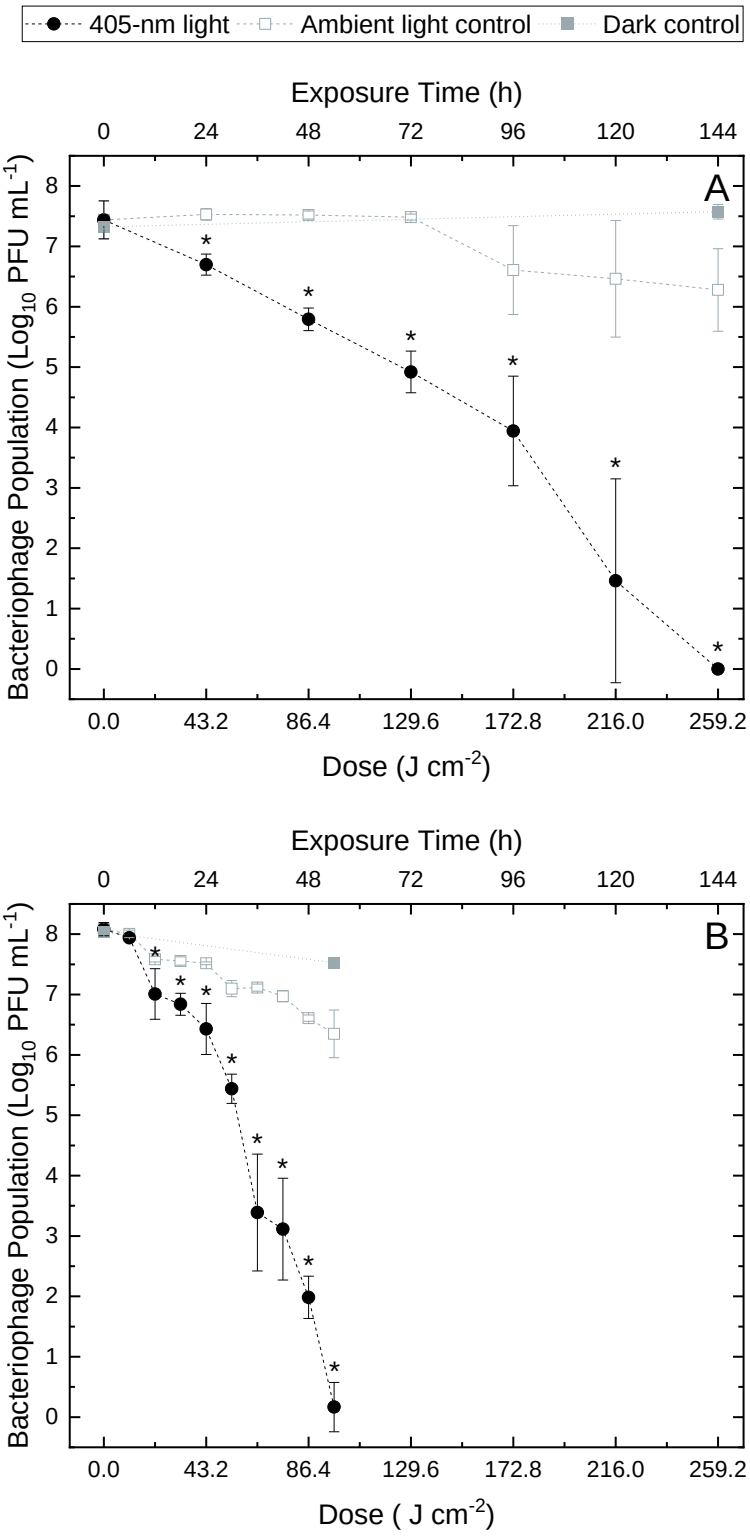

Figure 7.4 Inactivation of bacteriophage phi6 suspended in (A) SM buffer and (B) artificial human saliva at population densities of $10^{7–8}$ PFU mL^{-1} upon exposure to increasing doses of 405-nm light at an irradiance of ~0.5 mW cm^{-2}. Each data point represents the mean value ± SD ($n \geq 4$). Asterisks (*) indicate significant differences between exposed and non-exposed phi6 populations (two sample t-test; $P \leq 0.05$, Minitab Statistical Software v19).

7.3.2 Comparative Susceptibility of a SARS-CoV-2 Surrogate to Inactivation by High-Irradiance 405-nm Light

A comparison of the inactivation achieved for low- and high-density populations of bacteriophage phi6 exposed in both SM buffer and artificial saliva using 50 mW cm^{-2} 405-nm light is provided in Table 7.1. Samples were exposed to this higher irradiance light for durations which resulted in the dose delivered being equivalent to that required to achieve complete/near-complete (≥99.4%) bacteriophage inactivation when exposed to 0.5 mW cm^{-2} 405-nm light (Equation 3.1). The mean GE was calculated as described in Section 3.5.1 for bacteriophage inactivation under the various exposure conditions at both irradiance applications for comparative purposes.

Table 7.1 Comparison of the log_{10} reduction and germicidal efficiency values associated with 405-nm light inactivation of bacteriophage phi6 upon exposure to respective irradiances of 0.5 and 50 mW cm^{-2}. Each data point represents the mean value ± SD (n ≥ 4). Asterisks (*) represent values which are significantly higher than that of the other irradiance application (P≤0.05).

Exposure Conditions		Dose (J cm^{-2})	0.5 mW cm^{-2}		50 mW cm^{-2}	
			Log_{10} Reduction	GE	Log_{10} Reduction	GE
10^3 PFU mL^{-1}	SM Buffer	172.8	3.046 (±0.154)	0.018 (±0.001)	3.403* (±0.011)	0.020* (±0.000)
	Artificial Saliva	43.2	2.411* (±0.539)	0.056* (±0.012)	0.030 (±0.085)	0.002 (±0.002)
10^7 PFU mL^{-1}	SM Buffer	259.2	6.278* (±0.652)	0.024* (±0.003)	3.033 (±0.036)	0.011 (±0.000)
	Artificial Saliva	97.2	6.182* (±0.005)	0.064* (±0.005)	0.443 (±0.069)	0.004 (±0.001)

With the exception of low seeding density exposures in SM buffer, log_{10} reductions and GE values were significantly higher when exposed using 0.5 mW cm^{-2} as opposed to 50 mW cm^{-2} (P≤0.05). At low seeding density in artificial saliva, exposure to 43.2 J cm^{-2} achieved a 2.41 log_{10} reduction with a GE value of 0.056 using 0.5 mW cm^{-2} light in comparison to just a 0.03 log_{10} reduction and 0.002 GE using 50 mW cm^{-2} light (P≤0.05). Similarly, at high seeding densities, exposure to 97.2 and 259.2 J cm^{-2} in artificial saliva and SM buffer, respectively, resulted in greater inactivation and GE values when exposed using 0.5 mW cm^{-2} as opposed to 50 mW cm^{-2} (6.182-6.278 log_{10} reductions and GE values of 0.024-0.064 versus 0.443-3.033 log_{10} reductions and GE values of 0.004-0.011, respectively; P≤0.05). This trend was however not apparent with the low-density exposures in SM buffer, where similar (but

significantly different) inactivation and GE values were observed at each irradiance (3.403 log_{10} reduction and 0.020 GE for 50 $mWcm^{-2}$; 3.046 log_{10} reduction and 0.018 GE for 0.5 $mWcm^{-2}$; $P \leq 0.05$).

7.4 Discussion

The results in this chapter provide the first evidence demonstrating the efficacy of low irradiance 405-nm ceiling-mounted light systems for the inactivation of a SARS-CoV-2 surrogate, bacteriophage phi6, using parameters (irradiance and treatment distance) representative of practical system deployment. Importantly, results demonstrate the significant enhancement in phage susceptibility when exposed whilst suspended in artificial saliva: an important consideration given that the virus is commonly expelled into the environment within respiratory secretions.

For environmental decontamination applications involving occupied areas, it is essential that low irradiance (<1 $mWcm^{-2}$) 405-nm light sources are employed such that the illumination produced is within the limits considered safe for continuous human exposure (ICNIRP, 2013). For this study, exposures were conducted at approximately 1.5 m below the light source (using an irradiance of 0.5 mW cm^{-2}), with these parameters selected as being representative of the illumination expected within high-touch areas of a typical occupied public setting (Chapter 4).

The results of this chapter demonstrate bacteriophage phi6 can be successfully reduced when exposed in minimal SM buffer media; highlighting that 405-nm light inactivation is attainable in the absence of exogenous photosensitisers, as previously demonstrated for SARS-CoV-2 or appropriate surrogates (Gardner *et al.*, 2021; Lau *et al.*, 2021; Rathnasinghe *et al.*, 2021; Vatter *et al.*, 2021). Due to their lack of porphyrins, viruses and bacteriophages demonstrate the lowest susceptibility of all microorganisms to 405-nm light inactivation (Tomb *et al.*, 2018) and minimal inactivation has previously been indicated for non-enveloped viruses unless exposed to very high doses or suspended in organically-rich media (Tomb *et al.*, 2014, 2017b). As previously discussed in Chapter 2, the inactivation demonstrated in these studies may be the result of low-level UV-A exposure and/or 420-430 nm exposure at the tail ends of the 405-nm LED emission spectrum, which are known to induce oxidative damage to viral/phage proteins (Richardson and Porter, 2005; Girard *et al.*, 2011) and thus over extended time periods will likely induce such effects. Further, Rathnasinghe *et al*. (2021) recently demonstrated the significantly

enhanced susceptibility of enveloped viruses in comparison to non-enveloped viruses, hypothesising that the lipid envelope may be able to absorb 405-nm light wavelengths and contribute to the inactivation effect via either consequential ROS production instigating an oxidative effect, or simply destruction of the envelope. The results of this study can be considered to agree with this theory as, although significantly lower than that achieved when suspended in artificial saliva (i.e. in the presence of exogenous photosensitisers), statistically significant 0.06 and 0.83 $\log_{10}$ reductions of low- and high-density populations, respectively, were observed when exposed in SM buffer, after 24 h exposure ($P \leq 0.05$); suggesting the inactivation effect is likely somewhat accountable to light interactions with the phage envelope. In addition, the doses required for a 1 $\log_{10}$ reduction of high-density populations were found to be within the same orders of magnitude to that previously established for bovine coronavirus as a surrogate for SARS-CoV-2 exposed in PBS, which is also absent of photosensitive material (57.5 J cm^{-2} in comparison to 43.2 J cm^{-2} found in this study) (Lau *et al.*, 2021). Further investigation into the interactions of viral envelopes with 405-nm light, although beyond the scope of this thesis, will be essential in advancing understanding of its viricidal efficacy. It is also important to note

This chapter additionally evaluated the potential enhancement in phage susceptibility when exposed in artificial saliva; selected as it represents a significant vector media in the transmission of SARS-CoV-2 (Huang *et al.*, 2021). The mucins of saliva (or porcine stomach mucins as substituted in this thesis) contain light-sensitive chromophores that are likely predisposed to 405-nm light photosensitisation, and the potential for enhancing viral inactivation to 405-nm light has been previously demonstrated (Tomb *et al.*, 2017b). The hypothesis is that the photosensitive components within nutrient-rich media, such as saliva, can act as exogenous photosensitisers, absorbing the 405-nm photons and initiating Type I and Type II photodynamic reactions resulting in the local release of ROS which can impart oxidative damage to viral and phage structures in close proximity (Tomb *et al.*, 2014, 2017b). The results of this study are consistent with this theory, with 405-nm light inactivation significantly enhanced when exposed in artificial saliva compared to when in SM buffer: 83.3-87.5% and 50% less dose was required for a 1 $\log_{10}$ reduction of phi6 at low and high seeding densities, respectively. These results are comparable with that of previous findings (Tomb *et al.*, 2014, 2017b), which demonstrated 88-89% less dose was required for a 1 $\log_{10}$ reduction of both feline calicivirus and phage φC31, at similar population densities of 10^5 and 10^3 PFU mL^{-1}, respectively, when exposed to 405-nm light in organically-rich

media in comparison to minimal media. The dose requirements were significantly higher for feline calicivirus and φC31 in comparison to phi6 in this study (Tomb *et al.*, 2014, 2017b), however, it should be noted that both feline calicivirus and φC31 are non-enveloped and the increased susceptibility of enveloped vs non-enveloped viruses and bacteriophage to visible light inactivation is previously described (Hessling *et al.*, 2022). It is also of interest to note that the authors utilised significantly higher irradiances for viral and phage exposure than those employed here (155.8 and 56.7 mW cm^{-2}, respectively (Tomb *et al.*, 2014, 2017b)), suggesting this enhancement effect is apparent regardless of the light delivery method.

The log_{10} reductions and GE values shown in Table 7.1 indicate that lower irradiance 405-nm light is more efficient on a per-unit-dose basis for phage inactivation in comparison to that of equivalent higher irradiance exposures. At high seeding densities in both media, 0.5 mW cm^{-2} exposures achieved 2.07-5.79 greater log_{10} reductions and 2.18-16 times greater GE values than that of 50 mW cm^{-2} exposures. Similarly, in artificial saliva at low seeding densities, 0.5 mW cm^{-2} exposures achieved a 2.35 greater log_{10} reduction and a 28 times greater GE value than that of 50 mW cm^{-2} exposures. This trend was not demonstrated for low density exposures in SM buffer, with similar inactivation and GE values observed: this is most likely due to the fact that the time to apply this required dose using 50 mW cm^{-2} light (57.6 min) was, in this case, still sufficient to achieve complete inactivation of low-density populations and it is likely that sub-lethal doses would elucidate greater variation.

This enhancement in susceptibility observed with lower irradiance treatments is consistent with data gathered in previous studies. Vatter *et al*. (2021) exposed a 10^7 PFU mL^{-1} phi6 population in SM buffer to 405-nm light at a higher irradiance of 78.6 mW cm^{-2} and the dose required to achieve a 3 log_{10} reduction was significantly higher than that required in this study: approximately 1300 J cm^{-2} in comparison to approximately 129.6 J cm^{-2}. This is further corroborated by the recent findings of Rathnasinghe *et al*. (2021) who demonstrated that 405-nm light at a lower irradiance of 0.035 mW cm^{-2} could achieve a 1.03 log_{10} reduction of 10^5 PFU mL^{-1} SARS-CoV-2 following 24 h exposure (3.024 J cm^{-2}); a lower dose than that required at 0.5 mW cm^{-2} for similar 1 log_{10} reductions of 10^3 PFU mL^{-1} populations (>129.6 J cm^{-2}) and 10^7 PFU mL^{-1} populations (43.2 J cm^{-2}) in this study. This effect has also previously been demonstrated for nosocomial bacteria suspensions in Chapter 6 (Figures 6.4, 6.8 and 6.9), with evidence demonstrating up to six times less energy required to achieve

complete/near-complete (≥95.1%) inactivation when exposed using 5 mW cm^{-2} compared to 150 mW cm^{-2}, on a per-unit-dose basis. This is the first time, however, the enhanced efficacy of low irradiance 405-nm light, on a per-unit-dose basis, has been proposed for bacteriophage inactivation. It is suggested that delivering an identical 405-nm light dose using low irradiances over a longer exposure time may provide adequate time for either the 405-nm or low-level UV-A light exposure to evoke an antimicrobial effect on bacteriophage populations; whilst high irradiances over a shorter exposure time (up to 4.5 h in the case of Vatter *et al*. (2021)) may be insufficient. The results of the present study, both independently and when compared to the results of relevant earlier studies, provides fundamental evidence of the enhanced susceptibility of bacteriophage phi6 to 405-nm light when exposed at lower irradiances, further strengthening the proposal of visible violet-blue light systems for environmental decontamination of SARS-CoV-2. Further investigation into the associated photochemical mechanisms involved in 405-nm light inactivation of bacteriophage phi6 is required to further elucidate these findings and augment clinical translatability of this technology.

The high and low population densities utilised in this study were selected to represent the typical viral loads presented in the saliva of individuals infected with SARS-CoV-2 at day 0 (~10^7 copies mL^{-1}) and at day 24 (~10^3 copies mL^{-1}) post-symptom onset, respectively (Zhu *et al.*, 2020). The greater dose requirements for complete/near-complete inactivation at higher densities shown in this chapter has previously been demonstrated for the *Streptomyces* phage φC31 (Tomb *et al.*, 2014) and also in bacterial studies (Maclean *et al.*, 2009; Bumah *et al.*, 2013). For exposures in artificial saliva, the dose requirements for a 1 log_{10} reduction in low and high phi6 populations were similar ($P>0.05$), and this is comparable to the levels of φC31 inactivation at population densities of 10^3, 10^5 and 10^7 PFU mL^{-1} previously studied (Tomb *et al.*, 2014), suggesting bacteriophage density has little impact on the viricidal properties of 405-nm light when suspended in a nutrient rich medium. This is potentially due to the external photosensitisers present in the saliva, which are likely to elicit inactivation in a similar mechanism to bacterial inactivation and so would thus demonstrate similar levels of antimicrobial efficacy regardless of population density (Tomb *et al.*, 2018). Interestingly however, this same effect was not observed in minimal media: the dose required to achieve an initial 1-log_{10} reduction was significantly less for the higher population density in comparison to the lower population density (24 h exposure in comparison to 72-96 h exposure; $P\leq0.05$); however, once the higher density population was

reduced to an approximate 10^{3-4} PFU mL^{-1} population, akin to the lower density population, the dose requirements for the final 3-log_{10} reduction of both populations were identical (48 h exposure; ($P>0.05$). A possible explanation for this observation is that, at higher seeding densities, there are a significantly higher number of phage particles available to interact with the light photons, and so it is likely the maximum quantity of phage particles will be interacting with available photons at any given time, thus maximising the efficiency of photoinactivation. As populations become reduced, there will be fewer phage particles available to interact with light photons, and so it is likely that a larger proportion of photons will not be targeting a phage particle in the media and will be disengaged from the photoinactivation process, due to a lack of photosensitive material in the suspension media, reducing the efficiency of inactivation. Further research into this observation is required to fully understand the interaction and inactivation of phage particles upon 405-nm light exposure.

For all exposures, ambient light control populations were found to decrease significantly over time in comparison to their starting populations ($P\leq0.05$), with decay occurring significantly earlier in saliva compared with SM buffer suspensions ($P\leq0.05$). These findings are consistent with previous work by Tomb *et al*. (2014), who demonstrated that broadband lighting was also capable, albeit much less efficiently than that of 405-nm light, of inducing photosensitiser excitation for phage inactivation. It is expected that phage populations will naturally decay over an extended time period (DSMZ, 2014), and this effect will likely be enhanced in the presence of external photosensitisers. This theory was further corroborated by the inclusion of controls held in complete darkness in this chapter, which showed no significant decay in SM buffer ($P>0.05$), and some decay in saliva ($P\leq0.05$), albeit significantly less than that observed in ambient lighting ($P\leq0.05$). These results are encouraging as they suggest that, not only will the 405-nm light inactivation of SARS-CoV-2 occur more efficiently when exposed in saliva, SARS-CoV-2 will also be unlikely to survive for extended periods of time in occupied environments irrespective of treatment. Regardless of decay observed, exposed populations were significantly lower than that of control populations for the durations of treatments ($P\leq0.05$) and so it can be deduced that 405-nm light exposure did significantly decrease phi6 populations in all cases.

7.5 Conclusions

Overall, the findings of this chapter have successfully demonstrated the ability of low irradiance antimicrobial 405-nm light systems to inactivate bacteriophage phi6 populations, as a surrogate for SARS-CoV-2. Key findings associated with this chapter are detailed as follows:

- Complete/near-complete inactivation of bacteriophage phi6 suspended in minimal media was successfully demonstrated within 4 days for low-density populations (3.1 $\log_{10}$ reductions) and 6 days for high-density populations (6.3 $\log_{10}$ reductions); suggesting 405-nm light viral inactivation is possible in the absence of exogenous photosensitisers.
- The susceptibility of phi6 to inactivation was significantly enhanced when suspended in artificial saliva, which is known to possess photosensitisers, in comparison to minimal media (requiring 83.3-87.5% and 50% less dose for a 1 $\log_{10}$ reduction at low and high seeding densities, respectively). These findings suggest photosensitive components within artificial saliva can act as exogenous photosensitisers and impact localised oxidative damage to phage structures in close proximity.
- Comparisons indicated, on a per-unit-dose basis, lower irradiance (0.5 mW cm^{-2}) 405-nm light was more efficient for phage inactivation than that of higher irradiance (50 mW cm^{-2}) light sources, with up to 28 times greater GE demonstrated.

The exposure conditions used in these instances were chosen to replicate those employed for the decontamination of whole-room environments and as such, findings enhance understanding of the antimicrobial capabilities of low irradiance 405-nm light systems. In conjunction with its established safety benefits, this furthers the implementation of this technology as a novel approach to achieve widespread decontamination within occupied settings and help tackle environmental transmission of COVID-19, and potentially other common viral infections such as influenza and the common cold. An evaluation of the efficacy of 405-nm light for the inactivation of aerosolised SARS-CoV-2 without the use of a surrogate, across a greater range of irradiances likely to be produced by these systems in a typical room setting, will be essential to further implementation of low-irradiance 405-nm light systems for environmental decontamination purposes.

CHAPTER 8

Conclusions & Recommendations for Future Work

8.0 Overview

This thesis was conducted to generate new information on the antimicrobial efficacy and GE of low irradiance 405-nm light technology, with specific regard to its application for continuous environmental decontamination. This chapter will summarise the key findings from each section of this thesis, and discuss recommendations for future work to augment clinical translatability of the technology.

8.1 Conclusions

8.1.1 Antibacterial Efficacy of the 405-nm Light EDS

The experimental work in Chapter 4 sought to characterise the irradiance output profile of a 405-nm light EDS, and then establish the broad-spectrum antibacterial efficacy of irradiance levels within this range for the inactivation of clinically-relevant bacteria.

Optical output profiling of the 405-nm light EDS installed centrally in a typical 32 m^3 room recorded irradiances in the range 0.001-2.066 mW cm^{-2}; with values shown to decrease as both linear and angular displacement from the light source increased. From these results, the irradiance level recorded at a distance of ~1.5 m below the light source (~0.5 mW cm^{-2}) was employed for subsequent bacterial testing to represent the typical distances between the light source and high-touch surfaces within public areas.

The broad-spectrum antibacterial efficacy of the 405-nm light EDS using 0.5 mW cm^{-2} was successfully established, with ≥93.28% inactivation (~2 log_{10} reductions) demonstrated within exposure times realistic of those employed for environmental decontamination (2-16 h; 3.6-28.8 J cm^{-2}). Spatial analysis of the decontamination efficacy indicated that shorter treatment times were required for significant levels ($P \leq 0.05$) of inactivation when exposed closer to the light source, thus at higher irradiances; however, on a per-unit-dose basis, inactivation efficacy was enhanced when exposed at

lower irradiances. Despite variation, significant reductions ($P \leq 0.05$) were achieved in all cases – using irradiances ≤0.021 mW cm^{-2} – suggesting these factors will unlikely have a substantial impact on the overall inactivation achieved, and that longer exposures may be required for adequate decontamination of surfaces further from the light source.

Overall, these findings provide a comprehensive laboratory evaluation of the broad-spectrum antibacterial efficacy of the 405-nm light EDS for surface-simulated decontamination. This furthers the work of previous studies which have demonstrated the clinical efficacy of the 405-nm light EDS, as discussed in Section 2.4.2, by elucidating the inactivation kinetics of key clinical pathogens exposed to 405-nm light using irradiances (≤1 mW cm^{-2}) and exposure distances (up to 2.56 m) typically expected with practical deployment. These findings, in combination with its inherent safety benefits, furthers the understanding of this technology for environmental decontamination applications.

8.1.2 Operational Considerations Associated with the 405-nm Light EDS

The experimental work conducted in Chapter 5 sought to build upon the results of the previous chapter by investigating the efficacy of the 405-nm light EDS for inactivation of microbial contamination under a range of conditions representative of those likely to be encountered within dynamic clinical settings.

A miniaturised 405-nm light EDS prototype was developed to enable bench-top testing of the range of irradiance levels (0.001-2.066 mW cm^{-2}) typically emitted from the ceiling-mounted EDS. Testing evaluated the antibacterial efficacy of 405-nm light at the lower range of irradiances produced within a whole room setting (≤0.31 mW cm^{-2}), and in all cases, results demonstrated greater reductions upon increasing dose ($P \leq 0.032$); implying that with continuous use, consistently low levels of contamination have the potential to be maintained. An exception to this was exposures to 0.001 mW cm^{-2} - the lowest irradiance tested - where no significant reductions were demonstrated within 7 days ($P \geq 0.089$); implying the ROS produced were within levels capable of being detoxified by antioxidant defence mechanisms.

Inactivation of bacteria suspended in clinically-relevant substances known to contain photosensitisers was additionally established, with susceptibility significantly enhanced when exposed in artificial human saliva compared to PBS ($P < 0.001$). Significantly longer exposures were required to achieve significant reductions in whole blood and faeces, which was likely due to the limited penetrability of 405-nm light. The efficacy of the 405-nm light EDS was then established for bacteria dried onto

common healthcare surfaces, with results indicating ≥0.59 log_{10} reductions following 4 h exposure and ≥2.0 log_{10} reductions following 24 h exposure on all materials investigated; providing a more comprehensive understanding of the practical exposure times likely required to achieve adequate inactivation on healthcare surfaces. These studies emulated realistic clinical deployment, whereby bacteria are likely to be either suspended or associated with biological substrates, which may contain photosensitive media capable of enhancing ROS generation and inactivation; or stressed via desiccation on surfaces, thus likely enhancing their susceptibility to inactivation.

This study was then furthered to assess the efficacy of the 405-nm light EDS against bacterial biofilms - both in terms of the potential to inhibit the formation of, and inactivate established, monolayer and mature biofilms, on inert surfaces. Results indicated that exposure to 0.5 mW cm^{-2} 405-nm light inhibited the development of both monolayer and mature biofilms on all surfaces by 0.35-0.94 and 2.8-4.6 log_{10}, respectively; and inactivated formed monolayer and mature biofilms by 0.92-1.71 and 0.78-2.41 log_{10}, respectively, following 24 h exposure. Contact angle measurements of the four clinical surfaces indicated that wettability may be influential on the adherence and subsequent inactivation of bacteria using 405-nm light; however, it is likely that other surface characteristics, such as roughness, will also be influential.

Overall, these findings provide further insight into the efficacy of the 405-nm light EDS under conditions more tangible to those expected within dynamic healthcare environments, which will be crucial in augmenting clinical translatability.

8.1.3 Bactericidal Efficacy and Energy Efficiency of Low Irradiance 405-nm Light

On the basis of the aforementioned results, Chapter 6 sought to establish the GE of low irradiance 405-nm light in comparison to that of higher irradiance exposures, on a per-unit-dose basis, for bacterial inactivation. Testing, using the ESKAPE pathogens, focused initially on inactivation of surface-seeded bacteria at various population densities – representative of differing degrees of surface contamination – but also expanded to establish the efficacy of 405-nm light for inactivation of bacteria in suspension, coupled with investigation of the associated cytotoxic responses within the exposed bacteria.

Complete/near-complete (≥96%) inactivation was demonstrated in all cases for lower irradiance (≤5 mW cm^{-2}) exposures. Comparisons indicated, on a per unit dose basis, that significantly lower doses

were required for significant reductions of all species when exposed at lower irradiances: 3-30 J cm^{-2}/0.5 mW cm^{-2} compared to 9-75 J cm^{-2}/50 mW cm^{-2} for low density (10^2 CFU $plate^{-1}$) surface exposures and 22.5 J cm^{-2}/5 mW cm^{-2} compared to 67.5 J cm^{-2}/150 mW cm^{-2} for low density (10^3 CFU mL^{-1}) liquid exposures ($P \leq 0.05$). Similar patterns were observed at higher population densities – excluding *S. aureus* exposed at 10^9 CFU mL^{-1}, whereby light transmission was shown to be significantly hampered in comparison to that of both lower densities and *P. aeruginosa* – suggesting bacterial density, at levels likely to contaminate healthcare environments, has minimal influence on decontamination efficacy.

In terms of bacterial cytotoxic responses to such exposures, greater levels of intracellular ROS were indicated in *P. aeruginosa* when exposed to a fixed dose using lower irradiances, corresponding with the inactivation data. However, enhanced nucleic acid leakage was demonstrated for *P. aeruginosa* when exposed to a fixed dose using higher irradiances, suggesting the cellular membrane may not be the target of low irradiance 405-nm light inactivation. Results for *S. aureus* were more variable, highlighting the potential species-specific differences in response to 405-nm light treatment and the necessity for further study to clarify this effect. These studies required exposures of 10^9 CFU mL^{-1} bacterial suspensions; which for *S. aureus*, demonstrated different inactivation trends to those performed at lower densities. It is thus important to consider the potential bearing this may have had on results, and that testing at lower densities, better representative of typical contamination levels within the environment, may have produced differing findings.

Overall, these studies provide fundamental evidence of the enhanced susceptibility of ESKAPE pathogens to low irradiance 405-nm light, on a per-unit-dose basis, at normally occurring environmental contamination levels. This enhanced efficacy was associated with higher levels of ROS and lower levels of membrane damage for *P. aeruginosa*, with results for *S. aureus* less conclusive. In conjunction with its established safety benefits, these findings further promote use of the technology for environmental decontamination, or indeed any treatments involving exposure of sensitive tissues or materials.

8.1.4 Antiviral Efficacy of Low Irradiance 405-nm Light

Given its clinical relevance at the time of this thesis, the experimental work in Chapter 7 aimed to assess the antiviral efficacy of the 405-nm light EDS for the inactivation of bacteriophage phi6, as a surrogate for SARS-CoV-2. The influence of population density and suspension media on viral inactivation was

additionally assessed, and preliminary investigations into the comparative efficacy of higher irradiances of 405-nm light for phi6 inactivation were conducted.

Findings indicated phi6 could be successfully inactivated upon exposure to low irradiance 405-nm light, at both low and high seeding densities in SM buffer and biologically-relevant artificial saliva. Successful reductions in minimal media indicated the ability of 405-nm light to inactivate a SARS-CoV-2 surrogate in the absence of external photosensitisers; hypothesised to be due to light interactions with the phage envelope (Rathnasinghe *et al.*, 2021). Results indicated enhanced inactivation – requiring 50-87.5% less dose for a 1 $\log_{10}$ reduction – when exposed in artificial saliva compared to SM buffer, hypothesised to be due to photosensitive components within the suspension acting as external photosensitisers. These findings were of particular clinical significance given saliva represents a common vector media in SARS-CoV-2 transmission (Huang *et al.*, 2021). Significantly longer exposure times – approximately 1.5-2.3 times greater – were required for complete/near-complete (99.4%) inactivation of higher density populations; however, the dose requirements for a 1 $\log_{10}$ reduction were similar regardless of seeding density; suggesting potential efficacy of the technology to inactivate SARS-CoV-2 at various viral loads.

The efficacy of higher irradiance 405-nm light for phi6 inactivation was established and compared to that of the lower irradiance exposures conducted, with findings indicating enhanced inactivation (2-28 times greater GE) in all cases when exposed using 0.5 mW cm^{-2} compared to 50 mW cm^{-2}. This was potentially due to either the extended exposure periods associated with the lower irradiance regimes providing greater time for the light exposure to evoke an antimicrobial effect, or currently unknown differences in the response of photosensitive materials to low irradiance/longer exposure periods compared to higher irradiance/short exposure times.

Overall, these studies successfully demonstrated the ability of low irradiance 405-nm light to inactivate bacteriophage phi6 populations at both low and high seeding densities in both minimal and biologically-relevant media, with susceptibility significantly enhanced when exposed in suspension media known to contain photosensitisers. These findings indicate the potential for this novel technology to reduce environmental levels of SARS-CoV-2, and thus subsequently reduce COVID-19 transmission, within

indoor public spaces, along with its potential capacity to inactivate a range of other viral infections such as Influenza (Rathnasinghe *et al.*, 2021).

8.2 Recommendations for Future Work

8.2.1 Mechanism of 405-nm Light Inactivation

To better understand the suitability of 405-nm light for different applications, it is essential that further research to elucidate the exact inactivation mechanisms for both bacteria and viruses is conducted.

Studies conducted in this thesis have indicated that the cytotoxic responses of bacteria to a fixed dose of 405-nm light likely differ when exposed using low irradiance/long duration times versus high irradiance/short duration times. As previously discussed in Chapter 6, this thesis performed a preliminary investigation into the damage inflicted upon microbial cells in response to such exposures, however it is essential that future work further establishes the mechanisms accountable for these differences in order to enable treatments to be tailored for specific applications. It is firstly recommended that levels of intracellular oxidative stress produced in response to such exposures is further explored using additional methods for detection of ROS, such as OxyELISA^{TM} analysis (Krisko and Radman, 2010) and measurement of glutathione oxidation (Ramakrishnan *et al.*, 2016), and also for the detection of individual ROS; to comprehensively enhance understanding of the levels of oxidative stress, and the relative contribution of each species, generated in bacterial cells in response to such exposures. It is also recommended that microbial antioxidant levels are measured, using spectrometry or chromatography techniques for example, to better understand how cellular ROS defence mechanisms comparatively react to a fixed dose of 405-nm light delivered using relatively gentle oxidative stress levels for a prolonged time period, versus higher levels of oxidative stress delivered over a shorter time period. As previously discussed in Chapter 6, the ROS detection methods utilised in this thesis could only provide an indication of ROS levels at the time a measurement was taken. Samples were collected from bacteria exposed to identical doses to ensure adequate comparisons could be made; however, given the different irradiances employed, this resulted in bacterial populations being exposed to light treatments for substantially different time periods before measurements were taken (varying from minutes to hours). Given the short diffusion distance of ROS, it is likely that any

ROS produced prior to measurement would have decayed and thus be no longer detectable, with this effect likely to be heightened over longer exposure periods (and thus lower irradiances). The inability to characterise ROS production continuously and cumulatively was a limiting factor in these studies, and it is therefore of interest to measure oxidative stress levels over extended periods when exposed using low irradiance/long duration times versus high irradiance/short duration times. This could possibly be achieved using electrochemical sensing methods, which are growing in popularity for the real-time measurement of ROS at the single-cell level (Zhang *et al.,* 2017; Ma *et al*., 2023).

It is also suggested that, upon exposure to a fixed dose of 405-nm light using low irradiance/long duration exposures versus high irradiance/short duration exposures, the extent of damage exerted on precise cellular targets is further examined by employing additional assessment techniques. To provide a more comprehensive understanding of how these exposures affect the cell membrane, it is recommended that differences in permeability, efflux activity and transmembrane potential are quantified and compared (McKenzie *et al.*, 2016; Biener *et al*., 2017). It is also important that other cellular elements are examined, including DNA, lipids and proteins, using techniques such as lipid peroxide assays, SDS-PAGE, the Comet assay and Western blotting (St. Denis *et al.*, 2011b; Oh *et al.*, 2015; Kuchařová *et al.*, 2019). A greater understanding of these mechanisms will be essential in the appropriate design of light treatments for specific applications.

As previously discussed in Chapter 6, experiments performed in this thesis to assess damage mechanisms associated with exposure to a fixed dose using low irradiance/long duration times versus high irradiance/short duration times were limited in that they required exposure of bacteria at densities of 10^9 CFU mL^{-1} – much higher than typically expected environmental contamination levels – such that the techniques employed to measure oxidative stress and membrane damage could yield quantifiable results. The bacterial inactivation kinetics at this density level demonstrated differing characteristics to those at all other seeding densities, most likely due to the limited penetration of light through the samples. It is thus suggested that future studies assess cellular damage using techniques which would not require work to be conducted at such a high seeding density, such as measuring the loss of salt and bile tolerance as an indicator of membrane damage (McKenzie *et al.*, 2016), in order to better understand bacterial responses to such exposures at levels better representative of those likely to be found as contamination in clinical settings.

The mechanisms associated with 405-nm light inactivation of viruses is still relatively unknown, and various research questions pertaining to the antiviral efficacy of 405-nm light require attention. It is initially important to establish the exact mechanism of viral inactivation in the absence of external photosensitisers. It is suggested that future studies expose viruses to a broadband UV-visible light source and employ a selection of narrow bandpass filters to identify the causative wavelength range associated with viral inactivation. This would facilitate an enhanced understanding as to the comparative contributions of UV-A exposure at the tail end of the 405-nm light emission spectrum, and 405-nm wavelengths individually, in the antiviral effects observed. Further, previous studies have indicated an enhanced susceptibility of enveloped versus non-enveloped viruses to 405-nm light inactivation, likely due to cytotoxic interactions with the envelope (Rathnasinghe *et al.*, 2021), and it is thus of interest to further examine the mechanisms associated with inactivation of both viral sub-types. It is suggested that levels of ROS generated in both enveloped and non-enveloped viruses in response to identical light exposures is measured to indicate if 405-nm light is indeed absorbed by the envelope, and if this induces oxidative stress. Further, it is recommended that the exact viral targets of 405-nm light inactivation are identified. This could be achieved via integrity assessment of viral genomes, nucleocapsids and envelope proteins, using techniques such as scanning and transmission electron microscopy, PCR, gel electrophoresis and OxyELISA analysis, for example. These findings would ultimately enhance understanding of the antiviral mechanisms of 405-nm light exposure, and better justify its implementation for broader infection control applications.

Furthermore, studies conducted in this thesis have indicated variations in both bacterial and viral susceptibility to 405-nm light inactivation when exposed in the presence and absence of external photosensitisers, and thus it is recommended that future work further establishes the contribution of such additives to cellular inactivation. To indicate damage imparted by exogenous photosensitisers on microbial cells, the extent of damage to various cellular targets, as previously discussed, could be comparatively assessed when microbes are suspended in both minimal media and nutritious media known to contain photosensitive components. It will be of interest to determine whether ROS generated outside the cell primarily imparts damage to exterior microbial structures, such as cellular membranes/envelopes, in comparison to more interior structures such as DNA or RNA structures, given the short lifespan and diffusion distance of ROS (Moan, 1990). Given the likelihood that biological

fluids known to contain photosensitive components will constitute vector mediums for microbial transmission, an enhanced understanding of the influence of external photosensitisers on 405-nm light inactivation will be crucial in evaluating the technology for practical infection control applications.

8.2.2 Antibacterial Efficacy of the 405-nm light EDS

Studies conducted in this thesis have successfully demonstrated the broad-spectrum antibacterial efficacy of the 405-nm light EDS. There are, however, additional areas of research which require addressing to support widespread implementation of this technology.

It is firstly recommended that clinical studies investigating the broad-spectrum antibacterial efficacy of the 405-nm light EDS are conducted to substantiate the findings of the laboratory studies conducted in this thesis. As discussed, previous clinical investigations of the 405-nm light EDS have primarily demonstrated general reductions in bacterial contamination levels using contact agar plate sampling of staphylococcal-type organisms or total viable bacterial counts (Maclean *et al.*, 2010, 2013a; Bache *et al.*, 2012a, 2018a; Murrell *et al.*, 2019); however, identification and quantification of the reductions in distinct nosocomial pathogens within hospital areas will be essential in demonstrating clinical translatability of the studies conducted in this thesis. In addition to using Baird Parker contact plates for detection of *S. aureus* contamination as indicated in the aforementioned studies, it is recommended that future studies employ additional contact plate types for surface microbial monitoring, such as violet red bile glucose for the detection of *Enterobacteriaceae* or TSA for general bacterial detection, followed by a bacterial identification technique, such as PCR or MALDI-TOF, to quantify individual species. This would be useful in providing an indication of the comparative susceptibility of individual bacterial contaminants in the clinical setting, to ensure it aligns with that demonstrated in the laboratory.

It is recommended that such studies also monitor HAI rates following implementation of the 405-nm light EDS. Reductions in the instances of HAI is the utmost goal of any healthcare disinfection strategy, and thus establishing the translatability of reduced environmental contamination as a result of 405-nm light EDS exposure into reduced HAI rates therein is of paramount importance to achieving widespread implementation of the technology. A longitudinal study with an equivalent ‘control’ environmental area would be necessary to do this, ensuring all ward activities were accounted for. As discussed, Murrell *et al*. (2019) successfully demonstrated this effect within an operating room – with both microbial surface

contamination and SSI rates therein shown to be reduced – however, it is essential that additional investigations are conducted to corroborate this effect in other hospital settings and for reductions in other prominent HAIs, including UTIs, BSIs and LRTIs.

As previously discussed, although bacterial tolerance to 405-nm light inactivation is unlikely to develop given its non-selective and multi-targeted approach, it is essential that the comparative susceptibility of MDR and susceptible bacterial strains to the 405-nm light EDS is further established, given the increasing emergence of MDR strains in healthcare settings.

Studies performed in this thesis primarily assessed efficacy of the 405-nm light EDS for surface bacterial contamination, given that high-touch surfaces in the patient area constitute the biggest risk of HAI transmission (Dancer, 2009; Huslage *et al.*, 2010; Shams *et al.*, 2016). However, airborne transmission of HAI-inducing pathogens is increasingly prevalent given the overburdened nature of healthcare settings and the presence of immunosuppressed patients (Shrivastava *et al.*, 2013). As such, it is recommended that the efficacy of the 405-nm light EDS for inactivation of aerosolised bacteria is assessed. Dougall *et al.* (2018) previously demonstrated >99% inactivation of aerosolised bacteria within a suspension chamber following 30 min exposure to 22 mW cm^{-2} of 405-nm light; however, its efficacy at irradiances similar to that employed by the 405-nm light EDS is relatively unknown. The aforementioned study by Murrell *et al.* (2019), investigating the efficacy of the 405-nm light EDS with an operating room, additionally observed reductions in contamination levels/SSI rates in an adjacent room with no light source but a shared circulatory system, indicating its likely antimicrobial effect on bacterial aerosols. Further, studies assessing the efficacy of the 405-nm light EDS within a hospital isolation room have demonstrated decontamination of surfaces in areas of the room which were indirectly exposed to the light source; suggesting the installation position of the light source may not be critical as the inactivation of airborne bacteria, which will sediment at random within the room, will contribute to general reductions in surface bacterial levels (Bache *et al*., 2018). Further studies to quantify the relative inactivation effects of bacteria on surfaces and suspended in the air upon 405-nm light EDS exposure is essential. Eadie *et al*. (2022) recently demonstrated the ability of far UV-C to inactivate *S. aureus* within a laboratory-controlled room-sized chamber; which could serve as a promising mode of testing in this instance prior to clinical investigation. Studies which monitor levels of environmental airborne contaminants, using a sieve impactor sampler for example, at regular

intervals before, during and after use of the 405-nm light EDS in various clinical settings, will be essential to fully quantify its effect.

It is also recommended that the efficacy of the EDS for the inactivation of bacterial biofilms is further elucidated, by investigating its ability to inactivate biofilms of varying and of mixed species, at varying stages within the biofilm life cycle, to better comprehend its realistic clinical efficacy.

8.2.3 Antiviral Efficacy of the 405-nm light EDS

on the Hazard Group classification of SARS-CoV-2 (HG3) and the containment level of the laboratory utilised (BSL2), experimental

With regards to the antiviral studies conducted in this thesis, work was limited by the necessity to employ a SARS-CovV-2 surrogate species given the Hazard Group classification of SARS-CoV-2 (HG3) and the containment level of the laboratory utilised (BSL2). Although bacteriophage phi6 is a well-established surrogate species for coronaviruses (Fedorenko *et al.*, 2020; Rockey *et al.*, 2020; Bangiyev *et al.*, 2021; Ordon *et al.*, 2021; Vatter *et al.*, 2021; Ahuja *et al.*, 2022; Baker *et al.*, 2022; Dey *et al.*, 2022; Gomes *et al.*, 2022; Karaböce *et al.*, 2022; Zargar *et al.*, 2022), it is recommended that further work is conducted to establish the efficacy of low irradiance 405-nm light for the inactivation of SARS-CoV-2 without the requirement for a surrogate species, to further justify its clinical efficacy. Further, given the likelihood that contaminants will be presented at various distances from the EDS, and thus illuminated at various irradiances, it is important that efficacy is established across a range of irradiance levels typically expected within a whole-room setting (~0.001-2.066 mW cm^{-2}; as established in Chapter 4).

SARS-CoV-2 is known to be transmitted in both respiratory droplets and aerosols (WHO, 2020c). It is therefore recognised that a limitation of the work provided in this thesis is the absence of data demonstrating the ability of low irradiance 405-nm light to inactivate phi6 suspended in the air. Due to the sensitivity of the surrogate species employed and time constrains, a robust methodology for exposing and quantifying reductions of aerosolised phi6 was unfortunately not developed in this instance; however, it is essential that future studies establish the inactivation efficacy of the 405-nm light EDS against aerosolised SARS-CoV-2, such to better comprehend its ability to reduce COVID-19 transmission. It is suggested that initial studies of this nature are performed in a small-scale laboratory

aerosol chamber, using a similar methodology to that employed by Dougall *et al.* (2018), before then expanding to clinical studies.

It is additionally recommended that clinical studies assessing efficacy of the 405-nm light EDS, similar to those conducted previously for bacterial contamination (Maclean *et al.*, 2010, 2013a; Bache *et al.*, 2012a, 2018a; Murrell *et al.*, 2019), are conducted to assess the ability of the technology to inactivate SARS-CoV-2 in practical settings. The current study demonstrated the ability of low irradiance 405-nm light to inactivate the employed surrogate at various viral loads associated with infection progression (Zhu *et al.*, 2020), and so it is likely that similar reductions would be observed clinically; however, it is important that this is properly established given the dynamic nature of healthcare environments.

It is also proposed that the antiviral efficacy of the 405-nm light EDS is established for additional viruses associated with HAI development. Tomb *et al.* demonstrated the ability of low irradiance (0.5 mW $cm^{-2)}$ 405-nm light to inactivate both bacteriophage phi C31 and feline calicivirus, as a surrogate for norovirus (Tomb, 2017); however, it is important that is additionally demonstrated for other HAI-associated species, including influenza, rotavirus and adenovirus, as this could significantly enhance the applicability of the technology for public health decontamination applications.

8.3 Overall Summary

Comprehensively, this thesis presents novel findings pertaining to the low irradiance application of antimicrobial 405-nm light for continuous environmental decontamination. Key findings include:

(1) The broad-spectrum antibacterial efficacy of low irradiance 405-nm light exposure, at levels analogous to those produced by the 405-nm light EDS, has been established for a panel of clinically-relevant bacteria **(Sinclair *et al.*, 2023b)**.

(2) The antibacterial efficacy of the 405-nm light EDS under exposure conditions representative of those likely to be encountered with practical system deployment (low-level light exposures, suspended in biological media, dried onto inert surfaces and presented as biofilms) was demonstrated; furthering insight into clinical translatability.

(3) An enhancement in bactericidal efficacy and GE in response to low irradiance 405-nm light exposure, in comparison to that of higher irradiance exposures, was demonstrated on a per-

unit-dose basis; further validating its employment at these levels for infection control applications and the energy efficiency of such lighting systems **(Sinclair *et al.*, 2024)**.

(4) The antiviral efficacy of the 405-nm light EDS for the inactivation of a SARS-CoV-2 surrogate was established at various seeding densities in both minimal and biologically-relevant media; demonstrating the potential for this technology to be used to reduce the spread of SARS-CoV-2 and other viral infections within the clinical environment **(Sinclair *et al.*, 2023a)**.

These findings advance fundamental knowledge and development of this platform antimicrobial technology, which has the potential to reduce microbial transmission, and thus subsequent HAI rates, across the infection control sector.

REFERENCES

Abad-Lozano, J.L. and Rodriguez-Valera, F. (1984) 'Photodynamic inactivation of *Bacillus subtitis* spores', *Journal of Applied Bacteriology*, 57(2), pp. 339–343. Available at: https://doi.org/10.1111/j.1365-2672.1984.tb01399.x.

Abrahamse, H. and Hamblin, M.R. (2016) 'New photosensitizers for photodynamic therapy', *Biochemical Journal*, 473(4), pp. 347–364. Available at: https://doi.org/10.1042/BJ20150942.

Adair, C., Gorman, S., Byers, L., Jones, D., Goldsmith, C., Moore, J., Kerr, J., Curran, M., Hogg, G., Webb, C., Mccarthy, G., Milligan, K. and Feron, B. (1999) 'Implications of endotracheal tube biofilm for ventilator-associated pneumonia', *Intensive Care Medicine*, 25(10), pp. 1072-1076. Available at: https://doi.org/10.1007/s001340051014.

Ahmadipour, M., Dehghan, M., Ahmadinejad, M., Jabarpour, M., Shahrbabaki, P.M. and Rigi, Z.E. (2022) 'Barriers to hand hygiene compliance in intensive care units during the COVID-19 pandemic: A qualitative study', *Frontiers in Public Health*, 10, 968231. Available at: https://doi.org/10.3389/fpubh.2022.968231.

Ahuja, S., Kumar, M.S., Nandeshwar, R., Kondabagil, K. and Tallur, S. (2022) 'Longer amplicons provide better sensitivity for electrochemical sensing of viral nucleic acid in water samples using PCB electrodes', *Scientific Reports*, 12, 8814. Available at: https://doi.org/10.1038/s41598-022-12818-w.

Aitken, C. and Jeffries, D.J. (2001) 'Nosocomial spread of viral disease', *Clinical Microbiology Reviews*, 14(3), pp. 528–546. Available at: https://doi.org/10.1128/CMR.14.3.528-546.2001.

Akhtar, F., Khan, A.U., Misba, L., Akhtar, K. and Ali, A. (2021) 'Antimicrobial and antibiofilm photodynamic therapy against vancomycin resistant *Staphylococcus aureus* (VRSA) induced infection in vitro and in vivo', *European Journal of Pharmaceutics and Biopharmaceutics*, 160(1), pp. 65–76. Available at: https://doi.org/10.1016/j.ejpb.2021.01.012.

Ali, S., Muzslay, M., Bruce, M., Jeanes, A., Moore, G. and Wilson, A.P.R. (2016) 'Efficacy of two hydrogen peroxide vapour aerial decontamination systems for enhanced disinfection of methicillin-resistant *Staphylococcus aureus, Klebsiella pneumoniae* and *Clostridium difficile* in single isolation rooms', *Journal of Hospital Infection*, 93(1), pp. 70–77. Available at: https://doi.org/10.1016/j.jhin.2016.01.016.

Allison, R.R., Downie, G.H., Cuenca, R., Hu, X.H., Childs, C.J.H. and Sibata, C.H. (2004) 'Photosensitizers in clinical PDT', *Photodiagnosis and Photodynamic Therapy*, 1(1), pp. 27–42. Available at: https://doi.org/10.1016/S1572-1000(04)00007-9.

Alrahmany, D., Omar, A., Alreesi, A., Harb, G. and Ghazi, I. (2022) *'Acinetobacter baumannii* infection-related mortality in hospitalized patients: Risk factors and potential targets for clinical and antimicrobial stewardship interventions', *Antibiotics*, 11(8), 1086. Available at https://doi.org/10.3390/antibiotics11081086.

Al-Tawfiq, J.A. and Tambyah, P.A. (2014) 'Healthcare associated infections (HAI) perspectives', *Journal of Infection and Public Health*, 7(4), pp. 339–344. Available at: https://doi.org/10.1016/j.jiph.2014.04.003.

Amador, C.I., Stannius, R.O., Røder, H.L. and Burmølle, M. (2021) 'High-throughput screening alternative to crystal violet biofilm assay combining fluorescence quantification and imaging', *Journal of Microbiological Methods*, 190, 106343. Available at: https://doi.org/10.1016/j.mimet.2021.106343.

American Thoracic Society. (2005) 'Guidelines for the management of adults with hospital-acquired, ventilator-associated, and healthcare-associated pneumonia', *American Journal of Respiratory and Critical Care Medicine*, 171(4), pp. 388-416. Available at: https://doi.org/10.1164/rccm.200405-644ST.

Amin, R.M., Bhayana, B., Hamblin, M.R. and Dai, T. (2016) 'Antimicrobial blue light inactivation of *Pseudomonas aeruginosa* by photo-excitation of endogenous porphyrins: In vitro and in vivo studies', *Lasers in Surgery and Medicine*, 48(5), pp. 562–568. Available at: https://doi.org/10.1002/lsm.22474.

Amodeo, D., Lucarelli, V., De Palma, I., Puccio, A., Nante, N., Cevenini, G. and Messina, G. (2022) 'Efficacy of violet–blue light to inactive microbial growth', *Scientific Reports*, 12, 20179. Available at: https://doi.org/10.1038/s41598-022-24563-1.

Anderson, J., Maclean, M., MacGregor, S.J. and Woolsey, G.A. (2008) 'Lighting device'. Patent: US8398264B2.

Andrady, A.L., Heikkilä, A.M., Pandey, K.K., Bruckman, L.S., White, C.C., Zhu, M. and Zhu, L. (2023) 'Effects of UV radiation on natural and synthetic materials', *Photochemical and Photobiological Sciences*, 22(5), pp. 1177–1202. Available at: https://doi.org/10.1007/s43630-023-00377-6.

Angarano, V., Smet, C., Akkermans, S., Watt, C., Chieffi, A. and Van Impe, J.F.M. (2020) 'Visible light as an antimicrobial strategy for inactivation of *Pseudomonas fluorescens* and *Staphylococcus epidermidis* biofilms', *Antibiotics*, 9(4), 171. Available at: https://doi.org/10.3390/antibiotics9040171.

dos Anjos, C., Leanse, L.G., Ribeiro, M.S., Sellera, F.P., Dropa, M., Arana-Chavez, V.E., Lincopan, N., Baptista, M.S., Pogliani, F.C., Dai, T. and Sabino, C.P. (2023) 'New insights into the bacterial targets of antimicrobial blue light', *Microbiology Spectrum*, 11(2), e02833-22. Available at: https://doi.org/10.1128/spectrum.02833-22.

Antimicrobial Resistance Collaborators (2022) 'Global burden of bacterial antimicrobial resistance in 2019: a systematic analysis', *Lancet*, 399(10325), pp. 629–655. Available at: https://doi.org/ 0.1016/S0140-6736(21)02724-0.

Aranda-Michel, J. and Giannella, R.A. (1999) 'Acute diarrhea: A practical review', *American Journal of Medicine,* 106(6), 670-676. Available at: https://doi.org/10.1016/s0002-9343(99)00128-x.

ARHAI Scotland. (2020) *Healthcare Associated Infections 2019 Annual Report*. Scotland: ARHAI Scotland. Available at: https://www.nss.nhs.scot/publications/healthcare-associated-infections-2019-annual-report/. (Accessed October 2020).

ARHAI Scotland (2021) *Existing and emerging technologies used for the decontamination of the healthcare environment: Steam*. Scotland: ARHAI Scotland. Available at: https://www.nss.nhs.scot/media/2166/novel-tech-steam-literature-revi.pdf. (Accessed: February 2024).

Ashkenazi, H., Malik, Z., Harth, Y. and Nitzan, Y. (2003) 'Eradication of *Propionibacterium acnes* by its endogenic porphyrins after illumination with high intensity blue light', *FEMS Immunology & Medical Microbiology*, 35(1), pp. 17–24. Available at: https://doi.org/10.1016/S0928-8244(02)00423-6.

ASP. (2015) *GLOSAIR™ 400 system.* Available at: https://www.aspjj.com/emea/products/area-decontamination/glosair-400-system (Accessed: March 2024).

Asri, N., Ahmad, S., Mohamud, R., Hanafi, N., Zaidi, N., Irekeola, A., Shueb, R., Yee, L., Noor, N., Mustafa, F., Yean, C. and Yusof N (2021) 'Global prevalence of nosocomial multidrug-resistant *Klebsiella pneumoniae*: A systematic review and meta-analysis', *Antibiotics*, 10(12), 1508. Available at https://doi.org/10.3390/antibiotics10121508.

Azeredo, J., Azevedo, N.F., Briandet, R., Cerca, N., Coenye, T., Costa, A.R., Desvaux, M., Di Bonaventura, G., Hébraud, M., Jaglic, Z., Kačániová, M., Knøchel, S., Lourenço, A., Mergulhão, F., Meyer, R.L., Nychas, G., Simões, M., Tresse, O. and Sternberg, C. (2017) 'Critical review on biofilm methods', *Critical Reviews in Microbiology*, 43(3), pp. 313–351. Available at: https://doi.org/10.1080/1040841X.2016.1208146.

Bache, S.E., Maclean, M., Gettinby, G., Anderson, J.G., MacGregor, S.J. and Taggart, I. (2018) 'Universal decontamination of hospital surfaces in an occupied inpatient room with a continuous 405 nm light source', *Journal of Hospital Infection*, 98(1), pp. 67–73. Available at: https://doi.org/10.1016/j.jhin.2017.07.010.

Bache, S.E., Maclean, M., Gettinby, G., Anderson, J.G., MacGregor, S.J. and Taggart, I. (2018) 'Universal decontamination of hospital surfaces in an occupied inpatient room with a continuous 405 nm light source', *Journal of Hospital Infection*, 98(1), pp. 67–73. Available at: https://doi.org/10.1016/j.jhin.2017.07.010.

Bache, S.E, Maclean, M., MacGregor, S.J., Anderson, J.G., Gettinby, G., Coia, J.E. and Taggart, I. (2012) 'Clinical studies of the High-Intensity Narrow-Spectrum light Environmental Decontamination System (HINS-light EDS), for continuous disinfection in the burn unit inpatient and outpatient settings', *Burns*, 38(1), pp. 69–76. Available at: https://doi.org/10.1016/j.burns.2011.03.008.

Bache, S.E., Maclean, M., MacGregor, S.J., Anderson, J.G., Gettinby, G., Coia, J.E. and Taggart, I. (2012) 'Clinical studies of the high-intensity narrow-spectrum light environmental decontamination system (HINS-light EDS), for continuous disinfection in the burn unit inpatient and outpatient settings', *Burns*, 38(1), pp. 69–76. Available at: https://doi.org/10.1016/j.burns.2011.03.008.

Badia, J., Casey, A., Petrosillo, N., Hudson, P., Mitchell, S. and Crosby, C. (2017) 'Impact of surgical site infection on healthcare costs and patient outcomes: a systematic review in six European countries', *Journal of Hospital Infection*, 96(1), pp. 1-15. Available from: https://doi.org/10.1016/j.jhin.2017.03.004.

Bae, Y.S., Oh, H., Rhee, S.G. and Yoo, Y.D. (2011) 'Regulation of reactive oxygen species generation in cell signalling', *Molecules and Cells*, 32(6), pp. 491–509. Available at: https://doi.org/10.1007/s10059-011-0276-3.

Bak, A., Mugglestone, M.A., Ratnaraja, N. V, Wilson, J.A., Rivett, L., Stoneham, S.M., Bostock, J., Moses, S.E., Price, J.R., Weinbren, M., Loveday, H.P., Islam, J. and Wilson, A.P.R. (2021) 'SARS-CoV-2 routes of transmission and recommendations for preventing acquisition: joint British Infection Association (BIA), Healthcare Infection Society (HIS), Infection Prevention Society (IPS) and Royal College of Pathologists (RCPath) guidance', *Journal of Hospital Infection*, 114, pp. 79–103. Available at: https://doi.org/10.1016/j.jhin.2021.04.027.

Baker, C.A., Gutierrez, A. and Gibson, K.E. (2022) 'Factors impacting persistence of Phi6 bacteriophage, an enveloped virus surrogate, on fomite surfaces', *Applied and Environmental Microbiology*, 88(7), 02552-21. Available at: https://doi.org/10.1128/aem.02552-21.

Banerjee, S., Ghosh, D., Vishakha, K., Das, S., Mondal, S. and Ganguli, A. (2020) 'Photodynamic antimicrobial chemotherapy (PACT) using riboflavin inhibits the mono and dual species biofilm produced by antibiotic resistant *Staphylococcus aureus* and *Escherichia coli*', *Photodiagnosis and Photodynamic Therapy*, 32, 102002. Available at: https://doi.org/10.1016/j.pdpdt.2020.102002.

Bangiyev, R., Chudaev, M., Schaffner, D.W. and Goldman, E. (2021) 'Higher concentrations of bacterial enveloped virus Phi6 can protect the virus from environmental decay', *Applied and Environmental Microbiology*, 87(21), e0137121. Available at: https://doi.org/10.1128/AEM.01371-21.

Barbut, F., Yezli, S. and Otter, J.A. (2012) 'Activity in vitro of hydrogen peroxide vapour against *Clostridium difficile* spores', *Journal of Hospital Infection*, 80(1), pp. 85–87. Available at: https://doi.org/10.1016/j.jhin.2011.10.005.

Bardossy, A.C. and Zervos, J. (2016) 'Preventing hospital-acquired infections in low-income and middle-income countries: Impact, gaps, and opportunities', 30(3), pp. 805-818. Available at: https://doi.org/ 10.1016/j.idc.2016.04.006.

Barneck, M.D., Rhodes, N.L.R., de la Presa, M., Allen, J.P., Poursaid, A.E., Nourian, M.M., Firpo, M.A. and Langell, J.T. (2016) 'Violet 405-nm light: a novel therapeutic agent against common pathogenic bacteria', *Journal of Surgical Research*, 206(2), pp. 316–324. Available at: https://doi.org/10.1016/j.jss.2016.08.006.

BCCM. (2015) *Lab instruction videos; How to open a BCCM/LMG ampoule?* Available at: https://bccm.belspo.be/knowledge/labvideos. (Accessed: May 2023).

Beggs, C.B. (2003) 'The airborne transmission of infection in hospital buildings: Fact or fiction?', *Indoor and Built Environment*, 12(1-2), pp. 9–18. Available at: https://doi.org/10.1177/142032603032201.

Bell, E., Brassel, S., Oliver, E., Schirrmacher, H., Arnetorp, S., Berg, K., Darroch-Thompson, D., Pohja-Hutchison, P., Mungall, B., Carroll, S., Postma, M. and Steuten, L. (2022) 'Estimates of the Global Burden of COVID-19 and the Value of Broad and Equitable Access to COVID-19 Vaccines', *Vaccines*, 10(8), 1320. Available at: https://doi.org/10.3390/vaccines10081320.

Bernady, C. and Malley, J. (2023) 'Impact of surface characteristics and dew point on the blue light (BL_{405}) inactivation of viruses', *Microorganisms*, 11(11), 2638. Available at: https://doi.org/ 10.3390/microorganisms11112638.

Berríos-Torres, S.I., Umscheid, C.A., Brazler, D.W., Leas, B., Stone, E.C., Kelz, R.R., Reinke, C.E., Morgan, S., Solomkin, J.S., Mazuski, J.E., Dellinger, E.P., Itani, K.M.F., Berbari, E.F., Segreti, J., Parvizi, J., Blanchard, J., Allen, G., Kluytmans, J.A.J.W., Donlan, R. and Schecter, W.P. (2017) 'Centers for Disease Control and Prevention Guideline for the prevention of surgical Site infection, 2017', *JAMA Surgery*, 152(8), pp. 784-791. Available at: https://doi.org/10.1001/jamasurg.2017.0904.

Berrie, E., Andrews, L., Yezli, S. and Otter, J.A. (2011) 'Hydrogen peroxide vapour (HPV) inactivation of adenovirus', *Letters in Applied Microbiology*, 52(5), pp. 555–558. Available at: https://doi.org/10.1111/j.1472-765X.2011.03033.x.

Bertoloni, G., Lauro, F.M., Cortella, G. and Merchat, M. (2000) 'Photosensitizing activity of hematoporphyrin on *Staphylococcus aureus* cells', *Biochimica et Biophysica Acta (BBA) - General Subjects*, 1475(2), pp. 169–174. Available at: https://doi.org/10.1016/s0304-4165(00)00071-4.

Bhatta, D.R., Hamal, D., Shrestha, R., Hosuru Subramanya, S., Baral, N., Singh, R.K., Nayak, N. and Gokhale, S. (2018) 'Bacterial contamination of frequently touched objects in a tertiary care hospital of Pokhara, Nepal: How safe are our hands?', *Antimicrobial Resistance and Infection Control*, 7, 97. Available at: https://doi.org/10.1186/s13756-018-0385-2.

Biasin, M., Strizzi, S., Bianco, A., Macchi, A., Utyro, O., Pareschi, G., Loffreda, A., Cavalleri, A., Lualdi, M., Trabattoni, D., Tacchetti, C., Mazza, D. and Clerici, M. (2021) 'UV-A and UV-B can neutralize SARS-CoV-2 infectivity'. *Journal of Photochemistry and Photobiology*, 10, 100107. Available at: https://doi.org/10.1101/2021.05.28.21257989.

Biener, G., Masson-Meyers, D.S, Bumah, V.V, Hussey, G., Stoneman, M.R., Enwemeka, C.S. and Raicu, V. (2017) 'Blue/violet laser inactivates methicillin-resistant *Staphylococcus aureus* by altering its transmembrane potential', *Journal of Photochemistry and Photobiology B: Biology*, 170, pp. 118–124. Available at: https://doi.org/10.1016/j.jphotobiol.2017.04.002.

Bioquell. (2024) *Bioquell L-4*. Available at: https://www.bioquell.com/life-sciences/systems-and-services/l-4/?lang=en-uk (Accessed: May 2023).

Blee, J.A., Roberts, I.S. and Waigh, T.A. (2020) 'Membrane potentials, oxidative stress and the dispersal response of bacterial biofilms to 405 nm light', *Physical Biology*, 17(3), 036001. Available at: https://doi.org/10.1088/1478-3975/ab759a.

Boer, H.E.L. de, van Elzelingen-Dekker, C.M., van Rheenen-Verberg, C.M.F. and Spanjaard, L. (2006) 'Use of gaseous ozone for eradication of methicillin-resistant *Staphylococcus aureus* from the home environment of a colonized hospital employee', *Infection Control & Hospital Epidemiology*, 27(10), pp. 1120–1122. Available at: https://doi.org/10.1086/507966.

Bonadonna, L., Briancesco, R. and Coccia, A.M. (2017) 'Analysis of microorganisms in hospital environments and potential risks', in *Indoor Air Quality in Healthcare Facilities*, 42, pp. 53–62. Available at: https://doi.org/10.1007/978-3-319-49160-8_5.

Boncristiani, H.F. (2009) '*Respiratory Viruses',* in Criado, M.F. and Arruda, E. Encyclopedia of Microbiology. [Online]. Available at: https://doi.org/ 10.1016/B978-012373944-5.00314-X (Accessed January 2023).

Boyce, J.M. (2009) 'New approaches to decontamination of rooms after patients are discharged', *Infection Control & Hospital Epidemiology*, 30(6), pp. 515–517. Available at: https://doi.org/DOI: 10.1086/598999.

Braatsch, S., Moskvin, O. V, Klug, G. and Gomelsky, M. (2004) 'Responses of the *Rhodobacter sphaeroides* transcriptome to blue light under semiaerobic conditions', *Journal of Bacteriology*, 186(22), pp. 7726–7735. Available at: https://doi.org/10.1128/JB.186.22.7726-7735.2004.

Bradley, C. (2022) *Miniaturisation of the HINS-light environmental decontamination system (EDS).* Engineering Design and Manufacture Project Report. University of Strathclyde.

Brenner, D.J. (2022) 'Far-UVC light at 222 nm is showing significant potential to safely and efficiently inactivate airborne pathogens in occupied indoor locations', *Photochemistry and Photobiology*, 99(3), 1047-1050. Available at: https://doi.org/10.1111/php.13739.

Bridier, A., Briandet, R., Thomas, V. and Dubois-Brissonnet, F. (2011) 'Resistance of bacterial biofilms to disinfectants: A review', *Biofouling*, 27(9), pp. 1017–1032. Available at: https://doi.org/10.1080/08927014.2011.626899.

Brinkwirth, S., Ayobambi, O., Eckmanns, T. and Markwart, R. (2021) 'Hospital-acquired infections caused by enterococci: A systematic review and meta-analysis, WHO European Region, 1 January 2010 to 4 February 2020', *Eurosurveillance*, 26(45), 2001628. Available at https://doi.org/10.2807/1560-7917.ES.2021.26.45.2001628.

Buchovec, I., Paskeviciute, E. and Luksiene, Z. (2010) 'Photosensitization-based inactivation of food pathogen *Listeria monocytogenes* in vitro and on the surface of packaging material', *Journal of Photochemistry and Photobiology B: Biology*, 99(1), pp. 9–14. Available at: https://doi.org/https://doi.org/10.1016/j.jphotobiol.2010.01.007.

Bumah, V.V., Aboualizadeh, E., Masson-Meyers, D.S., Eells, J.T., Enwemeka, C.S. and Hirschmugl, C.J. (2017) 'Spectrally resolved infrared microscopy and chemometric tools to reveal the interaction between blue light (470 nm) and methicillin-resistant *Staphylococcus aureus*', *Journal of Photochemistry and Photobiology B: Biology*, 167, pp. 150–157. Available at: https://doi.org/10.1016/j.jphotobiol.2016.12.030.

Bumah, V.V, Masson-Meyers, D.S., Cashin, S.E. and Enwemeka, C.S. (2013) 'Wavelength and bacterial density influence the bactericidal effect of blue light on methicillin-resistant *Staphylococcus aureus* (MRSA)', *Photomedicine and Laser Surgery*, 31(11), pp. 547–553. Available at: https://doi.org/10.1089/pho.2012.3461.

Buonanno, M., Ponnaiya, B., Welch, D., Stanislauskas, M., Randers-Pehrson, G., Smilenov, L., Lowy, F.D., Owens, D.M. and Brenner, D.J. (2017) 'Germicidal efficacy and mammalian skin safety of 222-nm UV light', *Radiation Research*, 187(4), pp. 483–491. Available at: https://doi.org/10.1667/RR0010CC.1.

Buonanno, M., Welch, D., Shuryak, I. and Brenner, D.J. (2020) 'Far-UVC light (222 nm) efficiently and safely inactivates airborne human coronaviruses', *Scientific Reports*, 10(1). Available at: https://doi.org/10.1038/s41598-020-67211-2.

Byrd, A.L., Belkaid, Y. and Segre, J.A. (2018) 'The human skin microbiome', *Nature Reviews Microbiology*, 16(3), pp. 143–155. Available at: https://doi.org/10.1038/nrmicro.2017.157.

Cahill, O.J., Claro, T., O'Connor, N., Cafolla, A.A., Stevens, N.T., Daniels, S. and Humphreys, H. (2014) 'Cold air plasma to decontaminate inanimate surfaces of the hospital environment', *Applied and Environmental Microbiology*, 80(6), pp. 2004–2010. Available at: https://doi.org/10.1128/AEM.03480-13.

Cairns, S., Gibbons, C., Milne, A., King, H., Llano, M., MacDonald, L., Malcolm, W., Robertson, C., Sneddon, J., Weir, J. and Reilly, J. (2018) 'Results from the third Scottish National Prevalence Survey: Is a population health approach now needed to prevent healthcare-associated infections?', *Journal of Hospital Infection*, 99(3), pp. 312–317. Available at: https://doi.org/10.1016/j.jhin.2018.03.038.

Cassini, A., Plachouras, D., Eckmanns, T., Abu, S.M., Blank, H., Ducomble, T., Haller, S., Harder, T., Klingeberg, A., Sixtensson, M., Velasco, E., Weiß, B., Kramarz, P., Monnet, D., Kretzschmar, M. and Suetens, C. (2016) 'Burden of six healthcare-associated infections on European population health: Estimating incidence-based disability-adjusted life years through a population

prevalence-based modelling study', *PLoS Medicine*, 13(10), e1002150. Available at: https://doi.org/10.1371/journal.pmed.1002150.

Carr, B.G., Kaye, A.J., Wiebe, D.J., Gracias, V.H., Schwab, C.W. and Reilly, P.M. (2007) 'Emergency department length of stay: a major risk factor for pneumonia in intubated blunt trauma patients', *Journal of Trauma*, 63(1), pp. 9–12. Available at: https://doi.org/10.1097/TA.0b013e31805d8f6b.

Casas, A., Di Venosa, G., Hasan, T. and Batlle, A. (2011) 'Mechanisms of resistance to photodynamic therapy', *Current Medicinal Chemistry*, 18(16), pp. 2486–2515. Available at: https://doi.org/10.1038/jid.2014.371.

Casewell, M. and Phillips, I. (1977) 'Hands as route of transmission for Klebsiella species', *British Medical Journal*, 2(6098), pp. 1315–1317. Available at: https://doi.org/10.1136/bmj.2.6098.1315.

Cassell, G.H. and Mekalanos, J. (2001) 'Development of antimicrobial agents in the era of new and reemerging infectious diseases and increasing antibiotic resistance', *Journal of the American Medical Association*, 285(5), pp. 601–605. Available at: https://doi.org/10.1001/jama.285.5.601.

Castano, A.P., Demidova, T.N. and Hamblin, M.R. (2004) 'Mechanisms in photodynamic therapy: part one-photosensitizers, photochemistry and cellular localization', *Photodiagnosis and photodynamic therapy*, 1(4), pp. 279–293. Available at: https://doi.org/10.1016/S1572-1000(05)00007-4.

CDC. (2011) 'Vital signs: Central line–associated blood stream infections — United States', *Morbidity and Mortality Weekly Report*, 60(8), pp. 243-248. Available at: https://doi.org/10.1016/j.annemergmed.2011.07.035.

CDC (2019). CRPA Carbapenem-resistant *Pseudomonas aeruginosa.* Available at: www.cdc.gov/drugresistance/ar-lab-networks/domestic.html (Accessed: October 2020).

CDC (2023). *Best Practices for Environmental Cleaning in Global Healthcare Facilities with Limited Resources*. Available at: https://www.cdc.gov/hai/prevent/resource-limited/cleaning-procedures.html (Accessed: July 2023).

Cecchini, M., Langer, J. and Slawomirski, L. (2015) *Antimicrobial Resistance in G7 Countries and Beyond: Economic Issues, Policies and Options for Action*. Available at: http://www.oecd.org/els/health-systems/Antimicrobial-Resistance-in-G7-Countries-and-Beyond.pdf (Accessed: December 2019).

Ceri, H., Olson, M.E., Stremick, C., Read, R.R., Morck, D. and Buret, A. (1999) 'The calgary biofilm device: New technology for rapid determination of antibiotic susceptibilities of bacterial biofilms', *Journal of Clinical Microbiology*, 37(6), pp. 1771–1776. Available at: https://doi.org/10.1128/jcm.37.6.1771-1776.1999.

Cetinkaya, Y., Falk, P. and Mayhall, C.G. (2000) 'Vancomycin-Resistant Enterococci', *Clinical Microbiology Reviews,* 13(4), 686-707. Available at: https://doi.org/10.1128/CMR.13.4.686.

Chaoui, L., Mhand, R., Mellouki, F. and Rhallabi, N. (2019) 'Contamination of the surfaces of a health care environment by multidrug-resistant (MDR) bacteria', *International Journal of Microbiology*, 2019, 3236526. Available at: https://doi.org/10.1155/2019/3236526.

Chatterjee, A., Rai, S., Guddattu, V., Mukhopadhyay, C. and Saravu, K. (2018) 'Is methicillin-resistant *Staphylococcus aureus* infection associated with higher mortality and morbidity in hospitalized patients? A cohort study of 551 patients from south western India', *Risk Management and Healthcare Policy*, 11, pp. 243–250. Available at: https://doi.org/10.2147/RMHP.S176517.

Cheadle, W.G. (2006) 'Risk factors for surgical site infection', *Surgical Infections*, 7(1), pp. 7–11. Available at: https://doi.org/10.1089/sur.2006.7.s1-7.

Chen, H., Cheng, Y. and Moraru, C.I. (2023) 'Blue 405 nm LED light effectively inactivates bacterial pathogens on substrates and packaging materials used in food processing', *Scientific Reports*, 13, 15472. Available at: https://doi.org/10.1038/s41598-023-42347-z.

Chen, Z., Garcia, G., Arumugaswami, V. and Wirz, R.E. (2020) 'Cold atmospheric plasma for SARS-CoV-2 inactivation', *Physics of Fluids*, 32(11), 111702. Available at: https://doi.org/10.1063/5.0031332.

Chi, S., Kim., T., Park, C., Yu, J., Lee, B., Lee, S., Kim, Y., Lim, S. and Kwon, Y. (2012) 'Bacterial pathogens of ventilator associated pneumonia in a tertiary referral hospital', *Tuberculosis and Respiratory Diseases*, 73(1), pp. 32-37. Available at: https://doi.org/ 10.4046/trd.2012.73.1.32.

Chu, Z., Hu, X., Wang, X., Wu, J., Dai, T. and Wang, X. (2019) 'Inactivation of *Cronobacter sakazakii* by blue light illumination and the resulting oxidative damage to fatty acids', *Canadian Journal of Microbiology*, 65(12), pp. 922–929. Available at: https://doi.org/10.1139/cjm-2019-0054.

Church, D., Elsayed, S., Reid, O., Winston, B. and Lindsay, R. (2006) 'Burn wound infections', *Clinical Microbiology Reviews*, 19(2), pp. 403–434. Available at: https://doi.org/10.1128/CMR.19.2.403-434.2006.

Cimiotti, J.P., Aiken, L.H., Sloane, D.M. and Wu, E.S. (2012) 'Nurse staffing, burnout, and health care–associated infection', *American Journal of Infection Control*, 40(6), pp. 486–490. Available at: https://doi.org/10.1016/j.ajic.2012.02.029.

Cobb, T.C. (2016) 'UV-C decontamination: NASA, prions, and future perspectives', *Applied Biosafety*, 21(2), pp. 84–88. Available at: https://doi.org/10.1177/1535676016646217.

Cobrado, L., Silva-Dias, A., Azevedo, M.M. and Rodrigues, A.G. (2017) 'High-touch surfaces: microbial neighbours at hand', *European Journal of Clinical Microbiology and Infectious Diseases*, 36(11), pp. 2053–2062. Available at: https://doi.org/10.1007/s10096-017-3042-4.

Colón, J., Forbis-Stokes, A.A. and Deshusses, M.A. (2015) 'Anaerobic digestion of undiluted simulant human excreta for sanitation and energy recovery in less-developed countries', *Energy for Sustainable Development*, 29, pp. 57–64. Available at: https://doi.org/10.1016/j.esd.2015.09.005.

Coohill, T.P. (1986) 'Virus-cell interactions as probes for vacuum-ultraviolet radiation damage and repair', *Photochemistry and Photobiology*, 44(3), pp. 359–363. Available at: https://doi.org/10.1111/j.1751-1097.1986.tb04676.x.

Coraça-Huber, D.C., Kreidl, L., Steixner, S., Hinz, M., Dammerer, D. and Fille, M. (2020) 'Identification and morphological characterization of biofilms formed by strains causing infection in orthopedic implants', *Pathogens*, 9(8), pp. 1–18. Available at: https://doi.org/10.3390/pathogens9080649.

Cosgrove, S.E., Sakoulas, G., Perencevich, E.N., Schwaber, M.J., Karchmer, A.W. and Carmeli, Y. (2003) 'Comparison of Mortality Associated with Methicillin-Resistant and Methicillin-Susceptible Staphylococcus aureus Bacteremia: A Meta-analysis', *Clinical Infectious Diseases*, 36(1), 53-59. Available at: https://doi.org/10.1086/345476.

Costa, D.M., Johani, K., Melo, D.S., Lopes, L.K.O., Lopes Lima, L.K.O., Tipple, A.F. V, Hu, H. and Vickery, K. (2019) 'Biofilm contamination of high-touched surfaces in intensive care units: epidemiology and potential impacts', *Letters in Applied Microbiology*, 68(4), pp. 269–276. Available at: https://doi.org/10.1111/lam.13127.

Coyle, A., Maclean, M., Anderson, J.G., Gettinby, G., MacGregor, S.J. and Taggart, I. (2011) 'High-intensity narrow-spectrum light decontamination of a staff changing room in a burns ward', *Burns*, 37(1), pp. 17. Available at: https://doi.org/10.1016/s0305-4179(11)70069-9.

Dadgostar, P. (2019) 'Antimicrobial resistance: implications and costs', *Infection and Drug Resistance*, 12, pp. 3903–3910. Available at: https://doi.org/10.2147/IDR.S234610.

Dai, T., Fuchs, B.B., Coleman, J.J., Prates, R.A., Astrakas, C., St. Denis, T.G., Ribeiro, M.S., Mylonakis, E., Hamblin, M.R. and Tegos, G.P. (2012) 'Concepts and principles of photodynamic therapy as an alternative antifungal discovery platform', *Frontiers in Microbiology*, 3, 120. Available at: https://doi.org/10.3389/fmicb.2012.00120.

Dai, T., Gupta, A., Huang, Y.-Y., Sherwood, M.E., Murray, C.K., Vrahas, M.S., Kielian, T. and Hamblin, M.R. (2013) 'Blue light eliminates community-acquired methicillin-resistant *Staphylococcus aureus* in infected mouse skin abrasions', *Photomedicine and Laser Surgery*, 31(11), pp. 531–538. Available at: https://doi.org/10.1089/pho.2012.3365.

Dai, T., Gupta, A., Huang, Y.-Y., Yin, R., Murray, C.K., Vrahas, M.S., Sherwood, M.E., Tegos, G.P. and Hamblin, M.R. (2013) 'Blue light rescues mice from potentially fatal *Pseudomonas aeruginosa* burn infection: efficacy, safety, and mechanism of action', *Antimicrobial Agents and Chemotherapy*, 57(3), pp. 1238–1245. Available at: https://doi.org/10.1128/AAC.01652-12.

Dai, T., Vrahas, M.S., Murray, C.K. and Hamblin, M.R. (2012) 'Ultraviolet C irradiation: An alternative antimicrobial approach to localized infections?', *Expert Review of Anti-Infective Therapy*, 10(2), pp. 185–195. Available at: https://doi.org/10.1586/eri.11.166.

Dancer, S.J. (2008) 'Importance of the environment in methicillin-resistant *Staphylococcus aureus* acquisition: the case for hospital cleaning', *The Lancet Infectious Diseases*, 8(2), pp. 101–113. Available at: https://doi.org/10.1016/S1473.

Dancer, S.J. (2009) 'The role of environmental cleaning in the control of hospital-acquired infection', *Journal of Hospital Infection*, 73(4), pp. 378–385. Available at: https://doi.org/10.1016/j.jhin.2009.03.030.

Dancer, S.J. (2014) 'Controlling hospital-acquired infection: Focus on the role of the environment and new technologies for decontamination', *Clinical Microbiology Reviews*, 27(4), pp. 665–690. Available at: https://doi.org/10.1128/CMR.00020-14.

Davin-Regli, A., Lavigne, J. and Pagès, J. (2019) '*Enterobacter* spp.: update on taxonomy, clinical aspects, and emerging antimicrobial resistance', *Clinical Microbiology*, 32(4), e00002-19. Available at https://doi.org/10.1128/cmr.00002-19.

St. Denis, T.G., Dai, T., Izikson, L., Astrakas, C., Anderson, R.R., Hamblin, M.R. and Tegos, G.P. (2011a) 'All you need is light: antimicrobial photoinactivation as an evolving and emerging discovery strategy against infectious disease', *Virulence*, 2(6), pp. 509–520. Available at: https://doi.org/10.4161/viru.2.6.17889.

St. Denis, T.G., Huang, L., Dai, T. and Hamblin, M.R. (2011b) 'Analysis of the bacterial heat shock response to photodynamic therapy-mediated oxidative stress', *Photochemistry and Photobiology*, 87(3), pp. 707–713. Available at: https://doi.org/10.1111/j.1751-1097.2011.00902.x.

Department of Health (2013). *Health Building Note 00-03: Clinical and clinical support spaces*. Available at: https://www.england.nhs.uk/wp-content/uploads/2021/05/HBN_00-03_Final.pdf (Accessed: May 2023).

Devasagayam, T.P.A., Tilak, J.C., Boloor, K.K., Sane, K.K., Ghaskadbi, S.S. and Lele, R.D. (2004) 'Free radicals and antioxidants in human health: current status and future prospects', *Journal of the Association of Physicians of India*, 52, pp. 794–804.

Dey, R., Dlusskaya, E. and Ashbolt, N.J. (2022) 'SARS-CoV-2 surrogate (Phi6) environmental persistence within free-living amoebae', *Journal of Water and Health*, 20(1), pp. 83–91. Available at: https://doi.org/10.2166/WH.2021.167.

Djouiai, B., Thwaite, J.E., Laws, T.R., Commichau, F.M., Setlow, B., Setlow, P. and Moeller, R. (2018) 'Role of DNA repair and protective components in *Bacillus subtilis* spore resistance to inactivation by 400-nm-wavelength blue light', *Applied and Environmental Microbiology*, 84(19), 1604-1618. Available at: https://doi.org/10.1128/AEM.01604-18.

Doan, L., Forrest, H., Fakis, A., Craig, J., Claxton, L. and Khare, M. (2012) 'Clinical and cost effectiveness of eight disinfection methods for terminal disinfection of hospital isolation rooms contaminated with *Clostridium difficile*', *Journal of Hospital Infection*, 82(2), pp. 114–121. Available at: https://doi.org/10.1016/j.jhin.2012.06.014.

Donlan, R.M. (2002) 'Biofilms: Microbial Life on Surfaces', *Emerging Infectious Diseases',* 8(9), pp. 881-890. Available at: https://doi.org/ 10.3201/eid0809.020063.

van Doremalen, N., Bushmaker, T., Morris, D.H., Holbrook, M.G., Gamble, A., Williamson, B.N., Tamin, A., Harcourt, J.L., Thornburg, N.J., Gerber, S.I., Lloyd-Smith, J.O., de Wit, E. and Munster, V.J. (2020) 'Aerosol and surface stability of SARS-CoV-2 as compared with SARS-CoV-1', *New England Journal of Medicine*, 382(16), pp. 1564–1567. Available at: https://doi.org/10.1056/nejmc2004973.

Dougall, L., Anderson, J.G., Timoshkin, I. V, MacGregor, S.J. and Maclean, M. (2018) 'Efficacy of antimicrobial 405 nm blue-light for inactivation of airborne bacteria', 10479, 10479G. Available at: https://doi.org/10.1117/12.2289987.

Dougall, L.R., Booth, M.G., Khoo, E., Hood, H., MacGregor, S.J., Anderson, J.G., Timoshkin, I. V and Maclean, M. (2019) 'Continuous monitoring of aerial bioburden within intensive care isolation rooms and identification of high-risk activities', *Journal of Hospital Infection*, 103(2), pp. 185–192. Available at: https://doi.org/10.1016/j.jhin.2019.05.010.

Dröge, W. (2002) 'Free radicals in the physiological control of cell function', *Physiological Reviews*, 82(1), pp. 47–95. Available at: https://doi.org/10.1152/physrev.00018.2001.

DSMZ. (2014) *Handling of Cultures and Ampoules*. Available at: https://www.dsmz.de/fileadmin/Bereiche/Microbiology/Dateien/Kultivierungshinweise/Kultivierungshinweise_neu_CD/Opening_17new.pdf (Accessed: February 2021).

Eadie, E., Hiwar, W., Fletcher, L., Tidswell, E., O'Mahoney, P., Buonanno, M., Welch, D., Adamson, C.S., Brenner, D.J., Noakes, C. and Wood, K. (2022) 'Far-UVC (222 nm) efficiently inactivates an airborne pathogen in a room-sized chamber', *Scientific Reports*, 12(1), 4373. Available at: https://doi.org/10.1038/s41598-022-08462-z.

ECDC. (2016) *Annual Epidemiological Report for 2016: Healthcare-associated infections in intensive care units.* Available at: https://www.ecdc.europa.eu/sites/default/files/documents/AER_for_2016-HAI_0.pdf (Accessed: June 2020).

ECDC. (2017) *Healthcare-associated infections - a threat to patient safety in Europe*. Available at: https://antibiotic.ecdc.europa.eu/en/publications-data/healthcare-associated-infections-threat-patient-safety-europe (Accessed: December 2019).

ECDC (2024) *Point prevalence survey of healthcare-associated infections and antimicrobial use in European acute care hospitals*. Available at: https://www.ecdc.europa.eu/en/publications-data/PPS-HAI-AMR-acute-care-europe-2022-2023 (Accessed: May 2024).

ECVM. (2023) *PVC in healthcare*. Available at: https://pvc.org/pvc-applications/pvc-in-healthcare/ (Accessed: December 2023).

Endarko. (2011) *Optimisation of ultra-violet and visible light based technologies for disinfection applications in clinical and other environments.* PhD Thesis. University of Strathclyde. Available at: https://stax.strath.ac.uk/concern/theses/fq977t82f (Accessed February 2020).

Endarko, E., Maclean, M., Timoshkin, I. V, MacGregor, S.J. and Anderson, J.G. (2012) 'High-intensity 405 nm light inactivation of *Listeria monocytogenes'*, *Photochemistry and Photobiology*, 88(5), pp. 1280–1286. Available at: https://doi.org/10.1111/j.1751-1097.2012.01173.x.

Endarko, E., Maclean, M., Timoshkin, I. V., MacGregor, S.J. and Anderson, J.G. (2012) 'High-intensity 405 nm light inactivation of *Listeria monocytogenes'*, *Photochemistry and Photobiology*, 88(5), pp. 1280–1286. Available at: https://doi.org/10.1111/j.1751-1097.2012.01173.x.

Enwemeka, C.S., Bumah, V.V and Mokili, J.L. (2021) 'Pulsed blue light inactivates two strains of human coronavirus', *Journal of Photochemistry and Photobiology B: Biology*, 222, 112282. Available at: https://doi.org/10.1016/j.jphotobiol.2021.112282.

Enwemeka, C.S., Williams, D., Hollosi, S., Yens, D. and Enwemeka, S.K. (2008) 'Visible 405 nm SLD light photo-destroys methicillin-resistant *Staphylococcus aureus* (MRSA) in vitro', *Lasers in Surgery and Medicine*, 40(10), pp. 734–737. Available at: https://doi.org/10.1002/lsm.20724.

Erb, S., Frei, R., Dangel, M. and Widmer, A.F. (2016) 'Multidrug-resistant organisms detected more than 48 hours after hospital admission are not necessarily hospital-acquired', *Infection Control & Hospital Epidemiology*, 38(1), pp. 18–23. Available at: https://doi.org/10.1017/ice.2016.226.

Essentra Components. (2023) *What is surgical steel? The role of stainless in healthcare*. Available at: https://www.essentracomponents.com/en-gb/news/industries/medical-equipment/what-is-surgical-steel-the-role-of-stainless-in-healthcare (Accessed: December 2023).

Eurosurveillance Editorial Team (2020) 'Note from the editors: World Health Organization declares novel coronavirus (2019-nCoV) sixth public health emergency of international concern', *European communicable disease bulletin*, 25(5), 200131. Available at: https://doi.org/10.2807/1560-7917.ES.2020.25.5.200131e.

Exner, M., Kramer, A., Lajoie, L., Gebel, J., Engelhart, S. and Hartemann, P. (2005) 'Prevention and control of health care–associated waterborne infections in health care facilities', *American Journal of Infection Control*, 33(5), pp. 26–40. Available at: https://doi.org/10.1016/j.ajic.2005.04.002.

Fasnacht, M. and Polacek, N. (2021) 'Oxidative Stress in Bacteria and the Central Dogma of Molecular Biology', *Frontiers in Molecular Biosciences*. 8, 671037. Available at: https://doi.org/10.3389/fmolb.2021.671037.

Fedorenko, A., Grinberg, M., Orevi, T. and Kashtan, N. (2020) 'Survival of the enveloped bacteriophage Phi6 (a surrogate for SARS-CoV-2) in evaporated saliva microdroplets deposited on glass surfaces', *Scientific Reports*, 10(1), pp. 1–10. Available at: https://doi.org/10.1038/s41598-020-79625-z.

Ferrer-Espada, R., Liu, X., Goh, X.S. and Dai, T. (2019) 'Antimicrobial blue light inactivation of polymicrobial biofilms', *Frontiers in Microbiology*, 10, 721. Available at: https://doi.org/10.3389/fmicb.2019.00721.

Ferrer-Espada, R., Wang, Y., Goh, X.S. and Dai, T. (2020) 'Antimicrobial blue light inactivation of microbial isolates in biofilms', *Lasers in Surgery and Medicine*, 52(5), pp. 472–478. Available at: https://doi.org/10.1002/lsm.23159.

Feuerstein, O., Ginsburg, I., Dayan, E., Veler, D. and Weiss, E.I. (2005) 'Mechanism of visible light phototoxicity on *Porphyromonas gingivalis* and *Fusobacterium nucleatum*', *Photochemistry and Photobiology*, 81(5), pp. 1186–1189. Available at: https://doi.org/10.1562/2005-04-06-RA-477.

Fila, G., Kawiak, A. and Grinholc, M.S. (2017a) 'Blue light treatment of pseudomonas aeruginosa: Strong bactericidal activity, synergism with antibiotics and inactivation of virulence factors', *Virulence*, 8(6), pp. 938–958. Available at: https://doi.org/10.1080/21505594.2016.1250995.

Flores-Mireles, A.L., Walker, J.N., Caparon, M. and Hultgren, S.J. (2015) 'Urinary tract infections: epidemiology, mechanisms of infection and treatment options', *Nature Reviews Microbiology*, 13(5), pp. 269-284. Available at: https://doi.org/10.1038/nrmicro3432.

Founou, R.C., Founou, L.L. and Essack, S.Y. (2017) 'Clinical and economic impact of antibiotic resistance in developing countries: A systematic review and meta-analysis', *PLoS ONE*, 12(12), pp. 1–18. Available at: https://doi.org/10.1371/journal.pone.0189621.

Franco, L.C., Tanner, W., Ganim, C., Davy, T., Edwards, J. and Donlan, R. (2020) 'A microbiological survey of handwashing sinks in the hospital built environment reveals differences in patient room and healthcare personnel sinks', *Scientific Reports*, 10(1), 8234. Available at: https://doi.org/10.1038/s41598-020-65052-7.

Franke, G., Knobling, B., Brill, F.H., Becker, B., Klupp, E.M., Belmar Campos, C., Pfefferle, S., Lütgehetmann, M. and Knobloch, J.K. (2021) 'An automated room disinfection system using ozone is highly active against surrogates for SARS-CoV-2', *Journal of Hospital Infection*, 112, pp. 108–113. Available at: https://doi.org/10.1016/j.jhin.2021.04.007.

Frenkel, J. (1930) 'On the correct formulation of Pauli's exclusion principle', *Nature*, 125(1), pp. 235–236. Available at: https://doi.org/10.1038/125235b0.

Fu, T.Y., Gent, P. and Kumar, V. (2012) 'Efficacy, efficiency and safety aspects of hydrogen peroxide vapour and aerosolized hydrogen peroxide room disinfection systems', *Journal of Hospital Infection*, 80(3), pp. 199–205. Available at: https://doi.org/10.1016/j.jhin.2011.11.019.

Gahlot, R., Nigam, C., Kumar, V., Yadav, G. and Anupurba, S. (2014) 'Catheter-related bloodstream infections', *International Journal of Critical Illness and Injury Science*, 4(2), pp. 162–167. Available at: https://doi.org/10.4103/2229-5151.134184.

Gardner, A., Ghosh, S., Dunowska, M. and Brightwell, G. (2021) 'Virucidal efficacy of blue LED and far-UVC light disinfection against feline infectious peritonitis virus as a model for SARS-CoV-2', *Viruses*, 13(8), 1436. Available at: https://doi.org/10.3390/v13081436.

Gardner, S.E. and Frantz, R.A. (2008) 'Wound bioburden and infection-related complications in diabetic foot ulcers', *Biological Research for Nursing*, 10(1), pp. 44–53. Available at: https://doi.org/10.1177/1099800408319056.

Gerba, C.P. (2009) 'Environmentally transmitted pathogens', in Maier, R.M., Pepper, I.L and Gerba, C.P. (eds.) *Environmental microbiology (Second edition).* Elsevier, pp. 445-484. Available at: https://doi.org/ 10.1016/B978-0-12-394626-3.00022-3.

Giovannetti, R. (2012) 'The use of spectrophotometry UV-Vis for the study of porphyrins', in Uddin, J. (ed.) *Macro To Nano Spectroscopy*, InTech, pp. 87-110. Available at: https://doi.org/10.5772/38797.

Girard, P.M., Francesconi, S., Pozzebon, M., Graindorge, D., Rochette, P., Drouin, R. and Sage, E. (2011) 'UVA-induced damage to DNA and proteins: Direct versus indirect photochemical processes', *Journal of Physics: Conference Series*, 261, 012002. Available at: https://doi.org/10.1088/1742-6596/261/1/012002.

Goldoni, A. (2002) 'Porphyrins: Fascinating molecules with biological significance', *ELETTRA Highlights 2001-2002*, pp. 64-65. Available at: https://www.elettra.eu/images/Documents/SCIENCE/elettra_highlights_2001-2002.pdf (Accessed: March 2020).

Gomes, M., Bartolomeu, M., Vieira, C., Gomes, A.T.P.C., Faustino, M.A.F., Neves, M.G.P.M.S. and Almeida, A. (2022) 'Photoinactivation of phage Phi6 as a SARS-CoV-2 model in wastewater: Evidence of efficacy and safety', *Microorganisms*, 10(3), 659. Available at: https://doi.org/10.3390/microorganisms10030659.

Gomez, G.G.F., Lippert, F., Ando, M., Zandona, A.F., Eckert, G.J. and Gregory, R.L. (2019) 'Photoinhibition of streptococcus mutans biofilm-induced lesions in human dentin by violet-blue light', *Dentistry Journal*, 7(4), 113. Available at: https://doi.org/10.3390/DJ7040113.

Goodman, E.R., Piatt, R., Bass, R., Onderdonk, A.B., Yokoe, D.S. and Huang, S.S. (2008) 'Impact of an environmental cleaning intervention on the presence of methicillin-resistant *Staphylococcus aureus* and vancomycin-resistant *Enterococci* on surfaces in

intensive care unit rooms', *Infection Control & Hospital Epidemiology*, 29(7), pp. 593–599. Available at: https://doi.org/10.1086/588566.

Gorr, S.U. (2009) 'Antimicrobial peptides of the oral cavity', *Periodontology 2000*, 51(1), pp. 152–180. Available at: https://doi.org/10.1111/j.1600-0757.2009.00310.x.

Gorwitz, R.J., Kruszon-Moran, D., McAllister, S.K., McQuillan, G., McDougal, L.K., Fosheim, G.E., Jensen, B.J., Killgore, G., Tenover, F.C. and Kuehnert, M.J. (2008) 'Changes in the prevalence of nasal colonization with *Staphylococcus aureus* in the United States, 2001-2004', *Journal of Infectious Diseases*, 197(9), pp. 1226–1234. Available at: https://doi.org/10.1086/533494.

Goto, M. and Al-Hasan, M. (2013) 'Overall burden of bloodstream infection and nosocomial bloodstream infection in North America and Europe', *Clinical Microbiology and Infection*, 19(6), pp. 501-509. Available at: https://doi.org/ 10.1111/1469-0691.12195.

Goyal, S.M., Chander, Y., Yezli, S. and Otter, J.A. (2014) 'Evaluating the virucidal efficacy of hydrogen peroxide vapour', *Journal of Hospital Infection*, 86(4), pp. 255–259. Available at: https://doi.org/10.1016/j.jhin.2014.02.003.

Griendling, K.K., Touyz, R.M., Zweier, J.L., Dikalov, S., Chilian, W., Chen, Y.R., Harrison, D.G. and Bhatnagar, A. (2016) 'Measurement of reactive oxygen species, reactive nitrogen species, and redox-dependent signalling in the cardiovascular system: A scientific statement from the American Heart Association', *Circulation Research*, 119(5), pp. 39–75. Available at: https://doi.org/10.1161/RES.0000000000000110.

Grogan, M.D., Bartow-McKenney, C., Flowers, L., Knight, S.A.B., Uberoi, A. and Grice, E.A. (2019) 'Research techniques made simple: Profiling the skin microbiota', *Journal of Investigative Dermatology,* 139(4), pp. 747-752. Available at: https://doi.org/10.1016/j.jid.2019.01.024.

Gruber, I., Heudorf, U., Werner, G., Pfeifer, Y., Imirzalioglu, C., Ackermann, H., Brandt, C., Besier, S. and Wichelhaus, T.A. (2013) 'Multidrug-resistant bacteria in geriatric clinics, nursing homes, and ambulant care - Prevalence and risk factors', *International Journal of Medical Microbiology*, 303(8), pp. 405–409. Available at: https://doi.org/10.1016/j.ijmm.2013.05.002.

Guffey, J.S., Payne, W., Jones, T. and Martin, K. (2013) 'Evidence of resistance development by *Staphylococcus aureus* to an in vitro, multiple stage application of 405 nm light from a supraluminous diode array', *Photomedicine and Laser Surgery*, 31(4), pp. 179–182. Available at: https://doi.org/10.1089/pho.2012.3450.

Guffey, J.S. and Wilborn, J. (2006) 'Effects of combined 405-nm and 880-nm light on *Staphylococcus aureus* and *Pseudomonas aeruginosa* in vitro', *Photomedicine And Laser Surgery*, 24(6), pp. 680–683. Available at: https://doi.org/10.1089/PHO.2006.1028.

Guffey, S. and Wilborn, J. (2007) 'In vitro bactericidal effects of 405-nm and 470-nm blue light', *Photomedicine and Laser Surgery*, 24(6), pp. 684–688. Available at: https://doi.org/10.1089/PHO.2006.24.684.

Güzel Tunccan, Ö., Kalkanci, A., Unal, E.A., Abdulmajed, O., Erdoğan, M., Dizbay, M. and Çaglar, K. (2018) 'The in vitro effect of antimicrobial photodynamic therapy on *Candida* and *Staphylococcus* biofilms', *Turkish Journal of Medical Sciences*, 48(4), pp. 873–879. Available at: https://doi.org/10.3906/sag-1803-44.

El Haddad, L., Ghantoji, S.S., Stibich, M., Fleming, J.B., Segal, C., Ware, K.M. and Chemaly, R.F. (2017) 'Evaluation of a pulsed xenon ultraviolet disinfection system to decrease bacterial contamination in operating rooms', *BMC Infectious Diseases*, 17(1), 672. Available at: https://doi.org/10.1186/s12879-017-2792-z.

Haley, R.W., Culver, D.H., White, J.W., Morgan, W.M., Emori, T.G., Munn, V.P. and Hooton, T.M. (1985) 'The efficacy of infection surveillance and control programs in preventing nosocomial infections in US hospitals', *American Journal of Epidemiology*, 121(2), pp. 182–205. Available at: https://doi.org/10.1093/oxfordjournals.aje.a113990.

Hall, L., Otter, J.A., Chewins, J. and Wengenack, N.L. (2007) 'Use of hydrogen peroxide vapor for deactivation of *Mycobacterium tuberculosis* in a biological safety cabinet and a room', *Journal of Clinical Microbiology*, 45(3), pp. 810–815. Available at: https://doi.org/10.1128/JCM.01797-06.

Halstead, F.D., Thwaite, J.E., Burt, R., Laws, T.R., Raguse, M., Moeller, R., Webber, M.A. and Oppenheim, B.A. (2016) 'Antibacterial activity of blue light against nosocomial wound pathogens growing planktonically and as mature biofilms', *Applied and Environmental Microbiology*, 82(13), pp. 4006–4016. Available at: https://doi.org/10.1128/AEM.00756-16.

Hamblin, M.R. and Hasan, T. (2004) 'Photodynamic therapy: a new antimicrobial approach to infectious disease?', *Photochemical & Photobiological Sciences*, 3(5), pp. 436–450. Available at: https://doi.org/10.1039/b311900a.

Hamblin, M.R., Viverios, C., Yang, A., Ahmadi, R., Ganz, A. and Tolkoff, M.J. (2005) '*Helicobacter pylori* accumulates photoactive porphyrins and is killed by visible light', *Current Opinion in Microbiology*, 49(7), pp. 2822–2827. Available at: https://doi.org/10.1128/AAC.49.7.2822-2827.2005.

Hanberger, H., Walther, S., Leone, M., Barie, P.S., Rello, J., Lipman, J., Marshall, J.C., Anzueto, A., Sakr, Y., Pickkers, P., Felleiter, P., Engoren, M. and Vincent, J.L. (2011) 'Increased mortality associated with methicillin-resistant *Staphylococcus aureus* (MRSA) infection in the intensive care unit: Results from the EPIC II study', *International Journal of Antimicrobial Agents*, 38(4), pp. 331–335. Available at: https://doi.org/10.1016/j.ijantimicag.2011.05.013.

Harkins, C.P., Pichon, B., Doumith, M., Parkhill, J., Westh, H., Tomasz, A., de Lencastre, H., Bentley, S.D., Kearns, A.M. and Holden, M.T.G. (2017) 'Methicillin-resistant *Staphylococcus aureus* emerged long before the introduction of methicillin into clinical practice', *Genome Biology*, 18, 130. Available at: https://doi.org/10.1186/s13059-017-1252-9.

Hayden, M.K., Blow, D.W., Lyle, E.A., Moore, C.G. and Weinstein, R.A. (2008) 'Risk of hand or glove contamination after contact with patients colonized with vancomycin-resistant *Enterococcus* or the colonized patients' environment', *Infection Control & Hospital Epidemiology*, 29(2), pp. 149–154. Available at: https://doi.org/10.1086/524331.

He, Y., Pang, J., Yang, Z., Zheng, M., Yu, Y., Liu, Z., Zhao, B., Hu, G. and Yin, R. (2022) 'Toluidine blue O-induced photoinactivation inhibit the biofilm formation of methicillin-resistant *Staphylococcus aureus*', *Photodiagnosis and Photodynamic Therapy*, 39, 102902. Available at: https://doi.org/10.1016/j.pdpdt.2022.102902.

Health Protection Scotland (2012). *Scottish National Point Prevalence Survey of Healthcare Associated Infection and Antimicrobial Prescribing 2011*. Available at: https://www.nss.nhs.scot/publications/national-point-prevalence-survey-of-healthcare-associated-infection-and-antimicrobial-prescribing-2016/ (Accessed: March 2020).

Health Protection Scotland (2017a). *Literature Review and Practice Recommendations: Existing and emerging technologies used for decontamination of the healthcare environment: HINS light*. Available at: https://www.nss.nhs.scot/publications/literature-review-and-practice-recommendations-existing-and-emerging-technologies-for-decontamination-of-the-health-and-care-environment-hins-light-v10/ (Accessed: March 2020).

Health Protection Scotland (2017b). *Literature Review and Practice Recommendations: Existing and emerging technologies used for decontamination of the healthcare environment: Chlorine Dioxide*. https://www.nss.nhs.scot/publications/literature-review-and-practice-recommendations-existing-and-emerging-technologies-for-decontamination-of-the-health-and-care-environment-chlorine-dioxide-v10/ (Accessed: April 2020).

Health Protection Scotland (2017c). *Literature Review and Practice Recommendations: Existing and emerging technologies used for decontamination of the healthcare environment: Ozone*. Available at: https://www.nss.nhs.scot/publications/literature-review-and-practice-recommendations-existing-and-emerging-technologies-used-for-decontamination-of-the-healthcare-environment-ozone (Accessed: April 2020).

Health Protection Scotland (2017d). *National Point Prevalence Survey of Healthcare Associated Infections and Antimicrobial Prescribing 2016*. Available at: https://www.nss.nhs.scot/publications/national-point-prevalence-survey-of-healthcare-associated-infection-and-antimicrobial-prescribing-2016 *(Accessed: April 2020).*

Health Protection Scotland (2019). *Healthcare Associated Infection Annual Report 2018*. Available at: https://www.nss.nhs.scot/publications/hai-annual-report-2018 (Accessed: April 2020).

Healthcare Associated Infection Task Force (2009). *The NHSScotland National Cleaning Services Specification*. Available at: https://www.nss.nhs.scot/media/1969/shfn-01-02-v50-jun-2016.pdf (Accessed: July 2020).

Heilingloh, C.S., Aufderhorst, U.W., Schipper, L., Dittmer, U., Witzke, O., Yang, D., Zheng, X., Sutter, K., Trilling, M., Alt, M., Steinmann, E. and Krawczyk, A. (2020) 'Susceptibility of SARS-CoV-2 to UV irradiation', *American Journal of Infection Control*, 48(10), pp. 1273–1275. Available at: https://doi.org/10.1016/j.ajic.2020.07.031.

Henderson, B.W. and Miller, A.C. (1986) 'Effects of scavengers of reactive oxygen and radical species on cell survival following photodynamic treatment in vitro: Comparison to ionizing radiation', *Journal of Radiation Research*, 108(2), pp. 196–205.

Herruzo, R., Vizcaíno, M.J. and Herruzo, I. (2014) 'Quantifying Glosair™ 400 efficacy for surface disinfection of American Type Culture Collection strains and micro-organisms recently isolated from intensive care unit patients', *Journal of Hospital Infection*, 87(3), pp. 175–178. Available at: https://doi.org/10.1016/j.jhin.2014.04.006.

Hessling, M., Haag, R., Sieber, N. and Vatter, P. (2021) 'The impact of far-UVC radiation (200-230 nm) on pathogens, cells, skin, and eyes-a collection and analysis of a hundred years of data', *GMS Hygiene and Infection Control*, 16, 7. Available at: https://doi.org/10.3205/dgkh000378.

Hessling, M., Lau, B. and Vatter, P. (2022) 'Review of virus inactivation by visible light', *Photonics*, 9(2), 113. Available at: https://doi.org/10.3390/photonics9020113.

HM Government (2019). *Tackling antimicrobial resistance 2019 to 2024*. Available at: https://assets.publishing.service.gov.uk/media/6261392d8fa8f523bf22ab9e/UK_AMR_5_year_national_action_plan.pdf (Accessed: August 2020).

Hoenes, K., Bauer, R., Meurle, T., Spellerberg, B. and Hessling, M. (2021) 'Inactivation effect of violet and blue light on ESKAPE pathogens and closely related non-pathogenic bacterial species – A promising tool against antibiotic-sensitive and antibiotic-resistant microorganisms', *Frontiers in Microbiology*, 11, 612367. Available at: https://doi.org/10.3389/fmicb.2020.612367.

Holmdahl, T., Lanbeck, P., Wullt, M. and Walder, M.H. (2011) 'A head-to-head comparison of hydrogen peroxide vapor and aerosol room decontamination systems.', *Infection Control & Hospital Epidemiology*, 32(9), pp. 831–836. Available at: https://doi.org/10.1086/661104.

HSE (2020). EH40/2005 Workplace exposure limits (Fourth Edition 2020). Available at: https://www.hse.gov.uk/pubns/books/eh40.htm (Accessed: March 2021).

Hu, B., Guo, H., Zhou, P. and Shi, Z.L. (2021) 'Characteristics of SARS-CoV-2 and COVID-19', *Nature Reviews Microbiology*, 19, pp. 141–154. Available at: https://doi.org/10.1038/s41579-020-00459-7.

Huang, N., Pérez, P., Kato, T., Mikami, Y., Okuda, K., Gilmore, R.C., Conde, C.D., Gasmi, B., Stein, S., Beach, M., Pelayo, E., Maldonado, J.O., Lafont, B.A., Jang, S.-I., Nasir, N., Padilla, R.J., Murrah, V.A., Maile, R., Lovell, W., Wallet, S.M., Bowman, N.M., Meinig, S.L., Wolfgang, M.C., Choudhury, S.N., Novotny, M., Aevermann, B.D., Scheuermann, R.H., Cannon, G., Anderson, C.W., Lee, R.E., Marchesan, J.T., Bush, M., Freire, M., Kimple, A.J., Herr, D.L., Rabin, J., Grazioli, A., Das, S., French, B.N., Pranzatelli, T., Chiorini, J.A., Kleiner, D.E., Pittaluga, S., Hewitt, S.M., Burbelo, P.D., Chertow, D., Frank, K., Lee, J., Boucher, R.C., Teichmann, S.A., Warner, B.M. and Byrd, K.M. (2021) 'SARS-CoV-2 infection of the oral cavity and saliva', *Nature Medicine*, 27(5), pp. 892–903. Available at: https://doi.org/10.1038/s41591-021-01296-8.

Huang, S.S., Datta, R. and Platt, R. (2006) 'Risk of acquiring antibiotic-resistant bacteria from prior room occupants', *Archives of Internal Medicine*, 166(18), pp. 1945–1951. Available at: https://doi.org/ 10.1001/archinte.166.18.1945.

Hubbell Lighting (2020) *SpectraClean*. Available at: https://www.hubbell.com/hubbelllightingci/en/spectraclean (Accessed: June 2021).

Hunter, J. (2012) 'Ventilator associated pneumonia', *BMJ*, 344, e3325. Available at: https://doi.org/10.1136/bmj.e3325.

Huslage, K., Rutala, William A, Sickbert-Bennett, E. and Weber, D.J. (2010) 'A Quantitative Approach to Defining "High-Touch" Surfaces in Hospitals', *Infection Control & Hospital Epidemiology*, 31(8), pp. 850–853. Available at: https://doi.org/10.1086/655016.

ICNIRP. (2013) 'ICNIRP guidelines on limits of exposure to incoherent visible and infrared radiation', *Health Physics*, 105(1), pp. 74–96. Available at: https://doi.org/10.1097/HP.0b013e318289a611.

Imlay, J.A. (2019) 'Where in the world do bacteria experience oxidative stress?', *Environmental Microbiology*, 21(2), pp. 521–530. Available at: https://doi.org/10.1111/1462-2920.14445.

Inagaki, H., Saito, A., Sugiyama, H., Okabayashi, T. and Fujimoto, S. (2020) 'Rapid inactivation of SARS-CoV-2 with Deep-UV LED irradiation', *Emerging Microbes and Infections*, 9, pp. 1744–1747. Available at: https://doi.org/10.1080/22221751.2020.1796529.

International Health Facility Guidelines (2022) *Infection Control.* Available at: https://healthfacilityguidelines.com/ViewPDF/ViewIndexPDF/iHFG_part_d_complete (Accessed: February 2023).

Jamal, M., Ahmad, W., Andleeb, S., Jalil, F., Imran, M., Nawaz, M.A., Hussain, T., Ali, M., Rafiq, M. and Kamil, M.A. (2018) 'Bacterial biofilm and associated infections', *Journal of the Chinese Medical Association*, 81(1), pp. 7–11. Available at: https://doi.org/10.1016/j.jcma.2017.07.012.

Jeffet, U., Shimon, R. and Sterer, N. (2020) 'Effect of high intensity blue light on *Fusobacterium nucleatum* membrane integrity', *Photochemistry and Photobiology*, 96(1), pp. 178–181. Available at: https://doi.org/10.1111/php.13151.

Jefri, U.H.N.M., Khan, A., Lim, Y.C., Lee, K.S., Liew, K. Bin, Kassab, Y.W., Choo, C.Y., Al-Worafi, Y.M., Ming, L.C. and Kalusalingam, A. (2022) 'A systematic review on chlorine dioxide as a disinfectant', *Journal of Medicine and Life*, 15(3), pp. 313–318. Available at: https://doi.org/10.25122/jml-2021-0180.

Jin, R.-Y, Hu, S.-Q, Zhang, Y.-G and Bo, T. (2009) 'Concentration-dependence of the explosion characteristics of chlorine dioxide gas', *Journal of Hazardous Materials*, 166(2–3), pp. 842–847. Available at: https://doi.org/10.1016/j.jhazmat.2008.11.124.

Jinadatha, C., Quezada, R., Huber, T.W., Williams, J.B., Zeber, J.E. and Copeland, L.A. (2014) 'Evaluation of a pulsed-xenon ultraviolet room disinfection device for impact on contamination levels of methicillin-resistant *Staphylococcus aureus*', *BMC Infectious Diseases*, 14, 187. Available at: https://doi.org/10.1186/1471-2334-14-187.

Johani, K., Abualsaud, D., Costa, D.M., Hu, H., Whiteley, G., Deva, A. and Vickery, K. (2018) 'Characterization of microbial community composition, antimicrobial resistance and biofilm on intensive care surfaces', *Journal of Infection and Public Health*, 11(3), pp. 418–424. Available at: https://doi.org/10.1016/j.jiph.2017.10.005.

Jori, G., Fabris, C., Soncin, M., Ferro, S., Coppellotti, O., Dei, D., Fantetti, L., Chiti, G. and Roncucci, G. (2006) 'Photodynamic therapy in the treatment of microbial infections: Basic principles and perspective applications', *Lasers in Surgery and Medicine*, 38(5), pp. 468–481. Available at: https://doi.org/10.1002/lsm.20361.

Josefsen, L.B. and Boyle, R.W. (2008) 'Photodynamic therapy and the development of metal-based photosensitisers', *Metal-Based Drugs*, 2008, 276109. Available at: https://doi.org/10.1155/2008/276109.

Kaidzu, S., Sugihara, K., Sasaki, M., Nishiaki, A., Igarashi, T. and Tanito, M. (2019) 'Evaluation of acute corneal damage induced by 222-nm and 254-nm ultraviolet light in Sprague–Dawley rats', *Free Radical Research*, 53(6), pp. 611–617. Available at: https://doi.org/10.1080/10715762.2019.1603378.

Kalanuria, A., Zai, W. and Mirki, M. (2014) 'Ventilator-associated pneumonia in the ICU', Critical *Care*, 18, 208. Available at: https://doi.org/10.1186/cc13775.

Karaböce, B., Saban, E., Aydın Böyük, A., Okan Durmuş, H., Hamid, R. and Baş, A. (2022) 'Inactivation of viruses on surfaces by infrared techniques', *International Journal of Thermal Sciences*, 179, 107595. Available at: https://doi.org/10.1016/j.ijthermalsci.2022.107595.

Kasloff, S.B., Leung, A., Strong, J.E., Funk, D. and Cutts, T. (2021) 'Stability of SARS-CoV-2 on critical personal protective equipment', *Scientific Reports*, 11, 984. Available at: https://doi.org/10.1038/s41598-020-80098-3.

Katzenberger, R.H., Rösel, A. and Vonberg, R.P. (2021) 'Bacterial survival on inanimate surfaces: a field study', *BMC Research Notes*, 14, 97. Available at: https://doi.org/10.1186/s13104-021-05492-0.

Kelly, S., Schnugh, D. and Thomas, T. (2022) 'Effectiveness of ultraviolet-C vs aerosolized hydrogen peroxide in ICU terminal disinfection', *Journal of Hospital Infection*, 121, pp. 114–119. Available at: https://doi.org/10.1016/j.jhin.2021.12.004.

Kenall Manufacturing. (2017) *Indigo-Clean*. Available at: https://kenall.com/Indigo-Clean (Accessed: June 2020).

Kennedy, J.C. and Pottier, R.H. (1992) 'New trends in photobiology: Endogenous protoporphyrin IX, a clinically useful photosensitizer for photodynamic therapy', *Journal of Photochemistry and Photobiology B: Biology*, 14(4), pp. 275–292. Available at: https://doi.org/https://doi.org/10.1016/1011-1344(92)85108-7.

Kessel, D. and Oleinick, N.L. (2009) 'Initiation of autophagy by photodynamic therapy', *Methods in Enzymology*, 453(1), pp. 1–16. Available at: https://doi.org/10.1038/jid.2014.371.

Khan, H.A., Ahmad, A. and Mehboob, R. (2015) 'Nosocomial infections and their control strategies', *Asian Pacific Journal of Tropical Biomedicine*, 5(7), pp. 509–514. Available at: https://doi.org/10.1016/j.apjtb.2015.05.001.

Khan, H.A., Baig, F.K. and Mehboob, R. (2017) 'Nosocomial infections: Epidemiology, prevention, control and surveillance', *Asian Pacific Journal of Tropical Biomedicine*, 7(5), pp. 478–482. Available at: https://doi.org/10.1016/j.apjtb.2017.01.019.

Khan, R., Petersen, F.C. and Shekhar, S. (2019) 'Commensal bacteria: An emerging player in defense against respiratory pathogens', *Frontiers in Immunology*, 10, 1203. Available at: https://doi.org/10.3389/fimmu.2019.01203.

Kim, D.-K and Kang, D.-H. (2020) 'Effect of surface characteristics on the bactericidal efficacy of UVC LEDs', *Food Control*, 108, 106869. Available at: https://doi.org/10.1016/j.foodcont.2019.106869.

Kim, D.-K. and Kang, D.-H. (2021) 'Efficacy of light-emitting diodes emitting 395, 405, 415, and 425 nm blue light for bacterial inactivation and the microbicidal mechanism', *Food Research International*, 141, 110105. Available at: https://doi.org/10.1016/j.foodres.2021.110105.

Kim, M.-J. and Yuk, H.-G. (2017a) 'Antibacterial mechanism of 405-nanometer light-emitting diode against *Salmonella* at Refrigeration Temperature', *Applied and Environmental Microbiology*, 83(5), e02582-16. Available at: https://doi.org/10.1128/AEM.02582-16.

King, M.F., Wilson, A.M., Weir, M.H., López-García, M., Proctor, J., Hiwar, W., Khan, A., Fletcher, L.A., Sleigh, P.A., Clifton, I., Dancer, S.J., Wilcox, M., Reynolds, K.A. and Noakes, C.J. (2022) 'Modeling fomite-mediated SARS-CoV-2 exposure through

personal protective equipment doffing in a hospital environment', *Indoor Air*, 32(1), e12938. Available at: https://doi.org/10.1111/ina.12938.

Kingsley, D.H., Perez-Perez, R.E., Boyd, G., Sites, J. and Niemira, B.A. (2017) 'Evaluation of 405-nm monochromatic light for inactivation of Tulane virus on blueberry surfaces', *Journal of Applied Microbiology*, 124(4), pp. 1017–1022. Available at: https://doi.org/10.1111/jam.13638.

Kitagawa, H., Nomura, T., Nazmul, T., Omori, K., Shigemoto, N., Sakaguchi, T. and Ohge, H. (2021) 'Effectiveness of 222-nm ultraviolet light on disinfecting SARS-CoV-2 surface contamination', *American Journal of Infection Control*, 49(3), pp. 299–301. Available at: https://doi.org/10.1016/j.ajic.2020.08.022.

Koenig, S. and Truwit, J. (2006) 'Ventilator-associated pneumonia: Diagnosis, treatment, and prevention', *Clinical Microbiology Reviews*, 19(4), pp. 637-657. Available at https://doi.org/10.1128/cmr.00051-05.

Kohli, R. (2018) 'Applications of dry vapor steam cleaning technique for removal of surface contaminants', in Kohli, R. and Mittal, K.L. (eds.) *Developments in Surface Contamination and Cleaning: Applications of Cleaning Techniques Volume 11*. Elsevier, pp. 681–702. Available at: https://doi.org/10.1016/B978-0-12-815577-6.00017-7.

van der Kooi, T.I.I., de Boer, A.S., Manniën, J., Wille, J.C., Beaumont, M.T., Mooi, B.W. and van den Hof, S. (2007) 'Incidence and risk factors of device-associated infections and associated mortality at the intensive care in the Dutch surveillance system', *Intensive Care Medicine*, 33(2), pp. 271–278. Available at: https://doi.org/10.1007/s00134-006-0464-3.

Kramer, A. and Assadian, O. (2014) 'Survival of microorganisms on inanimate surfaces', in Borkow, G. (ed.) *Use of Biocidal Surfaces for Reduction of Healthcare Acquired Infections*. Springer, pp. 7–26. Available at: https://doi.org/10.1007/978-3-319-08057-4_2.

Kramer, A., Schwebke, I. and Kampf, G. (2006) 'How long do nosocomial pathogens persist on inanimate surfaces? A systematic review', *BMC Infectious Diseases*, 6, pp. 1–8. Available at: https://doi.org/10.1186/1471-2334-6-130.

Krisko, A. and Radman, M. (2010) 'Protein damage and death by radiation in *Escherichia coli* and *Deinococcus radiodurans'*, *Proceedings of the National Academy of Sciences of the United States of America*, 107(32), pp. 14373–14377. Available at: https://doi.org/10.1073/pnas.1009312107.

Kruszewska-Naczk, B., Grinholc, M., Waleron, K., Bandow, J.E. and Rapacka-Zdończyk, A. (2023) 'Can antimicrobial blue light contribute to resistance development? Genome-wide analysis revealed aBL-protective genes in *Escherichia coli*', *Microbiology Spectrum,* 12(1), e02490-23. Available at: https://doi.org/10.1128/spectrum.02490-23.

Kuchařová, M., Hronek, M., Rybáková, K., Zadák, Z., Štětina, R., Josková, V. and Patková, A. (2019) 'Comet assay and its use for evaluating oxidative DNA damage in some pathological states', *Physiological Research*, 68, pp. 1–15. Available at: https://doi.org/10.33549/physiolres.933901.

Kucheria, R., Dasgupta, P., Sacks, S.H., Khan, M.S. and Sheerin, M.S. (2005) 'Urinary tract infections: New insights into a common problem', Postgraduate Medical Journal, 81(952), pp. 83-86. Available at: https://doi.org/10.1136/pgmj.2004.023036.

Van Kuijk, F.J.G.M. (1991) 'Effects of ultraviolet light on the eye: Role of protective glasses', *Environmental Health Perspectives*, 96(30), pp. 177–184. Available at: https://doi.org/10.1289/ehp.9196177.

Kumar, A., Ghate, V., Kim, M.J., Zhou, W., Khoo, G.H. and Yuk, H.G. (2015) 'Kinetics of bacterial inactivation by 405 nm and 520 nm light emitting diodes and the role of endogenous coproporphyrin on bacterial susceptibility', *Journal of Photochemistry and Photobiology B: Biology*, 149, pp. 37–44. Available at: https://doi.org/10.1016/j.jphotobiol.2015.05.005.

Lachiewicz, A.M., Hauck, C.G., Weber, D.J., Cairns, B.A. and Van Duin, D. (2017) 'Bacterial infections after burn injuries: Impact of multidrug resistance', *Clinical Infectious Diseases*, 65(12), pp. 2130–2136. Available at: https://doi.org/10.1093/cid/cix682.

Lai, Y. and Gallo, R.L. (2010) 'Commensal skin bacteria as the probiotic of the cutaneous immune response', *Expert Review of Dermatology*, 5(3), pp. 251–253. Available at: https://doi.org/10.1586/edm.10.24.

Lamers, M.M. and Haagmans, B.L. (2022) 'SARS-CoV-2 pathogenesis', *Nature Reviews Microbiology*, 20, pp. 270–284. Available at: https://doi.org/10.1038/s41579-022-00713-0.

Latka, A. and Drulis-Kawa, Z. (2020) 'Advantages and limitations of microtiter biofilm assays in the model of antibiofilm activity of *Klebsiella* phage KP34 and its depolymerase', *Scientific Reports*, 10(1), 20338. Available at: https://doi.org/10.1038/s41598-020-77198-5.

Lau, B., Becher, D. and Hessling, M. (2021) 'High intensity violet light (405 nm) inactivates coronaviruses in phosphate buffered saline (PBS) and on surfaces', *Photonics*, 8(10), 414. Available at: https://doi.org/10.3390/photonics8100414.

Laue, M., Kauter, A., Hoffmann, T., Möller, L., Michel, J. and Nitsche, A. (2021) 'Morphometry of SARS-CoV and SARS-CoV-2 particles in ultrathin plastic sections of infected Vero cell cultures', *Scientific Reports*, 11(1), 3515. Available at: https://doi.org/10.1038/s41598-021-82852-7.

Leanse, L.G., Harrington, O.D., Fang, Y., Ahmed, I., Goh, X.S. and Dai, T. (2018) 'Evaluating the potential for resistance development to antimicrobial blue light (at 405 nm) in gram-negative bacteria: And in vivo studies', *Frontiers in Microbiology*, 9, 2403. Available at: https://doi.org/10.3389/fmicb.2018.02403.

Ledwoch, K., Dancer, S.J., Otter, J.A., Kerr, K., Roposte, D., Rushton, L., Weiser, R., Mahenthiralingam, E., Muir, D.D. and Maillard, J.Y. (2018a) 'Beware biofilm! Dry biofilms containing bacterial pathogens on multiple healthcare surfaces; a multi-centre study', *Journal of Hospital Infection*, 100(3), pp. 47–56. Available at: https://doi.org/10.1016/j.jhin.2018.06.028.

Lee, A., De Lencastre, H., Garau, J., Kluytmans, J., Malhotra-Kumar, S., Peschel, A. and Harbarth, S. (2018) 'Methicillin-resistant Staphylococcus aureus', *Nature Reviews Disease Primers,* 4, 18033. Available at: https://doi.org/ 10.1038/nrdp.2018.33.

Lee Ventola, C. (2015) 'The antibiotic resistance crisis'*, Pharmacy and Therapeutics,* 40(4), 277-283.

Legeay, C., Bourigault, C., Lepelletier, D. and Zahar, J.R. (2015) 'Prevention of healthcare-associated infections in neonates: Room for improvement', *Journal of Hospital Infection*, 89(4), pp. 319–323. Available at: https://doi.org/10.1016/j.jhin.2015.02.003.

Lesage, S., Xu, H. and Durham, L. (1993) 'The occurrence and roles of porphyrins in the environment: possible implications for bioremediation', *Hydrological Sciences Journal*, 38(4), pp. 343–354. Available at: https://doi.org/10.1080/02626669309492679.

Leung, N.H.L. (2021) 'Transmissibility and transmission of respiratory viruses', *Nature Reviews Microbiology*, 19, pp. 528–545. Available at: https://doi.org/10.1038/s41579-021-00535-6.

Li, X., Kim, M.J., Bang, W.S. and Yuk, H.G. (2018) 'Anti-biofilm effect of 405-nm LEDs against *Listeria monocytogenes* in simulated ready-to-eat fresh salmon storage conditions', *Food Control*, 84, pp. 513–521. Available at: https://doi.org/10.1016/J.FOODCONT.2017.09.006.

Li, Y.J., Zhu, N., Jia, H.Q., Wu, J.H., Yi, Y. and Qi, J.C. (2012) 'Decontamination of *Bacillus subtilis* var. *niger* spores on selected surfaces by chlorine dioxide gas', *Journal of Zhejiang University: Science B*, 13(4), pp. 254–260. Available at: https://doi.org/10.1631/jzus.b1100289.

Lim, V.K. (1997) 'Prevention of infection in the immunocompromised', *Annals of the Academy of Medicine in Singapore*, 26(3), pp. 331–335.

Linley, E., Denyer, S.P., McDonnell, G., Simons, C. and Maillard, J.Y. (2012) 'Use of hydrogen peroxide as a biocide: new consideration of its mechanisms of biocidal action', *Journal of Antimicrobial Chemotherapy*, 67(7), pp. 1589–1596. Available at: https://doi.org/10.1093/jac/dks129.

Liu, J., Zhou, L., Chen, J.H., Mao, W., Li, W.J., Hu, W., Wang, S.Y. and Wang, C.M. (2014) 'Role of ozone in UV-C disinfection, demonstrated by comparison between wild-type and mutant conidia of *Aspergillus niger'*, *Photochemistry and Photobiology*, 90(3), pp. 615–621. Available at: https://doi.org/10.1111/php.12217.

Lockley, S.W., Brainard, G.C. and Czeisler, C.A. (2003) 'High sensitivity of the human circadian melatonin rhythm to resetting by short wavelength light', *Journal of Clinical Endocrinology and Metabolism*, 88(9), pp. 4502–4505. Available at: https://doi.org/10.1210/jc.2003-030570.

Lorca-Oró, C., Vila, J., Pleguezuelos, P., Vergara-Alert, J., Rodon, J., Majó, N., López, S., Segalés, J., Saldaña-Buesa, F., Visa-Boladeras, M., Veà-Baró, A., Campistol, J.M. and Abad, X. (2022) 'Rapid SARS-CoV-2 inactivation in a simulated hospital room using a mobile and autonomous robot emitting ultraviolet-C light', *Journal of Infectious Diseases*, 225(4), pp. 587–592. Available at: https://doi.org/10.1093/infdis/jiab551.

Lowe, J.J., Gibbs, S.G., Iwen, P.C., Smith, P.W. and Hewlett, A.L. (2013) 'Impact of chlorine dioxide gas sterilization on nosocomial organism viability in a hospital room', *International Journal of Environmental Research and Public Health*, 10(6), pp. 2596–2605. Available at: https://doi.org/10.3390/ijerph10062596.

Ma, Y., Hu, W., Ruan, M., Zhan, Z., Zhang, Y. and Hu, C. (2023) 'Electrochemical monitoring of intracellular reactive oxygen species based on automated nanoprobe platform', *2023 IEEE International Conference on Manipulation, Manufacturing and Measurement on the Nanoscale (3M-NANO),* Chendu, China, 31 Jul – 4 Aug 2023. Available at: https://doi.org/10.1109/3M-NANO58613.2023.10305373.

Maclean, M. (2006). *An investigation into the light inactivation of medically important microorganisms.* PhD Thesis. University of Strathclyde. Available at: https://stax.strath.ac.uk/concern/theses/zg64tk959?locale=en (Accessed: December 2019).

Maclean, M., Anderson, J.G., MacGregor, S.J., White, T. and Atreya, C.D. (2016) 'A new proof of concept in bacterial reduction: Antimicrobial action of violet-blue light (405 nm) in ex vivo stored plasma', *Journal of Blood Transfusion*, 2016, 2920514. Available at: https://doi.org/10.1155/2016/2920514.

Maclean, M., Gelderman, M.P., Kulkarni, S., Tomb, R.M., Stewart, C.F., Anderson, J.G., MacGregor, S.J. and Atreya, C.D. (2020) 'Non-ionizing 405 nm Light as a potential bactericidal technology for platelet safety: Evaluation of in vitro bacterial inactivation and in vivo platelet recovery in severe combined immunodeficient mice', *Frontiers in Medicine*, 6, 331. Available at: https://doi.org/10.3389/fmed.2019.00331.

Maclean, M., MacGregor, S.J., Anderson, J.G. and Woolsey, G. (2009) 'Inactivation of bacterial pathogens following exposure to light from a 405-nanometer light-emitting diode array', *Applied and Environmental Microbiology*, 75(7), pp. 1932–1937. Available at: https://doi.org/10.1128/AEM.01892-08.

Maclean, M., MacGregor, S.J., Anderson, J.G. and Woolsey, G.A. (2008a) 'High-intensity narrow-spectrum light inactivation and wavelength sensitivity of *Staphylococcus aureus*', *FEMS Microbiology Letters*, 285(2), pp. 227–232. Available at: https://doi.org/10.1111/j.1574-6968.2008.01233.x.

Maclean, M., MacGregor, S.J., Anderson, J.G. and Woolsey, G.A. (2008b) 'The role of oxygen in the visible-light inactivation of *Staphylococcus aureus'*, *Journal of Photochemistry and Photobiology B: Biology*, 92(3), pp. 180–184.

Maclean, M., MacGregor, S.J., Anderson, J.G., Woolsey, G.A., Coia, J.E., Hamilton, K., Taggart, I., Watson, S.B., Thakker, B. and Gettinby, G. (2010) 'Environmental decontamination of a hospital isolation room using high-intensity narrow-spectrum light', *Journal of Hospital Infection*, 76(3), pp. 247–251. Available at: https://doi.org/10.1016/j.jhin.2010.07.010.

Maclean, M, MacGregor, S.J., Anderson, J.G., Woolsey, G.A., Coia, J.E., Hamilton, K., Taggart, I., Watson, S.B., Thakker, B. and Gettinby, G. (2013a) 'Continuous decontamination of an intensive care isolation room during patient occupancy using 405 nm light technology', *Journal of Infection Prevention*, 14(5), pp. 176–181. Available at: https://doi.org/10.1177/1757177413483646.

Maclean, M, Murdoch, L.E., MacGregor, S.J. and Anderson, J.G. (2013b) 'Sporicidal effects of high-intensity 405 nm visible light on endospore-forming bacteria', *Photochemistry and Photobiology*, 89(1), pp. 120–126. Available at: https://doi.org/10.1111/j.1751-1097.2012.01202.x.

Maclean, M., McKenzie, K., Anderson, J.G., Gettinby, G. and MacGregor, S.J. (2014) '405 nm light technology for the inactivation of pathogens and its potential role for environmental disinfection and infection control', *Journal of Hospital Infection*, 88(1), pp. 1–11. Available at: https://doi.org/https://doi.org/10.1016/j.jhin.2014.06.004.

Maclean, M., McKenzie, K., Moorhead, S., Tomb, R.M., Coia, J.E., MacGregor, S.J. and Anderson, J.G. (2015) 'Decontamination of the hospital environment: New technologies for infection control', *Current Treatment Options in Infectious Diseases*, 7(1), pp. 39–51. Available at: https://doi.org/10.1007/s40506-015-0037-5.

Mahida, N., Vaughan, N. and Boswell, T. (2013) 'First UK evaluation of an automated ultraviolet-C room decontamination device (Tru-D^{TM})', *Journal of Hospital Infection*, 84(4), pp. 332–335. Available at: https://doi.org/10.1016/j.jhin.2013.05.005.

Maillard, J.Y. and Centeleghe, I. (2023) 'How biofilm changes our understanding of cleaning and disinfection', *Antimicrobial Resistance and Infection Control*, 12, 96. Available at: https://doi.org/10.1186/s13756-023-01290-4.

Maisch, T. (2009) 'A new strategy to destroy antibiotic resistant microorganisms: antimicrobial photodynamic treatment.', *Mini-Reviews in Medicinal Chemistry*, 9(8), pp. 974–983. Available at: https://doi.org/10.2174/138955709788681582.

Maisch, T. (2015) 'Resistance in antimicrobial photodynamic inactivation of bacteria', *Photochemical and Photobiological Sciences*, 14(8), pp. 1518–1526. Available at: https://doi.org/10.1039/c5pp00037h.

Maknuna, L., Tran, V.N., Lee, B.I and Kang, H.W. (2023) 'Inhibitory effect of 405 nm laser light on bacterial biofilm in urethral stent', *Scientific Reports*, 13, 3908. Available at: https://doi.org/10.1038/s41598-023-30280-0.

Mandal, J., Acharya, N.S., Buddhapriya, D. and Parija, S.C. (2012) 'Antibiotic resistance pattern among common bacterial uropathogens with a special reference to ciprofloxacin resistant *Escherichia coli'*, *Indian Journal of Medical Research*, 136(5), pp. 842-849.

Manoukian, S., Stewart, S., Graves, N., Mason, H., Robertson, C., Kennedy, S., Pan, J., Kavanagh, K., Haahr, L., Adil, M., Dancer, S.J., Cook, B. and Reilly, J. (2021) 'Bed-days and costs associated with the inpatient burden of healthcare-associated infection in the UK', *Journal of Hospital Infection*, 114, pp. 43-50. Available at: https://doi.org/10.1016/j.jhin.2020.12.027.

Margomenou, L., Birkmyre, L., Piggott, J.R. and Paterson, A. (2000) 'Optimisation and validation of the "Strathclyde simulated mouth" for beverage flavour research', *Journal of the Institute of Brewing*, 106(2), pp. 101–106. Available at: https://doi.org/10.1002/j.2050-0416.2000.tb00045.x.

Matafonova, G.G., Batoev, V.B., Astakhova, S.A., Gómez, M. and Christofi, N. (2008) 'Efficiency of KrCl excilamp (222 nm) for inactivation of bacteria in suspension', *Letters in Applied Microbiology*, 47(6), pp. 508–513. Available at: https://doi.org/10.1111/j.1472-765X.2008.02461.x.

Matsumura, Y. and Ananthaswamy, H.N. (2004) 'Toxic effects of ultraviolet radiation on the skin', *Toxicology and Applied Pharmacology*, 195(3), pp. 298–308. Available at: https://doi.org/10.1016/j.taap.2003.08.019.

McDonald, R., MacGregor, S.J., Anderson, J.G., Maclean, M. and Grant, M.H. (2011) 'Effect of 405-nm high-intensity narrow-spectrum light on fibroblast-populated collagen lattices: an in vitro model of wound healing', *Journal of Biomedical Optics*, 16(4), 48003. Available at: https://doi.org/10.1117/1.3561903.

McDonald, R.S., Gupta, S., Maclean, M., Ramakrishnan, P., Anderson, J.G., MacGregor, S.J., Meek, R.M. and Grant, M.H. (2013) '405 nm light exposure of osteoblasts and inactivation of bacterial isolates from arthroplasty patients: potential for new disinfection applications?', *European Cells and Materials*, 7(25), pp. 204–214. Available at: https://doi.org/10.22203/ecm.v025a15.

McKenzie, K. (2014) Inactivation of foodborne pathogens and spoilage microorganisms by 405 nm light: An investigation into potential decontamination applications. PhD Thesis. University of Strathclyde. Available at: https://stax.strath.ac.uk/concern/theses/rn301138p?locale=en (Accessed January 2020).

McKenzie, K., Maclean, M., Grant, M.H., Ramakrishnan, P., MacGregor, S.J. and Anderson, J.G. (2016) 'The effects of 405 nm light on bacterial membrane integrity determined by salt and bile tolerance assays, leakage of UV-absorbing material and SYTOX green labelling', *Microbiology,* 162(9), pp. 1680–1688. Available at: https://doi.org/10.1099/mic.0.000350.

McKenzie, K., Maclean, M., Timoshkin, I. V, Endarko, E., Macgregor, S.J. and Anderson, J.G. (2013) 'Photoinactivation of bacteria attached to glass and acrylic surfaces by 405 nm light: Potential application for biofilm decontamination', *Photochemistry and Photobiology*, 89(4), pp. 927–935. Available at: https://doi.org/10.1111/php.12077.

McKenzie, K., Maclean, M., Timoshkin, I. V, MacGregor, S.J. and Anderson, J.G. (2014) 'Enhanced inactivation of *Escherichia coli* and *Listeria monocytogenes* by exposure to 405nm light under sub-lethal temperature, salt and acid stress conditions', *International Journal of Food Microbiology*, 170, pp. 91–98. Available at: https://doi.org/10.1016/j.ijfoodmicro.2013.10.016.

McMullan, P., White, A.B., Coker, O., Opal, S., McGee, S.A. and Rogers, G. (2022) 'Antimicrobial Efficacy of Continuous Low-Irradiance Phototherapy Against Multidrug-Resistant Organisms', *Photobiomodulation, Photomedicine and Laser Surgery*, 40(9), pp. 613–621. Available at: https://doi.org/10.1089/photob.2022.0016.

Meurle, T., Knaus, J., Barbano, A., Hoenes, K., Spellerberg, B. and Hessling, M. (2021) 'Photoinactivation of Staphylococci with 405 nm light in a trachea model with saliva substitute at 37 °C', *Healthcare*, 9(3), 310. Available at: https://doi.org/10.3390/healthcare9030310.

Mietto, C., Pincireoli, R., Patel, N. and Berra, L. (2013) 'Ventilator associated pneumonia: Evolving definitions and preventive strategies', *Respiratory Care*, 58(6), pp. 990-1007. Available at: https://doi.org/10.4187/respcare.02380.

Milgrom, L.R. (1997) *The Colours of Life: An Introduction to the Chemistry of Porphyrins and Related Compounds*. New York: Oxford University Press. Available at: https://doi.org/10.1093/oso/9780198553809.001.0001 (Accessed June 2020)

Minor, M. and Sabillón, L. (2023) 'Effectiveness of ultra-high irradiance blue light-emitting diodes in inactivating *Escherichia coli* O157:H7 on dry stainless steel and cast-iron surfaces', *Foods*, 12(16), 3072. Available at: https://doi.org/10.3390/foods12163072.

Misba, L., Abdulrahman, H. and Khan, A.U. (2019) 'Photodynamic efficacy of toluidine blue O against mono species and dual species bacterial biofilm', *Photodiagnosis and Photodynamic Therapy*, 26, pp. 383–388. Available at: https://doi.org/10.1016/j.pdpdt.2019.05.001.

Misba, L., Kulshrestha, S. and Khan, A.U. (2016) 'Antibiofilm action of a toluidine blue O-silver nanoparticle conjugate on *Streptococcus mutans*: a mechanism of type I photodynamic therapy', *Biofouling*, 32(3), pp. 313–328. Available at: https://doi.org/10.1080/08927014.2016.1141899.

Mitchell, B.G., Dancer, S.J., Anderson, M. and Dehn, E. (2015) 'Risk of organism acquisition from prior room occupants: A systematic review and meta-analysis', *Journal of Hospital Infection*, 91(3), pp. 211–217. Available at: https://doi.org/10.1016/j.jhin.2015.08.005.

Mitchell, B.G., Gardner, A., Stone, P.W., Hall, L. and Pogorzelska-Maziarz, M. (2018) 'Hospital staffing and health care–associated infections: A systematic review of the literature', *The Joint Commission Journal on Quality and Patient Safety*, 44(10), pp. 613–622. Available at: https://doi.org/10.1016/j.jcjq.2018.02.002.

Moan, J. (1990) 'On the diffusion length of singlet oxygen in cells and tissues', *Photochemistry and Photobiology*, 6(3), pp. 343–347.

Moat, J., Cargill, J., Shone, J. and Upton, M. (2009) 'Application of a novel decontamination process using gaseous ozone', *Canadian Journal of Microbiology*, 55(8), pp. 928–933. Available at: https://doi.org/10.1139/w09-046.

Moccia, G., De Caro, F., Pironti, C., Boccia, G., Capunzo, M., Borrelli, A. and Motta, O. (2020) 'Development and improvement of an effective method for air and surfaces disinfection with ozone gas as a decontaminating agent', *Medicina*, 56(11), 578. Available at: https://doi.org/10.3390/medicina56110578.

Moorhead, S., Maclean, M., Coia, J.E., MacGregor, S.J. and Anderson, J.G. (2016) 'Synergistic efficacy of 405 nm light and chlorinated disinfectants for the enhanced decontamination of *Clostridium difficile* spores', *Anaerobe*, 37, pp. 72–77. Available at: https://doi.org/10.1016/j.anaerobe.2015.12.006.

Moorhead, S., Maclean, M., MacGregor, S.J. and Anderson, J.G. (2016) 'Comparative sensitivity of *Trichophyton* and *Aspergillus Conidia* to inactivation by violet-blue light exposure', *Photomedicine and Laser Surgery*, 34(1), pp. 36–41. Available at: https://doi.org/10.1089/pho.2015.3922.

Moseley, H., Allen, J.W., Ibbotson, S., Lesar, A., McNeill, A., Camacho-Lopez, M.A., Samuel, I.D.W., Sibbett, W. and Ferguson, J. (2006) 'Ambulatory photodynamic therapy: A new concept in delivering photodynamic therapy', *British Journal of Dermatology*, 154(4), pp. 747–750. Available at: https://doi.org/10.1111/j.1365-2133.2006.07145.x.

Muralidar, S., Ambi, S.V., Sekaran, S. and Krishnan, U.M. (2020) 'The emergence of COVID-19 as a global pandemic: Understanding the epidemiology, immune response and potential therapeutic targets of SARS-CoV-2', *Biochimie*, 179, pp. 85–100. Available at: https://doi.org/10.1016/j.biochi.2020.09.018.

Murdoch, L.E., Bailey, L., Banham, E., Watson, F., Adams, N.M.T. and Chewins, J. (2016) 'Evaluating different concentrations of hydrogen peroxide in an automated room disinfection system', *Letters in Applied Microbiology*, 63(3), pp. 178–182. Available at: https://doi.org/10.1111/lam.12607.

Murdoch, L.E., MacLean, M., Endarko, E., MacGregor, S.J. and Anderson, J.G. (2012) 'Bactericidal effects of 405nm light exposure demonstrated by inactivation of *Escherichia*, *Salmonella*, *Shigella*, *Listeria*, and *Mycobacterium* species in liquid suspensions and on exposed surfaces', *The Scientific World Journal*, 2012, 137805. Available at: https://doi.org/10.1100/2012/137805.

Murdoch, L.E., MacLean, M., MacGregor, S.J. and Anderson, J.G. (2010) 'Inactivation of *Campylobacter jejuni* by exposure to high-intensity 405-nm visible light', *Foodborne Pathogens and Disease*, 7(10), pp. 1211–1216. Available at: https://doi.org/10.1089/fpd.2010.0561.

Murdoch, L.E., McKenzie, K., Maclean, M., MacGregor, S.J. and Anderson, J.G. (2013) 'Lethal effects of high-intensity violet 405-nm light on *Saccharomyces cerevisiae*, *Candida albicans*, and on dormant and germinating spores of *Aspergillus niger*', *Fungal Biology*, 117(7–8), pp. 519–527. Available at: https://doi.org/10.1016/j.funbio.2013.05.004.

Murray, B., Ohmine, S., Tomer, D., Jensen, K., Johnson, F., Kirsi, J., Robinson, R. and O'Neill, K. (2008) 'Virion disruption by ozone-mediated reactive oxygen species', *Journal of Virological Methods*, 153(1), pp. 74-79. Available at: https://doi.org/10.1016/j.jviromet.2008.06.004.

Murrell, L.J., Hamilton, E.K., Johnson, H.B. and Spencer, M. (2019) 'Influence of a visible-light continuous environmental disinfection system on microbial contamination and surgical site infections in an orthopedic operating room', *American Journal of Infection Control*, 47(7), pp. 804–810. Available at: https://doi.org/10.1016/j.ajic.2018.12.002.

Narita, K., Asano, K., Naito, K., Ohashi, H., Sasaki, M., Morimoto, Y., Igarashi, T. and Nakane, A. (2020) 'Ultraviolet C light with wavelength of 222 nm inactivates a wide spectrum of microbial pathogens', *Journal of Hospital Infection*, 105(3), pp. 459–467. Available at: https://doi.org/10.1016/j.jhin.2020.03.030.

National Collection of Type Cultures (2019) *A Guide for opening of NCTC glass ampoules and reconstitution of freeze dried material*. https://www.culturecollections.org.uk/training-and-support/how-to-handle-bacteria-and-fungi-on-receipt/ (Accessed November 2021).

National Institutes of Health (2023) *Clinical Spectrum of SARS-CoV-2 Infection*. Available at: https://www.covid19treatmentguidelines.nih.gov/overview/clinical-spectrum/ (Accessed: January 2023).

Neely, A.N. and Maley, M.P. (2000) 'Survival of Enterococci and Staphylococci on Hospital Fabrics and Plastic', *Journal of Clinical Microbiology,* 38(2), pp. 724-726. Available at: https://doi.org/10.1128/JCM.38.2.724-726.2000.

Nerandzic, M.M., Cadnum, J.L., Pultz, M.J. and Donskey, C.J. (2010) 'Evaluation of an automated ultraviolet radiation device for decontamination of Clostridium difficile and other healthcare-associated pathogens in hospital rooms', *BMC Infectious Diseases,* 10, 197. Available at: https://doi.org/ 10.1186/1471-2334-10-197.

NHS (2022) 'Chapter 2: Transmission based precautions (TBPs)', in *National infection prevention and control manual (NIPCM) for England*. Available at: https://www.england.nhs.uk/national-infection-prevention-and-control-manual-nipcm-for-england/chapter-2-transmission-based-precautions-tbps/ (Accessed: July 2023).

NHS England (2008). *An integrated approach to hospital cleaning: microfibre cloth and steam cleaning technology*. Available at: https://www.england.nhs.uk/publication/an-integrated-approach-to-hospital-cleaning-microfibre-cloth-and-steam-cleaning-technology/ (Accessed January 2022).

NHS England (2019). *New NHS online training to help people get home from hospital quicker*. Available at: https://www.england.nhs.uk/2019/11/new-nhs-online-training-to-help-people-get-home-from-hospital-quicker/ (Accessed: October 2020).

NHS Scotland (2012). *National Infection Prevention and Control Manual*. Available at: https://www.nipcm.hps.scot.nhs.uk/ (Accessed: September 2020).

NICE (2016). *Healthcare-associated infections*. Quality standard [QS113]. Available at: https://www.nice.org.uk/guidance/qs113 (Accessed: April 2020).

Nicolle, L. (2014) 'Catheter associated urinary tract infections', *Antimicrobial Resistance and Infection Control*, 3, 23. Available at: https://doi.org/10.1186/2047-2994-3-23.

Ning, P., Shan, D., Hong, E., Liu, L., Zhu, Y., Cui, R., Zhou, Y. and Wang, B. (2020) 'Disinfection performance of chlorine dioxide gas at ultra-low concentrations and the decay rules under different environmental factors', *Journal of the Air and Waste Management Association*, 70(7), pp. 721–728. Available at: https://doi.org/10.1080/10962247.2020.1769768.

Nitzan, Y., Gutterman, M., Malik, Z. and Ehrenberg, B. (1992) 'Inactivation of Gram-negative bacteria by photosensitized porphyrins', *Photochemistry and Photobiology*, 55(1), pp. 89–96. Available at: https://doi.org/10.1111/j.1751-1097.1992.tb04213.x.

Nitzan, Y., Salmon-Divon, M., Shporen, E. and Malik, Z. (2004) 'ALA induced photodynamic effects of Gram positive and negative bacteria', *Photochemical & Photobiological Sciences*, 3(5), pp. 430–435. Available at: https://doi.org/10.1039/b315633h.

Noszticzius, Z., Wittmann, M., Kály-Kullai, K., Beregvári, Z., Kiss, I., Rosivall, L. and Szegedi, J. (2013) 'Chlorine dioxide is a size-selective antimicrobial agent', *PLoS ONE*, 8(11), e79157. Available at: https://doi.org/10.1371/journal.pone.0079157.

Novo, D., Perlmutter, N.G., Hunt, R.H. and Shapiro, H.M. (1999) 'Accurate flow cytometric membrane potential measurement in bacteria using diethyloxacarbocyanine and a ratiometric technique', *Cytometry*, 35(1), pp. 55–63. Available at: https://doi.org/10.1002/(SICI)1097-0320(19990101)35:1<55::AID-CYTO8>3.0.CO;2-2.

NPSA (2009). *The Revised Healthcare Cleaning Manual*. Available at: https://www.ahcp.co.uk/wp-content/uploads/NRLS-0949-Healthcare-clea-ng-manual-2009-06-v1.pdf (Accessed: July 2020).

O'Connor, N., Cahill, O., Daniels, S., Galvin, S. and Humphreys, H. (2014) 'Cold atmospheric pressure plasma and decontamination. Can it contribute to preventing hospital-acquired infections?', *Journal of Hospital Infection*, 88(2), pp. 59–65. Available at: https://doi.org/10.1016/j.jhin.2014.06.015.

Office for National Statistics (2017). *Causes of death over 100 years*. Available at: https://www.ons.gov.uk/peoplepopulationandcommunity/birthsdeathsandmarriages/deaths/articles/causesofdeathover100years/2017-09-18 (Accessed: December 2023).

Oh, E., McMullen, L. and Jeon, B. (2015) 'Impact of oxidative stress defense on bacterial survival and morphological change in *Campylobacter jejuni* under aerobic conditions', *Frontiers in Microbiology*, 6, 295. Available at: https://doi.org/10.3389/fmicb.2015.00295.

Oh, J.K., Yegin, Y., Yang, F., Zhang, M., Li, J., Huang, S., Verkhoturov, S. V., Schweikert, E.A., Perez-Lewis, K., Scholar, E.A., Taylor, T.M., Castillo, A., Cisneros-Zevallos, L., Min, Y. and Akbulut, M. (2018) 'The influence of surface chemistry on the kinetics and thermodynamics of bacterial adhesion', *Scientific Reports*, 8, 17247. Available at: https://doi.org/10.1038/s41598-018-35343-1.

Olagüe, C., Mitxelena-Iribarren, O., Sierra-García, J.E., Rodriguez-Merino, F., Maestro, S., Pérez-Lorenzo, E., Guillen-Grima, F., González-Aseguinolaza, G., Arana, S. and Smerdou, C. (2022) 'Rapid SARS-CoV-2 disinfection on distant surfaces with UV-C: The inactivation is affected by the type of material', *Journal of Photochemistry and Photobiology*, 11, 100138. Available at: https://doi.org/10.1016/j.jpap.2022.100138.

De Oliveira, D., Forde, B., Kidd, T., Harris, P., Schembri, M., Beatson, S., Paterson, D. and Walker, M. (2020) 'Antimicrobial resistance in ESKAPE pathogens', *Clinical Microbiology Reviews*, 33(3), e00181-19. Available at https://doi.org/10.1128/cmr.00181-19.

O'Neill, J. (2016). *Tackling Drug-Resistant Infections Globally: Final Report and Recommendations.* Available at: https://amr-review.org/sites/default/files/160518_Final%20paper_with%20cover.pdf (Accessed: May 2020).

Ordon, M., Nawrotek, P., Stachurska, X. and Mizielí Nska, M. (2021) 'Polyethylene films coated with antibacterial and antiviral layers based on CO_2 extracts of raspberry seeds, of pomegranate seeds and of rosemary', *Coatings*, 11(10), 1179. Available at: https://doi.org/10.3390/coatings11101179.

Otter, Jonathan A. and French, G.L. (2009) 'Survival of nosocomial bacteria and spores on surfaces and inactivation by hydrogen peroxide vapor', *Journal of Clinical Microbiology*, 47(1), pp. 205–207. Available at: https://doi.org/10.1128/JCM.02004-08.

Otter, J.A., Puchowicz, M., Ryan, D., Salkeld, J.A., Cooper, T.A., Havill, N.L., Tuozzo, K. and Boyce, J.M. (2009) 'Feasibility of routinely using hydrogen peroxide vapor to decontaminate rooms in a busy United States hospital', *Infection Control and Hospital Epidemiology*, 30(6), pp. 574–577. Available at: https://doi.org/10.1086/597544.

Otter, J.A., Yezli, S., Barbut, F. and Perl, T.M. (2019) 'An overview of automated room disinfection systems: When to use them and how to choose them,' in Walker, J. (ed.) *Decontamination in Hospitals and Healthcare*. Elsevier, pp. 323-369. Available at: https://doi.org/10.1016/B978-0-08-102565-9.00015-7.

Otter, J.A., Yezli, S., Salkeld, J.A.G. and French, G.L. (2013) 'Evidence that contaminated surfaces contribute to the transmission of hospital pathogens and an overview of strategies to address contaminated surfaces in hospital settings', *American Journal of Infection Control*, 41(5), p. S6-S11. Available at: https://doi.org/10.1016/j.ajic.2012.12.004.

Owens, C. and Stoessel, K. (2008) 'Surgical site infections: epidemiology, microbiology and prevention', *Journal of Hospital Infection*, 70(2), pp. 3-10. Available at: https://doi.org/10.1016/S0195-6701(08)60017-1.

Oxy'Pharm. (2021) *Nocospray*. Available at: https://www.oxypharm.net/en/nocotech/nocospray/ (Accessed: March 2022).

Oztoprak, N., Kizilates, F. and Percin, D. (2019) 'Comparison of steam technology and a two-step cleaning (water/detergent) and disinfecting (1,000 resp. 5,000 ppm hypochlorite) method using microfiber cloth for environmental control of multidrug-resistant organisms in an intensive care unit', *GMS Hygiene and Infection Control*, 14, 15. Available at: https://doi.org/10.3205/dgkh000330.

Pang, Z., Raudonis, R., Glick, B.R., Lin, T.J. and Cheng, Z. (2019) 'Antibiotic resistance in *Pseudomonas aeruginosa*: Mechanisms and alternative therapeutic strategies', *Biotechnology Advances,* 37(1), pp. 177–192. Available at: https://doi.org/10.1016/j.biotechadv.2018.11.013.

Papageorgiou, P., Katsambas, A. and Chu, A.C. (2000) 'Phototherapy with blue (415 nm) and red (660 nm) light in the treatment of acne vulgaris', *British Journal of Dermatology*, 142(5), pp. 973–978. Available at: https://doi.org/10.1046/j.1365-2133.2000.03481.x.

Parameswaren, R., Sherchan, J.B., Varma, M.D., Mukhopadhyay, C. and Vidyasagar, S. (2010) 'Intravascular catheter-related infections in an Indian tertiary care hospital', *Journal of Infection in Developing Countries*, 5(6), pp. 452-458. Available at: https://doi.org/10.0.15.15/jidc.1261.

Parry, M.F., Sestovic, M., Renz, C., Pangan, A., Grant, B. and Shah, A.K. (2022) 'Environmental cleaning and disinfection: Sustaining changed practice and improving quality in the community hospital', *Antimicrobial Stewardship and Healthcare Epidemiology*, 2(1), e113. Available at: https://doi.org/10.1017/ash.2022.257.

Pendleton, J., Gorman, S. and Gilmore, B. (2013) 'Clinical relevance of the ESKAPE pathogens', *Expert Review of Anti-Infective Therapy*, 11(3), pp. 297-308. Available at: https://doi.org/10.1586/eri.13.12.

Peng, Z., Rojas, A.L.P., Kropff, E., Bahnfleth, W., Buonanno, G., Dancer, S.J., Kurnitski, J., Li, Y., Loomans, M.G.L.C., Marr, L.C., Morawska, L., Nazaroff, W., Noakes, C., Querol, X., Sekhar, C., Tellier, R., Greenhalgh, T., Bourouiba, L., Boerstra, A., Tang, J.W., Miller, S.L. and Jimenez, J.L. (2022) 'Practical indicators for risk of airborne transmission in shared indoor environments and their application to COVID-19 outbreaks', *Environmental Science and Technology*, 56(2), pp. 1125–1137. Available at: https://doi.org/10.1021/acs.est.1c06531.

Pittet, D. (2001) 'Improving adherence to hand hygiene practice: A multidisciplinary approach', *Emerging Infectious Diseases*, 7(2), pp. 234–240. Available at: https://doi.org/10.3201/eid0702.010217.

Pittet, D., Dharan, S., Touveneau, S., Sauvan, V. and Perneger, T. V (1999) 'Bacterial contamination of the hands of hospital staff during routine patient care', *Archives of Internal Medicine*, 159(8), pp. 821–826. Available at: https://doi.org/10.1001/archinte.159.8.821.

Plaetzer, K., Krammer, B., Berlanda, J., Berr, F. and Kiesslich, T. (2009) 'Photophysics and photochemistry of photodynamic therapy: Fundamental aspects', *Lasers in Medical Science*, 24(2), pp. 259–268. Available at: https://doi.org/10.1007/s10103-008-0539-1.

Ploydaeng, M., Rajatanavin, N. and Rattanakaemakorn, P. (2021) 'UV-C light: A powerful technique for inactivating microorganisms and the related side effects to the skin', *Photodermatology, Photoimmunology and Photomedicine*, 37(1), pp. 12–19. Available at: https://doi.org/10.1111/phpp.12605.

Pourhajibagher, M., Kazemian, H., Chiniforush, N., Hosseini, N., Pourakbari, B., Azizollahi, A., Rezaei, F. and Bahador, A. (2018) 'Exploring different photosensitizers to optimize elimination of planktonic and biofilm forms of *Enterococcus faecalis* from infected root canal during antimicrobial photodynamic therapy', *Photodiagnosis and Photodynamic Therapy*, 24, pp. 206–211. Available at: https://doi.org/10.1016/j.pdpdt.2018.09.014.

Raab, O. (1900) 'The effect of fluorescent agents on infusoria (in German)', *Journal of Biology*, 39, pp. 524–526.

Ragupathy, V., Haleyurgirisetty, M., Dahiya, N., Stewart, C., Anderson, J., MacGregor, S., Maclean, M., Hewlett, I. and Atreya, C. (2022) 'Visible 405 nm violet-blue light successfully inactivates HIV-1 in human plasma', *Pathogens*, 11(7), 778. Available at: https://doi.org/10.3390/pathogens11070778.

Ramakrishnan, P., Maclean, M., MacGregor, S.J., Anderson, J.G. and Grant, M.H. (2014) 'Differential sensitivity of osteoblasts and bacterial pathogens to 405-nm light highlighting potential for decontamination applications in orthopedic surgery', *Journal of Biomedical Optics*, 19(10), 105001. Available at: https://doi.org/10.1117/1.JBO.19.10.105001.

Ramakrishnan, P., Maclean, M., MacGregor, S.J., Anderson, J.G. and Grant, M.H. (2016) 'Cytotoxic responses to 405nm light exposure in mammalian and bacterial cells: Involvement of reactive oxygen species', *Toxicology in Vitro*, 33, pp. 54–62. Available at: https://doi.org/https://doi.org/10.1016/j.tiv.2016.02.011.

Rapacka-Zdonczyk, A., Wozniak, A., Kruszewska, B., Waleron, K. and Grinholc, M. (2021) 'Can gram-negative bacteria develop resistance to antimicrobial blue light treatment?', *International Journal of Molecular Sciences*, 22(21), 11579. Available at: https://doi.org/10.3390/ijms222111579.

Rapacka-Zdonczyk, A., Wozniak, A., Pieranski, M., Woziwodzka, A., Bielawski, K.P. and Grinholc, M. (2019) 'Development of *Staphylococcus aureus* tolerance to antimicrobial photodynamic inactivation and antimicrobial blue light upon sub-lethal treatment', *Scientific Reports*, 9, 9423. Available at: https://doi.org/10.1038/s41598-019-45962-x.

Rapozo, D.C.M., Bernardazzi, C. and De Souza, H.S.P. (2017) 'Diet and microbiota in inflammatory bowel disease: The gut in disharmony', *World Journal of Gastroenterology*, 23(12), pp. 2124–2140. Available at: https://doi.org/10.3748/wjg.v23.i12.2124.

Rathnasinghe, R., Jangra, S., Miorin, L., Schotsaert, M., Yahnke, C. and García-Sastre, A. (2021) 'The virucidal effects of 405 nm visible light on SARS-CoV-2 and influenza A virus', *Scientific Reports*, 11(1), pp. 1–10. Available at: https://doi.org/10.1038/s41598-021-97797-0.

Ray, A., Perez, F., Beltramini, A.M., Jakubowycz, M., Dimick, P., Jacobs, M.R., Roman, K., Bonomo, R.A. and Salata, R.A. (2010) 'Use of vaporized hydrogen peroxide decontamination during an outbreak of multidrug-resistant *Acinetobacter baumannii* infection at a long-term acute care hospital', *Infection Control & Hospital Epidemiology*, 31(12), pp. 1236–1241. Available at: https://doi.org/10.1086/657139.

Ray, P.D., Huang, B.-W. and Tsuji, Y. (2012) 'Reactive oxygen species (ROS) homeostasis and redox regulation in cellular signalling', *Cell Signalling*, 24(5), pp. 981–990. Available at: https://doi.org/10.1016/j.cellsig.2012.01.008.Reactive.

Redanz, S., Enz, A., Podbielski, A. and Warnke, P. (2021) 'Targeted swabbing of implant-associated biofilm formation—a staining-guided sampling approach for optimizing routine microbiological diagnostics', *Diagnostics*, 11(6), 1038. Available at: https://doi.org/10.3390/diagnostics11061038.

Reichman, D. and Greenberg, J. (2009) 'Reducing surgical site infections: A review', *Reviews in Obstetrics and Gynecology,* 2(4), pp. 212-221. Available at: https://doi.org/10.3909/riog0084.

Reygaert, W.C. (2018) 'An overview of the antimicrobial resistance mechanisms of bacteria', *AIMS Microbiology*, 4(3), pp. 482–501. Available at: https://doi.org/10.3934/microbiol.2018.3.482.

Richardson, T.B. and Porter, C.D. (2005) 'Inactivation of murine leukaemia virus by exposure to visible light', *Virology*, 341(2), pp. 321–329. Available at: https://doi.org/10.1016/j.virol.2005.07.025.

Riddell, S., Goldie, S., Hill, A., Eagles, D. and Drew, T.W. (2020) 'The effect of temperature on persistence of SARS-CoV-2 on common surfaces', *Virology Journal*, 17(1), 145. Available at: https://doi.org/10.1186/s12985-020-01418-7.

Rinninella, E., Raoul, P., Cintoni, M., Franceschi, F., Miggiano, G.A.D., Gasbarrini, A. and Mele, M.C. (2019) 'What is the healthy gut microbiota composition? A changing ecosystem across age, environment, diet, and diseases', *Microorganisms*, 7(1), 14. Available at: https://doi.org/10.3390/microorganisms7010014.

Robertson, S.N., Gibson, D., MacKay, W.G., Reid, S., Williams, C. and Birney, R. (2017) 'Investigation of the antimicrobial properties of modified multilayer diamond-like carbon coatings on 316 stainless steel', *Surface and Coatings Technology*, 314, pp. 72–78. Available at: https://doi.org/10.1016/j.surfcoat.2016.11.035.

Rockey, N., Arts, P.J., Li, L., Harrison, K.R., Langenfeld, K., Fitzsimmons, W.J., Lauring, A.S., Love, N.G., Kaye, K.S., Raskin, L., Roberts, W.W., Hegarty, B. and Wigginton, K.R. (2020) 'Humidity and deposition solution play a critical role in virus inactivation by heat treatment of N95 respirators', *mSphere*, 5(5), 00588-20. Available at: https://doi.org/10.1128/msphere.00588-20.

Rodríguez, M.E., Cogno, I.S., Sanabria, L.S.M., Morán, Y.S. and Rivarola, V.A. (2016) 'Heat shock proteins in the context of photodynamic therapy: Autophagy, apoptosis and immunogenic cell death', *Photochemical & Photobiological Sciences*, 15(9), pp. 1090–1102. Available at: https://doi.org/10.1039/c6pp00097e.

Rogers, G.S. (2012) 'Continuous low-irradiance photodynamic therapy: A new therapeutic paradigm', *Journal of the National Comprehensive Cancer Network*, 10(2), pp. S14-S17. Available at: https://doi.org/10.6004/jnccn.2012.0166.

Rutala, W., Gergen, M. and Weber, D. (2010) 'Room decontamination with UV radiation', *Infection Control & Hospital Epidemiology*, 31(10), pp. 1025–1029. Available at: https://doi.org/10.1086/656244.

Rutala, W. and Weber, D.J. (2013) 'Disinfectants used for environmental disinfection and new room decontamination technology', *American Journal of Infection Control*, 41(5), pp. 36–41. Available at: https://doi.org/10.1016/j.ajic.2012.11.006.

Rutala, W.A., Kanamori, H., Gergen, M.F., Sickbert-Bennett, E.E., Sexton, D.J., Anderson, D.J., Laux, J. and Weber, D.J. (2018) 'Antimicrobial activity of a continuous visible light disinfection system', *Infection Control and Hospital Epidemiology*, 39(10), pp. 1250–1253. Available at: https://doi.org/10.1017/ice.2018.200.

Rutala, W.A. and Weber, D.J. (2016) 'Disinfection and sterilization in health care facilities: An overview and current issues', *Infectious Disease Clinics of North America*, 30(3) pp. 609–637. Available at: https://doi.org/10.1016/j.idc.2016.04.002.

Rutala, W.A., Weber, D.J. and Healthcare Infection Control Practices Advisory Committee. (2008) *Guideline for Disinfection and Sterilization in Healthcare Facilities, 2008*. Available at: https://www.cdc.gov/infectioncontrol/pdf/guidelines/disinfection-guidelines-H.pdf (Accessed: May 2020).

Sandhu, R., Murillo, M., Wyatt, D., Bhanot, N.Min, Z. and Thomas, J. (2016) 'Environmental decontamination of medical intensive care unit suites using high-intensity narrow-spectrum light', *Open Forum Infectious Diseases*, 3(1), 265. Available at: *https://doi.org/10.1093/ofid/ofw172.131*.

Sandiumenge, A. and Rello, J. (2012) 'Ventilator-associated pneumonia caused by ESKAPE organisms', *Current Opinion in Pulmonary Medicine,* 18(3), pp. 187-193. Available at https://doi.org/10.1097/mcp.0b013e328351f974.

Santajit, S. and Indrawattana, N. (2016) 'Mechanisms of antimicrobial resistance in ESKAPE pathogens', *BioMed Research International*, 2016, 2475067. Available at: https://10.1155/2016/2475067.

Sasahara, T., Ae, R., Watanabe, M., Kimura, Y., Yonekawa, C., Hayashi, S. and Morisawa, Y. (2016) 'Contamination of healthcare workers' hands with bacterial spores', *Journal of Infection and Chemotherapy*, 22(8), pp. 521–525. Available at: https://doi.org/10.1016/j.jiac.2016.04.007.

Schapira, A.-J., Drame, M., Olive, C. and Marion-Sanchez, K. (2024) 'Bacterial viability in dry surface biofilms in healthcare facilities – A systematic review', *Journal of Hospital Infection*, 144, pp. 94-110. Available at: https://doi.org/10.1016/j.jhin.2023.11.004.

Schieber, M. and Chandel, N.S. (2014) 'ROS function in redox signalling and oxidative stress', *Current Biology*, 24(10), pp. 453-462. Available at: https://doi.org/10.1016/j.cub.2014.03.034.

Seixas, A.F., Quendera, A.P., Sousa, J.P., Silva, A.F.Q., Arraiano, C.M. and Andrade, J.M. (2022) 'Bacterial response to oxidative stress and RNA oxidation', *Frontiers in Genetics,* 12, 821535. Available at: https://doi.org/10.3389/fgene.2021.821535.

Serra-Burriel, M., Keys, M., Campillo-Artero, C., Agodi, A., Barchitta, M., Gikas, A., Palos, C. and López-Casasnovas, G. (2020) 'Impact of multi-drug resistant bacteria on economic and clinical outcomes of healthcare-associated infections in adults: Systematic review and meta-analysis', *PLoS ONE*, 15(1), pp. 1–14. Available at: https://doi.org/10.1371/journal.pone.0227139.

Setlow, P. (2014) 'Spore resistance properties', *Microbiology Spectrum*, 2(5), 0003-2012. Available at: https://doi.org/10.1128/microbiolspec.TBS-0003-2012.

van Seventer, J.M. and Hochberg, N.S. (2016) 'Principles of Infectious Diseases: Transmission, Diagnosis, Prevention, and Control', in Quah, S.R. (ed.) *International Encyclopedia of Public Health*. Elsevier, pp. 22-39. Available at: https://doi.org/10.1016/B978-0-12-803678-5.00516-6.

Shams, A.M., Rose, L.J., Edwards, J.R., Cali, S., Harris, A.D., Jacob, J.T., LaFae, A., Pineles, L.L., Thom, K.A., McDonald, L.C., Arduino, M.J. and Noble-Wang, J.A. (2016) 'Assessment of the overall and multidrug-resistant organism bioburden on environmental surfaces in healthcare facilities', *Infection Control & Hospital Epidemiology*, 37(12), pp. 1426–1432. Available at: https://doi.org/10.1017/ice.2016.198.

Shirasaki, Y., Matsuura, A., Uekusa, M., Ito, Y. and Hayashi, T. (2016) 'A study of the properties of chlorine dioxide gas as a fumigant', *Experimental Animals*, 65(3), pp. 303–310. Available at: https://doi.org/10.1538/expanim.15-0092.

Shrivastava, S.R., Shrivastava, P.S. and Ramasamy, J. (2013) 'Airborne infection control in healthcare settings', *Infection Ecology & Epidemiology*, 3(1), 21411. Available at: https://doi.org/10.3402/iee.v3i0.21411.

Simmons, S.E., Carrion, R., Alfson, K.J., Staples, H.M., Jinadatha, C., Jarvis, W.R., Sampathkumar, P., Chemaly, R.F., Khawaja, F., Povroznik, M., Jackson, S., Kaye, K.S., Rodriguez, R.M. and Stibich, M.A. (2021) 'Deactivation of SARS-CoV-2 with pulsed-xenon ultraviolet light: Implications for environmental COVID-19 control', *Infection Control and Hospital Epidemiology*, 42(2), pp. 127–130. Available at: https://doi.org/10.1017/ice.2020.399.

Sinclair, L.G., Anderson, J.G., MacGregor, S.J. and Maclean, M. (2024) 'Enhanced antimicrobial efficacy and energy efficiency of low irradiance 405-nm light for bacterial decontamination', *Archives of Microbiology*, 206(276). Available at: https://doi.org/10.1007/s00203-024-03999-1

Sinclair, L.G., Dougall, L.R., Ilieva, Z., McKenzie, K., Anderson, J.G., MacGregor, S.J. and Maclean, M. (2023) 'Laboratory evaluation of the broad-spectrum antibacterial efficacy of a low-irradiance visible 405-nm light system for surface-simulated decontamination', *Health and Technology*, 13, pp. 615-629. Available at: https://doi.org/10.1007/s12553-023-00761-3.

Sinclair, L.G., Ilieva, Z., Morris, G., Anderson, J.G., MacGregor, S.J. and Maclean, M. (2023) 'Viricidal efficacy of a 405-nm environmental decontamination system for inactivation of bacteriophage Phi6: Surrogate for SARS-CoV-2 ', *Photochemistry and Photobiology*, 99, pp. 1493-1500. Available at: https://doi.org/10.1111/php.13798.

Singh, D., Soorneedi, A.R., Vaze, N., Domitrovic, R., Sharp, F., Lindsey, D., Rohr, A., Moore, M.D., Koutrakis, P., Nardell, E. and Demokritou, P. (2023) 'Assessment of SARS-CoV-2 surrogate inactivation on surfaces and in air using UV and blue light-based intervention technologies', *Journal of the Air and Waste Management Association*, 73(3), pp. 200–211. Available at: https://doi.org/10.1080/10962247.2022.2157907.

Singh, J., Stoitsova, S., Zakrzewska, K., Henszel, L., Rosińska, M. and Duffell, E. (2022) 'Healthcare-associated hepatitis B and C transmission to patients in the EU/EEA and UK: A systematic review of reported outbreaks between 2006 and 2021', *BMC Public Health*, 22(1), 2260. Available at: https://doi.org/10.1186/s12889-022-14726-0.

Sinha, R. and Häder, D. (2002) 'UV-induced DNA damage and repair: A review', Photochemical and Photobiological Sciences, 1(4), pp. 225-236. Available at: https://doi.org/10.1039/b201230h.

Tru-D SmartUVC (2024) *About Tru-D*. Available at: https://tru-d.com/ (Accessed March 2020).

Smith, T.L., Pearson, M.L., Wilcox, K.R., Cruz, C., Lancaster, M. V, Robinson-Dunn, B., Tenover, F.C., Zervos, M.J., Band, J.D., White, E. and Jarvis, W.R. (1999) 'Emergence of vancomycin resistance in *Staphylococcus aureus*. Glycopeptide-

intermediate *Staphylococcus aureus* working group', *The New England Journal of Medicine*, 340(7), pp. 493–501. Available at: https://doi.org/10.1056/NEJM199902183400701.

Song, E., Park, K., Jang, E., Lee, E., Chong, Y., Cho, O., Kim, S., Lee, S., Sung, H., Kim, M., Jeong, J., Kim, Y., Woo, J. and Choi, S. (2010) 'Comparison of the clinical and microbiologic characteristics of patients with *Enterobacter cloacae* and *Enterobacter aerogenes* bacteremia: a prospective observation study', *Diagnostic Microbiology and Infectious Disease*, 66(4), pp. 436-440. Available at https://doi.org/10.1016/j.diagmicrobio.2009.11.007.

Soukos, N.S., Stultz, J., Abernethy, A.D. and Goodson, J.M. (2015) 'Phototargeting human periodontal pathogens in vivo', *Lasers in Medical Science*, 30(3), pp. 943–952. Available at: https://doi.org/10.1007/s10103-013-1497-9.

Spagnolo, A.M., Ottria, D., Amicizia, D., Perdelli, F. and Cristina, M.I. (2013) 'Operating theatre quality and prevention of surgical site infections', *Journal of Preventative Medicine and Hygiene*, 54(3), pp. 131-137.

STERIS (2021a). *VHP 1000ED biodecontamination unit*. Available at: https://www.sterislifesciences.com/products/equipment/vhp-sterilization-and-biodecontamination/vhp-1000ed-mobile-biodecontamination-system (Accessed: January 2022).

STERIS (2021b). *VHP Sterilization & Biodecontamination*. Available at: https://www.sterislifesciences.com/products/equipment/vhp-sterilization-and-biodecontamination (Accessed: January 2022).

Stewart, S., Robertson, C., Kennedy, S., Kavanagh, K., Haahr, L., Manoukian, S., Mason, H., Dancer, S., Cook, B. and Reilly, J. (2021) 'Personalized infection prevention and control: Identifying patients at risk of healthcare-associated infection', *Journal of Hospital Infection*, 114, pp. 32–42. Available at: https://doi.org/10.1016/j.jhin.2021.03.032.

Stibich, M. and Stachowiak, J. (2016) 'The microbiological impact of pulsed xenon ultraviolet disinfection on resistant bacteria, bacterial spore and fungi and viruses', *South African Journal of Infectious Disease*, 31(1), pp. 12–15. Available at: https://doi.org/10.4102/sajid.v31i1.103.

Stiller, A., Salm, F., Bischoff, P. and Gastmeier, P. (2016) 'Relationship between hospital ward design and healthcare-associated infection rates: A systematic review and meta-analysis', *Antimicrobial Resistance & Infection Control*, 5(1), 51. Available at: https://doi.org/10.1186/s13756-016-0152-1.

Strasfeld, L. and Chou, S. (2010) 'Antiviral drug resistance: Mechanisms and clinical implications', *Infectious Disease Clinics of North America*, 24(2), pp. 413–437. Available at: https://doi.org/10.1016/j.idc.2010.01.001.

Sukhum, K.V., Newcomer, E.P., Cass, C., Wallace, M.A., Johnson, C., Fine, J., Sax, S., Barlet, M.H., Burnham, C.-A.D., Dantas, G. and Kwon, J.H. (2022) 'Antibiotic-resistant organisms establish reservoirs in new hospital built environments and are related to patient blood infection isolates', *Communications Medicine*, 2(1), 62. Available at: https://doi.org/10.1038/s43856-022-00124-5.

Suleyman, G., Alangaden, G. and Bardossy, A.C. (2018a) 'The role of environmental contamination in the transmission of nosocomial pathogens and healthcare-associated infections', *Current Infectious Disease Reports*, 20(6), 12. Available at: https://doi.org/10.1007/s11908-018-0620-2.

Sutton, J., Cardinale, E., Epstein, S., Nummi, L., Bissinger, C., Holder, C. and Petersburg, B.H. St. (2016) 'Utilizing passive light-emitting diode disinfection technology to effectively reduce microbial contamination in a trauma room', *Open Forum Infectious Diseases*, 3(1), 266. Available at: https://doi.org/10.1093/ofid/ofw172.132.

Szemiel, A.M., Merits, A., Orton, R.J., MacLean, O.A., Pinto, R.M., Wickenhagen, A., Lieber, G., Turnbull, M.L., Wang, S., Furnon, W., Suarez, N.M., Mair, D., Da Silva Filipe, A., Willett, B.J., Wilson, S.J., Patel, A.H., Thomson, E.C., Palmarini, M., Kohl, A. and Stewart, M.E. (2021) 'In vitro selection of remdesivir resistance suggests evolutionary predictability of SARS-CoV-2', *PLoS Pathogens*, 17(9), e1009929. Available at: https://doi.org/10.1371/journal.ppat.1009929.

Tan, C. and Chlebicki, M. (2016) 'Urinary tract infections in adults', *Singapore Medical Journal*, 57(9), pp. 485-490. Available at: https://doi.org/ 10.11622/smedj.2016153

Tanielian, C., Mechin, R., Seghrouchni, R. and Schweitzer, C. (2000) 'Mechanistic and kinetic aspects of photosensitization in the presence of oxygen', *Photochemistry and Photobiology*, 71(1), p. 12-19. Available at: https://doi.org/10.1562/0031-8655(2000)071<0012:makaop>2.0.co;2.

von Tappeiner, H. (1904) 'On the knowledge of the effects of light (fluorescent) substances (in German)', *German Medical Weekly*, 1, pp. 579–580.

Terrosi, C., Anichini, G., Docquier, J.D., Savellini, G.G., Gandolfo, C., Pavone, F.S. and Cusi, M.G. (2021) 'Efficient inactivation of SARS-CoV-2 and other RNA or DNA viruses with blue LED light', *Pathogens*, 10(12), 1590. Available at: https://doi.org/10.3390/pathogens10121590.

Teska, P., Dayton, R., Li, X., Lamb, J. and Strader, P. (2020) 'Damage to common healthcare polymer surfaces from UV exposure', *Nano LIFE*, 10(03), 2050001. Available at: https://doi.org/10.1142/s1793984420500014.

Thermo Fisher Scientific. (2023) *Carboxy-H2DCFDA* (general oxidative stress indicator). Available at: https://www.thermofisher.com/order/catalog/product/C400 (Accessed: October 2022).

Tomb, R.M. (2017) Antimicrobial 405 nm light for clinical decontamination: Investigation of the antiviral efficacy and potential for bacterial tolerance. PhD Thesis. University of Strathclyde. Available at: https://stax.strath.ac.uk/concern/theses/jm214p149?locale=en (Accessed: October 2019).

Tomb, R.M., Maclean, M., Herron, P.R., Hoskisson, P.A., MacGregor, S.J. and Anderson, J.G. (2014) 'Inactivation of *Streptomyces* phage ϕC31 by 405 nm light', *Bacteriophage*, 4(3), e32129. Available at: https://doi.org/10.4161/bact.32129.

Tomb, R.M., Maclean, M., Coia, J.E., MacGregor, S.J. and Anderson, J.G. (2017a) 'Assessment of the potential for resistance to antimicrobial violet-blue light in *Staphylococcus aureus*', *Antimicrobial Resistance and Infection Control*, 6(1), pp. 1–13. Available at: https://doi.org/10.1186/s13756-017-0261-5

Tomb, R.M., Maclean, M., Coia, J.E., Graham, E., McDonald, M., Atreya, C.D., MacGregor, S.J. and Anderson, J.G. (2017b) 'New proof-of-concept in viral inactivation: virucidal efficacy of 405 nm light against feline calcivirus as a model for norovirus decontamination', *Food and Environmental Virology*, 9(2), pp. 159–167. Available at: https://doi.org/10.1007/s12560-016-9275-z.

Tomb, R.M, White, T.A., Coia, J.E., Anderson, J.G., MacGregor, S.J. and Maclean, M. (2018) 'Review of the comparative susceptibility of microbial species to photoinactivation using 380-480 nm violet-blue light', *Photochemistry and Photobiology*, 94(3), pp. 445–458. Available at: https://doi.org/10.1111/php.12883.

Tong, S.Y.C., Davis, J.S., Eichenberger, E., Holland, T.L. and Fowler, V.G. (2015) '*Staphylococcus aureus* infections: Epidemiology, pathophysiology, clinical manifestations, and management', *Clinical Microbiology Reviews*, 28(3), pp. 603–661. Available at: https://doi.org/10.1128/CMR.00134-14.

Troeger, C., Forouzanfar, M., Rao, P.C., Khalil, I., Brown, A., Swartz, S., Fullman, N., Mosser, J., Thompson, R.L., Reiner, R.C., Abajobir, A., Alam, N., Alemayohu, M.A., Amare, A.T., Antonio, C.A., Asayesh, H., Avokpaho, E., Barac, A., Beshir, M.A., Boneya, D.J., Brauer, M., Dandona, L., Dandona, R., Fitchett, J.R.A., Gebrehiwot, T.T., Hailu, G.B., Hotez, P.J., Kasaeian, A., Khoja, T., Kissoon, N., Knibbs, L., Kumar, G.A., Rai, R.K., Magdy Abd El Razek, H.M.A., Mohammed, M.S.K., Nielsen, K., Oren, E., Osman, A., Patton, G., Qorbani, M., Roba, H.S., Sartorius, B., Savic, M., Shigematsu, M., Sykes, B., Swaminathan, S., Topor-Madry, R., Ukwaja, K., Werdecker, A., Yonemoto, N., El Sayed Zaki, M., Lim, S.S., Naghavi, M., Vos, T., Hay, S.I., Murray, C.J.L. and Mokdad, A.H. (2017) 'Estimates of the global, regional, and national morbidity, mortality, and aetiologies of lower respiratory tract infections in 195 countries: A systematic analysis for the Global Burden of Disease Study 2015', *The Lancet Infectious Diseases*, 17(11), pp. 1133–1161. Available at: https://doi.org/10.1016/S1473-3099(17)30396-1.

Tseng, C. and Li, C. (2008) 'Inactivation of surface viruses by gaseous ozone', *Journal of Environmental Health*, 70(10), pp. 56–62.

Tsutsumi-Arai, C., Arai, Y., Terada-Ito, C., Imamura, T., Tatehara, S., Ide, S., Wakabayashi, N. and Satomura, K. (2022) 'Microbicidal effect of 405-nm blue LED light on *Candida albicans* and *Streptococcus* mutans dual-species biofilms on denture base resin', *Lasers in Medical Science*, 37(2), pp. 857–866. Available at: https://doi.org/10.1007/s10103-021-03323-z.

Tsutsumi-Arai, C., Arai, Y., Terada-Ito, C., Takebe, Y., Ide, S., Umeki, H., Tatehara, S., Tokuyama-Toda, R., Wakabayashi, N. and Satomura, K. (2019) 'Effectiveness of 405-nm blue LED light for degradation of *Candida* biofilms formed on PMMA denture base resin', *Lasers in Medical Science*, 34(7), pp. 1457–1464. Available at: https://doi.org/10.1007/s10103-019-02751-2.

Vatansever, F., de Melo, W.C.M.A., Avci, P., Vecchio, D., Sadasivam, M., Gupta, A., Chandran, R., Karimi, M., Parizotto, N.A., Yin, R., Tegos, G.P. and Hamblin, M.R. (2013) 'Antimicrobial strategies centered around reactive oxygen species - bactericidal antibiotics, photodynamic therapy, and beyond', *FEMS Microbiology Reviews*, 37(6), pp. 955–989. Available at: https://doi.org/10.1111/1574-6976.12026.

Vatter, P., Hoenes, K. and Hessling, M. (2021) 'Photoinactivation of the coronavirus surrogate phi6 by visible light', *Photochemistry and Photobiology*, 97(1), pp. 122–125. Available at: https://doi.org/10.1111/php.13352.

Vere Hodge, A. and Field, H.J. (2011) 'General mechanisms of antiviral resistance', in Tibayrenc, M. (ed.) *Genetics and Evolution of Infectious Diseases*. Elsevier, pp. 339–362. Available at: https://doi.org/10.1016/B978-0-12-384890-1.00013-3.

Viana Martins, C.P., Xavier, C.S.F. and Cobrado, L. (2022) 'Disinfection methods against SARS-CoV-2: A systematic review', *Journal of Hospital Infection*. 119, pp. 84–117. Available at: https://doi.org/10.1016/j.jhin.2021.07.014.

Vickery, K., Deva, A., Jacombs, A., Allan, J., Valente, P. and Gosbell, I.B. (2012) 'Presence of biofilm containing viable multiresistant organisms despite terminal cleaning on clinical surfaces in an intensive care unit', *Journal of Hospital Infection*, 80(1), pp. 52–55. Available at: https://doi.org/10.1016/j.jhin.2011.07.007.

Vidaver, A.K., Koski, R.K. and Van Etten, J.L. (1973) 'Bacteriophage φ6: a lipid-containing virus of *Pseudomonas phaseolicola*', *Journal of Virology*, 11(5), pp. 799–805. Available at: https://doi.org/10.1128/jvi.11.5.799-805.1973.

Vilar-Compte, D., Camacho-Ortiz, A. and Ponce-de-León, S. (2017) 'Infection control in limited resources countries: Challenges and priorities', *Current Infectious Disease Reports*, 19(5), 20. Available at: https://doi.org/10.1007/s11908-017-0572-y.

Vogler, E.A. (1998) 'Structure and reactivity of water at biomaterial surfaces,' *Advances in Colloid Interface Science,* 74(1-3), pp. 69-117. Available at: https://doi.org/10.1016/S0001-8686(97)00040-7.

Wagenvoort, J.H.T., Sluijsmans, W. and Penders, R.J.R. (2000) 'Better environmental survival of outbreak vs. sporadic MRSA isolates', *Journal of Hospital Infection*, 45(3), pp. 231–234. Available at: https://doi.org/10.1053/jhin.2000.0757.

Wainwright, M. (1998) 'Photodynamic antimicrobial chemotherapy (PACT)', *Journal of Antimicrobial Chemotherapy*, 42(1), pp. 13–28. Available at: https://doi.org/10.1093/jac/42.1.13.

Wang, D., Oppenländer, T., El-Din, M.G. and Bolton, J.R. (2010) 'Comparison of the disinfection effects of vacuum-UV (VUV) and UV light on *Bacillus subtilis* spores in aqueous suspensions at 172, 222 and 254 nm', *Photochemistry and Photobiology*, 86(1), pp. 176–181. Available at: https://doi.org/10.1111/j.1751-1097.2009.00640.x.

Wang, H.P., Qian, S.Y., Schafer, F.Q., Domann, F.E., Oberley, L.W. and Buettner, G.R. (2001) 'Phospholipid hydroperoxide glutathione peroxidase protects against singlet oxygen-induced cell damage of photodynamic therapy', *Free Radical Biology and Medicine*, 30(8), pp. 825–835. Available at: https://doi.org/10.1016/s0891-5849(01)00469-5.

Wang, M.Y., Zhao, R., Gao, L.J., Gao, X.F., Wang, D.P. and Cao, J.M. (2020) 'SARS-CoV-2: Structure, biology, and structure-based therapeutics development', *Frontiers in Cellular and Infection Microbiology*, 10, 587269. Available at: https://doi.org/10.3389/fcimb.2020.587269.

Wang, T., MacGregor, S.J., Anderson, J.G. and Woolsey, G.A. (2005) 'Pulsed ultra-violet inactivation spectrum of *Escherichia coli*', *Water Research*, 39(13), pp. 2921–2925. Available at: https://doi.org/10.1016/j.watres.2005.04.067.

Wang, Y., Ferrer-Espada, R., Baglo, Y., Goh, X.S., Held, K.D., Grad, Y.H., Gu, Y., Gelfand, J.A. and Dai, T. (2019) 'Photoinactivation of *Neisseria gonorrhoeae*: A paradigm-changing approach for combating antibiotic-resistant gonococcal infection', *Journal of Infectious Diseases*, 220(5), pp. 873–881. Available at: https://doi.org/10.1093/infdis/jiz018.

Wang, Y., Wu, X., Chen, J., Amin, R., Lu, M., Bhayana, B., Zhao, J., Murray, C.K., Hamblin, M.R., Hooper, D.C. and Dai, T. (2016) 'Antimicrobial blue light inactivation of gram-negative pathogens in biofilms: In vitro and in vivo studies', *Journal of Infectious Diseases*, 213(9), pp. 1380–1387. Available at: https://doi.org/10.1093/infdis/jiw070.

Warren, B.G., Turner, N., Smith, B., Addison, R., Marden, S., Weber, D.J., Rutala, W.A. and Anderson, D.J. (2020) 'Measuring the impact of continuous disinfection strategies on environmental burden in outpatient settings: A prospective randomized controlled trial', *Open Forum Infectious Diseases*, 7(10), ofaa431. Available at: https://doi.org/10.1093/ofid/ofaa431.

Wasson, C.J., Zourelias, J.L., Aardsma, N.A., Eells, J.T., Ganger, M.T., Schober, J.M. and Skwor, T.A. (2012) 'Inhibitory effects of 405nm irradiation on *Chlamydia trachomatis* growth and characterization of the ensuing inflammatory response in HeLa cells', *BMC Microbiology*, 12, 176. Available at: https://doi.org/10.1186/1471-2180-12-176.

Weber, D.J., Rutala, W.A., Miller, M.B., Huslage, K. and Sickbert-Bennett, E. (2010) 'Role of hospital surfaces in the transmission of emerging health care-associated pathogens: Norovirus, *Clostridium difficile*, and *Acinetobacter* species', *American Journal of Infection Control*, 38(5), pp. 25–33. Available at: https://doi.org/10.1016/j.ajic.2010.04.196.

Welch, D., Buonanno, M., Grilj, V., Shuryak, I., Crickmore, C., Bigelow, A.W., Randers-Pehrson, G., Johnson, G.W. and Brenner, D.J. (2018) 'Far-UVC light: A new tool to control the spread of airborne-mediated microbial diseases', *Scientific Reports*, 8, 2752. Available at: https://doi.org/10.1038/s41598-018-21058-w.

Weyrich, L.S., Dixit, S., Farrer, A.G., Cooper, A.J. and Cooper, A.J. (2015) 'The skin microbiome: Associations between altered microbial communities and disease', *Australasian Journal of Dermatology*, 56(4), pp. 268–274. Available at: https://doi.org/10.1111/ajd.12253.

WHO (2002). *Prevention of hospital-acquired infections.* Available at: https://iris.who.int/bitstream/handle/10665/67350/WHO_CDS_CSR_EPH_2002.12.pdf (Accessed: October 2019).

WHO (2011). *Report on the burden of endemic health care-associated infection worldwide: Clean care is safe.* Available at: https://www.who.int/publications/i/item/report-on-the-burden-of-endemic-health-care-associated-infection-worldwide (Accessed: October 2019).

WHO (2014). *Infection prevention and control of epidemic- and pandemic-prone acute respiratory infections in health care.* Available at: https://pubmed.ncbi.nlm.nih.gov/24983124/ (Accessed: November 2019).

WHO (2017). *Global priority list of antibiotic-resistant bacteria to guide research, discovery, and development of new antibiotics*. Available at: https://www.aidsdatahub.org/sites/default/files/resource/who-global-priority-list-antibiotic-resistant-bacteria.pdf (Accessed: October 2020).

WHO (2018). *Global guidelines for the prevention of surgical site infection*. Available at: https://www.who.int/publications/i/item/9789241550475 (Accessed: December 2019).

WHO (2020a). *Pneumonia of unknown cause – China*. Available at: https://www.who.int/emergencies/disease-outbreak-news/item/2020-DON229 (Accessed: July 2022).

WHO (2020b). *Situation Report-51*. Available at: https://www.who.int/publications/m/item/situation-report---51 (Accessed July 2022).

WHO (2020c). *WHO Director-General's opening remarks at the media briefing on COVID-19*. Available at: https://www.who.int/director-general/speeches/detail/who-director-general-s-opening-remarks-at-the-media-briefing-on-covid-19---11-march-2020 (Accessed July 2022).

WHO (2021a). *Antimicrobial Resistance*. Available at: https://www.who.int/news-room/fact-sheets/detail/antimicrobial-resistance (Accessed February 2022).

WHO. (2021b) Coronavirus disease (COVID-19): How is it transmitted? Available at: https://www.who.int/news-room/questions-and-answers/item/coronavirus-disease-covid-19-how-is-it-transmitted (Accessed: February 2022).

WHO. (2022a) *Global report on infection prevention and control.* Available at: https://www.who.int/publications/i/item/9789240051164 (Accessed March 2024).

WHO. (2022b) *WHO Coronavirus (COVID-19) dashboard*. Available at: https://data.who.int/dashboards/covid19/cases?n=c (Accessed: March 2022).

WHO. (2023) *Key facts and figures: World hand hygiene day 2023*. Available at: https://www.who.int/campaigns/world-hand-hygiene-day/2023/key-facts-and-figures#:~:text=On%20average%2C%201%20in%20every%2010%20affected%20patients,treated%20in%20adult%20intensive-care%20units%20are%20health%20care-associated. (Accessed: March 2024).

WHO. (2024) *Global technical consultation report on proposed terminology for pathogens that transmit through the air.* Available at: https://www.who.int/publications/m/item/global-technical-consultation-report-on-proposed-terminology-for-pathogens-that-transmit-through-the-air. (Accessed: May 2024).

Wilder-Smith, A. (2021) 'COVID-19 in comparison with other emerging viral diseases: Risk of geographic spread via travel', *Tropical Diseases, Travel Medicine and Vaccines*, 7, 3. Available at: https://doi.org/10.1186/s40794-020-00129-9.

Wilson, M. and Yianni, C. (1995) 'KilIing of methicillin-resistant *Staphylococcus aureus* by low-power laser light', *Journal of Medical Microbiology*, 42(1), pp. 62–66. Available at: https://doi.org/10.1099/00222615-42-1-62.

Wolf, C., Hochgräfe, F., Kusch, H., Albrecht, D., Hecker, M. and Engelmann, S. (2008) 'Proteomic analysis of antioxidant strategies of *Staphylococcus aureus*: Diverse responses to different oxidants', *Proteomics*, 8(15), pp. 3139–3153. Available at: https://doi.org/10.1002/pmic.200701062.

Wu, H.T., Li, Q.S., Dai, R.C., Liu, S., Wu, L., Mao, W. and Ji, C.H. (2021) 'Effects of air-conditioning systems in the public areas of hospitals: A scoping review', *Epidemiology and Infection*, 149, e201. Available at: https://doi.org/10.1017/S0950268821001990.

Xu, L., Sun, X. and Ma, X. (2017) Systematic review and meta-analysis of mortality of patients infected with carbapenem-resistant *Klebsiella pneumoniae'*, *Annals of Clinical Microbiology and Antimicrobials*, 16, 18. Available at: https://doi.org/10.1186/s12941-017-0191-3.

Xenex. (2022) *Light Strike Plus UV Advantage. Available at:* https://xenex.com/lightstrike-plus-uv-advantage/ (Accessed: March 2023).

Yang, K., Shi, J., Wang, L., Chen, Y., Liang, C., Yang, L. and Wang, L.N. (2022) 'Bacterial anti-adhesion surface design: Surface patterning, roughness and wettability: A review', *Journal of Materials Science and Technology*, 99, pp. 82–100. Available at: https://doi.org/10.1016/j.jmst.2021.05.028.

Yang, Y., Lu, S., Shen, W., Zhao, X., Shen, M., Tan, Y., Li, G., Li, M., Wang, J., Hu, F. and Le, S. (2016) 'Characterization of the first double-stranded RNA bacteriophage infecting *Pseudomonas aeruginosa*', *Scientific Reports*, 6, 38795. Available at: https://doi.org/10.1038/srep38795.

Zarb, P., Coignard. B., Griskeviciene, J., Muller, A., Vankerckhoven, V., Weist, K., Gossens, M.M., Vaerenberg, S., Hopkins, S., Catry, B., Monnet, D.L., Goossens, H. and Suetens, C. (2012) 'The European Centre for Disease Prevention and Control (ECDC) pilot point prevalence survey of healthcare-associated infections and antimicrobial use', *Euro Surveillance*, 17(46), 20316. Available at: https://doi.org/10.2807/ese.17.46.20316-en.

Zargar, B., Sattar, S.A., Kibbee, R., Rubino, J. and Khalid Ijaz, M. (2022) 'Direct and quantitative capture of viable bacteriophages from experimentally contaminated indoor air: A model for the study of airborne vertebrate viruses including SARS-CoV-2', *Journal of Applied Microbiology*, 132(2), pp. 1489–1495. Available at: https://doi.org/10.1111/jam.15262.

Zhang, X.-W., Qiu, Q.-F., Jiang, H., Zhang, F.-L., Liu, Y.-L., Amatore, C. and Huang, W.-H. (2017) 'Real-time intracellular measurements of ROS and RNS in living cells with single core-shell nanowire electrodes' Angewandte Chemie International Edition, 56(42), pp. 12997-13000. Available at: https://doi.org/10.1002/anie.201707187.

Zhang, Y., Zhu, Y., Chen, J., Wang, Y., Sherwood, M.E., Murray, C.K., Vrahas, M.S., Hooper, D.C., Hamblin, M.R. and Dai, T. (2016) 'Antimicrobial blue light inactivation of *Candida albicans*: In vitro and in vivo studies', *Virulence*, 7(5), pp. 536–545. Available at: https://doi.org/10.1080/21505594.2016.1155015.

Zhang, Y., Zhu, Y., Gupta, A., Huang, Y., Murray, C.K., Vrahas, M.S., Sherwood, M.E., Baer, D.G., Hamblin, M.R. and Dai, T. (2014) 'Antimicrobial blue light therapy for multidrug-resistant *Acinetobacter baumannii* infection in a mouse burn model: Implications for prophylaxis and treatment of combat-related wound infections', *Journal of Infectious Diseases*, 209(12), pp. 1963–1971. Available at: https://doi.org/10.1093/infdis/jit842.

Zhou, L., Ayeh, S.K., Chidambaram, V. and Karakousis, P.C. (2021) 'Modes of transmission of SARS-CoV-2 and evidence for preventive behavioural interventions', *BMC Infectious Diseases*, 21, 496. Available at: https://doi.org/10.1186/s12879-021-06222-4.

Zhu, J., Guo, J., Xu, Y. and Chen, X. (2020) 'Viral dynamics of SARS-CoV-2 in saliva from infected patients', *Journal of Infection*, 81(3) pp. 48–50. Available at: https://doi.org/10.1016/j.jinf.2020.06.059.

Zhou, X., Willems, R., Friedrich, A., Rossen, J. and Bathoorn, E. (2020) '*Enterococcus faecium*: From microbiological insights to practical recommendations for infection control and diagnostics', *Antimicrobial Resistance and Infection Control*, 9, 130. Available at: https://doi.org/10.1186/s13756-020-00770-1.

Zimmermann, J.L., Dumler, K., Shimizu, T., Morfill, G.E., Wolf, A., Boxhammer, V., Schlegel, J., Gansbacher, B. and Anton, M. (2011) 'Effects of cold atmospheric plasmas on adenoviruses in solution', *Journal of Physics D: Applied Physics*, 44(50), 505201. Available at: https://doi.org/10.1088/0022-3727/44/50/505201.

Zolfaghari, P. and Wyncoll, D. (2011) 'The tracheal tube: Gateway to ventilator-associated pneumonia', *Critical Care*, 15, 310. Available at: https://doi.org/10.0.4.162/cc10352.

Zoutman, D., Shannon, M. and Mandel, A. (2011) ‘Effectiveness of a novel ozone-based system for the rapid high-level disinfection of health care spaces and surfaces’, *American Journal of Infection Control*, 39(10), pp. 873–879. Available at: https://doi.org/10.1016/j.ajic.2011.01.012.

APPENDIX A

OPTICAL CHARACTERISATION OF THE 405-NM LIGHT EDS

This appendix contains the irradiance distribution produced by the 405-nm light EDS in a 2 × 2 × 4 m area, with measurements taken with the photodiode detector angled towards the light source to examine the irradiance levels likely to illuminate aerosolised matter in each area, as detailed in Chapter 4.

Optical characterisation in this configuration (Figure A.1) produced a total of 324 readings, with emitted irradiance values within the range of 0.001–2.066 mW cm^{-2}, with highest irradiance values were collected at the closest measurements taken to the 405-nm light EDS (directly under the light source at a distance of 0.5 m) and the lowest irradiance values were generally collected at maximum distances in X and Y directions from the light source, similar to that demonstrated for measurements taken with the photodiode detector held horizontal to the light source (Figure 4.5). Irradiance values gathered with the photodiode detector held horizontal to the 405-nm light EDS were overall lower than those gathered with the photodiode detector held angled towards the 405-nm light EDS: considering irradiance measurements for both X and Y planes, angular measurements were shown to be overall significantly greater than horizontal measurements at distances equal to or greater than 1.5 m from the light source ($P=<0.001$, 0.005, 0.187, 0.152, 0.8, 0.408, 0.124, 0.004 and <0.001 in the X plane and $P<0.001$, 0.004, 0.155, 0.495, 0.818, 0.368, 0.092, 0.002 and <0.001 in the Y plane, for distances of -2, -1.5, -1, -0.5, 0, 0.5, 1, 1.5 and 2 m from the light source, respectively). At distances less than 1.5 m from the light source in X and Y directions, no significant difference was overall found between horizontal and angular measurements. When considering the Z plane, statistical analysis demonstrated no significant difference overall between the measurements at each distance in the Z direction taken with the photodiode detector held horizontally and angled towards the 405-nm light EDS ($P=0.396$, 0.537, 0.579, 0.626 for distances of 0.5, 1, 1.5 and 2 m from the light source, respectively). Despite this, variation was still demonstrated between horizontal and angular measurements in the Z plane: at a distance of 0.5 m from the light source, the sum of all irradiance measurements was found to be 3.661 mW cm^{-2} for horizontal measurements and 4.367 mW cm^{-2} for angular measurements; these values were found to be 3.935 and

4.687 mW cm^{-2}, respectively, at a distance of 1 m; 3.998 and 5.02 mW cm^{-2}, respectively, at a distance of 1.5 m; and 3.913 and 5.454 mW cm^{-2}, respectively, at a distance of 2 m.

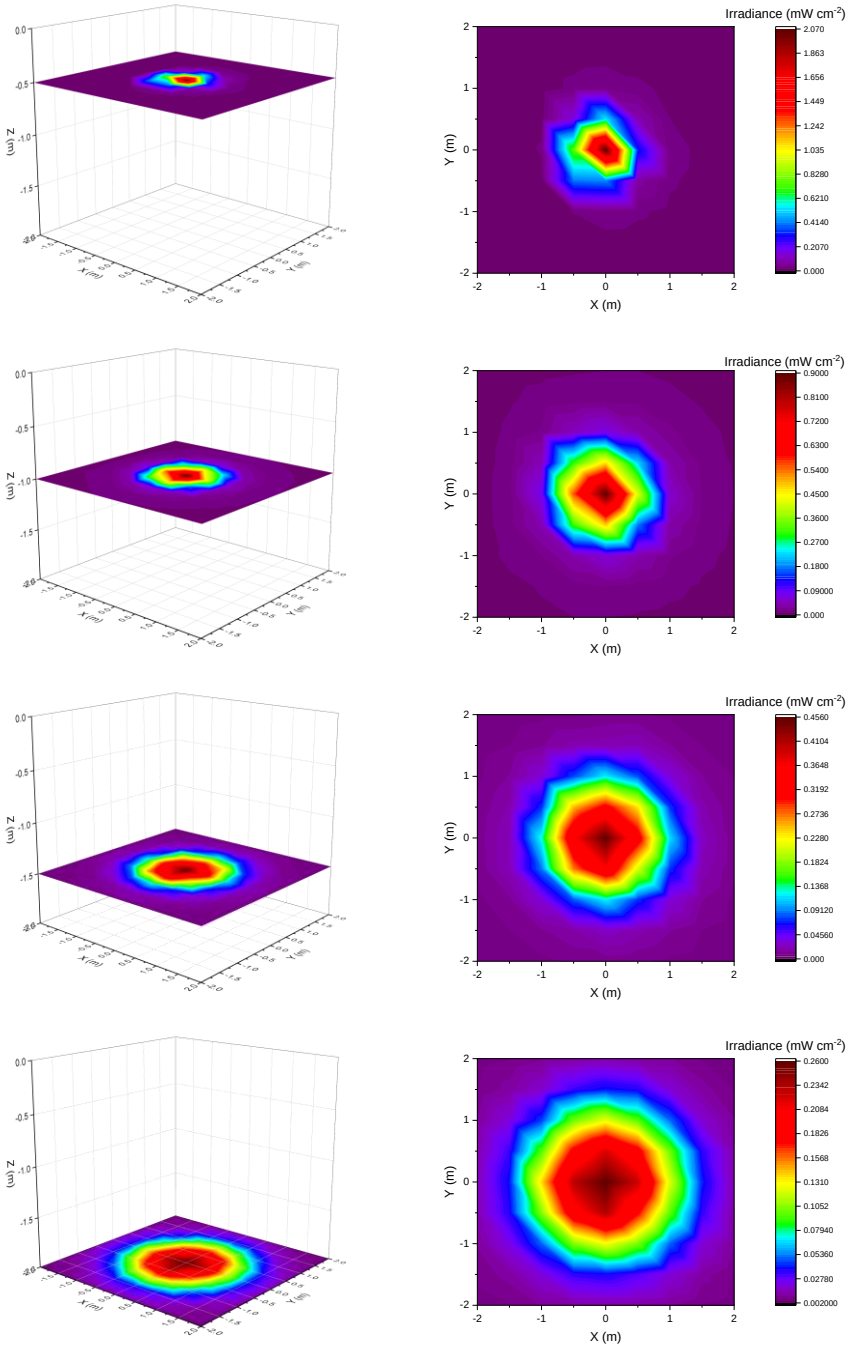

Figure A.1 Irradiance distribution produced by ceiling-mounted low-irradiance 405-nm light EDS at distances of (A) 0.5 m, (B) 1 m, (C) 1.5 m and (D) 2 m in the Z direction, with measurements taken with the photodiode detector angled to the light source (please note that the scale is different for each graph).

APPENDIX B

405-NM LIGHT INACTIVATION OF ESKAPE PATHOGENS ON SURFACES

This appendix contains displays agar plates seeded with *E. faecium* (Figure B.1), *K. pneumoniae* (Figure B.2), *A. baumannii* (Figure B.3) and *E. cloacae* (Figure B.4) at population densities of 10^1-10^8 CFU plate^{-1} and exposed to 0.5 mWcm^{-2} 405-nm light for 16-h (28.8 Jcm^{-2}) and 24-h (43.4 Jcm^{-2}), as detailed in Chapter 6.

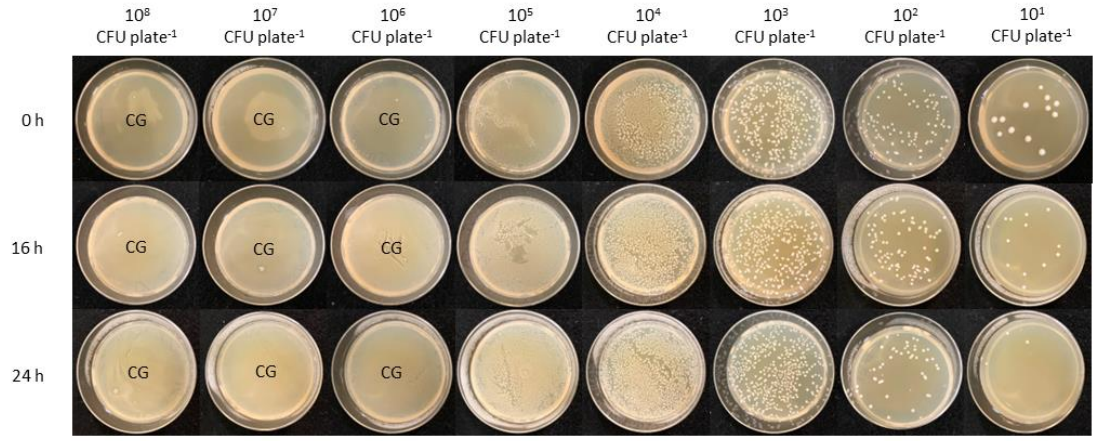

Figure B.1 Appearance of *E. faecium* at 10^8 – 10^1 CFU plate^{-1}, after exposure to 0.5 mWcm^{-2} 405-nm light for 16 h and 24 h (28.8 and 43.4 Jcm-2, respectively). CG represents plates with confluent growth of bacteria.

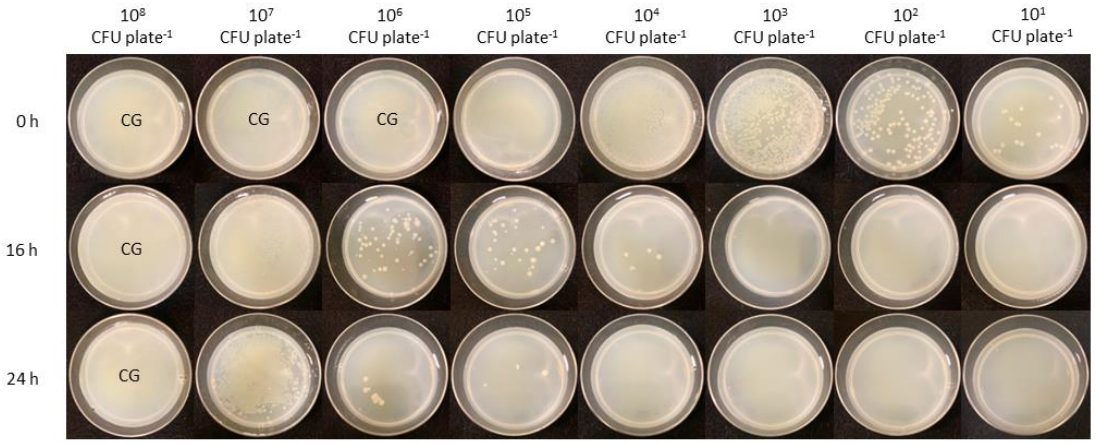

Figure B.2 Appearance of *K. pneumoniae* at 10^8 – 10^1 CFU plate^{-1}, after exposure to 0.5 mWcm^{-2} 405-nm light for 16 h and 24 h (28.8 and 43.4 Jcm-2, respectively). CG represents plates with confluent growth of bacteria.

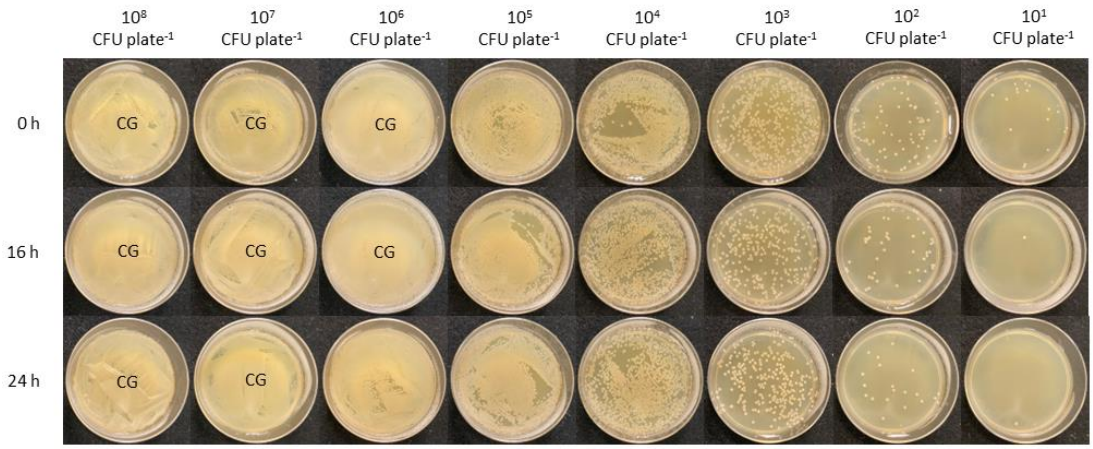

Figure B.3 Appearance of *A. baumannii* at 10^8 – 10^1 CFU plate^{-1}, after exposure to 0.5 mWcm^{-2} 405-nm light for 16 h and 24 h (28.8 and 43.4 Jcm-2, respectively). CG represents plates with confluent growth of bacteria.

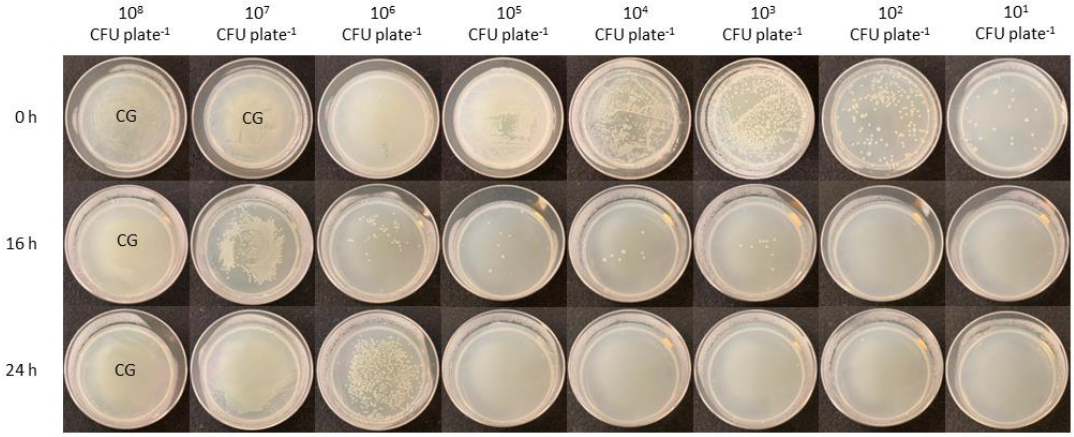

Figure B.4 Appearance of *E. cloacae* at 10^8 – 10^1 CFU plate^{-1}, after exposure to 0.5 mWcm^{-2} 405-nm light for 16 h and 24 h (28.8 and 43.4 Jcm-2, respectively). CG represents plates with confluent growth of bacteria.

APPENDIX C

PUBLICATION LIST

Peer-reviewed Journal Contributions:

- **Sinclair, L.G.**, Anderson, J.G., MacGregor, S.J. and Maclean, M. (2024) 'Enhanced antimicrobial efficacy and energy efficiency of low irradiance 405-nm light for decontamination of ESKAPE pathogens.' *Archives of Microbiology*, 206(276). Available at: https://doi.org/10.1007/s00203-024-03999-1
- **Sinclair, L.G.**, Dougall, L.R., Ilieva, Z., McKenzie, K., Anderson, J.G., MacGregor, S.J. and Maclean, M. (2023) 'Laboratory evaluation of the broad-spectrum antibacterial efficacy of a low-irradiance visible 405-nm light system for surface-simulated decontamination. *Health and Technology*, 13, 615-629. Available at: https://doi.org/10.1007/s12553-023-00761-3.
- **Sinclair, L.G.**, Ilieva, Z., Anderson, J.G., MacGregor, S.J. and Maclean, M. (2023) 'Viricidal efficacy of a 405nm environmental decontamination system for inactivation of bacteriophage phi6: Surrogate for SARS-CoV-2.' *Photochemistry and Photobiology*, 99(6), 1493-1500. Available at: https://doi.org/10.1111/php.13798 *

  *This paper was selected by Photochemistry and Photobiology to be a '*Feature Article*' on its website homepage and also to feature as the cover image of the issue in which it was published (https://onlinelibrary.wiley.com/doi/10.1111/php.13651).

Conference Poster Presentations:

- **Sinclair, L.G.**, MacGregor, S.J. and Maclean, M. (2023) 'Bactericidal efficacy and cytotoxic responses of *Pseudomonas aeruginosa* to low irradiance 405-nm light.' *20th Congress of the European Society of Photobiology*, Lyon, France, 27-31 Aug 2023.
- **Sinclair, L.G.**, Ilieva, Z., MacGregor, S.J. and Maclean, M. (2022) 'Efficacy of a low irradiance antimicrobial 405-nm visible light system for inactivation of bacteriophage phi6 as a surrogate for SARS-CoV-2.' *Federation of Infection Societies (FIS) 2022*, London, UK, 22-23 Sep 2022.

- **Sinclair, L.G.**, MacGregor, S. J., Anderson, J.G. and Maclean, M. (2022) 'Antimicrobial efficacy of a low irradiance 405-nm visible light system for broad spectrum inactivation of clinical bacterial pathogens.' *ASM Microbe 2022*, Washington DC, 9-13 June 2022.
- **Sinclair, L.G.**, MacGregor, S.J. and Maclean, M. (2021) 'Effect of bacterial bioburden and light intensity on the efficacy of antimicrobial 405-nm light.' *Federation of Infection Societies (FIS) 2021*, Online, 8-9 Nov 2021.
- **Sinclair, L.G.**, MacGregor, S.J. and Maclean, M. (2021) 'Antimicrobial efficacy and energy efficiency of low irradiance 405-nm light for inactivation of ESKAPE pathogens.' *World Microbe Forum*, Online, 20-24 June 2021.
- **Sinclair, L.G.**, MacGregor, S.J. and Maclean, M. (2021) 'Comparison of the antimicrobial efficacy and germicidal efficiency of 405-nm light for surface decontamination.' *Microbiology Society Annual Conference 2021*, Online, 26-30 Apr 2021.
- **Sinclair, L.G.**, MacGregor, S.J. and Maclean, M. (2020). 'Efficacy of low irradiance antimicrobial 405 nm violet-blue light for the inactivation of nosocomial bacteria.' *Federation of Infection Societies (FIS) / Healthcare Infection Society (HIS) International 2020*, Online, 9-11 Nov 2020.

Conference Oral Presentations:

- **Sinclair, L.G.**, MacGregor, S.J. and Maclean, M. (2023) 'Bactericidal efficacy and cytotoxic responses of *Pseudomonas aeruginosa* to low irradiance 405-nm light.' *20th Congress of the European Society of Photobiology*, Lyon, France, 27-31 Aug 2023.
- **Sinclair, L.G.**, MacGregor, S. J., Anderson, J. G. and Maclean, M. (2022) 'Antimicrobial efficacy of a low irradiance 405-nm visible light system for broad spectrum inactivation of clinical bacterial pathogens.' *ASM Microbe 2022*, Washington DC, 9-13 Jun 2022.